Universidade de Aveiro Departamento de Química
Ano 2017

Tânia Sofia Rodrigues de Melo

Estratégias analíticas baseadas em espectrometria de massa para identificação de modificações nitro oxidativas em fosfolípidos

Analytical strategies based on mass spectrometry toward identifying nitro oxidative modifications in phospholipids

Universidade de Aveiro Departamento de Química
Ano 2017

Tânia Sofia Rodrigues de Melo

Estratégias analíticas baseadas em espectrometria de massa para identificação de modificações nitro oxidativas em fosfolípidos

Analytical strategies based on mass spectrometry toward identifying nitro oxidative modifications in phospholipids

Tese apresentada à Universidade de Aveiro para cumprimento dos requisitos necessários à obtenção do grau de Doutor em Bioquímica, realizada sob a orientação científica da Doutora Maria do Rosário Gonçalves dos Reis Marques Domingues, Professora Associada com Agregação do Departamento de Química da Universidade de Aveiro, e da Doutora Marcela Alves Segundo, Professora Auxiliar da Faculdade de Farmácia da Universidade do Porto

Apoio financeiro do POCTI no âmbito do III Quadro Comunitário de Apoio.

Apoio financeiro da FCT e do FSE no âmbito do III Quadro Comunitário de Apoio.

Dedico este trabalho aos meus pais e irmã.

o júri

presidente

Prof. Doutor João Carlos de Oliveira Matias
Professor Catedrático do Departamento de Economia, Gestão, Engenharia Industrial e Turismo da Universidade de Aveiro

vogais

Prof. Doutora Maria de La Salette de Freitas Fernandes Hipólito Reis Dias Rodrigues
Professora Associado com Agregação da Faculdade de Farmácia da Universidade do Porto

Prof. Doutora Maria do Rosário Gonçalves dos Reis Marques Domingues
Professora Associada com Agregação da Universidade de Aveiro (orientadora)

Prof. Doutor Pedro Miguel Dimas Neves Domingues
Professor Auxiliar com Agregação da Universidade de Aveiro

Prof. Doutora Maria Teresa Teixeira da Cruz Rosete
Professora Auxiliar da Faculdade de Farmácia da Universidade de Coimbra

Prof. Doutora Maria Manuel Oliveira
Professora Auxiliar da Escola de Ciências da Vida e do Ambiente da Universidade de Trás-os-Montes e Alto Douro

agradecimentos

Agradeço à Professora Rosário Domingues e à Professora Marcela Segundo pela orientação deste trabalho, pelos conhecimentos transmitidos, pela disponibilidade e pelo incentivo constante.

Agradeço aos restantes coautores dos trabalhos apresentados nesta tese pelo seu contributo, em particular ao Professor Pedro Domingues pela sua disponibilidade e conhecimentos transmitidos.

Agradeço à Doutora Maria Fedorova por me ter recebido no seu laboratório, localizado no *Center for Biotechnology and Biomedicicne* em Leipzig. Agradeço à Ivana Milic e ao Andrea Annibal pelo apoio no laboratório e pelos bons momentos partilhados.

Agradeço à Doutora Dolores Pérez-Sala por me ter recebido no seu laboratório, localizado no *Centro de Investigaciones Biológicas* (CIB-CSIC) em Madrid (SAF2012-36519 and SAF2015-68590R from MINECO/FEDER). Agradeço pela enorme disponibilidade, pelos conhecimentos partilhados e pelo apoio no desenvolvimento do trabalho nesse laboratório.

De uma forma geral, agradeço aos colegas do grupo de Espectrometria de Massa pelo auxílio e pelo agradável ambiente de trabalho. Agradeço à Dra. Cristina Barros pelo apoio nos espectrómetros e no laboratório.

Agradeço aos meus pais e irmã pelo amor e pelo apoio incondicional.

Agradeço à unidade de investigação de Química Orgânica, Produtos Naturais e Agroalimentares (QOPNA) da Universidade de Aveiro (FCT Grant UID/QUI/00062/2013) e à Rede Nacional de Espectrometria de Massa (REDE/1504/REM/2005).

Agradeço à Fundação para a Ciência e a Tecnologia (FCT) pelo financiamento através de uma bolsa de doutoramento (SFRH/BD/84691/2012).

palavras-chave

Fosfolípidos, fosfatidilcolina, fosfatidiletanolamina, fosfatidilserina, stresse nitroxidativo, nitração, modificações estruturais, espectrometria de massa.

resumo

Os lípidos são considerados alvos importantes das espécies reativas de nitrogénio (RNS, do inglês *Reactive Nitrogen Species*), formadas em condições de stresse nitroxidativo. As RNS podem levar à formação de uma grande variedade de lípidos modificados, formados através de reações de nitração, nitrosação e nitroxidação. Os ácidos gordos nitrados (NO_2-FA) têm sido descritos como os principais produtos endógenos formados pela reação entre ácidos gordos e RNS, e já foram detetados em plasma, urina e tecidos. Os NO_2-FA são considerados compostos bioativos com um importante papel como agentes anti-inflamatórios, anti-hipertensivos e anti-trombóticos, estando envolvidos na modulação de complicações metabólicas e inflamatórias. Apesar da relevância da nitração de lípidos, maioritariamente descrita para os NO_2-FA, a nitração de fosfolípidos, que são os principais constituintes das membranas celulares, permanece um campo de investigação pouco explorado continuando a existir uma falha de conhecimento no que diz respeito ao tipo de produtos fosfolipídicos que podem ser formados em condições de stresse nitroxidativo, e quais os seus papéis nos sistemas biológicos.

Para ultrapassar esta questão, os principais objetivos desta tese de doutoramento consistiram no desenvolvimento de abordagens baseadas em espectrometria de massa (MS) para a) a identificação de diferentes fosfolípidos nitrados e nitroxidados, b) a identificação dos padrões de fragmentação característicos dos fosfolípidos modificados, c) aplicar as estratégias desenvolvidas e baseadas em espectrometria de massa para detetar fosfolípidos nitrados e nitroxidados *in vivo* em modelos de doença, d) avaliar o papel dos fosfolípidos nitrados e nitroxidados como agentes anti-inflamatórios e antioxidantes e e) avaliar a sua interação com proteínas. De um modo geral, pretendemos contribuir para o conhecimento das modificações químicas em fosfolípidos induzidas em condições de stresse nitroxidativo e a significância biológica desses produtos.

Para alcançarmos os objetivos propostos, os derivados nitrados dos fosfolípidos (NO_2-PL), nomeadamente os derivados nitro de fosfatidilcolinas (NO_2-PC), fosfatidiletanolaminas (NO_2-PE) e fosfatidilserinas (NO_2-PS), contendo diferentes ácidos gordos, foram estudados por MS. Os NO_2-PL foram sintetizados utilizando nitrónio tetraflouroborato (NO_2BF_4), mimetizando condições de stresse nitroxidativo, e foram posteriormente identificados por MS com ionização por *electrospray* (ESI-MS) e caracterizados por espectrometria de massa tandem (ESI-MS/MS). O seu padrão de fragmentação típico foi identificado e incluí a perda do grupo nitro (HNO_2) e a formação de ácidos gordos nitrados. Esta metodologia baseada em MS, permitiu a deteção de oito derivados nitrados de fosfolípidos, sete NO_2-PCs e uma NO_2-PE, em mitocôndrias isolados do coração de um modelo animal de diabetes *mellitus* tipo 1 obtido pela administração de streptozotocina (STZ).

Estas descobertas irão contribuir para a compreensão dos mecanismos de nitração em ambientes biológicos e para estabelecer a relevância fisiológica dos NO_2-PLs. Além disso, outros derivados nitrados e nitroxidados das PCs e PEs com diferentes combinações de ácidos gordos foram também sintetizados utilizando o modelo biomimético de nitroxidação e, posteriormente, foram estudados por cromatografia líquida (LC) acoplada à espectrometria de massa e MS/MS. Os derivados modificados de fosfolípidos incluíram: derivados nitroso e dinitroso, nitro e dinitro, e nitronitroso, em conjunto com derivados nitroxidados. A fragmentação típica para cada uma estas modificações foram a perda de HNO e HNO_2, as perdas combinadas de HNO (HNO_2) e a cabeça polar dos fosfolípidos, e ainda iões produto correspondentes às cadeias de ácido gordo modificadas, nomeadamente iões $[NO_n\text{-}FA+O_n+H]^+$ e $[NO_n\text{-}FA+O_n\text{-}H]^-$ (n=1-2). Estas fragmentações permitiram identificar PCs nitradas, incluindo NO_2-PC, $(NO_2)_2$-PCs, (NO_2)(NO)-PC, NO-PC; PEs nitradas, NO_2-PEs; e uma PC nitroxidada (NO_2)(2O)-PC em cardiomioblastos H9c2 em condições de *starvation*, mas não foram detetadas em células em condições de isquémia nem no controlo. A relevância fisiológica das PCs e PEs nitradas e nitroxidadas observadas exclusivamente em cardiomioblastos H9c2 em condições de *starvation* permanece desconhecida mas estas espécies podem ter um papel na cardioproteção que merece ser explorada.

Para avaliar os possíveis efeitos biológicos dos NO_2-PL, os produtos nitrados/nitroxidados da POPC, nomeadamente os derivados NO_2-POPC, foram incubados com macrófagos Raw 264.7, uma linha celular de monócitos de ratinho estimulada com LPS, demonstrando ter propriedades anti-inflamatórias pela diminuição da expressão da forma induzível da óxido nítrico sintase (iNOS). Os produtos nitrados/nitroxidados da POPC demonstraram ainda ter propriedades antioxidantes, nomeadamente como *scavengers*, demonstrada pela capacidade de reduzir os radicais $ABTS^{\bullet+}$, $DPPH^{\bullet}$ e peroxílo (ensaio ORAC).

Tendo em conta que os efeitos biológicos dos lípidos nitrados ocorre via modificações pós-transducionais de proteínas, também avaliámos a capacidade dos produtos nitrados/nitroxidados da POPC em interagir com proteínas, especificamente a adição dos derivados NO_2-POPC, principais produtos formados durante a nitração biomimética da POPC, com a vimentina que é um filamento intermediário. Para avaliar o efeito da NO_2-POPC foram utilizados ensaios de competição *in vitro*, onde as suas interações foram avaliadas utilizando *western blotting*. A interação dos produtos nitrados/nitroxidados da POPC com a vimentina protegeu-a da modificação pela iodoacetamida biotinilada. Os produtos nitrados/nitroxidados da POPC também induziram alterações na organização da rede de vimentina. Estes efeitos foram avaliados, utilizando microscopia confocal, em células de carcinoma adrenal SW13, as quais expressam construções específicas de vimentina.

Os resultados obtidos com esta tese de doutoramento fornecem novas informações baseadas em abordagens avançadas de MS para a identificação de modificações em PLs induzidas pelas RNS nomeadamente em condições de stresse nitroxidativo, o que irá ser crucial para a sua identificação em amostras biológicas, e ainda para o desvendar dos seus potenciais papéis a nível biológico.

keywords

Phospholipids, phosphatidylcholine, phosphatidylethanolamine, phosphatidylserine, nitroxidative stress, nitration, structural modifications, mass spectrometry.

abstract

Lipids are considered important targets of reactive nitrogen species (RNS), under nitroxidative stress conditions. Various RNS can lead to a great variety of modified lipids, formed via nitration, nitrosation and nitroxidation reactions. Nitro-fatty acids (NO_2-FA) have been reported as major endogenous products formed between fatty acids (FA) and RNS, and have been detected in plasma, urine, and tissues. NO_2-FA are considered important bioactive molecules with roles as anti-inflammatory, anti-hypertensive, and anti-thrombotic agents being involved in modulation of metabolic and inflammatory complications. In spite of the relevance of lipid nitration, it has been mainly focused on NO_2-FAs, but in contrast, putative nitration of phospholipids (PL), the major constituents of cell membranes, remains an unexplored field of research. There are no studies regarding the type of PL products that can be formed under nitroxidative stress conditions and their possible roles in biological systems.

To overcome this issue, the main goals of this PhD were the development of mass spectrometry (MS)-based approaches a) to identify different PL nitrated and nitroxidized products, b) to identify the characteristic fragmentation pattern of modified PL, c) to apply the developed MS-based strategies to detected nitrated and nitroxidized PL species in *in vivo* models of disease, d) to evaluate the role of nitrated and nitroxidized PLs as anti-inflammatory and as antioxidants, and c) to evaluate their adduction to proteins. Overall it is expected to contribute for the understanding of the chemical modifications induced by nitroxidative stress to PLs and their biological significance.

To accomplish our goal, first we analyzed nitrated PL species (NO_2-PL), namely nitro derivatives of phosphatidylcholine (NO_2-PC), phosphatidylethanolamine (NO_2-PE) and phosphatidylserine (NO_2-PS), bearing different FA by MS. NO_2-PL were synthesized using nitronium tetrafluoroborate (NO_2BF_4) in a biomimetic system of nitroxidative stress conditions. NO_2PL were identified by electrospray (ESI)-MS and characterized by ESI tandem mass spectrometry (ESI-MS/MS). The typical fragmentation pattern of NO_2-PL was determined and included the loss of nitro group (HNO_2) and the formation of nitrated fatty acids. The MS reported ions allowed us to detect eight nitrated derivatives of PLs, seven NO_2-PCs and one NO_2-PE, in cardiac mitochondria isolated from heart of a well-characterized animal model of type 1 diabetes mellitus (T1DM) obtained by administration of streptozotocin (STZ). These findings will contribute for the understanding of nitration in biological environments, and to establish the physiological relevance of NO_2-PL species.
In addition, different nitrated and nitroxidized derivatives of PCs and PEs with different combinations of FA were also generated using the biomimetic model of nitroxidation and were studied by liquid chromatography (LC)-MS and MS/MS approaches.

Single and multiple nitrated derivatives of PLs such as nitroso and dinitroso, nitro and dinitro, nitronitroso derivatives, together with nitroxidized derivatives were identified and their specific fragmentation pathways were assigned. Typical reporter product ions of these modifications were loss of HNO and HNO_2, the combined loss of HNO (or HNO_2) and polar head groups, and $[NO_n\text{-}FA+O_n+H]^+$ and $[NO_n\text{-}FA+O_n\text{-}H]^-$ (n=1-2) product ions corresponding to the modified fatty acyl chains, depending on each modification. These reported fragmentations allowed the identification of nitrated PCs, including NO_2-PC, $(NO_2)_2$-PCs, (NO_2)(NO)-PC, NO-PC; nitrated PEs, NO_2-PEs; and nitroxidized PCs, (NO_2)(2O)-PC in cardiomyoblast H9c2 cells under starvation conditions, but not in cells under ischemia neither in control. The physiological relevance of nitrated and nitroxidized PCs and PEs species observed exclusively in cardiomyoblast cells (H9c2) under starvation is still unknown but could have a role in cardioprotection that deserves to be explored.

To evaluate the putative biological effects of NO_2-PL, nitrated/nitroxidized products of POPC, namely the NO_2-POPC derivatives, were incubated with Raw 264.7 macrophages, a mouse leukaemic monocyte cell line, stimulated with LPS, and revealing anti-inflammatory properties by decreasing the expression of the inducible nitric oxide synthase (iNOS). Nitrated/nitroxidized products of POPC also showed antioxidant properties, namely as scavenging agents, demonstrated by reducing the $ABTS^{\bullet+}$, $DPPH^{\bullet}$ and peroxyl radicals (ORAC assay).

Considering that the biological effects of nitrated lipid occur via post-translational modification (PTM) of proteins, we had also evaluated the ability of nitrated/nitroxidized products of POPC to interact with proteins. For that it was studied the adduction of NO_2-POPC derivatives, the major product formed during biomimetic nitration of POPC, with vimentin, an intermediate filament protein, assessed using *in vitro* gel-based competition assay, and their interactions were evaluated using western blotting. The interaction of nitrated/nitroxidized products of POPC with vimentin shielded its modifications by biotinylated iodoacetamide. The effects of nitrated/nitroxidized products of POPC in the organization of vimentin network was also evaluated in SW13 adrenal carcinoma cell line expressing defined vimentin constructs using confocal microscopy. The results gathered in his study revealed that nitrated/nitroxidized products of POPC can interact with vimentin and induced changes in the organization of vimentin network.

Overall, the results gathered in this PhD thesis provide new tool based on advanced MS approaches to identify structural modification of phospholipids induced by RNS namely under nitroxidative stress, that can be successfully used to pinpoint these nitrated species in different systems, and will be crucial for their identification in biological samples, and to unveil some of their potential roles in biological systems.

Publications and communications

The results presented in this thesis already originated three publications in international scientific journals with Referee, one book chapter, as well as poster communications (as first author) in national and international meetings.

Publications in international scientific journals with Referee

Melo T, Domingues P, Ferreira R, Milic I, Fedorova M, Santos SM, Segundo MA, Domingues MRM (2016) Recent Advances on Mass Spectrometry Analysis of Nitrated Phospholipids. *Analytical Chemsitry*, 88, 2622-2629.

Melo T, Marques SS, Ferreira I, Cruz, MT, Domingues P, Segundo MA, Domingues MRM (2016) New Insights in Anti-inflammatory and Antioxidant Properties of Nitrated Phospholipids. *Chemistry and Physics of Lipids*, under revision.

Melo T, Domingues P, Ribeiro-Rodrigues TM, Girão H, Segundo MA, Domingues MRM (2016) Phospholipid Nitroxidation Profiling in H9c2 Myoblast using a Lipidomic Approach. *Free Radical Biology and Medicine*, under revision.

Book Chapter

Melo T, Domingues P, Segundo MA, Domingues MRM, Os benefícios dos ácidos gordos nitrados: uma viagem sobre o seu papel enquanto agentes anti-inflamatórios e na prevenção de doenças cardiovasculares, Bioquímica e Bem Estar@UA, Edições Afrontamento (*in press*).

Poster communications

Melo T, Domingues P, Segundo MA, Domingues MRM, Study of Phosphatidylcholine Nitration by Electrospray Ionization Tandem Mass Spectrometry. XX Encontro Luso Galego de Química, 26-28 November, Complexo Faculdade de Farmácia da University of Porto (FFUP)/ Instituto de Ciências Abel Salazar (ICBAS), Porto, Portugal, 2014.

Melo T, Domingues P, Segundo MA, Domingues MRM, Phosphatidylethanolamine Nitration – An Electrospray Ionization Tandem Mass Spectrometry Study. 7as Jornada da Bioquímica da Universidade de Aveiro, 29 de Abril, Universidade de Aveiro, Aveiro, Portugal, 2015

Melo T, Domingues P, Segundo MA, Domingues MRM, Structural Characterization of Nitrated Phosphatidylserine by Mass Spectrometry, 4º Workshop em Lipidómica, 6 de Maio, Universidade de Aveiro, Aveiro, Portugal, 2015.

Contents

List of Figures

CHAPTER I

CHAPTER III

APPENDIX A. SUPPLEMENTARY MATERIAL OF SECTION III.1.1

APPENDIX B. SUPPLEMENTARY MATERIAL OF SECTION III.1.2

APPENDIX C. SUPPLEMENTARY MATERIAL OF SECTION III.2.1

List of Tables

CHAPTER I

CHAPTER III

APPENDIX A. SUPPLEMENTARY MATERIAL OF SECTION III.1.1

APPENDIX B. SUPPLEMENTARY MATERIAL OF SECTION III.1.2

APPENDIX C. SUPPLEMENTARY MATERIAL OF SECTION III.2.1

Abbreviations

$[M+H]^+$	Protonated ion
$[M-H]^-$	Deprotonated ion
$[M+K]^+$	Potassium adduct ion
$[M+Na]^+$	Sodium adduct ion
AA-NO_2	Nitroarachidonato or Nitro arachidonic acid
AAPH	2,2′-azobis(2-methylpropionamidine) dihydrochloride
Abs	Absorbance
$ABTS^{\bullet+}$	2,2'-Azino-bis(3-ethylbenzothiazoline-6-sulfonic acid) diammonium salt
ACN	Acetonitrile
Ang-II	Angiotensin II
APS	Ammonium persulfate
ARE	Antioxidant-response element
AUC	Area under the curve
AT_1-R	Angiotensin II type I receptor
BME	β-Mercaptoethanol
$CaCl_2$	Calcium chloride
cGMP	Cyclic guanosine monophosphate
$CHCl_3$	Chloroform
CID	Collision-induced dissociation
Dha	Docosahexaenoic acid
DMEM	Dulbecco's modified eagle medium
dMPC	1,2-dimyristoyl-*sn*-glycero-3-phosphocholine
dMPE	1,2-dimyristoyl-*sn*-glycero-3-phosphoethanolamine
DMSO	Dimethyl sulfoxide
DNA	Deoxyribonucleic acid
$DPPH^{\bullet}$	2,2-Diphenyl-1-picrylhydrazyl
DTT	Dithiothreitol
ECL	Enhanced chemiluminescence
EGTA	Egtazic acid or Ethylene-bis(oxyethylenenitrilo)tetraacetic acid
ELISA	Enzyme-Linked Immunosorbent Assay
ESI	Electrospray ionization

EVOO	Extra virgin olive oil
FA	Fatty acid
FBS	Fetal bovine serum
GAPDH	Glyceraldehyde-3-phosphate dehydrogenase
GC	Gas chromatography
GFP	Green fluorescent protein
GLPC	1-octadecadienoyl-2-eicosenoyl-*sn*-glycero-3-phosphocholine
GSH	Glutathione
GSNO	Nitrosoglutathione
H_2O	Water
HCl	Hydrogen chloride
HEPES	4-(2-Hydroxyethyl)piperazine-1-ethanesulfonic acid
HILIC	Hydrophilic interaction liquid chromatography
HO-1	Heme oxygenase 1
HPLC	High-performance liquid chromatographic
HRMS	High resolution mass spectrometry
HRP	Horseradish peroxidase
Iac-B	Biotinylated iodoacetamide
Ig	Immunoglobulins
IL	Interleukin
iNOS	Inducible nitric oxide synthase
KCl	Potassium chloride
Keap1	Kelch-like ECH-associated protein 1
KH_2PO_4	Potassium dihydrogen phosphate
KOH	Potassium hydroxide
LC	Liquid chromatography
LIT	Linear Ion Trap
LNA	Linolenic acid
LPS	Lipopolysaccharide
m/z	mass to charge ratio
MALDI	Matrix assisted laser desorption/ionization
MAPK	Mitogen-activated protein kinase

MCP-1	Monocyte chemoattractant protein-1
MeOH	Methanol
$MgSO_4$	Magnesium sulfate
MPK-1	Mitogen-activated protein kinase phosphatase 1
MRM	Multiple reaction monitoring
MS	Mass spectrometry
MS/MS	Tandem mass spectrometry
MS^n	Multistage tandem mass spectrometry
MTT	3-(4,5-dimethylthiazol-2-yl)-2,5-diphenyl tetrazolium bromide
NaCl	Sodium chloride
NADPH	Nicotinamide adenine dinucleotide phosphate
$NaHCO_3$	Sodium bicarbonate
$NaH_2PO_4.2H_2O$	Sodium dihydrogen phosphate dihydrate
$NaMoO_4.H_2O$	Sodium molibdate
$NaNO_2$	Sodium nitrite
NF-κB	Nuclear factor kappa B
$NO^{\bullet}$	Nitric oxide
NO_2^-	Nitrite
$NO_2^{\bullet}$	Nitrogen dioxide
NO_2^+	Nitronium anion
NO_2-AA	Nitroarachidonato or Nitroarachidonic acid
NO_2BF_4	Nitronium tetrafluoroborate
NO_2-cLA	Conjugated nitrolinoleate or Conjugated nitro linoleic acid
NO_2-DhA	Nitro docosahexaenoic acid
NO_2-FA	Nitro-fatty acids
NO_2-LA	Nitrolinoleate or Nitro linoleic acid
NONOates	Diazeniumdiolates
NO_2-OA	Nitroleate or Nitro oleic acid
(NO_2)O-LA	Nitro-hydroxylinoleate or Nitro hydroxy linoleic acid
NO_2-PL	Nitrated phospholipids
Nrf2	Nuclear factor (erythroid-derived 2)-like 2
O_2	Molecular oxygen

OAc	Acetate
OAPC	1-oleoyl-2-arachidonoyl-*sn*-glycero-3-phosphocholine
$ONOO^-$	Peroxynitrite
ORAC	Oxygen radical absorbance capacity
PAPC	1-palmitoyl-2-arachidonoyl-*sn*-glycero-3-phosphocholine
PAPE	1-palmitoyl-2-arachidonoyl-*sn*-glycero-3-phosphoethanolamine
PAPS	1-palmitoyl-2-arachidonoyl-*sn*-glycero-3-phospho-L-serine
PBS	Phosphate buffer saline
PC	Phosphatidylcholine
PE	Phosphatidylethanolamine
PGHS	Prostaglandin endoperoxide H synthase
PIPES	1,4-piperazinediethanesulfonic acid
PIS	Product ion scanning
PLPC	1-palmitoyl-2-linoleoyl-*sn*-glycero-3-phosphocholine
PLPE	1-palmitoyl-2-linoleoyl-*sn*-glycero-3-phosphoethanolamine
PLPS	1-palmitoyl-2-linoleoyl-*sn*-glycero-3-phospho-L-serine
PPAR	Peroxisome proliferator activated receptor
PPAR-γ	Peroxisome proliferator activated receptor gamma
Pro MMP	Pro metalloproteinases
PS	Phosphatidylserine
POPC	1-palmitoyl-2-oleoyl-*sn*-glycero-3-phosphocholine
POPE	1-palmitoyl-2-oleoyl-*sn*-glycero-3-phosphoethanolamine
POPS	1-palmitoyl-2-oleoyl-*sn*-glycero-3-phospho-L-serine
PTM	Post-translational modifications
PVDF	Polyvinylidene difluoride
Q	Quadrupole
RFP	Red fluorescent protein (DsRed-Express2 protein)
RNS	Reactive nitrogen species
$ROO^\bullet$	Peroxyl radicals
ROS	Reactive oxygen species
RP	Reversed-Phase
RT	Retention time

SDPE	1-octadecanoyl-2-docosahexaenoyl-*sn*-glycero-3-phosphoethanolamine
SDS	Sodium dodecyl sulfate
SDS-PAGE	Sodium dodecyl sulfate-polyacrylamide gel electrophoresis
STZ	Streptozotocin
T1DM	Type 1 diabetes mellitus
TE	Trolox equivalents
TEMED	Tetramethylethylenediamine
TFA	Trifluoroacetic acid
TNF-α	Tumor necrosis factor alpha
TOF	Time-of-flight
Tris	2-Amino-2-(hydroxymethyl)-1,3-propanediol
Tris-HCl	2-Amino-2-(hydroxymethyl)-1,3-propanediol hydrochloride
Trolox	(±) 6-hydroxy-2,5,7,8-tetramethylchromane-2-carboxylic acid
TRP	Transient receptor potential
T-TBS	Tween-Tris Buffer Saline
wt	Wild type

CHAPTER I. INTRODUCTION

General Introduction

Phospholipids (PLs) are the most abundant lipids in mammalian, and are associated with several biological functions, as the main structural components of cellular membranes and lipoproteins, and playing key roles as signaling molecules [1, 2]. Under oxidative stress conditions, PLs can be easily modified due to the reaction with reactive oxygen species (ROS) generating a huge diversity of oxidized products structurally different from the unmodified PL precursors and also with dissimilar properties and functions in biological systems [1, 3]. These modified PL has been described to be either pro- or anti-inflammatory agents playing significant biological roles in the onset, development and progression of pathological conditions, such as cancer, neurodegenerative disease, cardiovascular diseases, diabetes inflammation and related complications [1-4]. But lipids can also be modified by reactive nitrogen species (RNS). Few *in vitro* studies suggested that the reactions of RNS with free fatty acids (FA) may generate a huge diversity of oxidized, nitroxidized, nitrated and/or nitrosated derivatives that have been characterized mostly using mass spectrometry based approaches [5, 6]. Free nitro-fatty acids (NO_2-FA) were already detected in biological samples [7-11] and were reported to play a widely range of signaling actions, especially as anti-inflammatory, anti-hypertensive and as anti-thrombotic agents [12-16]. The electrophilic nature of NO_2-FA facilitate their interaction with key proteins targets leading to the formation of lipid-protein adducts [12, 17, 18] and modulating protein function. Nevertheless, the knowledge of the effects of RNS in phospholipid itself has been scarcely explored. RNS may freely cross membranes, and easily accumulate in this hydrophobic environment, increasing the probability of PLs modifications under nitroxidative or nitrative stress conditions, similarly to which was observed for free FA, and nitrated/nitroxidized PLs may also have key biological properties [6, 11].

I.1. Reactive Nitrogen Species and Nitrative, Nitrosative and/or Nitroxidative Stress

Reactive nitrogen species (RNS) are endogenously produced reactive species that can be formed either by enzymatic and/or non-enzymatic reactions (Figure I.1), often concomitant with ROS, and usually under oxidative stress and inflammation conditions [19-21]. RNS are associated with key regulatory functions playing roles as signaling molecules [22]. There are also several exogenous sources of RNS (or their precursors), such as fruits, vegetables, cured meats, cereals from diet which are rich in the inorganic anions nitrite (NO_2^-) and nitrate (NO_3^-) [23, 24], chemicals and cigarette smoke, polluted air (Figure I.1).

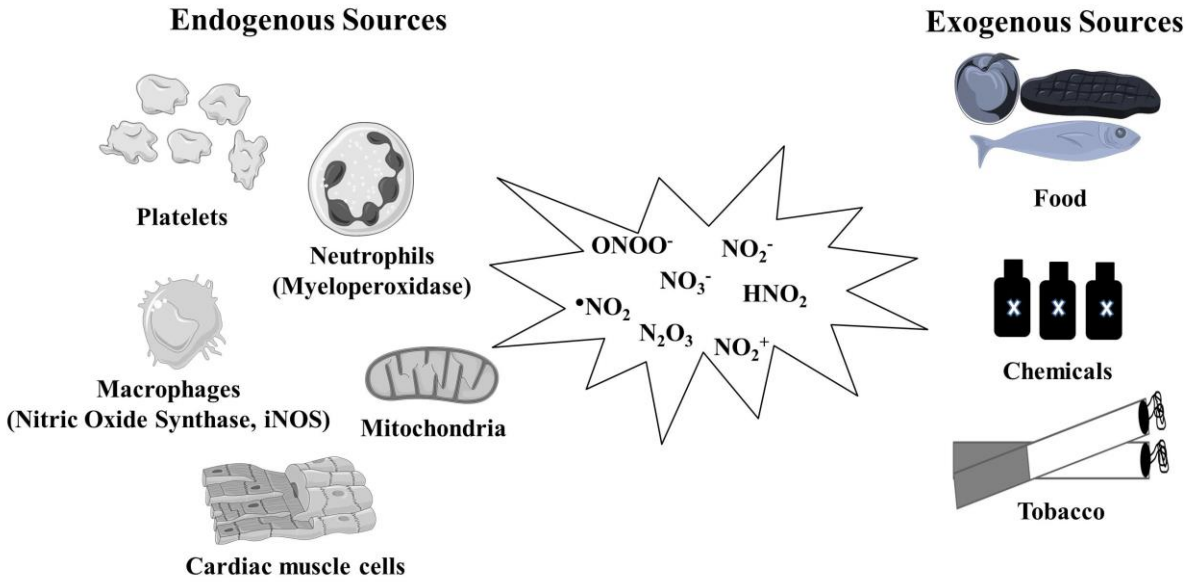

Figure I.1. Endogenous and exogenous sources of reactive nitrogen species (RNS).

RNS enclose different reactive species, with dissimilar structures and reactivity, including radical and non-radicalar species (Table I.1), that can be formed *in vivo*, namely nitric oxide ($NO^{\bullet}$), peroxynitrite ($ONOO^-$) and nitrogen dioxide ($NO_2^{\bullet}$), among others.

Nitric oxide ($NO^{\bullet}$), or nitrogen monoxide, is a small sized free radical molecule and the precursor of the other RNS. $NO^{\bullet}$ is endogenously produced by a wide variety of cells, such as neuronal, endothelial and smooth muscle cells, macrophages, neutrophils, platelets and fibroblasts. It is formed via oxidation of the amino acid L-arginine to $NO^{\bullet}$ and L-citrulline, in a reaction catalyzed by the enzyme nitric oxide synthase (NOS) in a tightly regulated way. There are three NOS isoforms: the neuronal-NOS (nNOS or NOS-I) [25,

26], inducible-NOS (iNOS or NOS-II) [27] and endothelial-NOS (eNOS or NOS-III) [28]. The neuronal and endothelial NOS are expressed constitutively and their activity is calcium-dependent (via activation by calmodulin). nNOS has been localized in the cytosol while eNOS is membrane-bounded [29]. In general, these constitutive isoforms regulate normal physiological functions [30]. The iNOS is also predominantly found in the cytosol and has a calcium-independent activity [29, 30]. iNOS is expressed in response to inflammatory stimuli such as cytokines being usually associated with the immune response [31]. In the lung and kidney, iNOS is constitutively expressed and represents a mechanism of constitutive generation of $NO^{\bullet}$ that is independent of calcium regulation [30].

In spite of being a free radical, nitric oxide has a short life time, is quite stable and thus is not a very reactive molecule [32]. However, it has the ability to react with lipid reactive species such as lipid peroxyl radicals ($LOO^{\bullet}$) to form non-radical end products of lipid peroxidation acting as a chain breaking antioxidant [6, 33]. $NO^{\bullet}$ is a small size, neutral and hydrophobic molecule [34, 35]. Due to these characteristics, $NO^{\bullet}$ cross lipid membrane bilayers, and easily diffuse through the hydrophilic surface into the hydrophobic layer where it is concentrated, triggering both intra and extracellular effects. $NO^{\bullet}$ is an important intracellular signaling messenger, and mediates and regulates multiple physiological processes, such as blood pressure and vascular relaxation, neurotransmission/neuronal communication, signal transduction, platelet aggregation, cell cycle regulation, inflammation, host defense, among others [36]. It has also antioxidant properties related to its chain breaking activity namely during lipid peroxidation [33, 37]. Their physiological effects as signaling molecule or cytoprotective factor are mediated by low concentrations. However, during inflammation and oxidative stress-associated pathologies, there is an excessive production of $NO^{\bullet}$ by key cells of the immune system, promoted by NOS. In fact, upon oxidative and inflammatory conditions where high concentration of $NO^{\bullet}$ and ROS are present, $NO^{\bullet}$ can be converted to more reactive RNS such as peroxynitrite [20, 29], that can further react with target biomolecules [38-40]. Thus, the indirect effects of $NO^{\bullet}$, transduced by these newly-formed RNS species, are also associated with the presence of ROS leading to the occurrence of different types of reactions via nitration, nitrosation and/or nitroxidation causing cell damage. Nitrative stress can be related to the nitration reactions that lead to the covalent addition of a nitro group (NO_2) to biomolecules such as lipids, while the nitrosative stress can be related to

nitrosation and the covalent addition of a nitroso group (NO). However, because of oxidative stress can occurs in simultaneous to nitrative stress and nitration reactions, the nitroxidative stress and nitroxidation reactions refers to both nitration and oxidation processes mediated by RNS [19, 40].

As reported, $NO^{\bullet}$ can be converted into other more reactive RNS. Removal of the unpaired electron from $NO^{\bullet}$ leads to the formation of the oxidized species nitrosonium cation (NO^{+}) that can be reduced by the addition of electrons leading to the formation of the nitroxyl anion (NO^{-}). NO^{-} can interact with $NO^{\bullet}$ yielding dinitrogen monoxide (N_2O) and hydroxyl radical ($^{\bullet}OH$). $NO^{\bullet}$ can react with hydrogen peroxide (H_2O_2) to yield several other RNS which include nitrous acid (HNO_2), dinitrogen trioxide (N_2O_3), NO_2^{-} and NO_3^{-} [41]. Dietary NO_3^{-} can be converted in NO_2^{-} which can also be obtained directly from diet. NO_2^{-} is highly abundant in biological fluids such as saliva.

Table I.1. Reactive nitrogen species grouped in radical and non-radical species.

Reactive Nitrogen Species	
Radical	**Non-radical**
$NO^{\bullet}$ Nitric oxide	$ONOO^{-}$ Peroxynitrite
$NO_2^{\bullet}$ Nitrogen dioxide	O_2NOO^{-} Peroxynitrate
	ONOOH Peroxynitrous acid
	$ONOOCO_2^{-}$ Nitrosoperoxycarbonate anion
	ROONO Alkyl peroxynitrite
	NO^{-} Nitroxyl anion
	NO_2^{-} Nitrite
	NO_3^{-} Nitrate
	NO^{+} Nitrosonium cation
	NO_2^{+} Nitronium cation
	HNO_2 Nitrous acid
	N_2O_3 Dinitrogen trioxide
	N_2O_4 Dinitrogen tetroxide
	N_2O_5 Dinitrogen pentoxide
	NO_2Cl Nitryl chloride
	RO_2ONO Alkyl peroxynitrate

Peroxynitrite ($ONOO^{-}$), a potent oxidant and cytotoxic agent, is the most reactive RNS [41]. $ONOO^{-}$ can be formed through the reaction between $NO^{\bullet}$ and superoxide anion ($O_2^{\bullet-}$) [42], two short-living molecules in biological systems, when both are present in the same cellular compartment. $NO^{\bullet}$ diffuses through the hydrophobic core of biological membranes, where it concentrates and reacts with $O_2^{\bullet-}$. This reaction occurs at the sites spatially associated with the sources of $O_2^{\bullet-}$ due to its restricted ability to diffusion across membranes. $O_2^{\bullet-}$ can be generated from peroxysomal fatty acid metabolism, cytochrome P-450 reactions, NADPH oxidase activity, and from mitochondrial electron transport chain

(complexes I, II and III) that is in fact the cell's most significant source of this ROS [43]. $ONOO^-$ can also be formed from the reaction of NO^- and O_2 [44]. On the other hand, reaction of $ONOO^-$ with transition metals as ferrous ions (Fe^{2+}) yields nitronium cation (NO_2^+). While stable at basic pH, at physiological pH (neutral pH), $ONOO^-$ is unstable undergoing different degradation routes. $ONOO^-$ can decompose directly to generate $NO_2^\bullet$ and NO_3^- or it can be protonated to form peroxynitrous acid (ONOOH) [45, 46]. ONOOH can undergo homolytic decomposition to yield nitrogen dioxide ($NO_2^\bullet$) and $^\bullet OH$ [45, 46]. $ONOO^-$ can also react with carbon dioxide (CO_2) generating nitrosoperoxycarbonate anion ($ONOOCO_2$), which may yields $NO_2^\bullet$ and carbonate ($CO_3^{\bullet-}$) by homolysis or NO_3^- and CO_2 [47]. Thus, CO_2 plays a role in the decomposition of $ONOO^-$ to $NO_2^\bullet$. $NO_2^\bullet$ can also be formed from the $NO^\bullet$ autoxidation.

As hydrophobic molecules, $NO^\bullet$ and molecular oxygen (O_2) can concentrate and diffuse in hydrophobic membrane, at similar extent favoring their mutual interaction and reaction. Thus, lipid membrane bilayers are the primary site for $NO^\bullet$ oxidation reactions to take place and be accelerated *in vivo* [48]. In fact, it was already demonstrated that $NO^\bullet$ oxidation to $NO_2^\bullet$ in aqueous solutions is greatly accelerated by phospholipids [48]. $NO_2^\bullet$ can also be generated from NO_2^- since, at acidic pH, the latter RNS species can form HNO_2. The low pH found in gastric compartment and phagocytic lysosomes allows NO_2^- to generate $NO_2^\bullet$ via HNO_2 generation. Dimerization of $NO_2^\bullet$ yields dinitrogen tetraoxide (N_2O_4) that decompose to produce NO_2^- and NO_3^-. $NO_2^\bullet$ can react with $NO^\bullet$ to form dinitrogen trioxide (N_2O_3). Both $NO_2^\bullet$ and N_2O_3 are unstable in aqueous phase. N_2O_3 rapidly hydrolyzes to form NO_2^- in aqueous solutions [38]. This RNS is stabilized in hydrophobic environments in which is a weak/mild oxidant agent but a powerful nitrosating agent. RNS can also be generated through enzymatic reactions. $NO_2^\bullet$ can be generated from reaction between NO_2^- and H_2O_2 catalyzed by peroxidases [49-51] including myeloperoxidase [52, 53] and lactoperoxidase [51, 54]. $NO_2^\bullet$ can also be formed from $ONOO^-$ in a reaction catalyzed by cytochrome P450 [55].

In an attempt to mimic biological reactions, there are some laboratorial procedures that aim to chemically synthesize some of these RNS naturally occurring *in vivo*. For example, $ONOO^-$ can be easily synthesized by mixing sodium nitrite ($NaNO_2$) and H_2O_2 in acidic conditions yielding ONOOH which was further neutralized in the presence of a alkaline solution to form the stabilized $ONOO^-$, as described by Robinson and co-authors [56] and

Beckman and co-authors [57]. This reaction is widely used in research published in scientific literature [6, 8-11, 58]. The decomposition of the NO-generating vasodilator 3-morpholinosydnonimine (SIN-1) also yields $ONOO^-$ continuously from a certain period of time after simultaneous generation and combination of $NO^\bullet$ and $O_2^{\bullet-}$ [5, 57]. Nitronium tetraflouroborate (NO_2BF_4), a salt of NO_2^+ ions [5, 9, 58, 59] and the $NO^\bullet$ donors (diazeniumdiolates or NONOates) has been also used in biomimetic models of nitrative/nitroxidative stress. $NO^\bullet$ can be generated from NONOates due to their ability to spontaneously release $NO^\bullet$ in aqueous media, under physiological conditions. Depending on their structure and pH of the solution, their half-life and consequently the rates of $NO^\bullet$ release are different [60].

The $NO^\bullet$-derived RNS including $ONOO^-$, $NO_2^\bullet$, NO_3^-, NO_2^+, in spite of having different reactivity, can potentially damage all type of biomolecules [19-21]. Peroxynitrite is a powerful nitrating, nitros(yl)aying and oxidizing agent [61, 62] which has been associated to post-translational modifications of biomolecules, such as glutathione (GSH), amino acid residues as cysteine and tyrosine, proteins, deoxyribonucleic acid (DNA), lipids (polyunsaturated fatty acids) and carbohydrates [19-21, 63]. Protein nitration has been widely studied and reported. In fact, the occurrence of protein tyrosine nitration is now a well-established footprint of the reaction of RNS, and nitrotyrosine is a well-known marker of nitroxidative stress [20, 45, 64]. This stable post-translational modification leads to changes in the structure [19] and function of proteins (loss of function or new and different function), and has been associated with the onset and progression of several pathologies [20] as cardiac, vascular and neurodegenerative diseases, autoimmune diseases, aging, asthma, cancer, inflammation, diabetes, and associated complications [20, 38, 46].

RNS can also react with lipids. The major work concerning the modifications induced by RNS to lipids is focused in the study of fatty acid nitration and nitroxidation, namely the generation and detection of nitroalkene derivatives of unsaturated FA (or nitro-fatty acids, NO_2-FA) both in *in vivo* samples [7, 9-11, 38, 46, 65-70] and in *in vitro* biomimetic model systems. In the following section we will describe how RNS can modify lipids based on the mechanisms decribed in the literature.

I.2. Nitrated Lipids: Occurrence and Proposed Mechanisms of Formation of Nitrated Fatty Acids

To understand lipid nitration, biomimetic systems using pure standards and chemically synthetized RNS have been used by several authors. Major work used FA and few RNS such as nitrite in acidic conditions [8-10, 71, 72], peroxynitrite and $NO_2^{\bullet}$ [5, 6, 11, 58]. These simplistic approaches aiming to mimic the biological conditions have the advantage of decreasing the complexity of the sample (in comparison with the more complex biological matrices such as urine or plasma) and produce an array of different nitrated/nitroxidized products in relatively high yields making easier to develop analytical strategies for their identification and characterization. These models can also contribute to the knowledge and understanding of the mechanism underlying nitroxidation, nitration and/or nitrosation processes and the type of modifications that can occurs in biological systems.

Among the modifications of FA induced by RNS, the nitroalkene derivatives of unsaturated fatty acids (nitro-fatty acids, NO_2-FA) are the most reported products of lipid modifications generated under (patho)physiological conditions associated with nitrative/nitroxidative stress, where oxidative stress and overproduction of $NO^{\bullet}$ occurs simultaneously, such as metabolic stress and inflammation [15, 73, 74].

NO_2-FA have been identified *in vivo*, in samples such as human red blood cells [7, 75], plasma [7, 9, 69, 75], urine, and in normal and inflamed mammalian tissues, including liver, kidney, muscle, adipose tissue [10, 11, 65-70] at concentrations ranging from the micromolar [11] to picomolar [69]. Nitro-fatty acids were already identified in cardiac tissue following ischemia/reperfusion [76] and ischemia preconditioning [77], oxidative stress and hypoxia [78]. More recently, a study of Fazzari and colleagues [23] reported the presence of NO_2-FAs in plants, specifically in fresh olives, and in extra virgin olive oil (EVOO). Moreover, olive oil and fish are rich in unsaturated fatty acids (namely, oleic and linoleic acids) while fruits, vegetables and cured meat are rich in inorganic anions nitrite and nitrate [23, 24]. The acidic and low oxygen conditions in the stomach provide the proper environment for the efficient nitration of unsaturated fatty acids by nitrite [79], which became protonated to yield a diversity of reactive intermediaries [80]. In fact, nitro-fatty acids were identified as major products of the acid-catalyzed reactions in gastric

compartment [81] and also from EVOO under acidic conditions which mimic the gastric pH and NO_2^- concentrations that occur during digestion [23]. Thus, dietary sources may also contribute to increase the endogenous presence of NO_2-FA [82]. The consumption of diets promoting increased NO_2-FA levels has recently been proposed to account for a significant element of the health benefits linked with Mediterranean diet. In this way, generation of nitrated fatty acids can occurs through acid-catalyzed unsaturated fatty acid nitration by dietary nitrite coming from vegetables and cured meats during digestion and/or free radical-mediated fatty acid nitration reactions during digestion, metabolic stress and inflammatory conditions (Figure I.2).

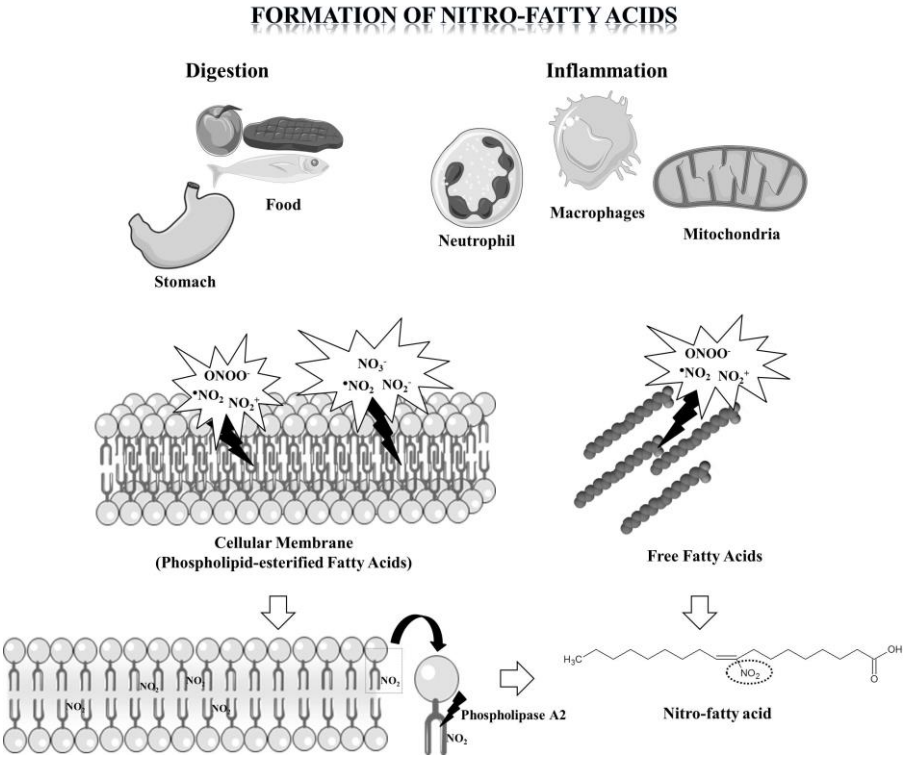

Figure I.2. Formation of NO_2-FA mediated by reactive nitrogen species occurs during digestion and inflammatory conditions.

From the nitroalkene FA derivatives, the nitroalkene derivative of oleic acid (nitro-oleic acid, NO_2-OA) is considered the most predominant derivative *in vivo* [7, 11] and two possible isomers can be formed depending on the position of the nitro group on the fatty acyl chain, namely in C9 (9-NO_2-OA) and C10 (10-NO_2-OA, Figure I.3). These isomers were detected in red blood cells and plasma [11], and in *in vitro* models [5, 83]. Nitroalkene derivatives of other fatty acids have been reported namely nitro-linoleic acid

(NO_2-LA), conjugated nitro linoleic acid (NO_2-cLA), and nitroarachidonic acid (NO_2-AA) [12, 16]. Specific isomers of NO_2-LA, namely C10 (10-NO_2-LA) and C12 (12-NO_2-LA) isomers, were detected and characterized in red blood cells and plasma [7]. These two isomers, together with C9 (9-NO_2-LA) and C13 (13-NO_2-LA) were also detected under *in vitro* experiments [5, 83, 84]. The synthesis and characterization of the C9 (9-NO_2-AA), C12 (12-NO_2-AA), C14 (14-NO_2-AA) and C15 (15-NO_2-AA) isomers of NO_2-AA were reported by Trostchansky and co-authors [10]. These four isomers plus the 11-NO_2-AA were also identified by Milic and co-authors [5]. They also identified and characterized the isomers of nitro-docosahexaenoic acid (NO_2-Dha), namely C10, C11, C13, C14, C16, C17, C19 and C20 isomers. The C9 (9-NO_2-cLA) and C12 (12-NO_2-cLA) isomers of NO_2-cLA were identified after *in vitro* nitration of cLA [72].

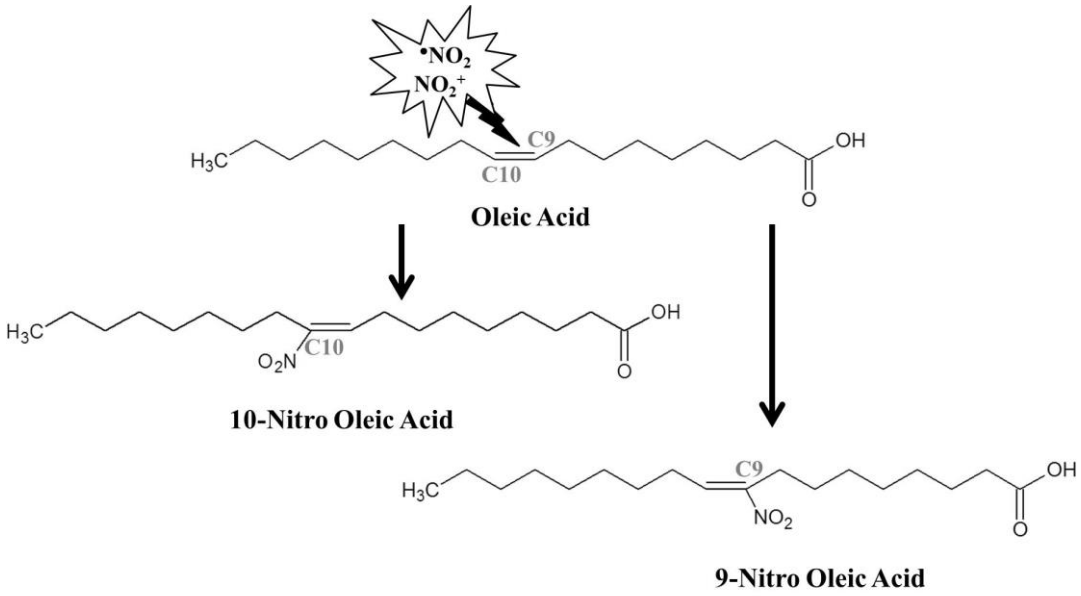

Figure I.3. Structure of oleic acid and its two nitroalkene isomers: the 9-nitro-oleic acid and the 10-nitro-oleic acid isomers.

In addition to the NO_2-FA, a wide spectrum of products can be generated from reaction of unsaturated fatty acids with RNS, including also different stereo- or positional isomers [7, 11]. Nitroso derivatives (NO-FA), multiply nitrated derivatives such as dinitroso ($(NO)_2$-FA), di- ($(NO_2)_2$-FA) and trinitro derivatives ($(NO_2)_3$-FA), and assorted nitroxidized products (nitrohydroxy ((NO_2)O-FA), nitro-hydroperoxy ((NO_2)2O-FA), nitro-epoxy, nitro-keto) has been detected and reported for both *in vivo* (cardiac tissue,

human blood and urine) and *in vitro* studies [6-8, 11, 13, 58, 59, 65, 78, 80, 85-88]. Non-nitrated geometrical *trans* isomers are considered byproducts of nitration reaction, formed due to elimination of nitro (NO_2) moiety from *cis* NO_2-FA, which decay and originates the *trans* double bond [89, 90]. The huge diversity of products is increased also due to the possibility of NO_2-FA to undergo β-oxidation, saturation and desaturation [78, 91].

The formation of nitrated and/or nitroxidized derivatives of unsaturated fatty acids is dependent of the concentration of reactive species (RNS and ROS), of the target species, secondary target molecules (scavengers, transition metals and thiols) and oxygen, pH, and of the partition between hydrophilic and hydrophobic environment in cellular compartments [15]. In membrane hydrophobic environments (and organic solvents in model systems), where RNS are soluble and can accumulate thus reaching higher concentrations, the lipid nitration products prevail. Otherwise, in aqueous milieu, where ROS prevail, the lipid peroxidation products predominate.

Different pathways have been considered to explain the mechanism of fatty acid nitration and nitroxidation (Figure I.4). Formation of NO_2-FA can occur through free-radical-induced nitration mediated by $NO_2^{\bullet}$ [80, 86]. Nitration mediated by $NO_2^{\bullet}$ involves a homolytic attack to the double bond of unsaturated fatty acids (or lipid radicals previously formed) yielding a β-nitro-alkyl radical (Figure I.4, step 1) that, at low oxygen concentrations, reacts with other molecule of $NO_2^{\bullet}$ to form nitro-nitrite or dinitro intermediates (Figure I.4, step 2). The loss of nitrous acid (HNO_2) from this intermediate leads to the formation of nitroalkenes (vinyl nitro) derivatives (Figure I.4, step 3), while its hydrolysis yields nitro-alcohol (nitrohydroxy) derivatives (Figure I.4, step 4). An alternative pathway may involve the abstraction of hydrogen atom from the bis-allylic carbon of β-nitro-alkyl radical by other $NO_2^{\bullet}$ leading to the formation of nitro-allyl derivatives in which both the position and the configuration of the double bond is changed (Figure I.4, step 5). Nitration by a free radical mechanism might suggest that all the double bonds would be susceptible to nitration, with additional double bond rearrangement and conjugation. Nitroalkene formation can also be achieved by nucleophilic reactions such as the electrophilic addition of nitronium cation (NO_2^+) at the double bond (Figure I.4, step 6) [58, 78, 92]. In this case, no rearrangement of double bond was observed [58]. According to the mechanism of nitration and depending on the RNS involved, different species can be formed. Addition reactions leads to formation of electrophilic products (also called

conjugated nitroalkenes, α,β-unsaturated nitroalkenes or vinyl nitro groups) while the hydrogen abstraction leads to non-electrophilic products (non-conjugated nitroalkenes, allylic nitro groups, nitroalkane alkene).

It is important to refer that $NO_2^{\bullet}$ can mediate oxidation, nitration, nitrosation and/or nitroxidation of unsaturated fatty acids. The yields of each process depends on the O_2 levels, because at low oxygen concentrations the formation of nitro derivatives will be favored, while under aerobic conditions lipid oxidation processes will predominate yielding hydroperoxides or *trans*-isomerized lipids derivatives [86, 88, 92]. At high O_2 concentrations, $NO_2^{\bullet}$ can generate a lipid carbon-centered radical (Figure I.4, step 7), which can react with O_2 to form lipid hydroperoxydes (Figure I.4, step 8), or can also produce β-nitro-alkyl radical (Figure I.4, step 9), which may lose HNO_2 and regenerate the unsaturated fatty acid, with formation of a *trans* configuration of the double bond (Figure I.4, step 10). Generation of trans isomers is a process that is usually mediated by $NO_2^{\bullet}$ [88] and peroxynitrite [90]. The β-nitro-alkyl radical can react with O_2 to form β-nitro-peroxyl radical whose rearrangement leads to the generation of nitrohydroxy derivatives after reduction; nitro-keto derivatives after loss of water; nitro-epoxy derivatives after deoxydation; nitroalkene (vinyl nitro) derivatives after elimination of O_2. Rotation around the C-C bond and elimination of O_2 and $NO_2^{\bullet}$ from β-nitro-peroxyl radical generated the *trans* derivative due to the isomerization of the double bond [88].

$NO_2^{\bullet}$, as well as $NO^{\bullet}$, can react with lipid radicals derived from peroxidation of unsaturated fatty acids such as lipid peroxyl radicals in hydrophobic milieu of membranes to terminate the radical chain propagation reactions. This can also lead to the formation of nitrated and nitroxidized products [33].

An additional biologically relevant mechanism for lipid nitroxidative modifications can arise from $ONOO^-$-derived reactions which may involve both radical ($NO_2^{\bullet}$) and electrophilic (NO_2^+) species as described above [73] or by $ONOO^-$ direct attack to the olefinic group of unsaturated fatty acids [93].

A diversity of nitrated and nitroxidized derivatives can be generated by reaction of unsaturated fatty acids and RNS. The formation of these new products has been associated with several biological activities as we will describe in the following section.

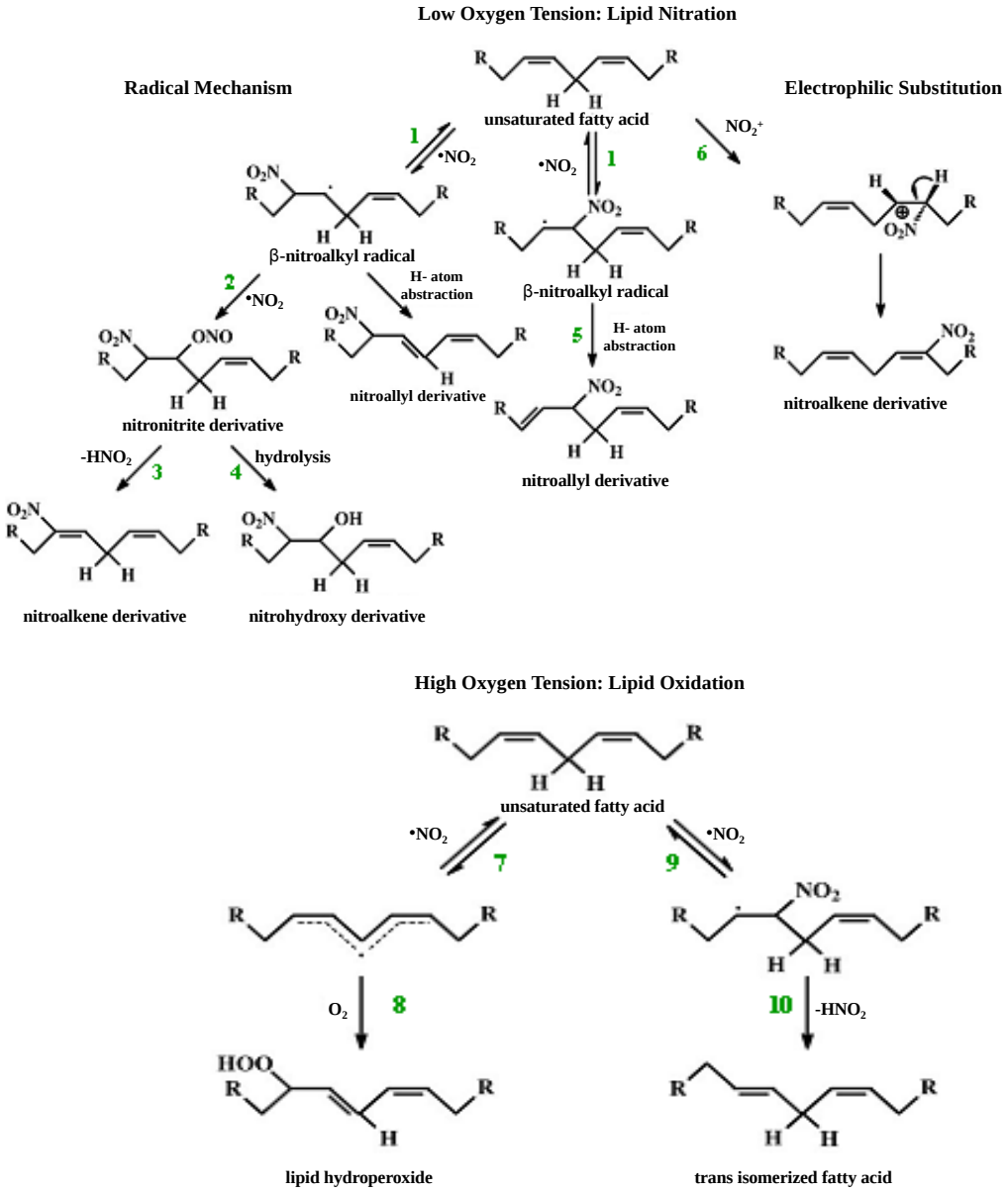

Figure I.4. Mechanism proposed for the formation of nitro-fatty acids (adapted from [73]).

I.3. Biological Properties of Nitrated Fatty Acids

Nitro-fatty acids have been recognized, in the last decade, as new signaling molecules being key mediators in physiological and pathophysiological processes [11, 13, 94]. The concentrations of NO_2-FA in biological samples range from the micromolar [11] to the picomolar range [69]. In spite of being present in very low concentrations, they have been reported to be high enough to mediate their potent biological signaling actions. Moreover, the levels of NO_2-FAs are increased under some metabolic and inflammatory situations

[71, 76, 77, 95]. Contrary to the initially believed, evidence is emerging that NO_2-FA play important biological role as anti-inflammatory [11, 13, 15, 70, 78, 91, 94, 96-108], anti-hypertensive agents [8, 65, 66, 73, 96, 97, 109, 110], and as inhibitors of platelet aggregation – anti-thrombotic properties [8, 111], rather than having pro-inflammatory potential. Their pleiotropic activities includes the modulation of platelet and macrophage activation [10, 99], inhibition of pro-inflammatory cytokine secretion [13, 94], prevention of leukocyte and platelet activation [99, 111], promotion of blood vessel relaxation, acting as mediators in $NO^{\bullet}$ signaling pathways [65, 109] and metabolism, among others. This complex array of signaling actions are mediated through different interdependent mechanisms including a) NO_2-FA decay reactions and transduction of $NO^{\bullet}$ signaling actions [7, 112], b) electrophilic reactions with cellular nucleophiles, namely proteins, inducing post-translational modifications in their structure, function, and localization (subcellular distribution) [18]; c) receptor-dependent mediated signaling roles.

NO_2-FAs can spontaneously decay to generate $NO^{\bullet}$ in aqueous environments acting as $NO^{\bullet}$ donors [109, 112, 113] and transducing the cell signaling actions usually mediate by $NO^{\bullet}$. This can explain the ability of NO_2-FA to mediate cyclic guanosine monophosphate (cGMP)-dependent cell signaling responses [112]. In this way, NO_2-FAs are both products of oxidative reactions between unsaturated fatty acids and $NO^{\bullet}$ and $NO^{\bullet}$-derived species, and mediators of signaling reactions [6, 99, 111] representing the convergence of lipid and $NO^{\bullet}$ signaling actions. One of the biological actions associated to $NO^{\bullet}$ is the ability to inhibit lipid peroxidation processes [33, 37] hindering the propagation reactions by chain breaking activity [33, 114]. $NO^{\bullet}$ released by nitroalkenes was thought to play an antioxidant and protective role on lipid oxidation in membranes and lipoproteins. Besides, the capacity to release $NO^{\bullet}$ has been also related to the vasorelaxation properties of NO_2-FA. NO_2-AA and nitroxydroxy-AA ((NO_2)O-AA) were described to have the ability to release $NO^{\bullet}$ and induce cGMP-dependent vasorelaxation in rat aortic ring in an endothelium-independent manner [8, 10, 65]. Also, NO_2-LA, conjugated nitro linoleic acid (NO_2-cLA) and (NO_2)O-LA promoted vessel relaxation via cGMP-dependent and endothelial-independent manner in preconstricted rat aortic rings [97, 109]. However, the exact mechanism by which NO_2-FAs can decay to release $NO^{\bullet}$ is controversial and remains unknown. Nevertheless, it is known that $NO^{\bullet}$ decay from NO_2-FA is regulated via hydrophobic reactions, since their organization in micelles and liposomes or incorporation

into lipoproteins and lipid membranes protects and stabilizes NO_2-FA, thus inhibiting $NO^\bullet$ release within the lipophilic milieus [112]. This suggests that NO_2-FAs are hydrophobically-stabilized $NO^\bullet$ reservoirs [112]. In fact, NO_2-FA decay has been reported to be faster in phosphate buffer, and probably in cytoplasm of cells, than in hydrophobic organic solvent [11, 109, 112]. In this way, $NO^\bullet$ is most probably released from NO_2-FAs that are free in the circulation. In spite of the ability of NO_2-FA to release $NO^\bullet$ has been demonstrated, only low yields of $NO^\bullet$ have been detected under aqueous conditions, thus NO_2-FAs signaling actions and antioxidant effects via $NO^\bullet$ release mechanism are considered to be of minor significance *in vivo* [10, 96, 109, 112, 115], at the endogenous concentrations.

Nitro-fatty acids were detected in human plasma, urine and tissues and in rodent models as free, esterified and as reversible nucleophilic-adducted species [71]. In fact, the predominant molecular mechanism associated to NO_2-FA biological signaling actions is based on their electrophilic nature. NO_2-FAs interact with key target proteins inducing post-translational modifications that alter protein function and modulate the patterns of gene expression programs, enzymatic activities, metabolic and inflammatory responses, and signaling network activities. The olefinic nitro group added to the double bond of the hydrocarbon chain leads to an alkenyl nitro-configuration that makes NO_2-FA powerful electrophilic species. The conjugation of a strongest electron-withdrawing NO_2 group with a carbon-carbon double bond of an alkene makes the β-carbon adjacent to the NO_2 group electron poor and with potential reactivity. The highly electrophilic properties of the nitroalkene β-carbon leads to post-translational modification of proteins because enable the occurrence of Michael addition reactions with nucleophiles groups of amino acids, such as deprotonated thiolate anions of cysteine (S-nitroalkylation) and imidazole moiety of histidine, in proteins via kinetically rapid and reversible cross linking adduction (Figure I.5) [12, 17, 18, 84, 94, 116]. These post-translational protein modifications can cause modulation of protein structure, function and (subcellular) distribution. Addition of a fatty acid moiety to protein can significantly influence their catalytic activity and hydrophobicity, and represent a new pathway for redox regulation of enzyme function, cell signaling, and protein trafficking [14, 18, 91]. NO_2FA-protein covalent adducts are reversible since β-mercaptoethanol (BME) is able to displace NO_2-FA [91, 117]. Hence, NO_2-FA can mediate signaling actions via covalent, reversible post-translational

modifications of target proteins. The reversible nature of these adducts seems to be related with a lack of toxicity [118], because irreversible post-translational modifications usually leads to protein damage and permanent loss of function, and raises the possibility of regulation. This reversible cross-linking adduction also inhibits NO_2-FA decay and $NO^{\bullet}$ release, thus manifesting signaling actions via cGMP-independent mechanisms [18]. The electrophilic nature of NO_2-FA is also related with the occurrence of nitrohydroxy derivatives [11, 94] which suggests the addition of hydroxide anion present in aqueous medium at physiological pH onto the double bond.

Examples of molecular targets for NO_2-FA electrophilic reactivity include small molecules as glutathione (GSH) [17, 18] to large regulatory proteins including transcription factors and enzymes. NO_2-FA were described to covalently bind to cysteine 38 (Cys38) of p65 subunit of nuclear factor κB (NF-κB) leading to inhibition of its activation controlling the pro-inflammatory process [13, 76]. Nitroalkylation of p65-Cys38 inhibits NF-κB activation and translocation to the nucleus inhibiting the DNA-binding activity and repression of NF-κB-dependent target pro-inflammatory gene expression leading to inhibition of secretion of pro-inflammatory cytokines (e.g., IL-6, TNF-α, and MCP-1) [13, 108]. NO_2-FAs are also irreversible inhibitors of xanthine oxidoreductase activity [117]. NO_2-FA stimulates the expression of heme oxygenase-1 (HO-1) leading to activation of endogenous cytoprotective pathway exerting antioxidant and anti-inflammatory actions [70, 98, 104, 105, 107, 119]. NO_2-FA induces mitogen-activated protein kinase (MAPK) phosphatase 1 (MPK-1) expression and activity leading to the inactivation and suppression of pro-inflammatory signal transducer and activator of transcription (STAT-1) [108] thus having an anti-atherosclerotic effects [120]. MKP-1 limits pro-inflammatory STAT-1 activity by reducing its phosphorylation. NO_2-FA interacts with Cys273 and Cys288 in Kelch-like ECH-associated protein 1 (Keap1) [105, 107, 121, 122]. Nuclear factor (erythroid-derived 2)-like 2 (Nrf2) is a transcription factor that is in its inactive form in cytoplasm due to being binding to Keap1. Activation of Nrf2 by nitroalkylation of Keap 1 leads to its migration to the nucleus where it binds to antioxidant-response element (ARE) in DNA activating gene expression, namely expression of antioxidant and phase II detoxifying enzymes. NO_2-FA are also involved in the modulation of peroxidase inhibitor of prostaglandin endoperoxide H synthases 1 and 2 (PGHS)-dependent gene expression [73, 123, 124]. NO_2-FA decreases the formation of

$NO^{\bullet}$ and inhibits the secretion of pro-inflammatory cytokines (IL-1β and TNF-α) during inflammatory processes, by inhibiting iNOS expression at transcriptional level rather than acting on iNOS activity or release of nitric oxide after decay, [10, 13, 71, 107]. NO_2-FA increased the expression of vascular eNOS [98, 125] limiting vasoconstriction and inflammatory cell margination and alleviated vascular injury. NO_2-FA covalently binds to Angiotensin II (Ang-II) type I receptor (AT_1-R) without inhibiting the binding of Ang-II to the receptor [96] leading to reduction of blood pressure and vasoconstriction induced by Ang II, and reduction of inositol-1,4,5-trisphosphate and calcium mobilization because inhibition of AT_1-R by NO_2-FA uncouples downstream effects of G-protein signaling. The human alpha-Synuclein (histidine (His) 50) [126], metalloproteinases (Cys70 for proMMP-7 and Cys100 for proMMP-9) [127], glyceraldehyde-3-phosphate dehydrogenase (GAPDH; Cys 149, Cys153, Cys244, His108, His134, His327) [17, 18] and transient receptor potential (TRP) channels [128-131] are also targets of NO_2-FAs.

NO_2-FA can display their biological signaling roles by receptor-dependent signaling actions and peroxisome proliferator-activated receptor (PPAR) family is one of the main targets, and particularly peroxisome proliferator-activated receptor gamma (PPARγ). PPARγ regulates glucose uptake and homeostasis, lipid metabolism and homeostasis, vascular tone, adipocyte differentiation, and inflammatory signaling being associated with anti-inflammatory actions such as modulation of the expression of several pro-inflammatory cytokines and chemokines. NO_2-FAs are potent endogenous ligands and activators of PPARγ [11, 13, 15, 94, 100, 107, 132-134] via hydrogen bonding interactions and covalent adduction to the Cys285 in the ligand binding domain [132].

Through these mechanisms, NO_2-FA potently control the expression and activity of key proteins regulating inflammation [13], metabolism [18, 117], cell proliferation, and cell differentiation [11, 94]. They modulate metabolic and inflammatory signaling pathways by promoting or inhibiting the expression and/or activity of both anti-inflammatory and pro-inflammatory proteins, heat shock and phase II antioxidant responses. In fact, murine and cell models showed that NO_2-FA limit pathologies linked to diabetes, metabolic syndrome and obesity [133, 135], ischemic episodes (cardiac and renal ischemia/reperfusion injury or ischemic-preconditioned hearts) [76, 77, 101, 136-138], cardiovascular disease [96, 99, 104, 111, 120, 123, 139, 140], bacterial LPS [71, 102, 139],

renal inflammation and kidney failure [136, 141-145], pulmonary inflammation [98, 102, 146, 147], chronic inflammatory disorders [100], and neurodegenerative diseases [148].

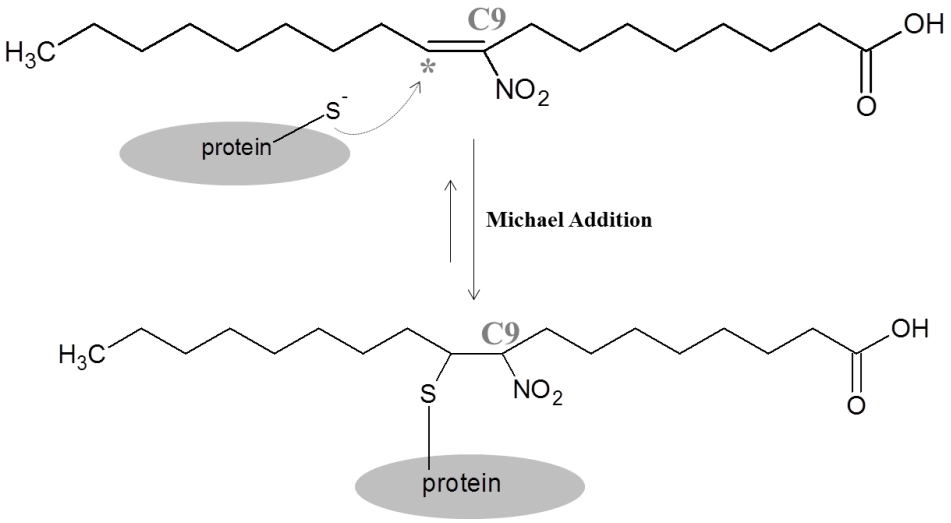

Figure I.5. Electrophilic addition of NO_2-FA to a protein/peptide. Michael addition between the nitro-oleic acid (the C9 isomer) to a cysteine residue of a protein with formation of a nitro-fatty acid-protein adduct.

The formation of NO_2-FA is not likely to be isomer specific and a mixture of different positional isomers can be randomly produced in biological system. However, some of the biological actions of NO_2-FA seem to be specific for a particular isomer. Michael addition reactions between NO_2-FA and peptide/protein seem to be remarkably selective and dependent on the nature and structural features of the electrophilic NO_2-FA. In fact, there is a high level of specificity regarding the structure of NO_2-FA with respect to its ability to modify proteins. NO_2-FA does not act randomly and only specific residues in proteins were identified as target sites for adduction. The position of the electrophilic carbon in relation to the target nucleophile is known to have a critical effect on the net reactivity and extent of formation of lipid-protein adducts [18, 100, 105, 117]. NO_2-LA has four possible isomers with different positions for the addition of the nitro group, namely in C9, C10, C12 and C13. The C9 isomer has been reported to be relatively unstable and rapidly degraded. The C10 and C12 are the species mostly frequently reported. In fact, the NO_2-LA C10 and C12 isomers were identified to selectively bind to PPARγ for its activation [132]. The major mechanism accounting for activation of PPARγ is the covalent adduction of NO_2-FA to Cys285 in the ligand binding domain. However, hydrogen bonds between C10 and C12

isomers and arginine (Arg) 288 and glutamate (glu) 343, respectively, have been suggested for selective and stable activation of PPARγ by NO_2-LA binding. Phenylalanine (Phe) 287 has also important roles for selective and stable activation of PPARγ by NO_2-LA [94, 132]. For NO_2-OA, the C10 isomer is more reactive toward to Cys285 in the ligand binding domain of PPARγ than the C9 isomer [133] while Keap1 is activated more readily by the C9 isomer via nitroalkylation of Cys273 and Cys288 [105, 122]. Xanthine oxidoreductase activity is preferentially inhibited by C9 isomer of NO_2-OA or a mixture of both C9 and C10 isomers [117]. Prostaglandin endoperoxide H synthases 1 and 2 activity and expression are only inhibited by NO_2-AA [123].

The associated covalent and reversible post-translational modifications that regulate protein structure, function and distribution may represent a new process in the redox- and $NO^{\bullet}$-dependent signaling in the resolution of inflammation and other associated complications.

Another important key point is that nitroxidation, nitration and/or nitrosation of fatty acids may occur when they are esterified in phospholipids. However, the signaling actions of NO_2-FA have been only reported for the free forms. This suggests that membrane phospholipid-esterified NO_2-FA need to be hydrolyzed and mobilized by esterases and phospholipase A_2 in order to mediate their actions [88, 112]. However, it is important to keep in mind that NO_2-FA esterified to phospholipid can also be formed and that can have different as well as key signaling actions that needs to be exploited in order to have a better knowledge of their signaling actions. So, future work is needed to identify and understand the chemical modifications induced by nitroxidative or nitrative and/or nitrosative stress to PLs and their biological roles such as their reactivity with key proteins and peptides, and the structural details and roles of the new adducts formed. Furthermore, the development of experimental approaches based on mass spectrometry (MS) and tandem mass spectrometry (MS/MS) strategies for the knowledge of the structural details and fragmentation patterns of NO_2-PL or other nitroxidative derivatives of PL will be crucial for their identification and characterization in biological systems and to unveil their biological roles as lipid signaling molecules in immune/inflammatory responses.

In the following section, we will describe the data published concerning the analysis of RNS-induced modifications in lipids, with focus on the identification and characterization of structural modifications in NO_2-FA using MS-based approaches.

I.4. Methodologies used for Identification and Characterization of Nitrated Fatty Acids

Mass spectrometry (MS) has been one of the mostly used analytical tool for the analysis of nitrated/nitroxidized derivatives of lipids in *in vitro* studies [112], to understand their reactivity, and also for their detection and quantification in biological samples and plants [23]. This analytical tool has high sensitivity, specificity and selectivity which allow to deal with the complexity and diversity of these products.

MS can be used alone or coupled with liquid chromatography (LC). Retention times for analyte separation and elution are based on the distribution and interaction of the components of a mixture with the mobile and stationary phases. Separation of analytes is achieved through adsorption of the analyte to the stationary phase due to the different affinity of the analytes for the mobile and stationary phases. In normal-phase, the non-polar (hydrophobic) components have more affinity to non-polar mobile phase and elute earlier than the polar components, which have higher affinity to the polar stationary phase and are more strongly retained. The retention time increases as the polarity of the mobile phase decreases. In reversed-phase occurs the partition of the hydrophobic components in a hydrophobic stationary phase while the mobile phase consists of polar solvents. Normal phase effectively separates PLs on the basis of class (polar head group) while reversed-phase separates PLs on the basis of their fatty acids residues. Hydrophilic interaction liquid chromatography (HILIC) is a variant of normal phase liquid chromatography. The stationary phase is polar like in normal-phase but the mobile phase has also a lower amount of water being more similar to the ones used in reversed-phase, but HILIC allows separation of lipids based on their polar head structure. Sample components interact with the water-rich layer that is formed in the surface of the polar stationary phase [149]. The coupling of liquid chromatographic separation technique with MS either online or offline can be advantageous in the analysis of complex mixtures, and also provides the separation of isomers, i.e. compounds having the same elemental composition, but with different structures, and thus not differentiable by direct MS. Additionally, LC-MS approaches avoids signal suppression effect caused by the different ionization efficiencies of the analytes present in samples. This effect is extremely important concerning the complex biological matrices like plasma, urine, and tissue, where nitrated/nitroxidized derivatives of lipids are present in low amount.

MS, usually coupled to LC, has been used with success for the identification and quantification of lipids and to elucidate their interaction with cell metabolism and function in biological systems, considering the aims of a lipidomic approach [150, 151]. It has also been used to identify chemical modifications of lipids and to pinpoint specific fragmentations to develop lipidomics targets analysis for the detection of modified lipids. Lipidomics approaches helps in the study of lipid profiles, their alterations in response to different stimulus or situations, and their function in biological systems. Typical study of lipids from biological samples using lipidomics approaches involve several steps starting with lipid extraction from tissues, cells, fluids, and analysis of lipid extracts through MS with or without prior chromatographic separation to obtain the lipid profile. This strategy has also been used for detection, quantification and characterization of nitroalkene and nitroxydroxy derivatives of fatty acids both in biological samples and in *in vitro* biomimetic model systems [5, 7, 9, 11, 23, 65, 75, 81, 91, 119].

Analysis of NO_2-FA by MS or LC-MS is based on the identification of the mass shifts of the products in comparison with the non-modified fatty acids and has been done mostly using the electrospray ionization (ESI) technique. Under ESI-MS conditions, NO_2-FA are usually analyzed in negative-ion mode as deprotonated $[M-H]^-$ ions. However, NO_2-FA can also be identified in positive-ion mode as protonated ions ($[M+H]^+$) [65], and as lithium ($[M+Li]^+$) [10], ammonium ($[M+NH_4]^+$) [75, 152] or sodium ($[M+Na]^+$) [75] adducts that helps in the fragmentation studies. Reversed-phase LC-MS has been applied for analysis of NO_2-FA and nitroxidized derivatives since their polarity is changed due to the presence of the NO_2 group and also oxygen atoms in the case of nitroxidized species. Besides, acidic solvents allow a better chromatographic resolution and isomers separation. Acetonitrile and formic acid have been used and provided good separation of NO_2-FA under reversed-phase LC-MS [153].

With only one MS analysis and identification of molecular ions, we can acquire information on a wide variety of modified products, with different structural features, gathered by the reaction of RNS with lipids, namely fatty acids. Accurate mass measurements achieved in high resolution mass spectrometry (HRMS), made the assignment of elemental composition for the identified ions possible, allowing the confirmation of the molecular formula of the lipid species. However, the confirmation of the structural details for the species identified by MS analysis can be obtained by tandem

mass spectrometry (MS/MS). Several authors reported the typical fragmentation pathways of each nitrated/nitroxidized FA by tandem mass spectrometry, because distinct products are expected to have different fragmentation pathways. Under MS/MS conditions, tandem mass spectrum of NO_2-FAs acquired both in positive- and negative-mode, shows several product ions that allows the structural characterization of these products [5, 7, 10, 59, 83]. The typical fragmentation pattern of NO_2-FA includes the neutral loss HNO_2 (loss of 47 u) which is observed in tandem mass spectra acquired in both ionization modes. The presence of product ions of the charged NO_2^- (*m/z* 46) can be also observed in negative-ion mode [153]. Additionally, MS/MS data of NO_2-FA also shows fragment ions that allow to pinpoint the position of the NO_2 group on the backbone of the lipid (Table I.2) [153]. Cyclization followed by heterolytic carbon chain fragmentation, which generates almost exclusively moieties containing an aldehyde and a nitrosamine, allows the correct identification of positional isomers [83]. Multiply nitrated products, such as dinitro fatty acids, displayed multiple losses of HNO_2 molecules [5]. For the polyunsaturated NO_2-FA, such as NO_2-LA and NO_2-AA, which have a *bis*-allylic interrupted diene and an additional double bond one or two carbons away from the NO_2 moiety already linked to the carbon chain, in addition to the previous fragments, were also observed products ions derived from cyclization reactions that facilitate the formation of 5- or 6-atom heterocycles [83]. Fragmentation pattern obtained after collision-induced dissociation (CID)-MS/MS induced fragmentation of (NO_2)O-FA allows to identify the specific position of NO_2 and hydroxyl groups [11]. These well-defined fragmentation pathways are very helpful for structural characterization of new and unidentified products, for confirmation of the already established products and allow the precise placement of double bonds and sites of nitration, predicting the NO_2 position. This reporter fragmentation can be used to search these modified lipids in biological samples using untargeted and target analysis.

There are several scan experiments useful for target analyses, which are possible by using MS/MS. In product ion scanning (PIS), the most common MS/MS experiment, a precursor ion with a specific *m/z* is selected and isolated in the first mass analyzer; its dissociation is induced in collision cell and then all the resulting masses (product ions) are separated in terms of *m/z* values and scanned in the second mass analyzer, reporting the fragments of a precursor ion. It allows to identify the fragmentation pattern of different nitrated or nitroxidized FA, providing information of their specific fragmentations that can

be further used to perform MS-based target analysis. In multiple reaction monitoring (MRM) scan mode the precursor ion is selected in the first analyzer, fragmented and the second analyzer instead of obtaining a full MS/MS scan with all possible fragments derived from the precursor, only a sequence-specific fragment ion is analyzed. MRM is applied for MS-based target analysis for scanning of specific transitions allowing to perform target detection and quantification of a particular nitrated or nitroxidized FA.

Therefore, analysis of NO_2-FA can be performed by MS alone or coupled to LC, or with MRM scan mode for target analysis. MS/MS analysis in negative ion-mode, without LC separation or MRM scan mode, was used for direct characterization of NO_2-LA derivative, synthetized *in vitro*, based on the presence of fragments formed due to the typical neutral loss of HNO_2 [84]. RP-LC-MS/MS was also applied for the identification of cLA nitrated products generated after *in vitro* nitration with NO_2^- under acidic conditions. Based on specific fragmentation, authors confirmed that only C9 and C12 isomers were generated [72]. This methodology was also applied in the identification and characterization of *in vitro* synthetized NO_2-LA [97].

RP-LC-MS and MS/MS analysis using MRM scan mode using specific transitions, namely the neutral loss of HNO_2 (47 u), has been widely used for identification, separation, characterization and quantification of nitrated and nitroxidized derivatives of unsaturated FAs. Through this RP-LC-MS-based approaches, nitrated and nitroxidized fatty acids were already identified and characterized in *in vitro* biomimetic models [5, 7, 9, 10, 71, 75, 81, 88] to be applied in their identification in biological samples such as plasma samples of healthy and hypercholesterolemic patients (NO_2-LA and (NO_2)O-LA) [9], in human red cells (positional isomers 10-NO_2-LA and 12-NO_2-LA) [7] and plasma (positional isomers 10-NO_2-LA and 12-NO_2-LA; 9-NO_2-OA and 10-NO_2-OA) [7, 69]; in plasma, red blood cells and urine of healthy humans (9-NO_2-OA and 10-NO_2-OA, nitroalkene derivatives of linoleic, linolenic, palmitic and arachidonic acids, and several nitrohydroxy fatty acids, namely 9-(NO_2)O-OA, 10-(NO_2)O-OA, 10-(NO_2)O-LA) [11]; in human plasma and lipoproteins, urine and tissues (NO_2-cLA) [75, 81]; from colon samples and plasma of mice with dextran sulfate sodium (DSS)-induced colitis (NO_2-OA and (NO_2)O-OA) [100]; in rat primary cardiomyocytes ($(NO_2)_2$-OA, NO_2-AA, NO_2-Dha, $(NO_2)_2$-Dha, (NO_2)O-Dha) [5]; in endothelial cells (NO_2-OA) [98]; in activated macrophages (NO_2-cLA) [71]; in rat serum and lung tissue [119].

Table I.2. Main specific fragments ions identified in the MS/MS spectra of NO_2-FA that can be used for pinpoint the position of the NO_2 group on hydrocarbon backbone of the NO_2-FA.

m/z	Ionization mode	Isomer	Specific fragment	Reference
m/z 310	$[M-H]^-$	9-NO-OA	*m/z* 168 ($C_9H_{14}NO_2^-$) *m/z* 182 ($C_{10}H_{16}NO_2^-$)	[5]
		10-NO-OA	*m/z* 157 ($C_8H_{13}O_3^-$) *m/z* 171 ($C_9H_{15}O_3^-$)	
m/z 324	$[M-H]^-$	9-NO_2-LA	*m/z* 168 ($C_9H_{14}NO_2^-$) *m/z* 210 ($C_{11}H_{16}NO_3^-$) *m/z* 224 ($C_{12}H_{18}NO_3^-$)	[5] [83]
		10-NO_2-LA	*m/z* 182 ($C_{10}H_{16}NO_2^-$) *m/z* 224 ($C_{12}H_{18}NO_3^-$) *m/z* 238 ($C_{13}H_{20}NO_3^-$)	[5] [83]
			m/z 168 and 228	[7]
		12-NO_2-LA	*m/z* 157 ($C_8H_{13}O_3^-$) *m/z* 171 ($C_9H_{15}O_3^-$) *m/z* 195 ($C_{11}H_{15}O_3^-$) *m/z* 213 ($C_{11}H_{17}O_4^-$)	[5] [83]
			m/z 196 and 157	[7]
		13-NO_2-LA	*m/z* 171 ($C_9H_{15}O_3^-$) *m/z* 185 ($C_{10}H_{17}O_3^-$) *m/z* 209 ($C_{12}H_{17}O_3^-$) *m/z* 227 ($C_{12}H_{19}O_4^-$)	[5] [83]
m/z 326	$[M-H]^-$	9-NO_2-OA	*m/z* 157 ($C_8H_{13}O_3^-$) *m/z* 168 ($C_9H_{14}NO_2^-$)	[5] [69] [83]
		10-NO_2-OA	*m/z* 169 ($C_9H_{12}O_3^-$) *m/z* 198 ($C_{10}H_{16}NO_2^-$)	
m/z 340	$[M-H]^-$	10,9-(NO_2)O-LNA	*m/z* 171 ($C_9H_{15}O_3^-$)	[11]
		9,10-(NO_2)O-LNA	*m/z* 202 ($C_9H_{16}NO_4^-$)	
		13,12-(NO_2)O-LNA	*m/z* 211 ($C_{12}H_{19}O_3^-$)	
		12,13-(NO_2)O-LNA	*m/z* 242 ($C_{12}H_{20}NO_4^-$)	
		15,14-(NO_2)O-LNA	*m/z* 251 ($C_{15}H_{23}O_3^-$)	
m/z 342*	$[M-H]^-$	10,9-(NO_2)O-LA	*m/z* 171 ($C_9H_{15}O_3^-$)	
m/z 342	$[M-H]^-$	9-oxo-10-NO_2-OA	*m/z* 169	[88]
		10-oxo-9-NO_2-OA	*m/z* 202	[88]
m/z 342	$[M-H]^-$	9,10-(NO_2)O-OA	*m/z* 202 ($C_9H_{16}NO_4^-$)	[5]
		10,9-(NO_2)O-OA	*m/z* 157 ($C_8H_{13}O_3^-$) *m/z* 171 ($C_9H_{15}O_3^-$)	
m/z 344*	$[M-H]^-$	9,10-(NO_2)O-OA	*m/z* 202 ($C_9H_{16}NO_4^-$)	[88] [11]
		10,9-(NO_2)O-OA	*m/z* 171 ($C_9H_{15}O_3^-$)	[88] [11]

*with saturation of the double bond

Table I.2. Main specific fragments ions identified in the MS/MS spectra of NO_2-FA that can be used for pinpoint the position of the NO_2 group on hydrocarbon backbone of the NO_2-FA (continuation).

m/z	Ionization mode	Isomer	Specific fragment	Reference
m/z 371	$[M-H]^-$	$(NO_2)_2$-OA	*m/z* 171 ($C_9H_{15}O_3^-$) *m/z* 202 ($C_9H_{16}NO_4^-$) *m/z* 214 ($C_{10}H_{16}NO_4^-$)	[5]
m/z 356	$[M+Li]^+$	5-NO_2-AA	*m/z* 136	[10]
		6-NO_2-AA	*m/z* 123	
		8-NO_2-AA	*m/z* 176	
		9-NO_2-AA	*m/z* 163	
			m/z 119 ($C_6H_8O_2Li^+$)	[5]
		11-NO_2-AA	*m/z* 216	
			m/z 133 ($C_8H_{10}O_2Li^+$) *m/z* 147 ($C_8H_{10}O_2Li^+$) *m/z* 149 ($C_7H_{10}O_3Li^+$) *m/z* 163 ($C_8H_{12}O_3Li^+$)	[5]
		12-NO_2-AA	*m/z* 203	[10]
			m/z 147 ($C_8H_{10}O_2Li^+$) *m/z* 159 ($C_9H_{12}O_2Li^+$) *m/z* 163 ($C_8H_{12}O_3Li^+$) *m/z* 175 ($C_9H_{12}O_3Li^+$) *m/z* 201 ($C_{11}H_{14}O_3Li^+$)	[5]
		14-NO_2-AA	*m/z* 256	[10]
			m/z 173 ($C_{10}H_{14}O_2Li^+$) *m/z* 187 ($C_{11}H_{14}O_2Li^+$)	[5]
		15-NO_2-AA	*m/z* 243	[10]
			m/z 187 ($C_{11}H_{14}O_2Li^+$) *m/z* 199 ($C_{12}H_{16}O_2Li^+$) *m/z* 215 ($C_{12}H_{16}O_3Li^+$) *m/z* 241 ($C_{14}H_{18}O_3Li^+$)	[5]
m/z 366	$[M-H]^-$	5,6-(NO_2)O-AA	*m/z* 146 ($C_5H_8NO_4^-$)	[65]
		6,5-(NO_2)O-AA	*m/z* 115 ($C_5H_7O_3^-$)	
		8,9-(NO_2)O-AA	*m/z* 186 ($C_8H_{12}NO_4^-$)	
		9,8-(NO_2)O-AA	*m/z* 155 ($C_8H_{11}O_3^-$)	
		11,12-(NO_2)O-AA	*m/z* 226 ($C_{11}H_{16}NO_4^-$)	
		12,11-(NO_2)O-AA	*m/z* 195 ($C_{11}H_{15}O_3^-$)	
		14,15-(NO_2)O-AA	*m/z* 266 ($C_{14}H_{20}NO_4^-$)	
		15,14-(NO_2)O-AA	*m/z* 235 ($C_{14}H_{19}O_3^-$)	

Table I.2. Main specific fragments ions identified in the MS/MS spectra of NO_2-FA that can be used for pinpoint the position of the NO_2 group on hydrocarbon backbone of the NO_2-FA (continuation).

m/z	Ionization mode	Isomer	Specific fragment	Reference
m/z 380	$[M+Li]^+$	10-NO_2-Dha	*m/z* 135 ($C_6H_8O_3Li^+$) *m/z* 149 ($C_7H_{10}O_3Li^+$)	[5]
		11-NO_2-Dha	*m/z* 149 ($C_7H_{10}O_3Li^+$) *m/z* 161 ($C_8H_{10}O_3Li^+$)	
		13-NO_2-Dha	*m/z* 175 ($C_9H_{12}O_3Li^+$) *m/z* 189 ($C_{10}H_{14}O_3Li^+$)	
		14-NO_2-Dha	*m/z* 189 ($C_{10}H_{14}O_3Li^+$) *m/z* 201 ($C_{11}H_{14}O_3Li^+$)	
		16-NO_2-Dha	*m/z* 215 ($C_{12}H_{16}O_3Li^+$) *m/z* 229 ($C_{13}H_{18}O_3Li^+$)	
		17-NO_2-Dha	*m/z* 229 ($C_{13}H_{18}O_3Li^+$) *m/z* 241 ($C_{14}H_{18}O_3Li^+$)	
		19-NO_2-Dha	*m/z* 255 ($C_{15}H_{20}O_3Li^+$) *m/z* 269 ($C_{16}H_{22}O_3Li^+$)	
		20-NO_2-Dha	*m/z* 269 ($C_{16}H_{22}O_3Li^+$) *m/z* 281 ($C_{17}H_{22}O_3Li^+$)	

Target tandem mass spectrometry analysis using MRM scan in positive ion-mode ($[M+H]^+$ ions), but without LC separation, was used for identification and characterization of 6-methyl-NO_2-AA allowing to pinpoint the NO_2 group to be linked in C6 instead of the usual C9, C12, C14 or C15 carbons of fatty acid [65]. RP-LC-MS/MS using MRM scan mode also allowed to study the nature and metabolism of NO_2-FA in plasma and liver of mice after intravenous injection of NO_2-OA, and allowed the identification of metabolites of β-oxidation, saturation or desaturation of the double bond of NO_2-OA [91]. Through this advanced analytical approach it was also possible to detect the endogenous presence of NO_2-FA, namely NO_2-cLA, in plants specially in olives and EVOO, and the formation of different isomers of NO_2-OA (9- and 10-NO_2-OA), NO_2-LA (9-, 12- and 13-NO_2-LA) and NO_2-cLA (8-, 9-, 11- and 12-NO_2-cLA) from EVOO under *in vitro* conditions that mimic gastric pH and NO_2^- concentrations during digestion [23].

Mass spectrometry coupled to LC has also been used for identification and characterization of reversible post-translational modifications of peptides and proteins by NO_2-FA. LC-ESI-MS and MS/MS was used to detect lipid-protein adducts formed

between NO_2-OA and NO_2-LA and with proteins and GSH *in vivo* in human red cells [18]. This methodology was also applied to confirm the post-translational modifications of matrix metalloproteinase by NO_2-OA [127], and identification of reversible Michael adducts of NO_2-OA and thiols of proteins and GSH in liver and plasma of NO_2-OA-treated mice, which were further confirmed by exchanged of NO_2-OA from proteins to the added BME [91]. LC-MS/MS allowed to define the specific sites of adduction since the typical fragmentation of NO_2-FAs were distinctive, demonstrating the usefulness of the assignment of the fragmentation fingerprints that are fundamental for detecting species in biological environments [127]. Significant levels of protein cysteine adducts of NO_2-OA were also observed in fresh olives, especially in the peel [23]. AT_1-R adducts with NO_2-OA were quantified by HPLC-MS/MS using MRM scan mode in negative-ion mode as BME adducts (BME-NO_2-OA adducts) after nucleophilic exchange of NO_2-OA from AT_1-R to BME. The presence of exchangeable NO_2-OA demonstrated the direct adduction of AT_1-R by NO_2-OA and therefore that AT_1-R is a relevant cellular target for NO_2-OA alkylation [96]. RP-LC-MRM scan in positive-ion mode ($[M+H]^+$ ions) was applied for the characterization of NO_2-LA-GSH adducts *in vitro* and their further identification in MCF7 cells treated with NO_2-LA [84].

One study also reported the direct analysis by MS and MS/MS, in positive-ion mode, of adenine nucleotide translocase 1 (ATN 1) adducts after NO_2-LA infusion into intact perfused heats allowing to pinpoint that the nitroalkylation of ANT1 by NO_2-LA occurred on Cys57 [138].

The effects of RNS in biological systems, namely lipid nitration, are reported to occur mainly in the hydrophobic environment of biological membranes [59] where phospholipids are predominant lipids, rather than free fatty acids, and thus expected to be key target for lipid nitration. The possibility of RNS to modified phospholipid-esterified fatty acids is very plausible but is still not explored and future work is needed to overcome this issue. Having this in mind, the development of sophisticated, robust, sensitive, specific and valid tools and technical approaches using MS to help on deciphering the structure and biologically relevant roles of phospholipid nitration products in the complex cellular network was one of the main aims of this work.

I.5. Aim of the work

The identification and structural characterization of the nitroxidative stress-induced modifications in PLs, and their possible biological roles, are completely uncharted and can be hindered by the diversity, structural complexity and probable lower amount of the derived products.

The aims of this work are to contribute for the understanding of the chemical modifications induced by nitroxidative stress to PLs and for the development of MS-based approaches that will allow their identification and structural characterization. MS-based strategies will be the basis of simple, specific, rapid and sensitive analytical methodologies for the *in vitro* and *in vivo* detection of nitrated/nitroxidized PL products. Nitration/nitroxidation of pure commercial PL standards comprising individual molecular species will be induced in controlled reaction conditions mimicking the ones found in biological systems. The nitrated/nitroxidized products formed will be analyzed by ESI-MS, ESI-MS/MS, LC-ESI-MS and LC-ESI-MS/MS allowing the separation of isomeric species, complemented with other analytical procedures. The MS-based approaches developed with model systems will be applied in the analysis of phospholipids extracts derived from biological samples to screen for the structural modifications and to validate the analytical strategy developed.

We also aim to evaluate the biological roles of nitrated/nitroxidized PLs. Their potential as lipid signaling molecules in immune/inflammatory response will be evaluated in macrophage immune/inflammatory models. The results obtained will be essential to understand their biological roles in diseases associated with oxidative/nitroxidative stress and inflammatory processes. Their antioxidant potential will also be assessed using well-established and reliable assays to determine the antioxidant capacity. The effect of nitrated PL in specific proteins will be also accessed.

All the experimental details are presented in Chapter II of this thesis. The results obtained and their discussion are presented in Chapter III. Results will be grouped in three subchapters, according to the specific aims of the different studies performed:

III.1. Understanding the nitroxidative stress-induced modifications of phospholipids

III.2. Understanding the biological activities of nitrated and nitroxidized derivatives of phospholipids

III.3. Understanding the cross reaction between nitrated and nitroxidized derivatives of phospholipids and proteins

The general concluding remarks are presented in Chapter IV while the references cited in the text are presented in Chapter V. In Appendices A-C are presented the supplementary material.

CHAPTER II. MATERIAL AND METHODS

II.1. Chemicals and Reagents

All chemicals and reagents used in the studies performed during this PhD work and presented in Section III were used without further purification.

II.1.1. Chemicals and reagents purchased from Abcam (Cambridge, UK):

- Primary antibody against inducible Nitric Oxide Synthase (iNOS; rabbit polyclonal anti-iNOS).

II.1.2. Chemicals and reagents purchased from Avanti® Polar Lipids, Inc. (Alabaster, USA):

- 1-Palmitoyl-2-oleoyl-*sn*-glycero-3-phosphocholine (POPC, C16:0/C18:1);
- 1-Palmitoyl-2-oleoyl-*sn*-glycero-3-phosphoethanolamine (POPE, C16:0/C18:1);
- 1-Palmitoyl-2-oleoyl-*sn*-glycero-3-phospho-L-serine (POPS, C16:0/C18:1);
- 1-Palmitoyl-2-linoleoyl-*sn*-glycero-3-phosphocholine (PLPC, C16:0/C18:2);
- 1-Palmitoyl-2-linoleoyl-*sn*-glycero-3-phosphoethanolamine (PLPE, C16:0/C18:2);
- 1-Palmitoyl-2-linoleoyl-*sn*-glycero-3-phospho-L-serine (PLPS, C16:0/C18:2);
- 1-Palmitoyl-2-arachidonoyl-*sn*-glycero-3-phosphocholine (PAPC, C16:0/C20:4);
- 1-Palmitoyl-2-arachidonoyl-*sn*-glycero-3-phosphoethanolamine (PAPE, 16:0/C20:4);
- 1-Palmitoyl-2-arachidonoyl-*sn*-glycero-3-phospho-L-serine (PAPS, C16:0/C20:4).

All phospholipid standards used in this PhD work had a purity of >99% and were used without further purification.

II.1.3. Chemicals and reagents purchased from Bio-Rad (Hercules, USA):

- Acrylamide/bis-acrylamide;
- Ammonium persulfate (APS);
- Precision plus protein™ dual color standard (161-0374).

II.1.4. Chemicals and reagents purchased from Chemicon (Madrid, Spain):

- Mouse monoclonal anti-tubulin antibody.

II.1.5. Chemicals and reagents purchased from Cytoskeleton, Inc (Denver, USA):

- Purified recombinant Syrian hamster vimentin (accession number AH001833).

II.1.6. Chemicals and reagents purchased from Dako (Copenhagen, Denmark):

- Peroxidase-conjugated anti-mouse immunoglobulins.

II.1.7. Chemicals and reagents purchased from Fisher Scientific Ltd. (Leicestershire, UK):

- Absolute ethanol;
- Chloroform (HPLC grade);
- Methanol (HPLC grade).

II.1.8. Chemicals and reagents purchased from Fluka (Buchs, Switzerland):

- 2,2'-Azino-bis(3-ethylbenzothiazoline-6-sulfonic acid) diammonium salt ($ABTS^{\bullet+}$).

II.1.9. Chemicals and reagents purchased from GE Healthcare (Carnaxide, Portugal):

- Alkaline phosphatase-linked anti-rabbit IgG antibody;

II.1.10. Chemicals and reagents purchased from GE Healthcare (Buckinghamshire, UK):

- Enhanced chemiluminiscence reagents;
- Horseradish peroxidase (HRP)-streptavidin.

II.1.11. Chemicals and reagents purchased from Gibco Life Technologies (Paisley, UK):

- Fetal bovine serum (for anti-inflammatory assays; Section II.8);
- Penicillin (for cross adduction with proteins; Section II.9);
- Streptomycin (for cross adduction with proteins; Section II.9);

II.1.12. Chemicals and reagents purchased from Invitrogen (Carlsbad, USA):

- 4,6-diamidino-2-phenylindole;

- Anti-rabbit-Alexa 568;
- Dulbecco's Modified Eagle Medium (DMEM) (for cross adduction with proteins, Section II.9).

II.1.13. Chemicals and reagents purchased from Life Technologies (Carlsbad, USA):

- GlutaMAX.

II.1.14. Chemicals and reagents purchased from Lonza Inc. (Walkersville, USA):

- Fetal bovine serum (FBS; for cross adduction with proteins, Section II.9).

II.1.15. Chemicals and reagents purchased from MatTek Corporation (Ashland, USA):

- Glass bottom dishes.

II.1.16. Chemicals and reagents purchased from Molecular Probes (Oregon, USA):

- Phalloidin-Alexa568

II.1.17. Chemicals and reagents purchased from Santa Cruz Biotechnology (Heidelberg, Germany):

- Anti-vimentin Alexa 488.

II.1.18.Chemicals and reagents purchased from Sigma-Aldrich (St Louis, MO, USA):

- (±) 6-Hydroxy-2,5,7,8-tetramethylchromane-2-carboxylic acid (Trolox);
- 2,2′-Azobis(2-methylpropionamidine) dihydrochloride (AAPH);
- 2,2-Diphenyl-1-picrylhydrazyl (DPPH$^{\bullet}$);
- 3-(4,5-Dimethylthiazol-2-yl)-2,5-diphenyl tetrazolium bromide (MTT);
- Anti-vimentin antibodies
- Biotinylated iodoacetamide (Iac-B)
- Dulbecco's Modified Eagle Medium (DMEM) (for anti-inflammatory assay, Section II.8);
- Fluorescein sodium salt;
- Laemmli Buffer
- Lipopolysaccharide (LPS) from Escherichia coli (serotype 026:B6);

- Nitronium tetrafluoroborate (NO_2BF_4);
- Penicillin (for anti-inflammatory assays; Section II.8);
- Potassium phosphate monobasic;
- Streptomycin (for anti-inflammatory assays; Section II.8);
- TEMED.

Milli-Q water (Synergy®, Millipore Corporation, Billerica, MA, USA) was also used.

II.2. Samples

II.2.1. Phospholipid Standards

II.2.1.1. Phosphatidylcholines

The commercial phosphatidylcholines (PCs) were used as models because PCs are the most abundant phospholipid class present in mammalian cell membranes and plasma lipoproteins. POPC is composed by a saturated fatty acyl chain in the *sn*-1 position (palmitic acid, C16:0) and a monounsaturated fatty acyl chain in the *sn*-2 position (oleic acid, C18:1), which mimics mammalian phosphatidylcholine composition. PLPC and PAPC are composed by a saturated fatty acyl chain in the *sn*-1 position (palmitic acid, C16:0) and a polyunsaturated fatty acyl chain in the *sn*-2 position (linoleic acid, C18:2 for PLPC; arachidonic acid, C20:4 for PAPC).

PCs standards (POPC, PLPC and PAPC) were used in the studies presented in Section III.1.1 and III.1.2. POPC standard was also used in the studies presented in Section III.2.1 and Section III.3.1.

II.2.1.2. Phosphatidylethanolamines

Phosphatidylethanolamines (PEs) commercial standards were used as models, since PE is the second most abundant phospholipid class in mammalian cells. POPE, PLPE and PAPE are composed by a saturated fatty acyl chain in the *sn*-1 position (palmitic acid, C16:0) and unsaturated fatty acyl chain in the *sn*-2 position (oleic acid, C18:1 for POPE; linoleic acid, C18:2 for PLPE; arachidonic acid, C20:4 for PAPE).

PEs standards (POPE, PLPE and PAPE) were used in the studies presented in Section III.1.1 and III.1.2.

II.2.1.3. Phosphatidylserines

The commercial phosphatidylserines (PSs) were chosen as models because PSs are the most abundant negatively charged phospholipid in eukaryotic cells. POPS, PLPS and PAPS are composed by a saturated fatty acyl chain in the *sn*-1 position (palmitic acid, C16:0) and unsaturated fatty acyl chain in the *sn*-2 position (oleic acid, C18:1 for POPS; linoleic acid, C18:2 for PLPS; arachidonic acid, C20:4 for PAPS).

PSs standards (POPS, PLPS and PAPS) were used in the studies presented in Section III.1.1.

II.2.2. Peptides and Proteins Standards

Vimentin was used as model in the studies of Section III.3.1.

II.2.3. Biological Samples for *In Vivo* and *In Vitro* Assays

In order to screen for the structural modification identified by using the phospholipid standard models (see Section II.2.1) in biological samples and to validate the MS and LC-MS-based experimental methodologies developed (see Section II.4 and II.5), we analyzed total lipids extracts from cardiac mitochondria from a well-characterized animal model of type 1 diabetes mellitus (T1DM) obtained by administration of streptozotocin (STZ) and total lipid extracts from cardiomyoblast cell line (H9c2), a suitable model for cardiac cells, with induced starvation and ischemia in order to mimic conditions to which cardiomyocytes are exposed during acute myocardial infarction were analyzed. Cardiac mitochondria were used in the study presented in Section III.1.1 while cardiomyoblast cell line (H9c2) was used in the study presented in Section III.1.2.

In order to evaluate the biological activity of nitrated POPC, namely its anti-inflammatory potential, the mouse leukaemic monocyte-macrophage Raw 264.7 cell line was used in the studies presented in Section III.2.1.

In order to evaluate the ability of nitrated POPC to interact with vimentin and the effects on vimentin network organization, the human adrenal tumor cell line SW13 was used in the studies of Section III.3.1.

II.3. Preparation of Phospholipid Standard Work Solutions and Biological Samples for the Identification and Structural Characterization of Nitrated and Nitroxidized derivatives of Phospholipids

II.3.1. Preparation of Phospholipid Standard Model Solutions and Nitration Reaction

Solutions of each PC, PE and PS (1 mg) were dissolved in 1 mL of chloroform and well-vortexed. Each solution was prepared immediately before nitration reaction using nitronium tetrafluoroborate (NO_2BF_4) as nitrating agent.

Nitration of phospholipid standard solutions was carried out with NO_2BF_4. A solution of each PC, PE or PS (1 mg) was prepared in chloroform (1 mL) in an amber vial tube. Then, an excess of solid NO_2BF_4 (≈ 1 mg) was added. NO_2BF_4 has been previously used as nitrating agent in fatty acid nitration studies and was chosen for mimicking the nitration occurring on biological membranes with peroxynitrite and nitrite [7, 9, 58, 154]. The concentration of NO_2BF_4 used was high allowing to obtain nitrated derivatives of phospholipids in high amount to perform all the mass spectrometry structural characterization studies. The reaction mixture was incubated at room temperature for 1 h, under orbital shaking at 750 rpm. After incubation, the reaction mixture was transferred to a centrifuge glass tube and the reaction was stopped by solvent extraction with Milli-Q water. The water is added to hydrolyze unreacted NO_2BF_4 and to separate water soluble contaminants as anions (*e.g.* nitrite (NO_2^-), nitrate (NO_3^-), and tetrafluoroborate (BF_4^-)) from phospholipids [9, 58, 59]. The mixture was vortex for 30 s and then centrifuged at 2000 rpm for 10 min at room temperature using a Mixtasel Centrifuge (Selecta). The organic layer containing the phospholipid products was collected, evaporated under nitrogen stream, and stored at -20 °C to be further quantified using phosphorous assay [155] (see Section II.3.2.4).

The extent of nitration reaction and formation of nitrated and nitroxidized products were monitored by ESI-MS and MS/MS analysis. The nitrated and nitroxidized products

were subsequently separated and identified by reversed phase liquid chromatography (LC) coupled to ESI-MS (C5-RP-LC-MS), and characterized by LC-MS/MS.

II.3.2. Preparation of Biological Samples

II.3.2.1. Animal Care Protocol, Induction of Hyperglycemia and Isolation of Cardiac Mitochondria

The animal care protocol, the induction and characterization of STZ-induced hyperglycemia and the cardiac mitochondria isolation was performed as previously described [156].

Briefly, Wistar male rats, aged 6–8 weeks, weighing 200 g at the beginning of the experiments were randomly divided into two groups: type 1 diabetic group (T1DM) and control. Housing and experimental treatment were in accordance with Guide for the Care and Use of Laboratory Animals from the Institute for Laboratory Animal Research (ILAR, 1996). The experimental procedures complied with the current national laws. The T1DM group was treated with a single intraperitoneal injection of streptozotocin (STZ; 60 mg/kg), after a 16 h fasting period. Control animals were injected with citrate solution. Animals were considered hyperglycemic when blood glucose exceeded 250 mg/dL, which was verified after 48 h of STZ injection. After 4 weeks of STZ administration, animals were sacrificed followed by thoracotomy with heart extraction. The excised hearts were minced in an ice-cold isolation medium containing 250 mmol/L sucrose, 0.5 mmol/L EGTA, 10 mmol/L HEPES-KOH (pH 7.4), and 0.1% defatted BSA. The minced blood-free tissue was resuspended in isolation medium containing protease subtilopeptidase A type VIII (1 mg/g tissue) and homogenized with tightly fitted Potter–Elvehjen homogenizer and Teflon pestle. The suspension was incubated for 1 min at 4 °C and re-homogenized. The homogenate was centrifuged at 14,500 ×g during 10 min. The supernatant fluid was decanted, and the pellet, essentially devoid of protease, was gently resuspended in isolation medium. The suspension was centrifuged at 750 ×g for 10 min, and the resulting supernatant was centrifuged at 12,000 ×g for 10 min. The pellet was resuspended and repelleted at 12,000 ×g for 10 min. The final pellet, containing the mitochondrial fraction, was resuspended in a washing medium containing 250 mmol/L sucrose, 10 mmol/L HEPES-KOH, pH 7.4.

II.3.2.2. Cell culture of Cardiomyoblast H9c2 cell line

The cardiomyoblast cell line H9c2 (Sigma-Aldrich, St. Louis, MO) was cultured in Dulbecco's Modified Eagle Medium (DMEM), supplemented with 10% fetal bovine serum (FBS), 1% penicillin/streptomycin (100 U/mL: 100 μg/mL) and 1% GlutaMAX, at 37 ºC under 5% CO_2. Metabolic ischemia was induced by a buffer exchange to an ischemia-mimetic solution (118 mmol/L NaCl, 4.7 mmol/L KCl, 1.2 mmol/L KH_2PO_4, 1.2 mmol/L $MgSO_4$, 1.2 mmol/L $CaCl_2$, 25 mmol/L $NaHCO_3$, 5 mmol/L calcium lactate, 20 mmol/L 2-deoxy-D-glucose, 20 mmol/L Na-HEPES, pH 6.6) and by placing the dishes in hypoxic pouches with an indicator (GasPak^{TM} EZ, BD Biosciences) for 2 h. As certified by the manufacturer, the Anaerobe Gas Generating Pouch System produces an atmosphere containing 10% CO_2 and 1% O_2. Starvation was induced by culturing H9c2 cells in DMEM with 1% antibiotics (100 U/ml penicillin, and 100 μg/ml streptomycin), and 1% GlutaMAX, but not supplemented with FBS. The cells were maintained at 37 ºC in a humidified chamber with 5% CO_2.

II.3.2.3. Lipid Extraction of Cardiac Mitochondria and of Cardiomyoblast H9c2 cell line

Lipid extraction of either each mitochondrial fraction and each myoblast H9c2 cell line condition was performed according to the method of Bligh and Dyer [157].

Briefly, 3.75 mL chloroform:methanol 1:2 (v/v) was added to each 1 mL of heart mitochondrial fraction and to the cell pellets previously dissolved in 1 mL of Milli-Q H_2O. Samples were vortexed and incubated on ice for 30 min. An additional volume of 1.25 mL of chloroform and 1.25 mL of H_2O were added followed by vortex for 1 min between each addition. The samples were centrifuged at 1000 rpm for 5 min at room temperature using a Mixtasel Centrifuge (Selecta) to obtain a two-phase system: an aqueous top phase and an organic bottom phase. The lipid extract was recovered from the organic bottom phase. In order to guarantee full extraction of lipid phase, 1.88 mL of chloroform were added to the aqueous phase followed by vortex and new centrifugation. The organic phase was recovered to the same tube as before and dried under a nitrogen stream. After drying, the total lipid extracts were re-suspended in 300 μL of chloroform, transferred to an amber

glass vial. The phospholipid amount in each lipid extract was determined by phosphorous measurement performed according to Bartlett and Lewis [155] with modifications (see Section II.3.2.4). Two different and independent mitochondrial extracts and three different and independent myoblast cultures were extracted and analyzed in order to verify the reproducibility of the results.

II.3.2.4. Phosphorous Measurement – for Phospholipid Quantification

Total amount of PL was quantified with the phosphorus assay as previously described by Bartlett and Lewis [155].

For cardiac mitochondria, 650 µL of concentrated perchloric acid (70% m/v) was added to an aliquot of 10 µL of each sample (cardiac mitochondria lipid extracts were dissolved in 300 µL of $CHCl_3$; the 10 µL of each sample was dried under a nitrogen stream before the addition of perchloric acid). Samples were then incubated for 1 h at 180 °C in the heating block (Stuart, UK). Afterwards, 3.3 mL of H_2O, 500 µL of 1% ammonium molybdate (m/v, 1 g of $NaMoO_4.H_2O$ in 100 mL of Milli-Q H_2O) and 4% ascorbic acid (m/v, 0.4 g in 10 mL of Milli-Q H_2O) were added to all samples. The reaction mixture was homogenized in a vortex mixer after each addition followed by incubation for 10 min at 100 °C in a water bath.

For myoblast H9c2 cell line and for nitrated and nitroxidized products of PLs recovered after extraction (see Section II.3.1), 125 µL of concentrated perchloric acid (70% m/v) was added to an aliquot of 10 µL of each sample (myoblast H9c2 cell lipid extracts were dissolved in 300 µL of $CHCl_3$ while nitrated and nitroxidized products of PLs were dissolved in 1 mL of $CHCl_3$; the 10 µL of each sample was dried under a nitrogen stream before the addition of perchloric acid). Samples were then incubated for 1 h at 180 °C in the heating block (Stuart, UK). Afterwards, 825 µL of H_2O, 125 µL of 2.5% ammonium molybdate (m/v; 2.5 g of $NaMoO_4.H_2O$ in 100 mL of Milli-Q H_2O) and 10% ascorbic acid (m/v; 0.1 g in 1 mL of Milli-Q H_2O) were added to all samples. The reaction mixture was homogenized in a vortex mixer after each addition followed by incubation for 10 min at 100 °C in a water bath. Samples were put on cold water afterward.

For all samples, standards from 0.1 to 2 µg of phosphate ($NaH_2PO_4.2H_2O$, 100 µg of phosphorus per mL) underwent the same sample treatment with exception of the heating block phase. Finally, 200 µL of each standard and sample were added to the 96-multiwell

plate and the absorbance was measured at 797 nm in a Multiskan GO Microplate Spectrophotometer (Multiskan GO 1.00.38, Thermo Scientific, Hudson, NH, USA) controlled by SkanIT software version 3.2 (Thermo Scientific™). The amount of phosphorus present in each sample was calculated by linear regression through the graph that relates the amount of phosphorus present in the standards (X-axis) and absorbance obtained from the duplicates of the different concentrations (Y-axis). For lipid extracts, the amount of phospholipid was directly calculated by multiplying the amount of result phosphorus by 25.

II.4. Electrospray Ionization Mass Spectrometry

Mass spectrometry (MS) with electrospray ionization (ESI), combined with tandem MS (MS/MS and MS^n) is a technique successfully applied in the identification and characterization of structural changes of lipids, especially nitro-fatty acids (NO_2-FA, see Section I.4). Liquid chromatography (LC) coupled online to ESI-MS was also applied.

The global strategy that was used in this PhD work for the structural characterization of nitrated and nitroxidized products of PCs, PEs and PSs was based in the analysis of the nitrogen-containing products by mass spectrometry (MS) or by high performance liquid chromatoghapy (HPLC) coupled to MS (LC-MS). Different mass spectrometers with different mass analyzers but equipped with the same soft ionization source, ESI, were used for direct ESI-MS analysis: LXQ linear ion trap (LIT) mass spectrometer (ThermoFinnigan, San Jose, CA, USA) and Q-TOF 2 hybrid quadrupole time-of-flight mass spectrometer (Micromass, Manchester, UK). The LIT spectrometer allowed to perform multistage tandem mass spectrometry (MS^n) analysis. The Q-TOF mass spectrometer was used to perform the accurate mass measurements and elemental composition determination.

The ESI-MS data were obtained either by direct infusion of sample into the mass spectrometer but also by online coupling to LC. The LC was used for separation of the diverse products formed including isomeric species.

II.4.1. Linear ion trap (LIT) Mass Spectrometry

An aliquot (4 µg) of each sample in methanol (2:100, v/v) was introduced through direct infusion for ESI-MS analysis on the LIT mass spectrometer operated both in

positive- and negative-ion modes. For the ESI-MS analysis of PCs in the negative-ion mode, 10 µL of 1 mmol/L ammonium acetate in methanol were added and the samples were incubated for 5 min before the analysis. The ESI operating conditions used were as follows: samples were introduced at a flow rate of 8 µL/ min into the ESI source; electrospray voltage was 4.7 kV in the negative-ion mode and 5 kV in the positive-ion mode; capillary temperature was 275 ºC and the sheath gas flow of 25 (arbitrary units). Nitrogen was used as nebulizing and drying gas. An isolation width of 0.5 Da was used with a 30 ms activation time for CID MS/MS experiments using helium as collision gas. Full scan MS spectra (acquired over the *m/z* range 200-2000) and MS/MS spectra were acquired with a 50 ms and 200 ms maximum ion injection time, respectively. For MS/MS experiments, a normalized collision energy^{TM} (CE) between 20 and 30 (arbitrary units) was used. Data acquisition and analysis were performed using Xcalibur Data System (version 2.0, ThermoFinnigan, San Jose, CA, USA).

II.4.2. Quadrupole Time-of-Flight (Q-TOF) Mass Spectrometry

ESI-MS and MS/MS analysis of the nitrated and nitroxidized products of PCs, PEs and PSs standards were carried out in positive-ion using a Q-TOF mass spectrometer. Samples (4 µg of each sample in methanol (2:100, v/v)) were introduced through direct infusion into ESI source conditions at a flow rate of 10 µL/ min. The cone voltage was set at 30 V; capillary voltage was maintained at 3 kV, source temperature was 80 °C; desolvation temperature was 150 °C. Mass spectra were acquired for 1 min scanning the mass range from *m/z* 100 to 2000. MS/MS spectra were accumulated for 1 min and acquired by CID using argon as the collision gas. The collision energy used was set between 20 and 40 eV. Data acquisition and analysis were performed using MassLynx 4.0 data system.

The identification of the new product ions resulting from nitration/nitroxidation of PL standards were confirmed by the accurate mass measurements and elemental composition determination using ESI-MS spectra acquired and processed using MassLynx 4.0 data system after locking the mass correction for the calculated monoisotopic mass of the $[M+H]^+$ ions of each native phospholipid (non-modified phospholipid).

II.5. High-Performance Liquid Chromatography Online Coupled with Electrospray Ionization Mass Spectrometry

Electrospray ionization sources can be easily coupled online to a high performance liquid chromatography (HPLC) system because of the production of gas-phase ions directly from a liquid solution. This allows the separation of components in complex mixtures.

In this PhD work, nitrated phospholipid standards mixtures were analyzed by reversed-phase LC-ESI-MS using a C5 column. For biological samples, Hydrophilic Interaction Liquid Chromatography Mass Spectrometry (HILIC-ESI-MS) was used.

II.5.1. Reversed- Phase HPLC-ESI-MS Analysis with a C5 column

The nitrated and nitroxidized products obtained after nitration reactions between phospholipid standards (PCs, PEs and PSs) and NO_2BF_4 were separated and identified by LC-ESI-MS and characterized by LC-ESI-MS/MS. These experiments were performed on a Waters Alliance 2690 HPLC system (Mildford, MA, USA) coupled online to the LXQ linear ion trap (LIT) mass spectrometer (ThermoFinnigan, San Jose, CA, USA). An aliquot of 60 μg of each nitrated mixture (previously dissolved in chloroform, transferred to an Eppendorf tube and dried under a nitrogen stream) was diluted in 60% of mobile phase A (30 μL), and then filtered using a PVDF Millex-GV syringe filter with a 0.22 μm pore size (Millipore, Billerica, MA, USA). Volumes of 5 μL of each diluted and filtered nitrated mixture (60 μg in 30 μL of mobile phase A) were introduced into a Discovery Bio Wide Pore C5 column (15 cm × 0.5 mm, 5 μm particle size; Supelco, Bellefonte, PA, USA), using a flow rate of 16 μL/min. The mobile phase A consisted of water with 5% acetonitrile and 0.1% formic acid. The mobile phase B consisted of acetonitrile, with 0.1% formic acid. Prior to use, the mobile phases were filtered with Supelco Nylon 66 membranes (0.45 μm pore size and 47 mm diameter; Sigma-Aldrich, St Louis, MO, USA), and degassed by ultrasonication for 15 min. The mobile phase gradient was programmed as follows: initial conditions were 60% of A; 0-35 min, linear increase gradient to 60% of B; 35–45 min linear increase gradient to 100% of B held in isocratic mode for 10 min; 55-60 min linear gradient to 60% of A in order to bring back to the mobile phase composition to

the initial conditions and held in isocratic mode for 5 min, allowing to equilibrate the column until the next injection. The LIT mass spectrometer was operated both in positive- and negative-ion mode. Typical ESI conditions were as follows: electrospray voltage of 4.7 kV in the negative-ion mode and 5 kV in the positive-ion mode; capillary temperature, 275 °C; and sheath gas (nitrogen) flow of 25 (arbitrary units). To obtain the product-ion spectra of the major components during LC experiments, cycles consisting of one full scan mass spectrum (*m/z* 100-1700) and three data-dependent MS/MS scans were repeated continuously throughout the experiments with the following dynamic exclusion settings: repeat count 3; repeat duration 30 s; exclusion duration 45 s. An isolation with of 0.5 Da was used with a 30 ms activation time for MS/MS experiments using helium as collision gas. Normalized collision energy was 27 (arbitrary units). Data acquisition and processing was carried out on an Xcalibur data system (version 2.0).

II.5.2. Hydrophilic Interaction Liquid Chromatography (HILIC)-ESI-MS

Phospholipid either from cardiac mitochondrial extracts from control and T1DM heart, and from cardiomyoblast H9c2 cells from control, starvation and ischemic groups were separated and identified by hydrophilic interaction liquid chromatography (HILIC)-ESI-MS and characterized by HILIC-ESI-MS/MS performed on a Waters Alliance 2690 HPLC system (Mildford, MA, USA) coupled online to the LXQ linear ion trap (LIT) mass spectrometer (ThermoFinnigan, San Jose, CA, USA). Aliquots of 25 µg from the total lipid extracts (previously dissolved in chloroform, transferred to an Eppendorf tube and dried under a nitrogen stream) were diluted in 90 µL of the mobile phase B (acetonitrile 60%, methanol 40% with 10 mmol/L ammonium acetate) and then filtered using a PVDF Millex-GV syringe filter with a 0.22 µm pore size (Millipore, Billerica, MA, USA). Volume of 5 µL of each diluted and filtered reaction mixture was introduced into an Ascentis Si HPLC Pore column (15 cm × 1.0 mm, 3 µm; Sigma–Aldrich). Prior to use, the mobile phases were filtered with Supelco Nylon 66 membranes (0.45 µm pore size and 47 mm diameter; Sigma-Aldrich, St Louis, MO, USA), and degassed by ultrasonication for 15 min. The solvent gradient for phospholipid class separation from cardiac mitochondrial extracts was programmed as follows: gradient started with 0% of A (acetonitrile 55%, methanol 35% and water 10% (v/v) with 10 mmol/L of ammonium acetate) and linear increase to 100% of A during 20 min, and held isocratically for 30 min, returning to the

initial conditions in 10 min. The solvent gradient for phospholipid class separation from cardiomyoblast H9c2 cells was programmed as follows: gradient started with 0% of A (acetonitrile 50%, methanol 25% and water 25% with 10 mmol/L of ammonium acetate) and 100% of B, and held isocratically for 8 min. It linearly increased to 60% of A and decreased to 40% of B during 7 min, and held isocratically for 22 min, returning, to the initial conditions in 5 min. The flow rate through the column was 60 µL/ min. The LXQ linear ion trap mass spectrometer was operated in positive-ion mode. Typical ESI conditions were as follows: electrospray voltage, 5 kV; capillary temperature, 275 ºC; and the sheath gas flow of 8 (arbitrary unis). To obtain the product-ion spectra of the major components during LC experiments, cycles consisting of one full scan mass spectrum and three data-dependent MS/MS scans were repeated continuously throughout the experiments with the following dynamic exclusion settings: repeat count 3; repeat duration 30 s; exclusion duration 45 s. For the identification and characterization of the nitrated and nitroxidized species of cardiomyoblast H9c2 cells under MS/MS, an inclusion list with the *m/z* values of the major plausible products was created. HILIC-LC-MS was performed with an internal standard to confirm the retention time (RT) for elution of each PL class. Internal standards were added to the lipid extracts aliquots (prior being dried under a nitrogen stream), and the amount added was adjusted to the percentage of each PL class in the total PL extract. For cardiac mitochondria, 7 µg of PC (dMPC 14:0/14:0) and 5 µg PE (dMPE 14:0/14:0) were used. The results obtained for T1DM and for control group are presented as mean±SD of two experiments that were measured independently in different days for each experimental group (Control and T1DM). For cardiomyoblast H9c2 cell line, PL standards used were 2 µg of PC (dMPC 14:0/14:0) and 3 µg of PE (dMPE 14:0/14:0). The results obtained for cardiomyoblast H9c2 cell line (control, starvation and ischemia groups) are presented as mean±SD of three experiments that were measured independently in different days for each experimental group. Data acquisition was carried out on an Xcalibur data system (V2.0). Relative quantification of each individual phospholipid species was obtained by the ratio between the area of reconstructed ion chromatogram of a given *m/z* value against the area of the reconstructed ion chromatogram of the respective standard.

II.6. Theoretical Calculations

All calculations were performed with Gaussian09 [158] at the DFT level using the B3LYP functional and the 6-31++G** basis set. Wiberg bond indices were obtained from a Natural Bond Orbital [159] analysis as implemented in Gaussian software, at the same level of theory, using previously geometry optimized conformations.

II.7. Antioxidant Assays

The role of the nitrated/nitroxidized products of POPC, namely the nitrated derivative (NO_2-POPC), generated as described in Section II.3.1 as potential antioxidant candidates was evaluated using the radical scavenging capacity assays against 2,2-diphenyl-1-picrylhydrazyl radical ($DPPH^{\bullet}$) and 2,2'-azinobis-3-ethylbenzothiazoline-6-sulfonic acid radical cation ($ABTS^{\bullet+}$), and also the oxygen radical absorbance capacity (ORAC) assay.

The $DPPH^{\bullet}$ assay is based on the reduction of the purple chromogen $DPPH^{\bullet}$ radical to the corresponding pale yellow hydrazine through electron transfer by antioxidant compound(s). The scavenging capacity was evaluated by monitoring the absorbance decrease at 517 nm. The blue-green $ABTS^{\bullet+}$ radical can be reduced either by antioxidant compound(s) by electron transfer or by hydrogen atom transfer. The scavenging capacity was assessed by monitoring of the absorbance decrease at 734 nm. The ORAC assay is based on the inhibition of the peroxyl radical ($ROO^{\bullet}$)-induced oxidation of a fluorescent probe (usually fluorescein) through hydrogen atom donation. The fluorescence intensity is monitored at λ_{exc} 485 nm, λ_{em} 535 nm.

Stock solutions for antioxidant assays were prepared from the dried non-modified POPC standard and nitrated POPC (1 mg), recovered after extraction and properly quantified (see Section II.3.1), which were dissolved in 1 mL of ethanol and well-vortexed. Work solutions of 7.5, 25 and 100 µg/mL for ORAC assay, and 250, 300 and 500 µg/mL for $DPPH^{\bullet}$ and $ABTS^{\bullet+}$ assays of each POPC (non-modified and nitrated) were prepared by dissolving the correct volume of stock solution (3.75, 12.5, 50, 125, 150 and 250 µL) in ethanol (final volume of 500 µL).

II.7.1. DPPH• Assay

The microplate DPPH• method previously described [160] was applied with some modifications. A stock solution of DPPH• in ethanol (250 µmol/L) was prepared and kept in dark at room temperature. On the day of analysis, different concentrations of DPPH• (between 10 and 300 µmol/L) were prepared in ethanol. Then, 150 µL of each dilution of DPPH• and 150 µL of ethanol were placed in each well of the 96-well flat-bottom UV transparent microplates and absorbance measurements at 517 nm were performed at room temperature, 2 min after incubation, using an UV-Vis spectrophotometer (Multiskan GO 1.00.38, Thermo Scientific, Hudson, NH, USA) controlled by SkanIT software version 3.2 (Thermo Scientific™). The DPPH• calibration curve was established, allowing to determine the necessary dilution of DPPH• stock solution to obtain absorbance values of 0.9. This solution was used for further experiments.

For evaluation of radical species scavenging, 150 µL of Trolox standard solutions (between 5 and 75 µmol/L in ethanol), non-modified POPC and nitrated POPC (250, 300 and 500 µg/mL in ethanol) were placed in each well, followed by addition of 150 µL of DPPH• in ethanol. The DPPH• scavenging activity of standards and samples was monitored at 517 nm every 5 min after the beginning of reaction during 120 min at room temperature. The microplate was automatically shaken for 5 s prior to each reading. For each sample, the experiment was performed in triplicate in three different days. In order to evaluate the stability of the radical upon reaction time, the absorbance of DPPH• in the absence of antioxidant species (blank) was monitored at 517 nm every 5 min after the beginning of reaction at room temperature, providing an absorbance decrease of 5% after 120 min. The percentage of DPPH• radical remaining was calculated using the equation:

$$\%\ DPPH^{\bullet}\ Remaining = (Abs_{sample\ after\ incubation\ time}/Abs_{sample\ at\ the\ beginning\ of\ reaction}) \times 100.$$

The antioxidant activity of the tested samples expressed as percentage of inhibition of DPPH• radical was calculated (60 and 120 min) using the following equation:

$$\%\ inhibition = ((Abs_{DPPH^{\bullet}} - Abs_{sample})/Abs_{DPPH^{\bullet}}) \times 100.$$

The IC20 values (concentration of sample that induces a reduction of 20% in the initial $DPPH^{\bullet}$ radical) after 120 min of reaction were calculated by linear regression from the concentration of sample versus percentage of inhibition. The results were also expressed as Trolox equivalent (TE, μmol Trolox/ g of sample). The equation used was:

TE = IC20 Trolox (μmol/L) x 1000/ IC20 of sample (μg/mL).

II.7.2. $ABTS^{\bullet+}$ Assay

The microplate $ABTS^{\bullet+}$ method previously described [161] was applied. 96-Well flat-bottom UV transparent microplates and microplate reader equipment were the same as described for $DPPH^{\bullet}$ assay. The $ABTS^{\bullet+}$ radical cation solution was prepared by mixing equal volumes of an ABTS stock solution (7 mmol/L in water) with potassium persulfate (2.45 mmol/L in water) [161, 162]. This mixture was kept for 12–16 h at room temperature in the dark. On the day of analysis, five different concentrations of the $ABTS^{\bullet+}$ solution (between 25 and 350 μmol/L) were prepared in acetate buffer (pH 4.6, 50 mmol/L). A linear relationship between the radical concentration and absorbance at 734 nm was established in order to determine the dilution of the $ABTS^{\bullet+}$ stock solution necessary to obtain an $ABTS^{\bullet+}$ concentration that provided an absorbance value of 0.9. Hence, 150 μL of each $ABTS^{\bullet+}$ dilution in acetate buffer (pH 4.6, 50 mmol/L) and 150 μL of ethanol were placed in each well. The absorbance measurements were performed at room temperature, after 2 min of incubation. In order to evaluate the stability of the radical upon reaction time, the absorbance of $ABTS^{\bullet+}$ in the absence of antioxidant species (blank) was monitored, and the absorbance decrease observed was 5% after 120 min of reaction.

For evaluation of radical species scavenging, 150 μL of Trolox standard solutions (between 5 and 75 μmol/L in ethanol), non-modified POPC and nitrated POPC (250, 300 and 500 μg/mL in ethanol) and 150 μL of $ABTS^{\bullet+}$ solution were placed in each well. The $ABTS^{\bullet+}$ scavenging activity of standards and samples was monitored at 734 nm every 5 min after the beginning of reaction during 120 min at room temperature. The microplate was automatically shaken for 5 s prior to each reading. The experiments were performed in triplicate and in three different days. The percentage of $ABTS^{\bullet+}$ radical remaining was calculated using the equation:

$$\% \text{ ABTS}^{\bullet+} \text{ Remaining} = (\text{Abs}_{\text{sample after incubation time}}/\text{Abs}_{\text{sample at the beginning of reaction}}) \times 100.$$

The antioxidant activity of the tested samples expressed as percentage of inhibition of $ABTS^{\bullet+}$ radical was calculated at specific time-points (60 and 120 min) using the following equation:

$$\% \text{ inhibition} = ((\text{Abs}_{\text{ABTS}^{\bullet+}} - \text{Abs}_{\text{sample}})/\text{Abs}_{\text{ABTS}^{\bullet+}}) \times 100.$$

The IC50 values (concentration of sample that induces the reduction of $ABTS^{\bullet+}$ radical to 50%) after 120 min of reaction were calculated by linear regression from concentration of sample versus percentage of inhibition. The results were also expressed as Trolox equivalent (TE, µmol Trolox/ g of sample). The equation used was:

$$\text{TE} = \text{IC50 Trolox (µmol/L)} \times 1000 / \text{IC50 of sample (µg/mL)}.$$

II.7.3. ORAC Assay

ORAC assay was carried out in black-walled 96-well plates, using a volume of 200 µL per well. Potassium phosphate buffer (75 mmol/L, pH 7.4) was used for the preparation of fluorescein and AAPH solutions. Control experiments were performed using 60 µL of potassium phosphate buffer and 20 µL of ethanol, ensuring 10% (v/v) ethanol per well. For the blank experiment (fluorescein + AAPH), 20 µL of ethanol were used instead of sample. Trolox standard solutions (10, 25, 50, 100, 150, 200, 250 µmol/L), non-modified POPC and nitrated POPC samples (7.5, 25 and 100 µg/mL) were prepared in ethanol. Twenty µL of each standard/sample were placed in the calibration or sample wells, respectively, providing a final concentration corresponding to the one-tenth value.

Then, 120 µL of fluorescein (117 nmol/L; 70 nmol/L per well) were added to all wells, after which the microplate was pre-incubated at 37°C for 15 min in the microplate reader (Cytation3 Cell Imaging Microplate Reader, Bio-Tek Instruments, Inc., Winooski, VT, USA). This pre-incubation step was followed by the addition of 60 µL of AAPH solution (40 mmol/L; 12 mmol/L per well), with the exception of control experiments, to initiate the reaction. The fluorescence intensity (λ_{exc} 485 nm, λ_{em} 528 nm) was recorded every min during 240 min.

The ORAC curves (fluorescence vs time) were normalized (relative fluorescence, %) and the reaction endpoint was fixed at 5 % of the initial fluorescence intensity. The area under the curve (AUC) was calculated by integrating the curve defined by the relative fluorescence curve as a function of the reaction time. The lag time was also determined as the initial period of constant fluorescence intensity, prior to signal decay. Trolox equivalent (TE) values for ORAC assay were determined by interpolation of the determined AUC values in the trolox calibration curve and expressed as mmol Trolox/g lipid.

II.8. Anti-Inflammatory Assays

The role of the nitrated products of POPC generated as described in Section II.3.1 in the inflammatory response, and consequently their potential anti-inflammatory properties were assessed using the murine-leukaemic monocyte-macrophage Raw 264.7 cell line. Macrophages are key players in immune system and the Raw 264.7 cell line has been widely used as a very useful model to assess the effects of compounds, both as pro- or anti-inflammatory agents, in inflammatory processes. The bacterial lipopolysaccharide (LPS) was used as pro-inflammatory stimuli, acting on macrophages and triggering a cascade of inflammatory processes which leads to the production of several inflammatory modulators (such as $NO^{\bullet}$ and cytokines) and activation of enzymes such as iNOS.

II.8.1. Cell culture of Raw 264.7 Macrophage cell line

Raw 264.7, a mouse leukaemic monocyte-macrophage cell line from American Type Culture Collection (ATCC number: TIB-71), was cultured in DMEM supplemented with 10% non-inactivated fetal bovine serum, 100 U/mL penicillin, and 100 μg/mL streptomycin at 37 °C in a humidified atmosphere of 95% air and 5% CO_2. Along the experiments, cells were monitored by microscope observation in order to detect any morphological change.

II.8.2. Cell viability by MTT Assay

Assessment of metabolically active cells was performed using 3-(4,5-dimethylthiazol-2-yl)-2,5-diphenyl tetrazolium bromide (MTT) reduction colorimetric assay, as previously

reported [163]. Raw 264.7 cells (0.3×10^6 cells/well) were plated and allowed to stabilize overnight. Afterwards, cells were either maintained in culture medium (control) or pre-incubated with different concentrations of non-modified POPC and nitrated POPC in PBS (7.5 μg/mL, 15 μg/mL and 30 μg/mL) for 1 h, and later activated with 1 μg/mL LPS (from E. *coli*-serotype 026:B6) for 24 h. After treatments, a solution of MTT (5 mg/mL in phosphate buffered saline) was added and cells were further incubated at 37 °C for 15 min [163]. Supernatants were removed and dark blue crystals of formazan solubilized with 300 μL of acid isopropanol (0.04N HCl in isopropanol). Quantification of formazan was performed using an ELISA automatic microplate reader (SLT, Austria) at 570 nm, with a reference wavelength of 620 nm.

II.8.3. Western Blot for Immunodetection of iNOS

Raw 264.6 cells were plated at 0.6 x 10^6 cells per well in 24 well culture plates and allowed to stabilize overnight. Afterwards, cells were either maintained in culture medium (control) or pre-incubated with non-cytotoxic concentrations of non-modified POPC and nitrated POPC for 1 h, and later activated with 1 μg/mL LPS for 24 h. Cells were then lysed with RIPA buffer (50 mmol/L Tris–HCl, pH 8.0, 1% Nonidet P-40, 150 mmol/L NaCl, 0.5% sodium deoxycholate, 0.1% sodium dodecyl sulfate and 2 mmol/L ethylenediamine tetraacetic acid) freshly supplemented with 1 mmol/L dithiothreitol, protease and phosphatase inhibitor cocktails, during 30 min in ice. The nuclei and the insoluble cell debris were removed by centrifugation at (12,000 g for 10 min, at 4 °C). The postnuclear extracts were collected and used as total cell lysates. Protein concentration was determined using the bicinchoninic acid method and cell lysates denatured at 95 ºC, for 5 min in sample buffer (0.125 mmol/L Tris pH 6.8, 2% (w/v) sodium dodecyl sulfate, 100 mmol/L dithiothreitol, 10% glycerol and bromophenol blue). Briefly, equivalent amounts of protein were electrophoretically separated on a 10% (v/v) sodium dodecyl sulfate – polyacrylamide gel and transferred to a PVDF membrane. The membranes were blocked with 5% (w/v) fat-free dry milk in Tris- buffered saline containing 0.1% (v/v) Tween 20 (T-TBS), for 1 h, at room temperature. Blots were then incubated overnight at 4 ºC with the primary antibody against iNOS (1:500). The membranes were then washed for 30 min with T-TBS and incubated for 1 h at room temperature with alkaline phosphatase-conjugated anti-rabbit antibody (1:20,000). The immune complexes were detected by

membrane exposure to the enhanced chemifluorescence reagent for 5 min, followed by scanning for blue excited fluorescence on the Typhoon FLA 9000 imager (GE Healthcare). The generated signals were analyzed using Image-Quant TL software. To ensure that equivalent amounts of protein were loaded for each sample, the membranes were stripped and reprobed with a monoclonal anti-tubulin antibody (1:20,000).

II.9. Cross Adduction with Proteins

II.9.1. *In vitro* Competition Assay for Vimentin Modification

For modification of vimentin and evaluation of non-modified POPC or nitrated POPC as potential electrophiles a competition assay was performed. Stock solutions (3.67 mmol/L) were prepared by dissolving the dried non-modified POPC standard and nitrated POPC (1 mg), recovered after extraction and properly quantified (see Section II.3.1) in 339 µL of dimethylsulfoxide (DMSO). Three work solutions of 100 µmol/L, 500 µmol/L and 1 mmol/L were prepared by dissolving the correct volume of stock solution (2.7, 13.6 and 27 µL) in DMSO (final volume of 100 µL). Stock solution of 28.3 µmol/L soluble vimentin (1.5 mg/mL) in 5 mmol/L PIPES (pH 7.0) and 0.1 mmol/L dithiothreitol (DTT) was used without further dilution. Vimentin at 2.8 µmol/L (1µL of 28.3 µmol/L vimentin stock solution in 5 mmol/L PIPES (pH 7.0)) was pre-incubated in the absence or presence of the previous designated compounds at 10, 50 and 100 µmol/L final concentration (1 µL of each PL work solution in DMSO; final volume of reaction mixture of 10 µL in 5 mmol/L PIPES (pH 7.0)). The assay was carried out at room temperature during 4 h. A work solution of 200 µmol/L of biotinylated iodoacetamide (Iac-B) was prepared in 5 mmol/L PIPES (pH 7.0) buffer (10 µL of Iac-B in a final volume of 500 µL) from the 10 mmol/L stock solution (in water). Subsequently, 20 µmol/L of Iac-B (1 µL of 200 µmol/L work solution of Iac-B in 5 mmol/L PIPES (pH 7.0)) was added to the samples and incubated for additional 30 min. Incorporation of Iac-B was assessed through biotin detection after the separation of aliquots from the incubations on 10% SDS–polyacrylamide gels (SDS–PAGE) followed by transfer to PVDF membranes (0.45 µm pore size; Sigma-Aldrich, St Louis, MO, USA). Blots were incubated with horseradish peroxidase (HRP)-streptavidin and enhanced chemiluminiscence (ECL). Western blot with specific antibodies was used for detection and to determine the vimentin amount.

II.9.2. Western blot and Immunoprecipitation for Vimentin Modification

Aliquots from the competition assays (final volume 10 µL) were separated on 10% SDS–polyacrylamide gels. A volume of 2.5 µL of Laemmli sample buffer (4% SDS, 20% glycerol, 10% β-mercaptoethanol, 0.004% bromophenol blue and 0.125 mol/L Tris-HCl, pH 6.8) was added and samples were incubated for 5 min at 95 °C for protein denaturation. After cooling, 6 µL of each sample and 4 µL aliquot of a protein marker were loaded on top of a 4% SDS–polyacrylamide stacking gel polymerized over a 10% SDS–polyacrylamide gels. Samples were separate by running the gel at 100 V until samples got into the running gel and then at 120 V until the end of the run using the running buffer 125 mmol/L Tris, 0.96 mol/L glycine, 20% SDS, pH 8.3. Gels were further transferred to PVDF membranes on a semidry trans-blot system from Bio-Rad set at 22 V, for 50 min. A three buffer system (anode buffer I, 0.3 mol/L Tris pH 10.4, 10% (v/v) MeOH; anode buffer II, 25 mmol/L Tris pH 10.4, 10% (v/v) MeOH; catode buffer, 25 mmol/L Tris pH 9.4, 40 mmol/L 6-aminohexanoic acid, 20% MeOH, pH 9.4) was used according to the instructions of the manufacturer. Membranes were then blocked by incubation with 2% defatted milk for 1 h at room temperature with shaking followed by three times washes of 5 min with Tween-Tris Buffer Saline (T-TBS; 20 mmol/L Tris-HCl pH 7.5, 500 mmol/L NaCl, 0.05% Tween 20). Then, membranes were incubated for 45 min with HRP-conjugated streptavidin diluted 1:1000 in 1% BSA prepared in T-TBS. A new step of three times washes of 5 min with T-TBS was performed. For detection, membranes were incubated with ECL reagents for 1 min as specified in the manufacturer instructions. Signal is obtained by exposing membranes to Hyperfilm (GE Healthcare, Buckinghamshire, UK) for various time periods to ensure non-saturated signals (1, 5, 15 and 30 seconds). Then, the stripping of membrane was performed. For that, membranes were washed three times for 5 min with water to remove the salts followed by a quick step of incubation with 8 mol/L guanidinium chloride pH 3 (only few seconds; membrane should become transparent). Membranes were washed three times for 5 min with water and three times for 5 min with T-TBS. In order to guarantee that protein was loaded and transferred, the membranes were incubated with anti-vimentin antibody (1:500) in 1% BSA prepared in T-TBS for 1 h, followed by three washes of 5 min with T-TBS. Then, incubation with an HRP-conjugated secondary antibody (anti-mouse (1:2000) for vimentin for 1h was

executed, and immunoreactive bands were detected with ECL according to standard western blot procedures. Levels of the proteins of interest were estimated by image scanning after exposing membranes to Hyperfilm for various time periods (1, 5, 15 and 30 s) to ensure non-saturated ECL signals. Afga Arcus 1200 scanner with the Fotolook software (version 32 v3.60.0) was used for scanning the gel images. Gel-imaging software (Scion Image from Scion Corporation, Inc.) was used for signal quantification.

II.9.3. Cell culture and Treatments of Adrenal Carcinoma SW13 cell line

The cell line SW13/cl.2 (SW13), which is a vimentin-deficient cell line devoid of cytosolic intermediate filaments, was stably transfected as previously described by Peréz-Sala and co-authors [225]. In RFP//vimentin, cells were co-transfected with a bicistronic expression plasmid coding for vimentin wild type (wt) or C328S mutant (vimentin wt or C328S and the red fluorescent protein RFP (DsRed-Express2 protein) as a marker of transfection were expressed as separated products). In these cells, both vimentin constructs form an extended radial network. SW13 cells were also stably transfected with constructs expressing the green fluorescent protein fused to vimentin wt or C328S mutant (GFP-vimentin wt or C328S). These cells are characterized by the formation of filamentous structures with two free ends consistent with vimentin squiggles or short vimentin filaments in the case of wt, but only bright vimentin dots in the case of GFP-vimentin C328S, which is not competent for the formation of squiggles.

RFP//vimentin wt and RFP//vimentin C238S SW13 cells were cultured on p-60 plates with glass bottom dishes in Dulbecco's Modified Eagle Medium (DMEM) supplemented with 10% (v/v) fetal bovine serum (FBS) and 1% antibiotics (100 U/mL penicillin and 100 µg/mL streptomycin) at 37 ºC under 5% CO_2. For experiments cells were plated on p-35 plates. Experiments were performed on confluent monolayers. Medium with FBS was removed, plates were washed with medium without FBS and then cells were treated in fresh medium without FBS. Treatments with 10 µmol/L non-modified POPC and nitrated POPC (from 3.67 mmol/L stock solution) were carried out at 37 ºC under 5% CO_2 for 6h. At the time point, cells were fixed, processed for immunofluorescence and observed by confocal microscopy.

GFP-vimentin wt stable transfectants were plated on 12-multiwell plate on glass bottom dishes in Dulbecco's Modified Eagle Medium (DMEM) supplemented with 10%

(v/v) fetal bovine serum (FBS) and 1% antibiotics (100 U/mL penicillin and 100 µg/mL streptomycin) at 37 ºC under 5% CO_2. Confluent monolayers were plated in DMEM medium deprived of FBS and were observed by confocal microscopy before and after treatments with 10 µmol/L and 30 µmol/L non-modified POPC and nitrated POPC (from 3.67 mmol/L stock solution), and 10 µmol/L and 30 µmol/L GSNO (from stock solution of 10 mmol/L) for imaging of live cells. Controls cells received an equivalent volume of DMSO. After treatments, cells were fixed, processed for immunofluorescence and observed by confocal microscopy.

II.9.4. Immunofluorescence

After the 6h treatment with 10 µmol/L non-modified and nitrated POPC, SW13 cells were washed twice with 1 mL 1x PBS, fixed with 4% paraformaldehyde for 20 min at room temperature, and washed again twice with 1 mL 1x PBS. Cells were permeabilized with 1 mL 0.1% Triton X-100 in PBS for 15 min, washed twice with 1 mL 1x PBS, blocked by incubation in 1% bovine serum albumin in PBS (blocking solution) for 1h, washed again twice with 1 mL 1x PBS and incubated with 500 µL anti-vimentin-Alexa 488 at 1:200 dilution in blocking solution for 1h. Cells were further washed three times for 5 min with 1 mL 1x PBS. For actin visualization, cells were counterstained with 100 µL of Phalloidin-Alexa 568 (5:200 dilution in blocking solution) for 30 min, and further washed three times for 5 min with 1 mL 1x PBS. The position of the nuclei was obtained by staining cells with 100 µL of 4,6-diamidino-2-phenylindole (DAPI) at 1:1500 dilution in PBS was added to cells and allowed to incubate for 20 min. Cells were washed twice with 1 mL 1x PBS and kept in 1 mL 1x PBS with 4 µL of 10% sodium azide solution (final concentration of 0.04%) for confocal microscopy.

II.9.5. Confocal Microscopy

Cells were visualized on confocal microscopes Leica SP2 (LEICA DMRE2, Heidelberg, Germany) or LEICA SP5 (Leica microsystem LAS AF6000 modular system, Heidelberg, Germany). Individual sections were taken every 0.5 µm with a numerical aperture of x63.

RFP//vimentin wt and C238S SW13 cells were observed after 6 hours of treatment on a LEICA SP2. Cross-sections of single confocal microscopy planes of SW13 cells stained for vimentin by immunofluorescence were plotted to obtain profiles using Fiji ImageJ software. The pattern of the vimentin network was assessed to evaluate the proportion of cells with vimentin filaments circumscribed to the perinuclear area or extending towards the periphery of the cells. A minimum of 100 cells per assay were monitored.

The Leica SP5 confocal microscope equipped with a thermostatic chamber at 37 °C was used for imaging of GFP-vimentin wt SW13 live cells after being treated with non-modified POPC, nitrated POPC, GSNO (10 and 30 µmol/L), and DSMO. Briefly, a pre-incubation image was taken, before the addition of the previous designated compounds. Further, cells underwent the treatments with 10 µmol/L and 30 µmol/L non-modified POPC and nitrated POPC (from 3.67 mmol/L stock solution), and 10 µmol/L and 30 µmol/L GSNO (from stock solution of 10 mmol/L). Prompt observations of post-treated cells were performed. Then, cells were monitored for the 75 min of incubation. After the immunofluorescence protocol, GFP-vimentin wt SW13 cells were observed on LEICA SP2.

II.10. Statistical Analysis

Statistical analysis was performed using PRISM® GraphPad Software, Inc (GraphPad Prism 5.0, La Jolla, CA, USA).

One-way analysis of variance (ANOVA) with the Bonferroni post-hoc test was used to determine significant differences ($p<0.05$) among phospholipid molecular species (non-modified and nitrated phospholipid (NO_2-PL) molecular species) for each experimental group in cardiac mitochondria from type 1 diabetes mellitus model (see Section II.5.2). The two-sided paired t-test was used to compare the conversion of phospholipid molecular species with formation of NO_2-PLs. The results were expressed as mean ± SD of two different and independent experiments.

One-way analysis of variance (ANOVA) with the Bonferroni post-hoc test was used to determine significant differences ($p<0.05$) among phospholipid molecular species (non-modified and nitrated phospholipid (NO_2-PL) molecular species) and to compare the conversion of phospholipid molecular species with formation of NO_2-PLs for each control

and starvation group in cardiomyoblast H9c2 cell line model (see Section II.5.2). The results were expressed as mean ± SD of three different and independent experiments.

In $DPPH^{\bullet}$ (see Section II.7.1) and $ABTS^{\bullet+}$ (see Section II.7.2) assays, the experiments were performed in triplicate and in three different days both for non-modified and nitrated POPC. The results were expressed as mean ± SD. One-way analysis of variance (ANOVA) with the Bonferroni post-hoc test was used to determine significant differences among samples. A P value <0.05 was considered significant. For ORAC assay (see Section II.7.3), the experiments were performed in triplicate and in two different days both for non-modified and nitrated POPC. The results were expressed as mean ± SD using two-sided unpaired t-test for a P value <0.05.

For cell viability (see Section II.8.2), the results were analyzed with one-way ANOVA followed by Dunnett's multiple comparison test. For iNOS protein expression (see Section II.8.3) the comparison was made between the treatment condition and control using the two-sided unpaired t-test. A P value <0.05 was considered statistically significant. For each experimental condition, the results were expressed as the mean ± SD of at least three independent experiments.

For *in vitro* gel-based competition method (see Section II.9.1), the results were analyzed with one-way ANOVA followed by Dunnett's multiple comparison test. The results were expressed as mean ± SD of three different and independent experiments. For SW13 cells treated with non-modified or nitrated POPC (see Section II.9.3), the results were analyzed with one-way ANOVA followed by Bonferroni post-hoc test. A P value <0.05 was considered statistically significant. For each experimental condition, the results were expressed as the mean ± SD of two independent experiments.

CHAPTER III. RESULTS AND DISCUSSION

III.1. UNDERSTANDING THE NITROXIDATIVE STRESS-INDUCED MODIFICATIONS OF PHOSPHOLIPIDS

III.1.1. RECENT ADVANCES ON MASS SPECTROMETRY ANALYSIS OF NITRATED PHOSPHOLIPIDS

III.1.2. PHOSPHOLIPID NITROXIDATION IN H9c2 MYOBLAST USING A LIPIDOMIC APPROACH

III.2. UNDERSTANDING THE BIOLOGICAL ACTIVITIES OF NITRATED AND NITROXIDIZED DERIVATIVES OF PHOSPHOLIPIDS

III.2.1. NEW INSIGHTS IN ANTI-INFLAMMATORY AND ANTIOXIDANT PROPERTIES OF NITRATED PHOSPHOLIPIDS

III.3. UNDERSTANDING THE CROSS REACTION BETWEEN NITRATED AND NITROXIDIZED DERIVATIVES OF PHOSPHOLIPIDS AND PROTEINS

III.3.1. MODIFICATION OF VIMENTIN BY NITRATED/NITROXIDIZED PRODUCTS OF POPC

CHAPTER III. RESULTS AND DISCUSSION

III.1. UNDERSTANDING THE NITROXIDATIVE STRESS-INDUCED MODIFICATIONS OF PHOSPHOLIPIDS

Reactive nitrogen species (RNS) has the ability to react with lipids, generating nitro-fatty acids that have been identified *in vitro* and *in vivo*. Considering that RNS can freely cross membranes, where it accumulates in higher concentrations, thus it is plausible that phospholipid nitration/nitroxidation can also occur. However, the identification and detailed structural characterization of nitrated and nitroxidized derivatives of phospholipids have been overlooked.

In order to better understand the nitrative/nitroxidative-induced modifications in phospholipids, phospholipid standards from distinct classes, including phosphatidylcholine, phosphatidylethanolamine, and phosphatidylserine, the most abundant phospholipids in membranes, bearing different fatty acyl chains with distinct unsaturation degrees, were submitted to nitration by nitronium tetraflouroborate (NO_2BF_4), in a biomimetic model of nitroxidation (Section III.1.1 and Section III.1.2). The products formed in *in vitro* model system were characterized by liquid chromatography (LC)-mass spectrometry (MS) and tandem mass spectrometry (MS/MS) and identified in biological samples using the developed MS-based approaches.

CHAPTER III. RESULTS AND DISCUSSION

III.1. UNDERSTANDING THE NITROXIDATIVE STRESS-INDUCED MODIFICATIONS OF PHOSPHOLIPIDS

III.1.1. RECENT ADVANCES ON MASS SPECTROMETRY ANALYSIS OF NITRATED PHOSPHOLIPIDS

The results and discussion presented in this section were integrally published as follow:

Melo T, Domingues P, Ferreira R, Milic I, Fedorova M, Santos SM, Segundo MA, Domingues MRM (2016) Recent Advances on Mass Spectrometry Analysis of Nitrated Phospholipids, *Analytical Chemsitry*, 88:2622-2629

III.1.1.1. Background and Aim of the Study

In recent years, there has been an increasing interest in nitro-fatty acids (NO_2-FA) as signaling molecules formed under nitroxidative stress. NO_2-FA were detected *in vivo* in a free form, although it is assumed that they may also be esterified to phospholipids (PL). Nevertheless, insufficient discussion about the nature, origin or role of nitro phospholipids (NO_2-PL) was reported up to now.

The aim of this study was to develop a mass spectrometry (MS)-based approach which allows identifying nitroalkenes derivatives of three major PL classes found in living systems: phosphatidylcholines (PCs), phosphatidylethanolamines (PEs) and phosphatidylserines (PSs). NO_2-PLs were generated by nitronium tetrafluoroborate (NO_2BF_4) in hydrophobic environment, mimicking biological systems. The NO_2-PLs were then detected by electrospray ionization (ESI-MS) and ESI-MS coupled to hydrophilic interaction liquid chromatography (HILIC). Identified NO_2-PLs were further analyzed by tandem MS in positive (as $[M+H]^+$ ions for all PL classes) and negative-ion mode (as $[M-H]^-$ ions for PEs and PSs and $[M+OAc]^-$ions for PCs) for characterization of their fragmentation patterns. The developed MS method was further validated by screening the identified NO_2-PL in cardiac mitochondria from a well-characterized animal model of type 1 diabetes mellitus.

III.1.1.2. Results and Discussion

In this study, we have induced the nitration of PC, PE and PS phospholipids, differing in degree of unsaturation of the hydrocarbon chains (oleic acid (OA), linoleic acid (LA) and arachidonic acid (AA)) (Supplementary Table S-1 and Figure S-1, Appendix A), by incubation with nitronium tetrafluoroborate (NO_2BF_4). NO_2BF_4 is a nitronium cation salt (NO_2^+) that has been previously used as nitrating agent in fatty acid nitration studies and was chosen for mimicking the nitration occurring on biological membranes with peroxynitrite and nitrite [7, 9, 58, 154] by allowing nitration to occur in hydrophobic environments [9, 58, 59].

Tandem Mass Spectrometry Characterization of NO_2-PLs

Nitro phospholipids, NO_2-PLs, were observed in the positive mass spectra as $[M+H]^+$ molecular ions and, in the negative mode mass spectra, as $[M-H]^-$ for PE and PS, and as $[M+OAc]^-$ molecular ions for PC. MS/MS spectra were acquired for both positive and negative precursor ions, to obtain complementary information, which could further be used for lipidomic studies on cell, tissues and biofluids [164, 165]. In the mass spectra, the nitro phospholipids (NO_2-PL) were observed with a mass increment of 45 u relative to the non-modified PL (Supplementary Table S-1, Appendix A). In order to confirm the formation of NO_2-PLs, accurate mass measurement and elemental composition determination were performed in a Q-TOF mass spectrometer. Based on the accuracy of the measurements, the structural assignments could be made with a high degree of confidence (Supplementary Table S-2, Appendix A).

Further, MS/MS spectra were acquired for the PC, PE and PS nitro derivatives both in positive- and negative-ion mode (Figure III.1) using collision induced dissociation (CID) conditions. All MS/MS spectra showed four main fragmentation pathways involving: a) the elimination of the nitro (NO_2) group, as neutral loss of HNO_2; b) formation of ionized nitrated fatty acids as $[NO_2\text{-FA+H}]^+$ and $[NO_2\text{-FA-H}]^-$; c) the fragmentation of the fatty acyl chain in the vicinity of the NO_2 group and; d) combined fragmentation of the NO_2 group and the polar head groups of each PL. The fragmentation pathways identified for NO_2-PLs are illustrated in Figure III.2 using NO_2-OA-PLs as model. The product ions arising from observed fragmentation pathways can be used for identifying nitrated PLs. These include product ions formed due to neutral loss of nitro group as HNO_2 (loss of 47 u), observed both in positive and negative mode MS/MS spectra of all NO_2-PL, as can be seen in Figure III.1 and Supplementary Figure S-2 to S-4 (Appendix A). Product ions arising from the neutral loss of H_2O and $2H_2O$ (loss of 18 u or 36 u) and combined loss of water and HNO_2 (65 u and 83 u) were also observed. Such product ions were already reported for NO_2-FA and thus can be used to unequivocally confirm the presence of a NO_2 group [7, 9, 10, 58, 69, 83, 100, 153, 154]. Other typical product ions that were observed in the MS/MS spectra are the protonated molecules of nitro-fatty acids, $[NO_2\text{-FA+H}]^+$, that occur due to cleavage between the fatty acid and the glycerol backbone, and which observation in MS^2 is favored due to charge retention in the nitro group [166, 167]. These

product ions were found at *m/z* 328.3 ($[NO_2\text{-}OA+H]^+$), *m/z* 326.3 ($[NO_2\text{-}LA+H]^+$) and *m/z* 350.4 ($[NO_2\text{-}AA+H]^+$) (Figure III.1 A to C, Figure III.2 and Supplementary Table S-3, Appendix A). When NO_2-PL were analyzed in the negative mode, we observed in all the MS/MS spectra peaks corresponding to the carboxylate anions of NO_2-FA ($[NO_2\text{-}FA\text{-}H]^-$) (Supplementary Table S-3, Appendix A). These ions allowed unequivocal identification of NO_2-FA esterified to the particular PL. Furthermore, MS^3 spectra of the nitro-fatty acids product ions, both in positive ($[NO_2\text{-}FA+H]^+$) and negative ion modes ($NO_2\text{-}FA\text{-}H]^-$), showed product ions confirming the presence of the NO_2 group (neutral loss of HNO_2), as reported previously for $[NO_2\text{-}FA\text{-}H]^-$ (Supplementary Figure S-5 and Table S-3, Appendix A) [5, 59, 83].

As previously indicated, the third identified fragmentation pathway produces typical fragment ions arising from cleavage of fatty acyl chain in the vicinity of the NO_2 group, as shown in Figure III.2. This fragmentation pathway is observed in the MS/MS spectra of both positive and negative NO_2-PLs precursor ions. Formed product ions are common for the NO_2-PLs with the same fatty acyl chain (OA, LA and AA), independently of the polar head group. However, the fragment ions, that were observed for each fatty acyl chain were different and thus, the nature of the NO_2-PLs was also different. In the case of NO_2-OA-PL, we have assigned the 9-NO_2-OA-PL and 10-NO_2-OA-PL species, which is in accordance with previously reported results for oleic acid nitration [5, 83]. The location of the nitro group at C9 or C10 was inferred by the observed cleavage between C8-C9 or C10-C11 occurring with a neutral loss of 169 u ($C_{10}H_{19}ON$) or 128 u ($C_8H_{16}O$), respectively [5, 83]. For NO_2-LA-PL, we have assigned three major isomers, with the nitro group attached at C9, C10, or C13, inferred by product ions formed by cleavages between C9-C10, C13-C14, C10-C11 and C12-C13, respectively. These backbone cleavages promote neutral losses of 156 u ($C_9H_{16}O_2$), 86 u ($C_5H_{10}O$), 139 u ($C_8H_{13}ON$) and 115 u ($C_6H_{13}ON$), respectively. For NO_2-AA-PLs, we assigned four major isomers, with the nitro group attached in C11, C12, C14 or C15. The location of the NO_2 group at C14 and C15 were inferred by the observation of cleavages between C10-C11 and C13-C14 with the correspondent neutral loss of 183 u ($C_{10}H_{17}O_2N$) or 143 u ($C_7H_{13}O_2N$). The 11- or 12-NO_2-AA-PLs were assigned due to neutral loss of 193 u ($C_{12}H_{19}ON$). Other minor product ions were observed, as reported in Figures S-5 and S-6 (Appendix A), which are well described

in literature [5, 83]. These product ions can be used to locate the position of the NO_2 group along the fatty acyl chain.

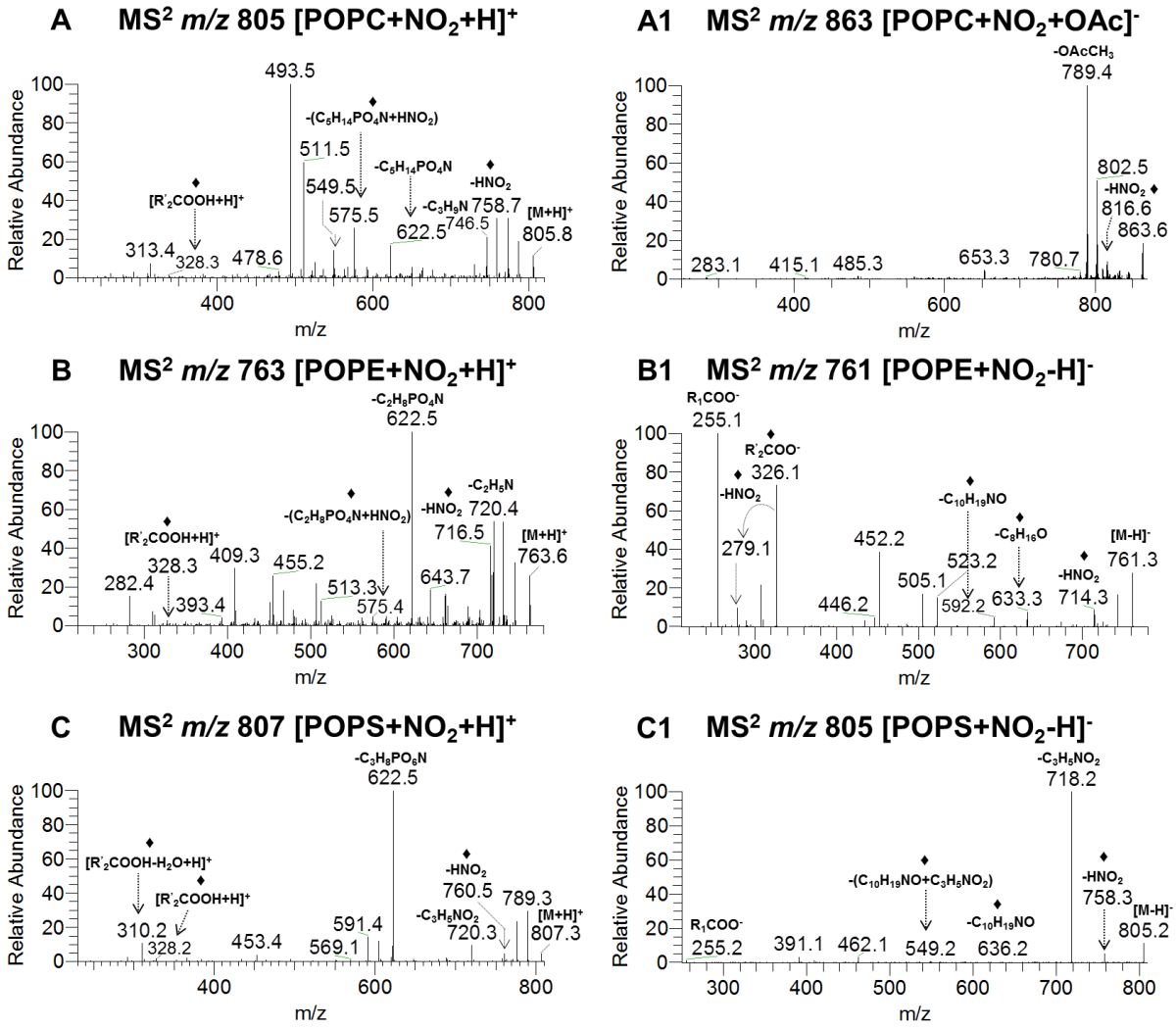

Figure III.1. ESI-MS/MS spectra of: A) $[M+NO_2+H]^+$ and $[M+NO_2+OAc]^-$ POPC molecular ions ($[POPC+NO_2+H]^+$; A1, $[POPC+NO_2+OAc]^-$); B) $[M+NO_2+H]^+$ and $[M+NO_2-H]^-$ POPE molecular ions ($[POPE+NO_2+H]^+$; B1, $[POPE+NO_2-H]^-$) and; C) POPS molecular ions ($[POPS+NO_2+H]^+$; C1, $[POPS+NO_2-H]^-$). Product ions indicating the presence of a NO_2 group were labeled with (♦).

Phospholipids usually show a typical MS/MS fragmentation pattern depending on the polar head, including the observation of a product ion at *m/z* 184 for $[PCs+H]^+$ ions, and neutral losses of 141 u for $[PEs+H]^+$ ions and of 185 u for $[PSs+H]^+$ precursor quasi-molecular ions. However, the MS/MS spectra of the $[M+H]^+$ ions of NO_2-PLs (Figure III.1

A to C) show fragmentations usually observed in the MS/MS spectra of cationized ions ($[M+X, X= Na, K, Li]^+$) of non-modified PLs [3, 164, 168-171]. These fragmentations involve the polar head group and are the neutral losses of 59 u (C_3H_9N, trimethylamine) and 183 u ($C_5H_{14}PO_4N$, phosphocholine) in the case of NO_2-PCs. The decomposition of NO_2-PEs and of NO_2-PSs showed, respectively, the neutral loss of 43 u (aziridine, C_2H_5N) and the neutral loss of 87 u (Supplementary Table S-3, Appendix A). The occurrence of these fragmentation pathways in NO_2-PL MS/MS spectra can lead to misassignment of the peaks in lipidomics studies. This behavior can be caused by proton retention in the NO_2 group, which modifies the lability of the chemical bonds, favoring different fragmentation pathways. Losses of 59 u, 43 u and 87 u involves cleavages of the O-C bond, namely between phosphate and PL-head group. The presence of the charge in the NO_2 group, rather than exclusively in the polar head, could to favor the cleavage between the phosphate and the polar head, which only occurs in cationized non-nitrated PL. In fact, sodium ions have been reported to randomly associate with several regions of the PL molecule and the free negatively charged phosphate oxygen, in the sodium adduct of PL, can undergo fragmentation via neutral loss of trimethylamine (loss of 59 u) [172].

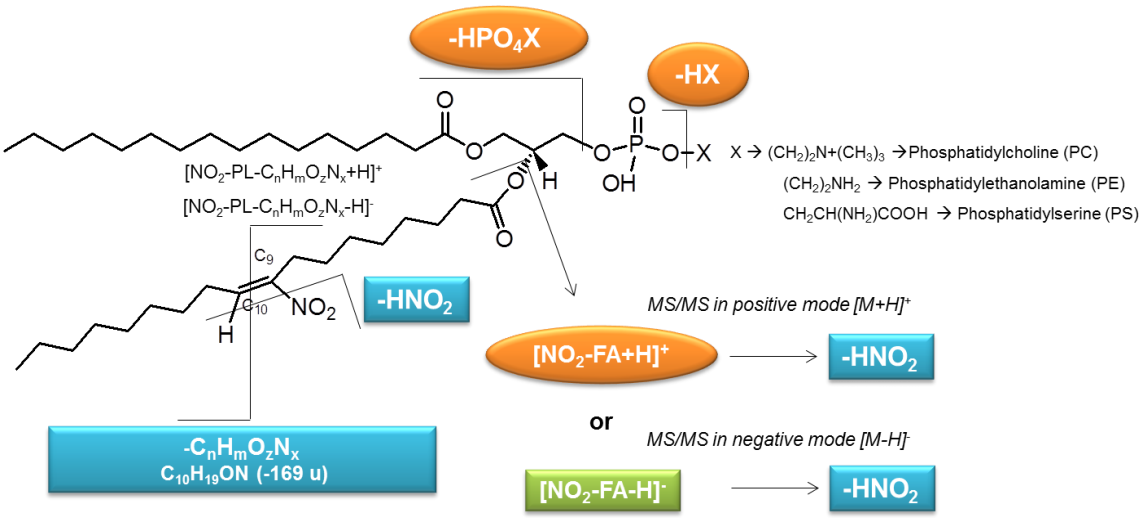

Figure III.2. Major fragmentation pathways identified for NO_2-PLs in positive- and negative-ion mode; NO_2-OA-PLs derivatives were used as examples. Common fragmentations observed both in positive and negative modes are the loss of HNO_2 and cleavages in the vicinity of the NO_2 group. Fragmentations observed only in negative-ion mode ($[M-H]^-$ ions) corresponding to the carboxylate anions of NO_2-FAs. Typical fragmentations observed in positive-ion mode ($[M+H]^+$ ions) involve the presence of

protonated NO_2-FA and loss of polar head group typically observed for the cationized ions of PLs.

Bond Energy Theoretical Studies

In order to gain atomistic insights into the mechanisms governing the different fragmentation patterns of the several compounds, namely the distinct fragments observed upon CID fragmentation of nitrated lipids, we have performed bond energy theoretical calculations. Since the distinct fragmentation was observed independently of the polar head and the fatty acyl chain, the theoretical calculations were performed considering the NO_2-PLPE system as a representative example of the common behavior of the remaining NO_2-PLs studied. The PE was chosen since it has the simplest polar head in terms of chemical structure and is more prone to theoretical calculation. The strategy involved analysis of the Wiberg bond indices obtained through Natural Bonding Orbital (NBO) analysis at the B3LYP/ 6-31++G** level using geometry optimized molecules (at the same level and theory). To decrease the conformational freedom and the total number of atoms, the saturated aliphatic chain was truncated to a simple methyl substitute. The lowest energy conformations of the PLPE models protonated at the -NO_2 and terminal -NH_2 groups (top and bottom, respectively) alongside the calculated Wiberg bond indices of the relevant bonds are shown in Supplementary Figure S-7 (Appendix A).

The lowest energy conformation for the -NO_2 protonated model presents the phosphate OH hydrogen bonded to the ester carbonyl (d_{NH--O}=1.88 Å) whereas the ethanolamine terminal chain is stretched and not involved in any intramolecular interaction. In contrast, the -NH_2 protonated structure shows an intramolecular hydrogen bond between one -NH_3^+ hydrogen and the ester carbonyl (d_{NH--O}=1.59 Å), resulting from the curling of the phosphoethanolamine fragment into itself. The protonation of the terminal NH_2 originates a significantly more stable isomer, suggesting that this species are the most abundant. Comparing the Wiberg bond indices between both species, depicted in Supplementary Figure S-7 (Appendix A), the C—O bond near the ester is slightly weaker (lower bond index) in the NH_2 protonated model (0.8674) than in the NO_2 one (0.8768), suggesting that the former is more likely to be cleaved during MS/MS experiments. In contrast, the C—O bond close to the terminal NH_2 is weaker in NO_2 model than in the NH_2 one, suggesting

that cleavage of the latter is more probable. These results are in clear agreement with the fragmentation patterns observed experimentally.

The MS/MS spectra of $[NO_2\text{-PLs+H}]^+$ ions (Figure III.1 A to C) also showed product ions arising from the combined loss of HNO_2 and polar head group. These were the product ions formed by the neutral loss of $59+HNO_2$ and $183+HNO_2$ for NO_2-PCs, $43+HNO_2$ and $141+HNO_2$ for NO_2-PEs and $87+HNO_2$ and $185+HNO_2$ for NO_2-PSs, as confirmed by MS^3 analysis (Supplementary Figures S-8 to S-10, Appendix A). We also observed combined loss of polar head and neutral losses due to the cleavage in the vicinity of the NO_2 group for $[M+H]^+$ ions (Supplementary Figure S-10 and S-11, Appendix A).

Overall, the typical fragmentation pattern reported in here is crucial to design targeted approaches for the identification of NO_2-PL in complex biological samples. Moreover, these can be used to propose specific multiple reaction monitoring (MRM), precursor ions scan (PIS) or neutral loss scan (NLS), essential to detect and quantify nitrated phospholipids in the lipidome, as is resumed in Table III.1.

Table III.1. Tandem MS fragment ions for diagnostic scan of NO_2-PLs in positive and negative mode.

	Fragment Ion/Diagnostic Scan	
	Positive Mode $[M+H]^+$	**Negative Mode $[M-H]^-$**
Nitro group (NO_2)	Neutral loss of 47 ($-HNO_2$)	Neutral loss of 47 ($-HNO_2$)
Head group		
Phosphatidylcholine	Neutral loss of 59 u	--
	Neutral loss of 183 u	--
Phosphatidylethanolamine	Neutral loss of 43 u	--
	Neutral loss of 141 u	--
Phosphatidylserine	Neutral loss of 87 u	Neutral loss of 87 u
	Neutral loss of 185 u	--
Nitrated Modifications		
$[NO_2\text{-OA}]^+$	Product ion 328	--
$[NO_2\text{-LA}]^+$	Product ion 326	--
$[NO_2\text{-AA}]^+$	Product ion 350	--
$NO_2\text{-OARCOO}^-$	--	Product ion 326
$NO_2\text{-LARCOO}^-$	--	Product ion 324
$NO_2\text{-AARCOO}^-$	--	Product ion 348
HNO_2+Head Group		
Phosphatidylcholine	Neutral loss of 106 u (HNO_2+59)	--
	Neutral loss of 230 u (HNO_2+183)	--
Phosphatidylethanolamine	Neutral loss of 90 u (HNO_2+43)	--
	Neutral loss of 188 u (HNO_2+141)	--
Phosphatidylserine	Neutral loss of 134 u (HNO_2+87)	Neutral loss of 134 u (HNO_2+87)
	Neutral loss of 232 u (HNO_2+185)	--

Identification of NO_2-PL in Mitochondria

Previously we have characterized the lipidome of cardiac mitochondria isolated from heart of an animal model of type 1 diabetes mellitus (T1DM) [156]. We observed an increase in the relative content of PC, and a decrease in the other classes of phospholipids (PI, SM and PG) in T1DM mitochondria in comparison with control group. Additionally, we detected higher amounts of carbonylated and nitrated proteins in T1DM mitochondria in comparison with control group [156]. In consequence, we decided to further investigate the presence of nitro phospholipids in the animal model of type 1 diabetes mellitus (T1DM), using the knowledge of the typical fragmentation pattern of NO_2-PL reported in the previous section. It is worth noting that, in the previous report, we did not identify any NO_2-PL.

In this study, samples were analyzed by HILIC-LC-MS and MS/MS. The retention time (RT) observed for PC class was between RT 45 and 57 min and for PE was between RT 22 and 30 min, based on elution of internal standards (dMPC and dMPE, respectively) (Supplementary Figure S-12, Appendix A). The major PC molecular species identified for mitochondria of control and T1DM group, and their relative amount are shown in Figure III.3A. The LC-MS/MS spectra were also interpreted using the fragmentation pathway of NO_2-PCs data. By doing so, we were able to identify nine NO_2-PC species in T1DM cardiac mitochondria: at *m/z* 803.6 (NO_2-PC 16:0/18:2); 805.7 (NO_2-PC 16:0/18:1); 851.6 (NO_2-PC 18:2/20:4); 853.7 (NO_2-PC 16:0/22:5, NO_2-PC 18:0/20:5 and NO_2-PC 18:1/20:4); 855.7 (NO_2-PC 18:0/20:4); 857.6 (NO_2-PC 18:2/20:1); and 879.6 (NO_2-PC 18:0/22:6) (Figures 3B and Supplementary Figure S-13, Appendix A). Only NO_2-PC 18:2/20:1 was detected in the control samples, although with a small relative abundance. As an example, the LC–MS/MS spectra obtained for ions at *m/z* 805.7 (Figure III.4) allowed to confirm the presence of NO_2-PC, based on typical fragmentation pattern namely loss of HNO_2 and loss of HNO_2+59 and HNO_2+183.

We calculated the ratio between the nitrated species and the corresponding non-modified PC (Figure III.3C). It was found that the ratio of NO_2-PC/non-modified PC was higher for PCs esterified with monounsaturated fatty acids such as for NO_2-PC 34:1 (NO_2-PC 16:0/18:1) at *m/z* 805.7, NO_2-PC 38:3 (NO_2-PC 18:2/20:1) at *m/z* 857.6 and NO_2-PC 38:5 (NO_2-PC 18:1/20:4) at *m/z* 853.7. This is in agreement with a recent report showing

that the increase in fatty acid length and in the unsaturation degree has a negative impact on the susceptibility towards NO_2^+ driven nitration [5]. Using kinetic studies, authors reported that NO_2-OA was formed faster compared to nitro-linoleic, nitro-arachidonic and nitro-docosahexaenoic acids. Interestingly, in our study, the non-modified PC molecular species (PC 16:0/18:1 at *m/z* 760.6 (POPC), PC 18:2/20:1 at *m/z* 812.7 (GLPC) and PC 18:1/20:4 at *m/z* 808.6 (OAPC)) precursors of the NO_2-PCs showing the higher percentage of conversion share the presence of one (mono)unsaturated fatty acyl chain in their composition.

In this study, we were able to identify one nitrated PE species at *m/z* 837.5 (NO_2-PE 18:0/22:6) formed from nitration of PE 18:0/22:6 at *m/z* 792.5 (SDPE) bearing docosahexaenoic acid (Dha) as unsaturated fatty acyl chain (Supplementary Figure S-14, Appendix A). We have reported earlier the presence of PEs molecular species from cardiac mitochondria with high percentage of polyunsaturated fatty acids, mainly AA and Dha [156]. This could justify the observed lack of nitrated PEs in T1DM cardiac mitochondria. Interestingly, rat primary cardiomyocytes treated with the peroxynitrite donor 3-morpholinosydnonimine (SIN-1) showed increased levels of Dha-NO_2 when compared with NO_2-AA (~3 fold) [5].

The present results are significant as they highlight the presence of NO_2-PCs and NO_2-PEs derivatives in biological samples, subjected to oxidative stress, allowing the quantification of the percentage of conversion of non-modified PL in NO_2-PL. However, more research on this topic needs to be undertaken before the *in vivo* significance of phospholipid nitration is understood.

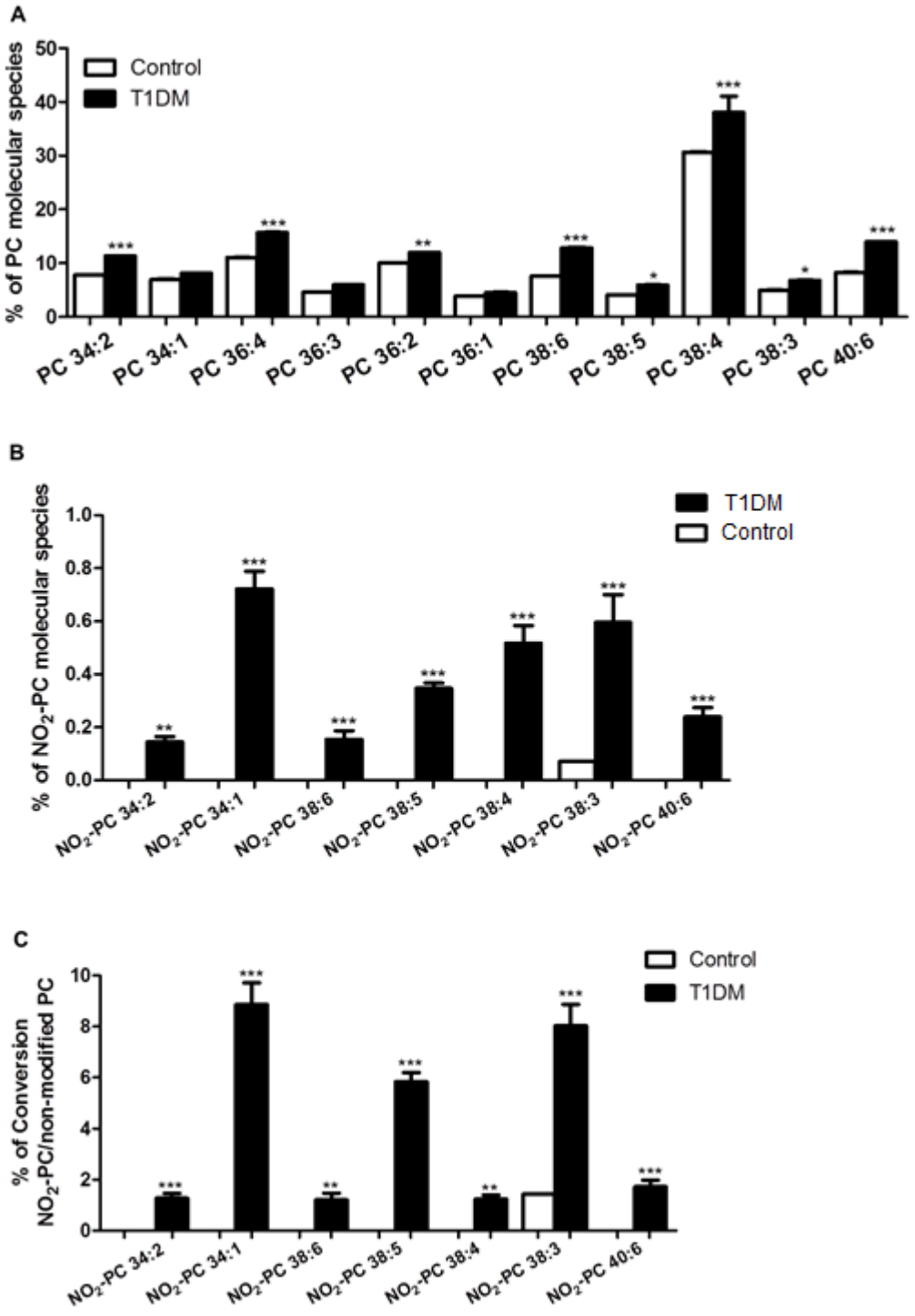

Figure III.3. A) Phosphatidylcholine (PC) molecular species profile observed for cardiac mitochondria of control group and type 1 diabetes mellitus (T1DM) group identified after LC-MS/MS analysis. B) NO_2-PC molecular species identified after LC-MS/MS analysis for cardiac mitochondria of control group and for type 1 diabetes mellitus (T1DM) group. The results were expressed as relative percentage obtained by dividing the ratio between

the peak areas of each PC molecular specie and the PC internal standard (dMPC) and the total of all ratio. Values are means±standard deviation. *p<0.05, **p<0.01 and ***p<0.0001, significantly different from control group. C) Ratio between non-modified PC molecular species and NO_2-PC in T1DM. The results were expressed as relative percentage determined by dividing the ratio between the peak areas of each NO_2-PC molecular specie and the PC internal standard (dMPC) and the ratio between the peak areas of the correspondent non-modified PC molecular specie and the PC internal standard (dMPC). Values are means±standard deviation. **p<0.01 and ***p<0.0001, significantly different from control group.

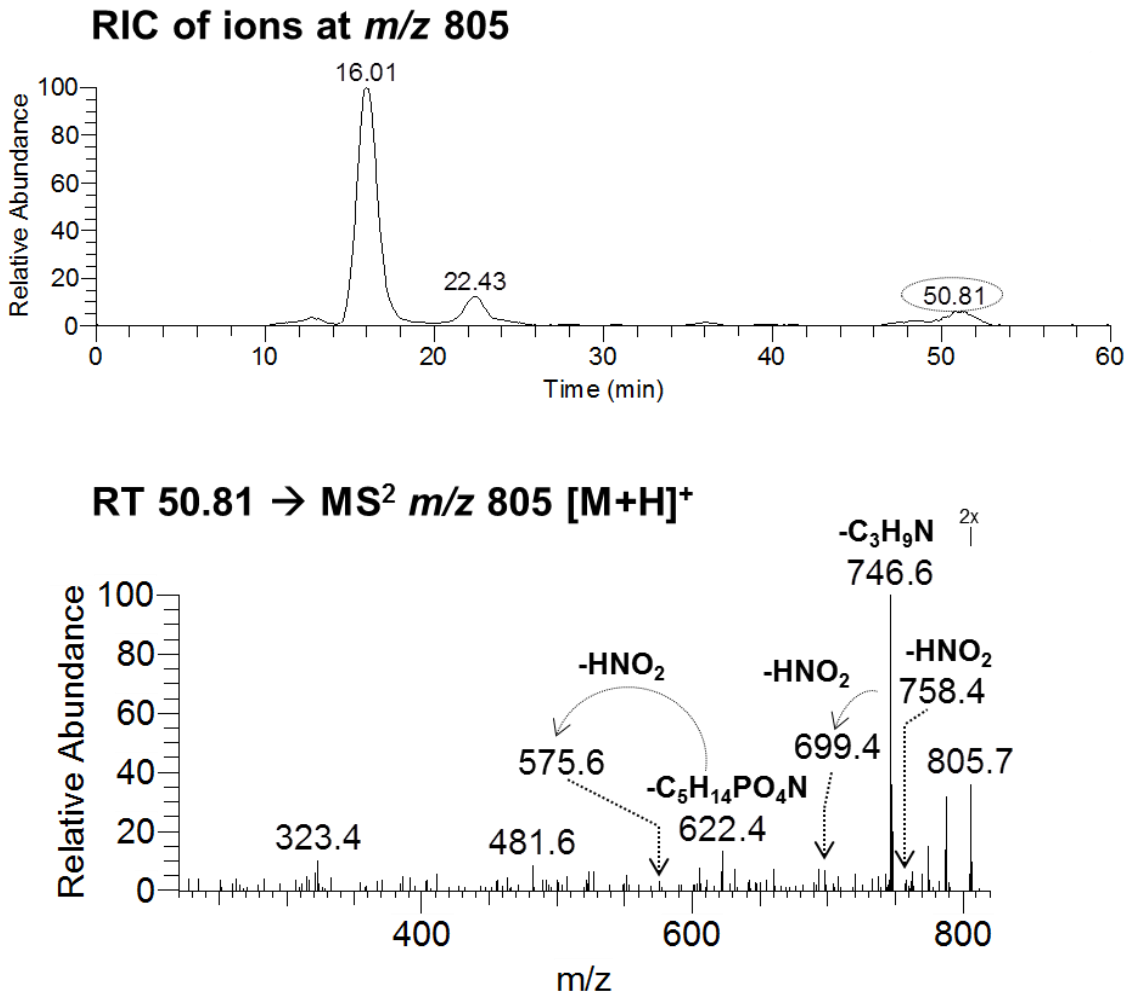

Figure III.4. Reconstructed ion chromatogram (RIC) and HILIC-ESI-MS/MS spectrum of ions at *m/z* 805.7 ($[M+H]^+$), retention time (RT) = 50.81 min, observed in mitochondria from T1DM heart.

III.1.1.3. Concluding Remarks

In this study, we studied the *in vitro* formation of nitroalkenes derivatives of PCs, PEs and PSs after reaction with NO_2BF_4. Tandem mass spectra of the identified species (NO_2-PC, NO_2-PE and NO_2-PS) were acquired in order to determine the main fragmentation pathways of NO_2-PLs. The fragmentation pattern observed in the MS/MS spectra of all PLs classes, showed product ions involving the neutral loss of HNO_2, product ions formed by cleavage in the vicinity of the NO_2 group and the presence of the nitrated fatty acyl chains.

This approach allowed us to propose MS-based strategies that can allow simple, specific, rapid and sensitive analytical methodologies for the *in vitro* and *in vivo* detection and characterization of phospholipid nitration products. These approaches include specific tandem mass spectrometry modes such as MRM, PIS or NLS and can be used to identify and quantify NO_2-PL in biological samples. On the basis of the typical fragmentation pattern observed for the NO_2-PLs standards, we were able to identify ten nitrated derivatives of phospholipids, nine NO_2-PCs and one NO_2-PE, in cardiac mitochondria isolated from heart of a well-characterized animal model of type 1 diabetes mellitus.

Nevertheless, more efforts are needed in order to test the propose scan modes and to extend the identification of nitrated PLs in other conditions. This will contribute for the understanding of nitration mechanisms in biological environments, and to establish the physiological relevance of NO_2-PL species.

CHAPTER III. RESULTS AND DISCUSSION

III.1. UNDERSTANDING THE NITROXIDATIVE STRESS-INDUCED MODIFICATIONS OF PHOSPHOLIPIDS

III.1.2. PHOSPHOLIPID NITROXIDATION IN H9c2 MYOBLAST USING A LIPIDOMIC APPROACH

The results and discussion presented in this section were integrally submitted as follow:

Melo T, Domingues P, Ribeiro-Rodrigues TM, Girão H, Segundo MA, Domingues MRM (2016) Phospholipid nitroxidation in H9c2 Myoblast using a lipidomic approach. *Free Radical Biology and Medicine*, under revision.

III.1.2.1. Background and Aim of the Study

Under nitroxidative stress conditions, lipids are prone to be modified by reaction with reactive nitrogen species (RNS) and different modifications were reported to occur in fatty acids. However, in the case of phospholipids (PL), studied under nitroxidative stress conditions, only nitroalkene derivatives of phosphatidylcholine (PC) and phosphatidylethanolamine (PE) were reported when using both *in vitro* biomimetic conditions and *in vivo* model system of type 1 diabetes mellitus. Therefore, in order to further explore other nitroxidative modifications of PL, a biomimetic model of nitroxidation combined with liquid chromatography mass spectrometry (MS) and MS/MS approaches were used to characterize the nitrated and nitroxidized derivatives of PCs and PEs.

Results gathered with *in vitro* biomimetic models were validated by screening the nitrated and nitroxidized PL species in a cardiomyoblast cell line (H9c2), a suitable model for cardiac cells, in conditions of starvation and ischemia, to mimic the conditions to which cardiomyocytes are exposed during acute myocardial infarction.

III.1.2.2. Results and Discussion

Nitrated and nitroxidized modifications of PLs were induced by co-incubation of nitronium tetrafluoroborate (NO_2BF_4) with PC (POPC, PLPC and PAPC) and PEs (POPE, PLE and PAPE). These PL species were selected considering that PCs and PEs are the major constituents in membranes and, as reported for free fatty acids, different degree of unsaturation were chosen and this can lead to different susceptibility to nitration [5].

The formation of nitrated and nitroxidized products of PLs was monitored by ESI-MS and LC-MS. These products were observed in positive-ion mode as $[M+H]^+$ ions for PCs and PEs and negative-ion mode as $[M-H]^-$ ions for PEs (Supplementary Figures S-2 and S-3, Appendix B). Analysis of the MS data revealed new ions observed at higher *m/z* values that the non-modified PLs, which are consistent with the formation of nitrated and nitroxidized products (Supplementary Tables S-1 and S-2; Figures S-2 and S-3, Appendix B). These ions were assigned as nitroso PL (NO-PL and $(NO)_2$-PL) and nitro PL (NO_2-PL and $(NO_2)_2$-PL). Products bearing concomitantly NO with NO_2 groups (nitronitroso, (NO_2)(NO)-PL), and products bearing one or two NO_2 with hydroxy or hydroperoxy

moieties were also observed (Supplementary Tables S-1 and S-2, Appendix B). Weak signals attributed to the well-known oxidized derivatives of PCs and PEs, namely keto, hydroxy and hydroperoxy derivatives were also observed [173, 174]. Elemental composition and mass accuracy measurements supported the structural assignments that could be made with a high degree of confidence (Supplementary Tables S-3 and S-4, Appendix B).

Typical fragmentation of nitrated and nitroxidized PL products was obtained performing reversed-phase LC-ESI-MS and LC/ESI-MS/MS, which allowed to confirm the proposed assignments, to identify specific fragmentation pattern that can be used for target lipidomics analysis of biological samples, and to unveil isomeric species.

LC-MS and LC-MS/MS analysis of Nitrated Phospholipids

Nitro PL derivatives (NO_2-PL) showed typical fragmentation assigned as loss of HNO_2 (-47 u) [175]. Nitroso derivatives, NO-PL and $(NO)_2$-PL (Tables S1 and S2), showed product ions arising from the loss of one or two nitroxyl groups (31 u, HNO), thus confirming the presence of a NO group. The absence of fragment ions arising from loss of HNO_2 (47 u) confirmed the proposed assignment and the nonexistence of a NO_2 group linked to PL (Figure III.5; Supplementary Figures S-4 A, B and S-5, Appendix B).

The LC-MS chromatogram of PL nitrated products with a mass shift of +45 u eluted in two distinct peaks (Supplementary Tables S-1 and S-2). The MS/MS data, obtained in each retention time, allowed to differentiate the isomeric nitrosohydroxy ((NO)O-PL) and the nitro derivatives (NO_2-PL). As exemplified for POPE + 45u (Figure III.6; Supplementary Figures S-6 to S-8, Appendix B), the MS/MS spectrum of the nitrosohydroxy derivative (RT 31.3 min) showed the fragment ions arising from the neutral of HNO typical of the nitroso derivatives, but no fragment ions arising from the neutral loss of HNO_2 were observed, while the isomer eluting at 44.0 min attributed to NO_2-POPE only displayed the neutral loss of HNO_2 [175]. Nitronitroso derivatives, (NO_2)(NO)-PL (Figure III.7A; Supplementary Figures S-4 C, E and S-9, Tables S-1 and S-2, Appendix B) showed in their MS/MS spectra fragment ions arising from both neutral losses of HNO_2 and HNO, while dinitro derivatives $(NO_2)_2$-PL showed fragment ions arising from from loss of one and two HNO_2 (Figure III.7B; Supplementary Figure S-4 D, F and S-10; Tables S-1 and S-2, Appendix B).

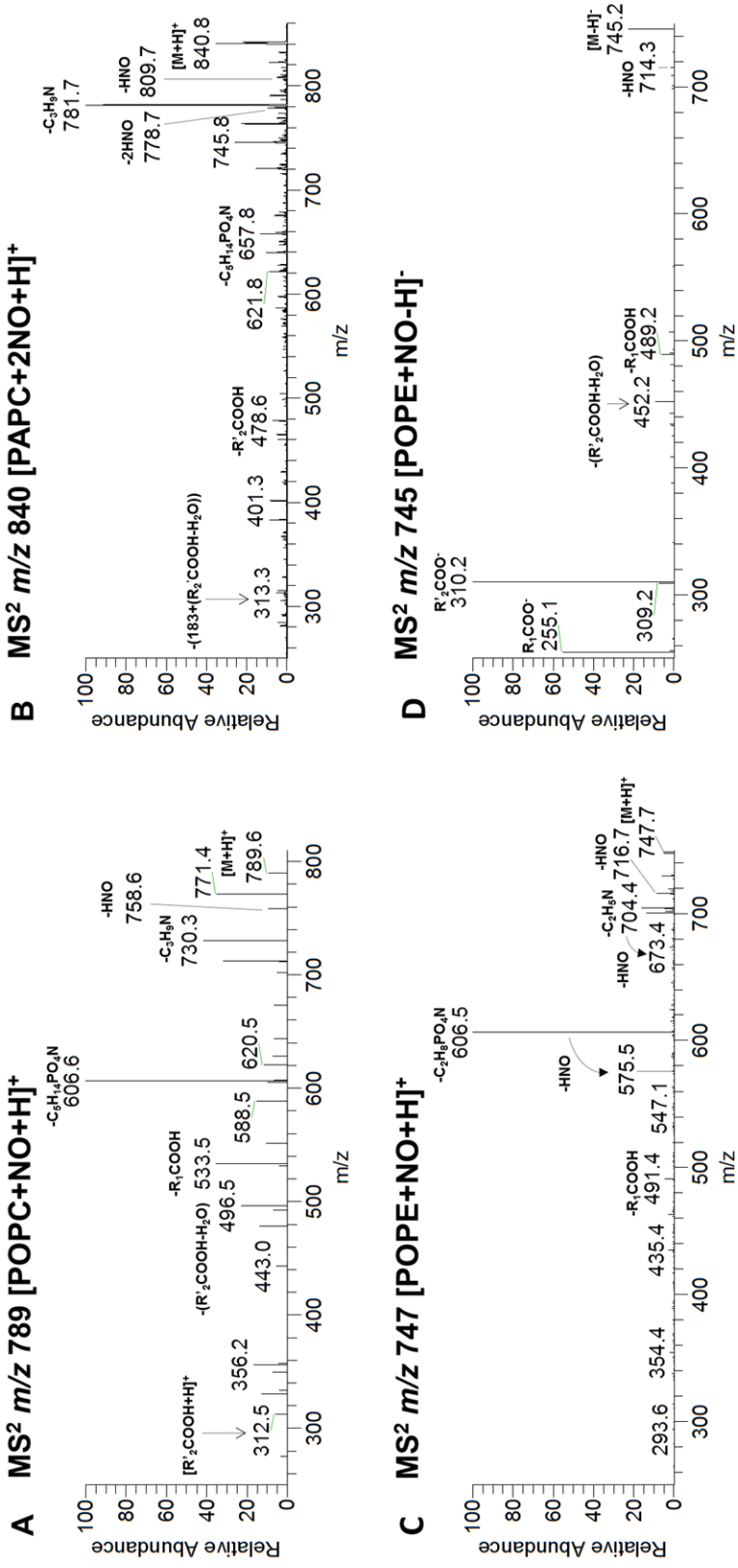

Figure III.5. LC tandem mass spectra of nitroso and dinitroso molecular species of PC and PE. LC-ESI-MS/MS spectra of $[M+H]^+$ ions at *m/z* 789.6 (POPC+NO), 840.8 (PAPC+2NO), 747.6 (POPE+NO) and LC-ESI-MS/MS spectrum of $[M-H]^-$ ions at *m/z* 745.2 (POPE+NO).

The LC-MS/MS spectra of PL products that were simultaneously oxidized and nitrated, namely nitrohydroxy, nitrohydroperoxy, dinitrohydroxy and dinitrohydroperoxy, showed fragment ions arising from the neutral losses of one or two HNO_2 depending on the presence of one or two NO_2 moieties, but no fragment ions arising from the neutral loss of HNO could be observed (Figure III.7 C and D; Supplementary Figures S-11 to 17; Tables S-1 and S-2, Appendix B). MS/MS of hydroperoxy derivatives showed losses of 32 u (O_2) or 34 u (H_2O_2) (Figure III.7 C and D; Supplementary Figures S-11 to 17, Appendix B) [174, 176]. The above described reporter fragmentations are typical for MS/MS obtained both positive- ($[M+H]^+$) and negative-ion mode ($[M-H]^-$) ions.

Besides the fragmentation patterns involving nitro and nitroso groups, the MS/MS data in positive mode ($[M+H]^+$ precursor ions) from nitrated precursor ions also showed typical fragmentation involving PCs and PEs polar head group: fragment ions arising from neutral loss of 59 u and 183 u for PCs; and 43 u and 141 u for PEs. Moreover, ions arising from combined neutral losses of polar head groups and loss of HNO and HNO_2 were also assigned (Table III.2).

Fragmentation patterns involving nitrated fatty acids linked to PL could also be seen in MS/MS data, as summarized in Tables III.2 and S5. In positive mode, there were abundant product ions formed by loss of nitrated or nitroxidized *sn*-2 fatty acyl chains as acid or keto derivatives, and product ions corresponding to protonated modified fatty acids $[NO_n\text{-}FA+O_n+H]^+$, $[NO_n\text{-}FA+O_n\text{-}H_2O+H]^+$, and $[NO_n\text{-}FA+O_n\ \text{-}2H_2O+H]^+$, n=1-2. In negative mode, modified carboxylate anions, namely $[NO_n\text{-}FA+O_n\text{-}H]^-$, $[NO_x\text{-}FA+O_x\text{-}H_2O\text{-}H]^-$, and $[NO_n\text{-}FA+O_n\text{-}2H_2O\text{-}H]^-$ (n=1-2) ions were assigned both in the nitrated or nitroxidized products.

Identification of nitrated and nitroxidized species of Phospholipids in Cardiomyoblasts

The information on the typical fragmentation pattern observed in this study for the nitrated and nitroxidized PCs and PEs derivatives in biomimetic *in vitro* model system, was used to search for the nitroxidative PCs and PEs modifications in cardiomyoblasts (H9c2) under starvation or ischemia conditions, mimicking the acute myocardial infarction conditions [177]. Notably, the generation of NO_2-FA was reported during ischemia/reperfusion [76] and heart ischemia preconditioning [77].

In our study, we have not identified any nitrated or nitroxidized PL products on cells under ischemia or control conditions. However, we identified nitrated and nitroxidized PCs and PEs species on H9c2 cells under starvation. The modified PCs we have identified were the following: one nitro derivative at *m/z* 805.8 (NO_2-PC 16:0/18:1); two dinitro derivatives at *m/z* 822.9 ($(NO_2)_2$-PC 16:0/16:1) and 850.8 ($(NO_2)_2$-PC 16:0/18:1); one nitroso derivative at *m/z* 817.7 (NO-PC 18:0/18:1); one nitronitroso derivative at *m/z* 858.4 ((NO_2)(NO)-PC 16:0/20:3); and one nitroxidized derivative at *m/z* 837.7 (NO_2)(2O)-PC 16:0/18:1 (Supplementary Figures S-19 and S-20, Appendix B).The relative amount of nitrated and nitroxidized PC molecular species and the ratio between the modified PCs molecular species and the corresponding non-modified PC were calculated and are shown in Figure III.8A to C. The modified PCs molecular species found to be present in higher relative amount was the nitro derivative (NO_2-PC 16:0/18:1) followed by the dinitro derivatives ($(NO_2)_2$-PC 16:0/18:1 and ($(NO_2)_2$-PC 16:0/16:1). The nitroso derivative (NO-PC 18:0/18:1) was the modified species with lower relative amount. In figure III.8C and D, the ratio of conversion, calculated by the ratio between nitrated and non-modified PL's, is shown. The modified species with higher ratio of conversion were the nitro NO_2-PC 16:0/18:1 followed by the dinitro $(NO_2)_2$-PC 16:0/18:1 and nitronitroso (NO_2)(NO)-PC 16:0/20:3 derivatives, respectively (Figure III.8C). In the case of PE, we were able to identify two nitrated PE species: NO_2-PE 34:1 and NO_2-PE 36:1, at *m/z* 763.7 and 791.5, respectively (Supplementary Figures S-21 and S-22, Appendix B), and their percentage of conversion are shown in Supplementary Figure III.8D (Appendix B).

Nitration seems to be favored in hydrophobic environment of biological membranes, where RNS easily diffuse, cross membranes and accumulate [48, 178, 179], being related with the formation of nitrated fatty acids [59]. As so, phospholipids in biomembranes are expected to be also a target for lipid nitration but these types of PL modifications are scarcely reported.

In the present study, biomimetic models with PC and PE, the most abundant PL in membranes, were used to simulate nitroxidative stress conditions using NO_2BF_4, a salt of nitronium ion (NO_2^+), recognized as a biomimetic agent of phospholipid [175] and fatty acid nitration [5, 9, 58]. Herein, we reported the fragmentation patterns of these nitrated species. This involved combined losses of HNO, HNO_2, for single and multiple nitrated species, and also combined losses with fragmentation of polar head groups of PC and PE.

These fragmentation pathways can be used to pinpoint nitro and nitroxidized modifications of PL in biological samples. Results gathered in this study allow to identify specific fragmentation pathways for NO-PL, $(NO)_2$-PL, NO_2-PL, $(NO_2)_2$-PL, $(NO_2)(NO)$-PL, $(NO)O$-PL, $(NO_2)O$-PL, $(NO_2)(2O)$-PL, $(NO_2)_2O$-PL and $(NO_2)_2(2O)$-PL species.

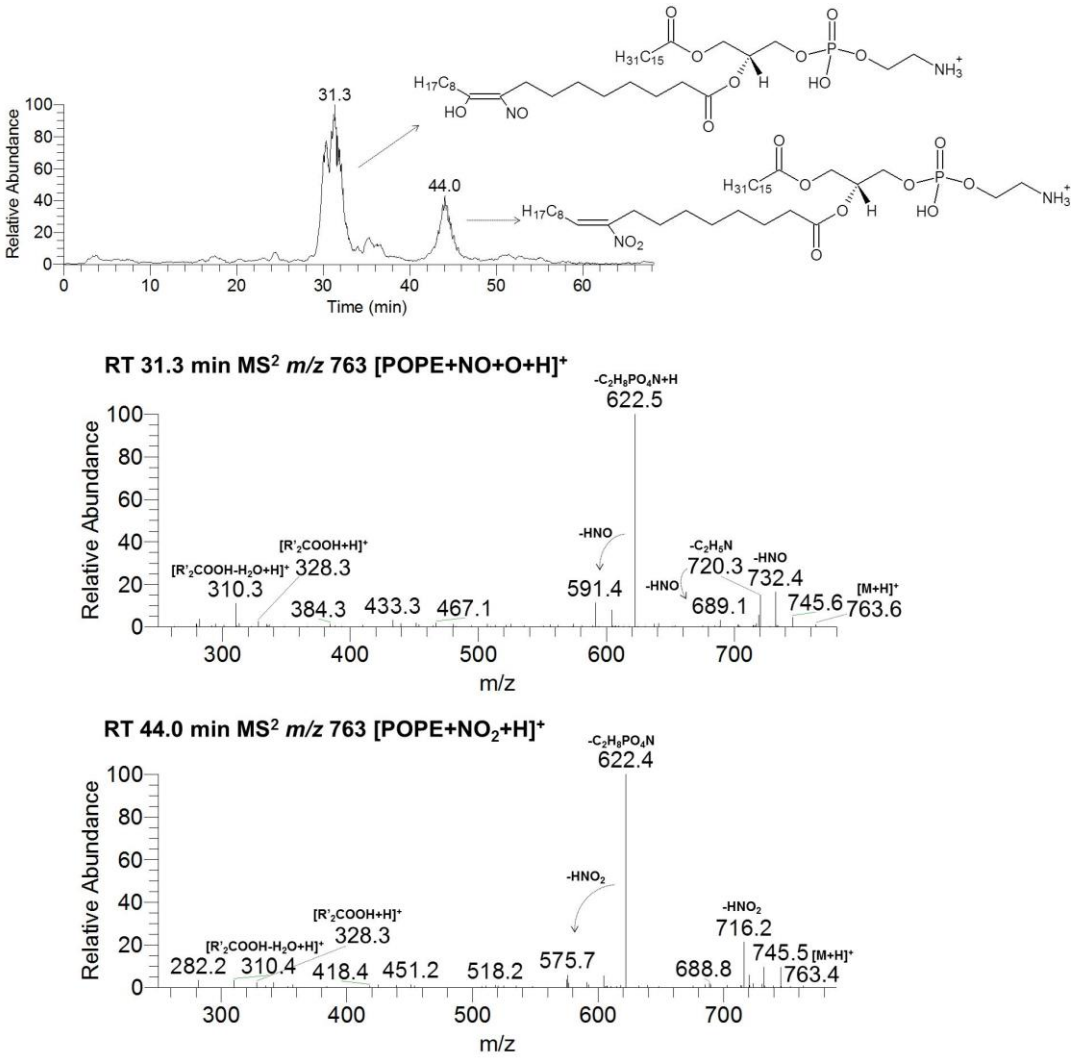

Figure III.6. LC tandem mass spectra of isomers of nitroxidized and nitrated PE. LC-ESI-MS/MS spectra of $[M+H]^+$ ions at *m/z* 763.5 (POPE+NO+O) and 763.4 (POPE+NO_2).

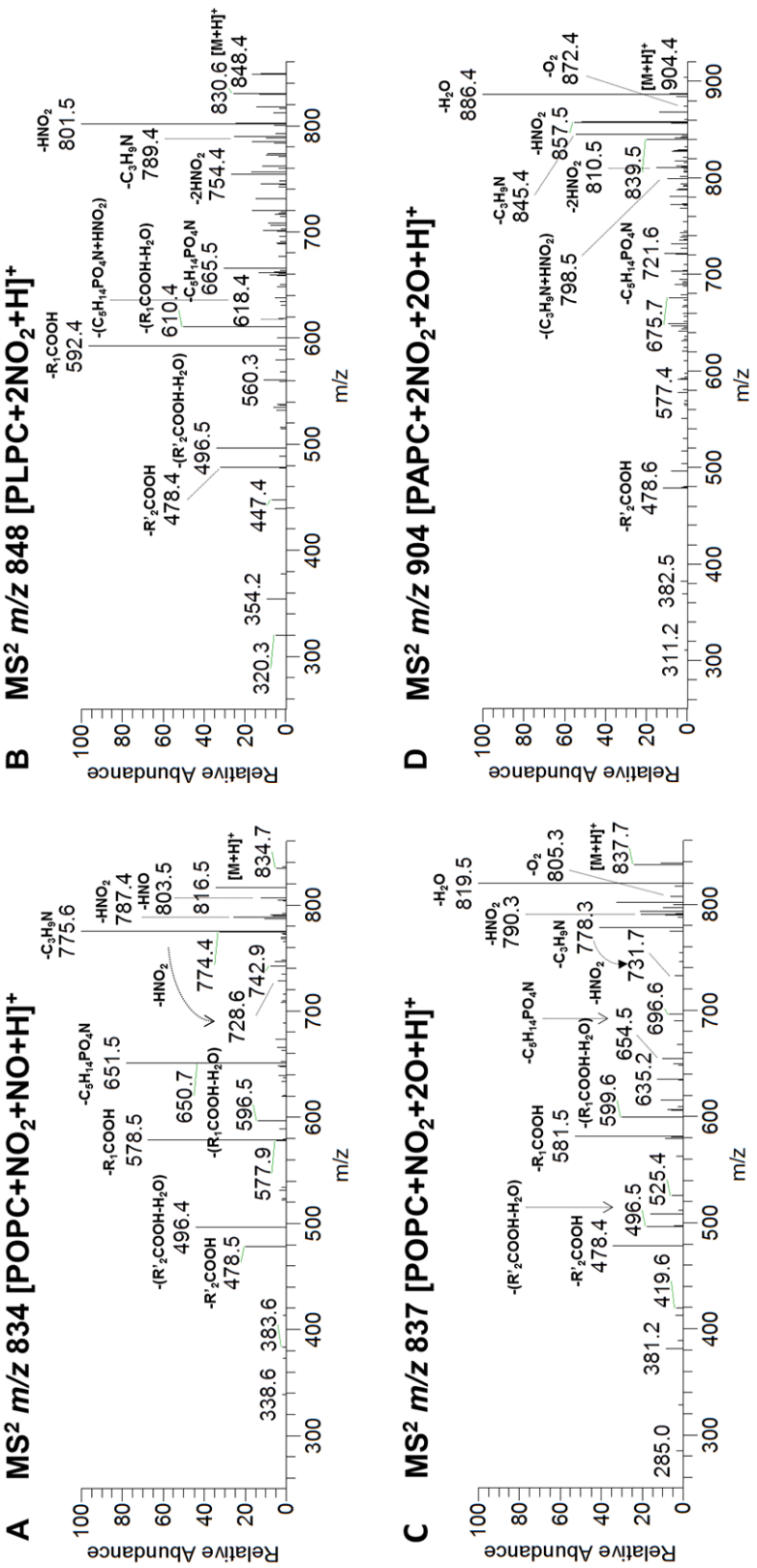

Figure III.7. LC tandem mass spectra of nitronitroso, dinitro and nitroxidized molecular species of PC. LC-ESI-MS/MS spectra of $[M+H]^+$ ions at *m/z* 834.7 (POPC+NO_2+NO), 848.4 (PLPC+2NO_2), 837.7 (POPC+NO_2+2O), and 904.4 (PAPE+2NO_2+2O).

Table III.2. Typical neutral losses and product ions observed in tandem mass spectra that can be used for diagnostic scan of nitrated and nitroxidized PLs in positive- and negative-ion mode.

		Mass shift to non-modified PLs	Typical Neutral Losses (NL) for Diagnostic Scan in MS^2
Nitrated derivatives			
NO-PL	**Nitroso**	+29	-31 u (HNO)
NO_2-PL	**Nitro**	+45	-47 u (HNO_2)
$(NO)_2$-PL	**Dinitroso**	+58	-31 u (HNO) -62 u (2HNO)
$(NO_2)(NO)$-PL	**Nitronitroso**	+74	- 47 u (HNO_2 -31 u (HNO)
$(NO_2)_2$-PL	**Dinitro**	+90	- 47 u (HNO_2) - 94 u ($2HNO_2$)
Nitroxidized derivatives			
(NO)O-PL	**Nitrosohydroxy**	+45	-18 u (H_2O) -31 u (HNO)
(NO_2)O-PL	**Nitrohydroxy**	+61	-18 u (H_2O) - 47 u (HNO_2)
$(NO_2)(2O)$	**Nitrohydroperoxy**	+77	-18 u (H_2O) - 32 u (O_2) -47 u (HNO_2)
$(NO_2)_2$O-PL	**Dinitrohydroxy**	+106	-18 u (H_2O) -47 u (HNO_2) -94 u ($2HNO_2$)
$(NO_2)_2(2O)$-PL	**Dinitrohydroperoxy**	+122	-18 u (H_2O) -32 u (O_2) -47 u (HNO_2) -94 u ($2HNO_2$)

Neutral losses of nitrated /and nitroxidized (-31 and -47 u) can be seen combined with the typical fragmentation of polar head of PLs [164]: PCs: NL+59 u (C_3H_9N) and NL+183 u ($C_5H_{14}PO_4N$); PEs: NL+43 u (C_2H_5N) and NL+141 u ($C_2H_8PO_4N$).

The reported fragmentations proposed in this study were further validated by allowing to pinpoint nitrated and nitroxidized PL species in the lipidome of the cardiomyoblast H9c2 cell line under starvation, but not upon ischemia or control conditions. It is known previously that phospholipid profile changes as an adaptation/response mechanism to these pathophysiological conditions and can have a role in cell survival or cell death [177]. In the case of starvation, a decrease in the relative abundance of PC 34:1, and an increase in PS 36:1 molecular species were observed, when comparing both with control and ischemia [177]. It was suggested that this could be associated with adaptive pathways related with cell recovery and survival, preventing the events that triggers apoptosis and cell death

[177]. Also, the decrease of PC 34:1 could be due to being modified by RNS, since the formation of their nitro derivatives was observed exclusively in starvation.

In our study, the PL nitro derivatives showed higher relative abundance in comparison with nitroso or nitroxidized derivatives. In biological systems, it is reasonable to assume the formation of the nitro derivatives of lipids as the first step of nitration reactions. These products can further react with ROS or other RNS to generate the other products, such as nitroso, dinitro, nitronitroso and nitroxidized derivatives. Also, reaction of nitro derivatives with O_2 can lead to the formation of a nitrohydroperoxide derivative, which can be further reduced to form the nitrohydroxy derivative [65]. These assumptions are also supported by the findings of Milic and co-authors [5] where, during both electrophilic (NO_2^+) and free-radical-mediated nitration of fatty acids, found that nitro derivatives do not represent the final products, but are prone to be further nitrated or oxidized leading to the formation of multiple nitrated, nitroso, nitronitroso and nitroxidized derivatives.

Also, in our study, we were unable to observe the formation of NO_2-PLs in ischemia simulating conditions. Interestingly, other authors have reported that endogenous generation of nitroalkene derivatives of fatty acids does not occur [76] or occurs in a very low extent, generating a minute amount of NO_2-FA [77] in myocardial ischemia without reperfusion. In fact, we only observed nitrated PL species in starvation condition but not in ischemia. In spite of the biological effects of nitrated and nitroxidized PLs have not been reported and remain unknown, it is well recognized that nitroalkene derivatives of fatty acids have important biological signaling actions as anti-thrombotic [111], anti-hypertensive [96, 97, 109] and anti-inflammatory agents [10, 11, 70, 94, 98, 100, 102, 105-108]. Nitroxidized fatty acids have also been reported as anti-hypertensive agents [65].

It is well-known that nitro-fatty acids trigger their biological signaling events by post-translational modifications (PTM) of key proteins such as PPARγ, NF-κB, Keap1-Nrf2, AT_1 receptor, heme oxygense 1 (HO-1) [11, 76, 94, 96, 100, 105, 121, 180], regulating pivotal signaling pathways essential to ensure cellular homeostasis and provide protection to the cardiovascular system by affecting various biological processes namely reduction of vascular inflammation [76, 181] and platelets aggregation [111], enhancement of vasodilatation [111], stimulation of anti-inflammatory and antioxidant mechanisms [13]. For all of these reasons, an important modulatory role have been ascribed to NO_2-FA in the

context of cardiovascular diseases [180], contributing to reduce the risk of atherosclerosis, myocardial infarction and stroke.

Although nitroalkene derivatives of arachidonic acid (NO_2-AA), linoleic acid (NO_2-LA) and oleic acid (NO_2-OA) can be involved in PTM, NO_2-OA seems to be a preferential player [11, 12]. Thus, it is conceivable that the main formation of NO_2-PL derivatives bearing OA could have a critical role in cell survival associated with autophagy and starvation. Moreover, there is now sound evidence that NO_2-OA may be an upstream signal-regulating species in autophagy [77, 138]. Indeed, NO_2-OA has been reported to potently activate all PPAR isoforms, including peroxisome proliferator-activated receptor-α (PPARα) and peroxisome proliferator-activated receptor-γ (PPARγ) [11, 94, 132]. PPARα is highly expressed in heart and cardiomyocytes [182-184], where upregulates the expression of many genes encoding enzymes of fatty acid transport, esterification, uptake, and utilization via β-oxidation [185]. Thus, its activation could be of remarkable importance in the adaptation to starvation conditions. PPARγ is involved in the regulation and maintenance of metabolic homeostasis [183, 185, 186] but has also been associated with anti-inflammatory pathways and regulation of inflammatory responses [182, 187, 188]. PPARγ activation has an important role in the maintenance of normal heart function, [182, 189] reversed myocardial lipid accumulation, increased glucose oxidation, improved and restored myocardial heart function in a rat model of type 2 diabetes [186]. Nitro- and nitrohydroxy derivatives of fatty acids are physiologically relevant candidates as endogenous ligands of PPARγ [78]. There are *in vitro* evidences that PPARγ activation is very sensitive to NO_2-OA [133] leading to PPARγ-mediated anti-inflammatory actions [100, 102, 187, 190]. Therefore, it is plausible that the presence of NO_2-PLs in cardiomyoblast H9c2 cells relates with PPARγ activation, which could sustain the resolution of myocardium infarction.

Additionally, PPARγ is reported to protect cardiomyocytes from oxidative stress-induced apoptosis, decreasing hydrogen peroxide (H_2O_2)-induced apoptosis in cardiomyocytes [188, 191, 192]. Upregulation of genes controlled by NF-κB transcription factor signaling pathways [193], which has been related with cardiomyocyte pro-inflammatory cytokine release and apoptosis, and the induction of intracellular accumulation of Ca^{2+} in cardiomyocytes leading to heart dysfunction [194], together with being a precursor of hydroxyl radical are some of the adverse roles attributed to H_2O_2.

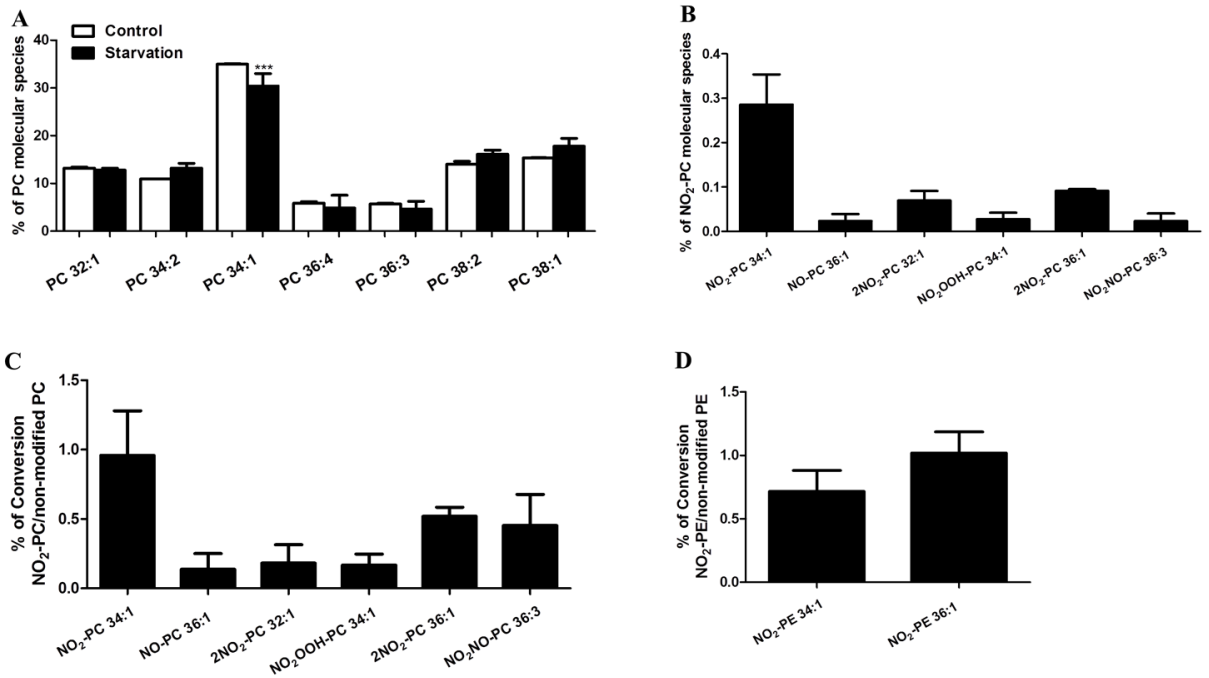

Figure III.8. Nitrated and nitroxidized PCs and PEs in cardiomyoblast cell line (H9c2) in a model of myocardium starvation. A) Major molecular species of phosphatidylcholine (PC) observed for H9c2 cells from control and starvation conditions, identified after HILIC-LC-MS/MS analysis. Values are mean±standard deviation. ***$p<0.0001$, significantly different from control group. B) Nitrated and nitroxidized molecular species of PC identified after HILIC-LC-MS/MS analysis for H9c2 cells from starvation condition. These results (from A and B) were expressed as relative percentage obtained by the ratio between the peak areas of each molecular species of PC and the PC internal standard (PC 14:0/14:0), normalized by the total area of PCs. C) Ratio between the relative abundance of nitrated or nitroxidized molecular species of PC and the corresponding non-modified molecular species of PC. D) Ratio between the relative abundance of nitrated molecular species of PE and the corresponding non-modified PE molecular species.

Activation of PPARγ by NO_2-OA has already been associated with a concomitant downstream regulation of NF-κB [100]. Thus, the presence of the NO_2-PLs could also be correlated with PPARγ activation, with anti-inflammatory and cardioprotective effects in H9c2 cardiomyoblast cells.

Nevertheless, activation of PPARγ is not the only mechanism by which NO_2-OA, and possibly NO_2-PLs bearing NO_2-OA, exerts their beneficial actions. NO_2-OA also demonstrated to have a potent inhibitory effect on NF-κB activation and translocation to the nucleus by alkylation of the p65 subunit, thus modulating the release of pro-inflammatory cytokines and inflammatory signaling [13, 76, 132, 181]. NO_2-OA up-regulates Nrf2 activity and expression by alkylation of the inhibitor protein keap1 [104, 105, 122, 195]. NO_2-OA is involved in heme oxygenase 1 (HO-1) expression and activation, which also mediates anti-inflammatory actions [13, 98, 104, 107]. NO_2-OA can induce heat shock factor 1 (HSF1)- and HSF2-dependent activation of heat shock responsive genes [105] in order to regulate the heat shock response, which is a ordered response to metabolic dysregulation and exposure to inflammatory-derived reactive species [196]. The fact that NO_2-OA being able to trigger the Keap1-Nrf2 pathway and the heat shock response is related to cellular adaptation and enhancement of cell survival [197]. In fact, NO_2-FA has been suggested to an upstream signal for regulation of autophagy, thus confering cardioprotection [77, 138]. Autophagy is an adaptive survival response that aims to replenish the energy and "building blocks" required for cells survival when nutrients are scarce [198] being therefore a key mechanism to ensure the maintenance of the cardiac homeostasis under nutrients and oxygen deprivation conditions [199]. Under myocardial ischemia, where both oxygen and nutrient deprivation (starvation) occur simultaneously, there is an activation of autophagy, that according to its duration and extent can determine the cell fate, either survival or death [200, 201]. It is also established that in ischemic conditions, the activity of nitric oxide synthase (NOS) (mostly eNOS and nNOS) is reduced leading to reduced or diminished $NO^{\bullet}$ generation and release [202]. Therefore, the low levels of $NO^{\bullet}$ may not be enough to lead the generation of RNS able to induce nitration or nitroxidation of PLs. Thus, it is conceivable that the presence of NO_2-FA esterified to PLs observed only in cardiomyoblasts under starvation may be also correlated with cardioprotective pathways.

III.1.2.3. Concluding Remarks

In this study, by using a lipidomics approach, we have been able to identify and characterize nitroalkene derivatives of PLs (NO_2-PLs) and other single and multiple nitrated species such as nitroso, dinitroso, dinitro and nitronitroso derivatives, together with nitroxidized species.

The tandem mass spectrometry typical fragmentation pattern obtained for nitrated and nitroxidized phospholipid standards showed to be a valuable tool for the detection of the nitrated and nitroxidized derivatives of phospholipids (PCs and PEs) *in vivo*.

In cardiomyoblasts subjected to starvation, but not in control or ischemia conditions, we were able to identified one NO_2-PC, two $(NO_2)_2$-PCs, one (NO_2)(NO)-PC, one NO-PC, one (NO_2)(2O)-PC and two NO_2-PEs. These products can have a role in cardioprotection by post-translational modifications of the key proteins, directly or after release of the nitrated/nitroxidized fatty acid moiety. These modifications of target proteins may initiate a cascade of signaling actions leading to the stimulation of anti-inflammatory and antioxidant pathways that can have an impact in reduction of the risk factors for onset and development of cardiovascular diseases.

Although this study contributed to unveil the products that can be formed under nitroxidative conditions *in vivo*, it is very important to further identify these modified lipids and increase our knowledge regarding susceptibility to be modified, mechanism of formation, and, ultimately to understand their biological actions.

CHAPTER III. RESULTS AND DISCUSSION

III.2. UNDERSTANDING THE BIOLOGICAL ACTIVITIES OF NITRATED AND NITROXIDIZED DERIVATIVES OF PHOSPHOLIPIDS

Nitro-fatty acids (NO_2-FA) and nitrohydroxy fatty acids ((NO_2)O-FA) have been described to exerts important biological signaling actions namely as anti-inflammatory, anti-hypertensive, and inhibitors of platelet aggregation – anti-thrombotic agents. Nitrated and nitroxidized phospholipids have been overlooked regarding both their identification/structural characterization and biological roles.

In order to give new insights in the biological activities of nitrated phospholipids, the antioxidant and anti-inflammatory activities of nitrated/nitroxidized phosphatidylcholine products were evaluated using different antioxidant assays, well recognized as tools to establish the antioxidant status of compounds or extracts, and evaluating their anti-inflammatory potential by measuring their effects on nitric oxide synthase expression in activated macrophages (Section III.2).

CHAPTER III. RESULTS AND DISCUSSION

III.2. UNDERSTANDING THE BIOLOGICAL ACTIVITIES OF NITRATED AND NITROXIDIZED DERIVATIVES OF PHOSPHOLIPIDS

III.2.1. NEW INSIGHTS IN ANTI-INFLAMMATORY AND ANTIOXIDANT PROPERTIES OF NITRATED PHOSPHOLIPIDS

The results and discussion presented in this section were integrally under revision as follow:

Melo T, Marques SS, Ferreira I, Cruz, MT, Domingues P, Segundo MA, Domingues MRM (2016) New Insights in Anti-inflammatory and Antioxidant Properties of Nitrated Phospholipids. *Chemistry and Physics of Lipids*, under revision.

III.2.1.1. Background and Aim of the Study

The nitroalkene derivatives of unsaturated fatty acids (NO_2-FA) have been widely studied regarding their identification, structural characterization and biological actions. NO_2-FA could also be present endogenously esterified to phospholipids (PL), and NO_2-PLs were already identified in cardiac mitochondria from a well-characterized animal model of type 1 diabetes mellitus. However, the biological actions of NO_2-PL have been overlooked.

The aim of this study was to evaluate the anti-inflammatory and antioxidant potential of the nitrated/nitroxidized 1-palmitoyl-2-oleoyl-*sn*-glycero-3-phosphocholine (POPC), namely the nitroalkene derivative (NO_2-POPC) that is the major product formed *in vitro* by incubation with nitronium tetraflouroborate (NO_2BF_4), in a well-recognized biomimetic model of nitroxidative stress. The antioxidant capacity was investigated through the evaluation of the radical scavenging capacity against 2,2-diphenyl-1-picrylhydrazyl radical ($DPPH^{\bullet}$), against 2,2'-azino-bis-3-ethylbenzothiazoline-6-sulfonic acid radical cation ($ABTS^{\bullet+}$) and through the oxygen radical absorbance capacity (ORAC) assay. Anti-inflammatory potential was assessed by evaluation the effects of nitrated POPC in the inducible nitric oxide synthase (iNOS) expression in RAW 264.7 macrophages activated by the *Toll-like* receptor 4 (TLR4) agonist lipopolysaccharide (LPS) in a well described *in vitro* model of inflammation.

III.2.1.2. Results and Discussion

Despite the mechanism of lipid nitration remains still under active investigation there are evidences concerning the formation and presence of NO_2-FA as free and esterified species *in vivo* [7, 9, 67, 69, 175]. Moreover, although *in vivo* concentrations of NO_2-FA are reported to range from the micromolar [11] to picomolar [9], during inflammatory conditions their levels have been shown to be greatly increased [71, 95]. These concentrations should be higher enough to allow NO_2-FA to exert biological actions namely as antioxidant and anti-inflammatory agents partially by counteracting the pro-inflammatory effects [16]. The biological actions described for NO_2-FA are based on their ability to potently regulate the expression of key inflammatory proteins [11, 94, 100, 117,

127, 128] and phase II antioxidant enzymes [70, 105, 107]. Inspired by the lack of knowledge concerning the anti-inflammatory and antioxidant potential of NO_2-FA esterified to phospholipids, we evaluated the anti-inflammatory and antioxidant capacity of a nitrated POPC. Nitrated POPC, whose nitroalkene derivative (NO_2-POPC) is the major product formed after biomimetic nitration, was chosen as a model system due to the high prevalence of phosphatidylcholine in mammalian cellular membranes and lipoproteins. In fact, POPC and oleic acid are, respectively, one of the major PC species and the most abundant monounsaturated fatty acid found in biological systems [68]. Besides, nitro-oleic acid is the most abundant nitroalkene derivative found in human plasma [10, 68] and NO_2-POPC was one of the major nitrated phospholipid specie recently detected *in vivo* [175]. Three common assays were used for measuring the antioxidant activity: $DPPH^{\bullet}$ assay, Trolox equivalent antioxidant capacity assay (with $ABTS^{\bullet+}$ radical cation) and ORAC assay. These assays are well recognized as instrumental tools to establish the antioxidant status of candidate compounds or extracts *in vitro* [205]. These methods differ in terms of their assay principles and experimental conditions, therefore, it is indispensable to consider all assays for the fully elucidation of the antioxidant capacity profile of a given compound or extract as no single method has the ability to accurately reflect the multiple mechanisms of antioxidant actions. The anti-inflammatory capacity of the nitrated POPC was assessed through evaluation of iNOS expression on LPS-stimulated RAW 264.7 macrophages. LPS is a TLR4 agonist able to evoke a pro-inflammatory profile in macrophages [163]. In all experiments, non-modified POPC was used as a control.

Antiradical Activity: $ABTS^{\bullet+}$ and $DPPH^{\bullet}$ Assay

The blue-green $ABTS^{\bullet+}$ radical can be reduced either by an antioxidant compound or a mixture by electron or hydrogen atom transfer, while the purple chromogen $DPPH^{\bullet}$ radical can be reduced through electron transfer to the corresponding pale yellow hydrazine [203].

The scavenging capacity of non-modified POPC and nitrated POPC (125, 150 and 250 µg/mL in ethanol) was evaluated by monitoring the absorbance decrease at 734 nm ($ABTS^{\bullet+}$) and 517 nm ($DPPH^{\bullet}$) during 120 min. Firstly, we assessed the amount (in percentage) of $ABTS^{\bullet+}$ (Supplementary Figure S-1A to A2, Appendix C) and $DPPH^{\bullet}$ radical (Supplementary Figure S-1B to B2, Appendix C) that remained in solution

throughout the reaction time. In the presence of the non-modified POPC, only a very slightly decreased in the percentage of both $ABTS^{\bullet+}$ and $DPPH^{\bullet}$ radical remaining was observed after 120 min of reaction as summarized in Table III.3. Thereby lower ability to scavenge the $ABTS^{\bullet+}$ and $DPPH^{\bullet}$ radicals can be attributed to non-modified POPC. These findings also allowed us to establish that both radicals are highly stable and not decayed by itself during the reaction time. In the presence of nitrated POPC, a marked decrease of the $ABTS^{\bullet+}$ radical remaining was found (Supplementary Figure S-1A to A2, Appendix C). The ability of nitrated POPC to reduce the $ABTS^{\bullet+}$ radical was concentration dependent, in spite of the response seems to be not linear. The percentage of inhibition of $ABTS^{\bullet+}$ radical obtained in the presence of non-modified POPC (control; white bar) and nitrated POPC (black bar, $P<0.0001$) was calculated and is shown in Figure III.9A and S2 A. In the presence of non-modified POPC the percentage of inhibition was found at basal levels thus the amount of $ABTS^{\bullet+}$ radical remaining was high, as reported above. For nitrated POPC, the percentage of inhibition was higher and enhanced by the increase of concentration (Figure III.9A). The IC50 value after 120 min of reaction was 124±2 µg/mL. Nitrated POPC also exhibits ability to reduce the $DPPH^{\bullet}$ radical since the percentage of $DPPH^{\bullet}$ radical remaining decreased during the reaction time (Supplementary Figure S-1B to B2, Appendix C). This ability seems to be dose-dependent since higher concentrations of nitrated POPC are reflected in a higher ability to reduce the $DPPH^{\bullet}$ radical (Table III.3). Figure III.9B and Supplementary Figure S-2B (Appendix C) show the percentage of inhibition of $DPPH^{\bullet}$ radical obtained in the presence of non-modified POPC (control; white bar) and nitrated POPC (black bar, $P<0.0001$). However, in comparison with the $ABTS^{\bullet+}$ assay, the decrease in the percentage of the remaining radical was lower and not allowed to achieve the 50% inhibition of $DPPH^{\bullet}$ radical (Figure III.9B and Supplementary Figure S-2B, Appendix C). For this reason, we were not able to calculate the IC50 value for $DPPH^{\bullet}$ assay. Instead, we calculate the IC20 value after 120 min of reaction, which was 225±4µg/mL. The obtained TE values were 152±9 µmol Trolox/g lipid for $ABTS^{\bullet+}$ assay and 86±6 µmol Trolox/g lipid for $DPPH^{\bullet}$ assay.

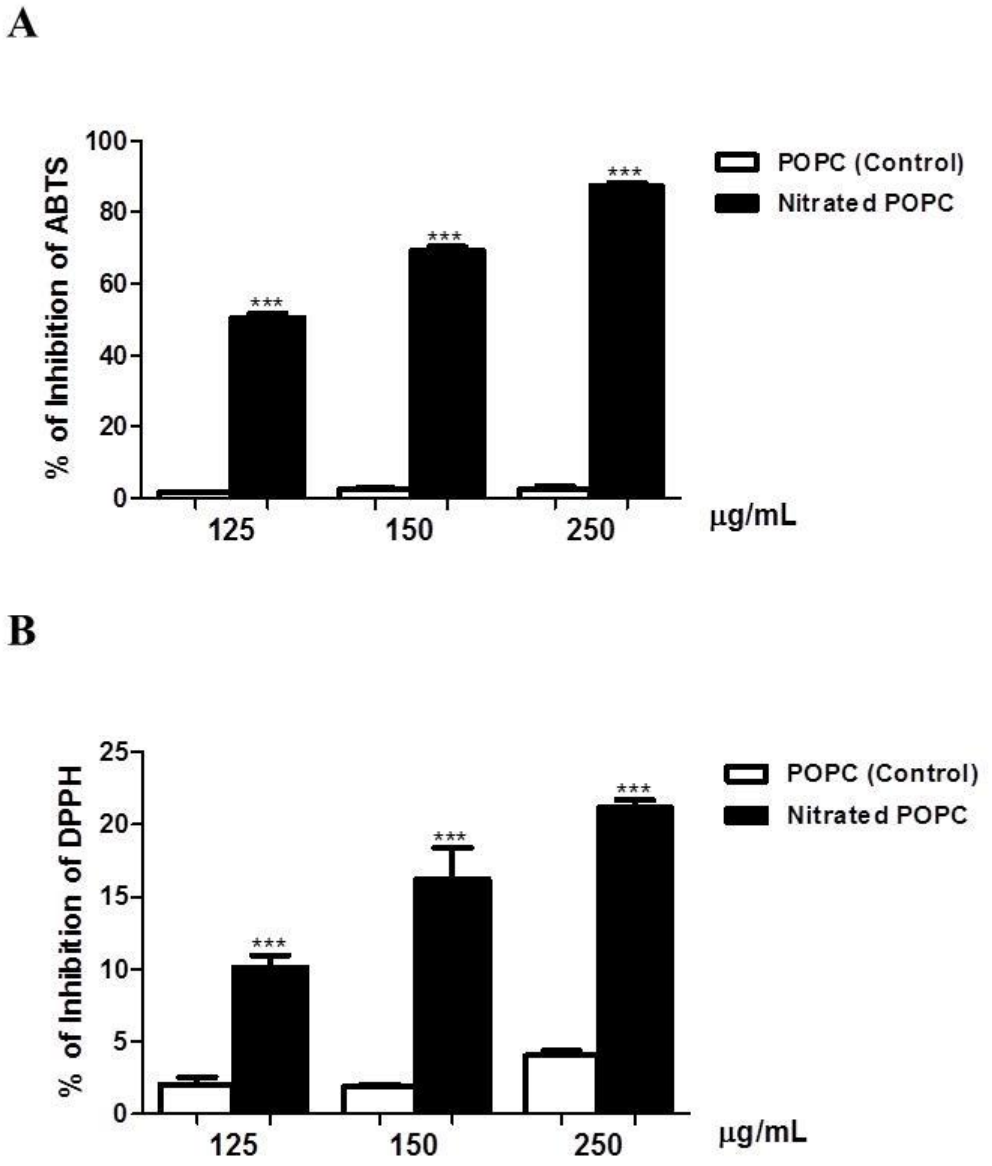

Figure III.9. (A) Percentage of inhibition of $ABTS^{\bullet+}$ (A) and $DPPH^{\bullet}$ radicals (B) obtained in the presence of non-modified POPC and nitrated POPC (125, 150 and 250 µg/mL) after 120 min of reaction. Values were the means±SD. ***, significantly different from control group ($P<0.0001$).

Table III.3. Amount of the residual $ABTS^{\bullet+}$ and $DPPH^{\bullet}$ radicals after 120 min of reaction in the presence of non-modified POPC and nitrated POPC at the three concentrations tested (125, 150 and 250 µg/mL) prepared in ethanol. The results were expressed as percentage of $ABTS^{\bullet+}$ and $DPPH^{\bullet}$ remaining.

[Non-modified POPC] (µg/mL)	**%ABTS Remaining**	**[Nitrated POPC] (µg/mL)**	**%ABTS Remaining**
125	95.1±2.1	125	60.5±3.3
150	95.7±2.0	150	47.9±4.8
250	94.5±2.4	250	21.5±1.0
[Non-modified POPC] (µg/mL)	**%DPPH Remaining**	**[Nitrated POPC] (µg/mL)**	**%DPPH Remaining**
125	95.3±1.0	125	86.3±0.3
150	93.9±0.4	150	80.0±2.4
250	91.8±0.8	250	74.3±1.0

These results indicate a higher reactivity of nitrated POPC in aqueous media ($ABTS^{\bullet+}$ assay) than in ethanolic media ($DPPH^{\bullet}$ assay). Trolox is a fast acting antioxidant in both assays and, this apparent difference in TE values result from kinetic differences. As observed in Supplementary Figure S-1 (Appendix C), $ABTS^{\bullet+}$ consumption reaches its end-point but this is not verified in $DPPH^{\bullet}$ assay.

As reported above, previous published work [85] evaluated the radical scavenging capacity against $DPPH^{\bullet}$ radical of two synthetic isomers of nitroalkene derivative of linoleic acid (NO_2-LA). Manini *et al* [85] found the 9-NO_2-LA isomer to be more prone to H-atom loss and thereby a higher decay of $DPPH^{\bullet}$ radical absorbance was observed. However, the absorbance decay in the presence of 10-NO_2-LA and non-modified linoleic acid was in the same order of magnitude of decay observed for nitrated POPC and non-modified POPC, respectively. Another key feature was the concentrations of both NO_2-FA and $DPPH^{\bullet}$ radical solution. The concentration of NO_2-FA used in the study of Manini *et al* [85] was 7.7 mmol/L while the concentrations used in our study for non-modified and nitrated POPC were undoubtedly lower (between 0.1 and 0.3 mmol/L). Regarding the $DPPH^{\bullet}$ radical solution, they used 100 µmol/L while we used 250 µmol/L. Based on the results displayed by Manini *et al* [85] we performed some calculations in order to establish the amount of $DPPH^{\bullet}$ radical consumed after 60 min of reaction (Supplementary Figure S-2 and Table S-1, Appendix C). The percentage of $DPPH^{\bullet}$ radical consumed was approximately 15.5%, 28.3% and 88% for non-modified linoleic acid, 10-NO_2-LA and 9-NO_2-LA, respectively. This corresponds to approximately 15.5, 28.3 and 88 µmol/L of

$DPPH^{\bullet}$ radical consumed. Considering the final fatty acid concentration used in their experiments (7.7 mmol/L), the amount of $DPPH^{\bullet}$ radical consumed was, respectively, 7.2, 11.3 and 35.0 μmol $DPPH^{\bullet}$ radical/g of non-modified linoleic acid, 10-NO_2-LA and 9-NO_2-LA [85]. In our work, the amount of $DPPH^{\bullet}$ radical consumed was 74 μmol $DPPH^{\bullet}$ radical/g of nitrated POPC, within a similar order of magnitude.

The $DPPH^{\bullet}$ and $ABTS^{\bullet+}$ assays are widely used for screening and routine determinations of radical scavenging activity of antioxidants candidates and mixtures due to their stability, availability and technical simplicity. Nevertheless, these assays have been criticized as the $DPPH^{\bullet}$ and $ABTS^{\bullet+}$ radicals are non-physiological radicals and thus not representative of biomolecules and not even found in any biological system [203]. In this way, we also performed the ORAC assay that is based in a biologically relevant radical source (peroxyl radicals) associated with physiological disturbance [203, 204].

ORAC Assay

The ORAC assay is based on the inhibition of the peroxyl radical ($ROO^{\bullet}$)-induced oxidation through hydrogen atom donation. Peroxyl radicals are produced in a time-dependent manner during the thermal decomposition of 2,2'-azobis-(2-methylpropionamidine) dihydrochloride (AAPH), and react with a fluorescent probe (usually fluorescein) inducing its oxidation and quenching the fluorescent signal. In the presence of a compound with chain-breaking antioxidant properties, the elimination of the peroxyl radicals occurs, and fluorescein is protected from oxidation and therefore the fluorescent signal is maintained until antioxidant depletion. Peroxyl radicals are formed *in vivo* during oxidation of biomolecules particularly during lipid peroxidation and are themselves capable of propagate the oxidation reactions bringing harmful effects [204]. Thus, ORAC assay has been widely used to measure the antioxidant capacity since this assay is considered one of the most relevant to define the antioxidant level in a biological system [205].

The ability of non-modified POPC and nitrated mixtures of this lipid (0.75, 2.5 and 10 μg/mL) to protect fluorescein from peroxyl radical induced-oxidation was assessed and compared with the fluorescence decrease for blank sample (fluorescein and AAPH). Both non-modified and nitrated POPC confer higher lag time and higher AUC values when compared to blank (t_{calc} values between -33.13 and -5.626, t_{tab} = 2.074, ν = 22, p = 0.05),

which indicates that the presence of both lipid samples retard fluorescein oxidation (Figure III.10). Non-modified POPC bears oleic acid in its composition. Indeed, oleic acid was already described to be able to protect PC12 rat cells against nanoparticle-induced oxidative stress enhancing cell survival [206]. However, for the $ABTS^{\bullet+}$ and $DPPH^{\bullet}$ assays no antioxidant activity was observed for non-modified POPC. Thereby, the inhibition of $ROO^{\bullet}$ radicals should occur through a different mechanism from the free radical scavenging. A possible explanation could be the reaction of $ROO^{\bullet}$ radicals with the double bond present in the oleic fatty acyl chain of POPC in a radical mechanism since POPC is susceptible to be oxidized [174, 207].

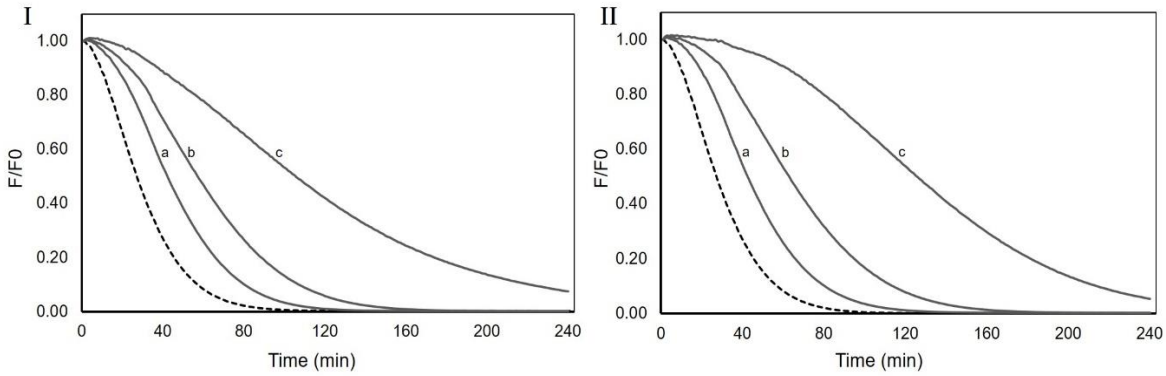

Figure III.10. ORAC profile of I) non-modified POPC and II) nitrated POPC at 0.75 (a), 2.5 (b) and 10 (c) µg/mL. Control experiment (dashed line) corresponds to fluorescein (70 nM) + AAPH (12 mM).

Considering non-modified and nitrated POPC, non-significant differences in the AUC values were attained ($|t_{calc}| < 1.797$, $t_{tab} = 2.145$, $\nu = 14$, $p = 0.05$), with slightly larger AUC values for nitrated POPC (Table III.4). Moreover, significant differences in the lag time values were observed between non-modified and nitrated POPC when higher concentrations (2.5 and 10 µg/mL) were analyzed showing concentration dependent behavior ($|t_{calc}|$ was 4.503 (2.5 µg/mL) and 16.358 (10 µg/mL), $t_{tab} = 2.145$, $\nu = 14$, $p = 0.05$). These results indicate that nitrated POPC reacts faster than non-nitrated POPC with peroxyl radicals, thus providing a more relevant initial protection against fluorescein oxidation. Nevertheless, the total protection (based on AUC values) did not differ significantly for non-modified and nitrated POPC. Indeed, the obtained TE values for the

highest lipid concentration were 1.03 ± 0.22 and 1.30 ± 0.16 mmol trolox/g lipid for non-modified and nitrated POPC, respectively.

Table III.4. Lag time and area under the curve (AUC) values for non-modified and nitrated POPC.

Concentration (µg/mL)	Non-modified POPC		Nitrated-POPC	
	Lag time (min)	AUC	Lag time (min)	AUC
0.75	13.6 ± 1.7	45.5 ± 4.5	13.8 ± 2.2	45.5 ± 7.1
2.5	14.9 ± 2.7	61.0 ± 5.6	22.1 ± 3.7	67.1 ± 7.8
10	23.7 ± 3.0	113 ± 24	51.7 ± 3.8	129 ± 16

Blank experiment: Lag time = 5.62 ± 1.44 min, AUC = 30.8 ± 2.9.

Taken together, the results obtained using these three common assays suggest that nitrated POPC has antioxidant potential. Its actions could be associated either to hydrogen- or electron-donation to radicals. The results obtained for ORAC assay could be quite important regarding that peroxyl radicals are formed *in vivo* bringing harmful effects[204].

Anti-Inflammatory Activity

Previous studies have reported that several anti-inflammatory drugs have shown an antioxidant and/or radical scavenging mechanism as part of their activity [208-211]. Additionally, considering that antioxidants and free radical scavengers present concomitant anti-inflammatory actions [212], we also investigate the anti-inflammatory capacity of the nitrated POPC. In our study, we investigated and compared the anti-inflammatory capacity of the non-modified POPC and a nitrated mixture of POPC on LPS-stimulated RAW 264.7 macrophages through the evaluation of their effects in iNOS expression. The expression of this enzyme is strongly increased under inflammatory conditions and inhibition of its intracellular levels is often used to disclose the anti-inflammatory potential of several drugs. In a first approach, and before testing the anti-inflammatory potential of nitrated POPC, we performed the MTT assay in order to select concentrations devoid of toxicity to macrophages. For that, macrophages were incubated with several concentrations of non-modified POPC and nitrated POPC. The *in vitro* cytotoxic effect of non-modified POPC (light grey bar) and nitrated POPC (dark grey bar) on macrophages viability was represented as percentage of control (non-stimulated cells; white bar), as shown in Figure

III.11. A cytotoxic effect was observed using concentrations of 15 and 30 μg/mL for nitrated POPC. Subsequently, for the further experiments concentrations of 7.5 μg/mL for both non-modified POPC and nitrated POPC we selected.

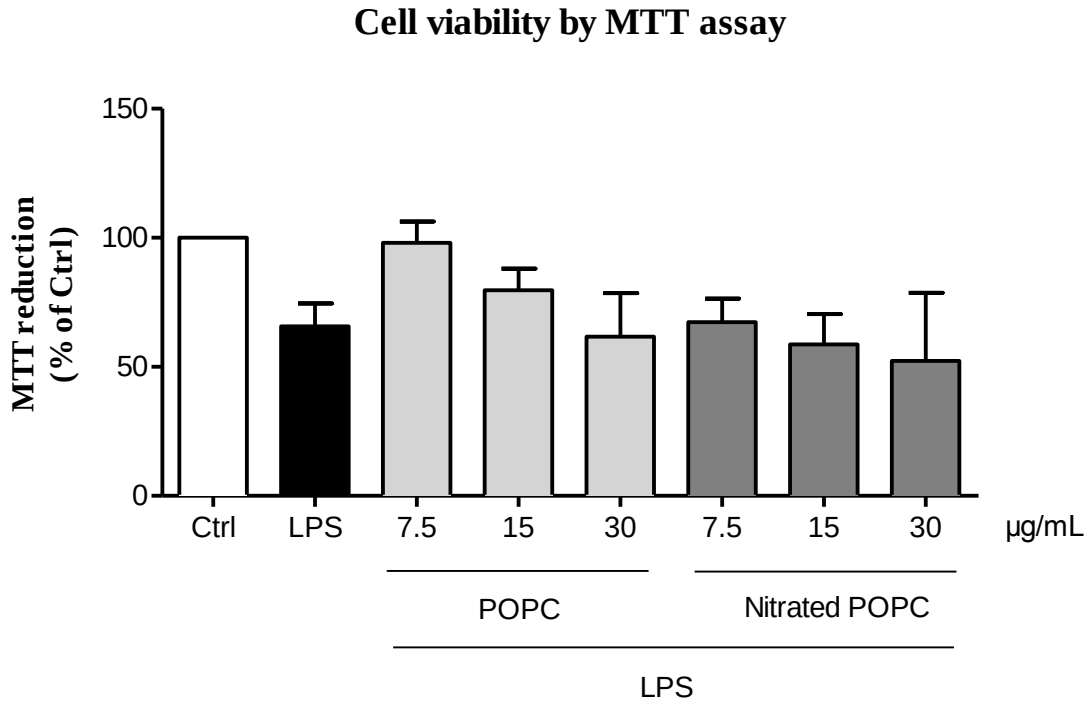

Figure III.11. Cell viability (% of the control) of Raw 264.7 cells incubated with non-modified POPC (light grey bar; 7.5, 15 and 30 μg/mL) or nitrated POPC (light grey bar; 7.5, 15 and 30 μg/mL) for 1 h, and later activated with LPS for 24 h. Results are expressed as a percentage of MTT reduction by control cells maintained in culture medium. Data represent mean ± SD of three independent assays.

In order to investigate the effects of nitrated POPC in iNOS expression on LPS-activated macrophages (Raw 264.7 cells), western blotting analysis was performed using a specific antibody against iNOS. Macrophages were incubated with LPS in the absence and the presence of 7.5 μg/mL of non-modified POPC or nitrated POPC. As shown in Figure III.12, non-stimulated cells (control; white bar) expressed low levels of iNOS protein. The iNOS expression is increased after stimulation with LPS for 24 h (black bar). The presence of nitrated POPC inhibited the expression of iNOS in LPS-activated macrophages in 20.2% (dark grey bar; $p<0.05$).

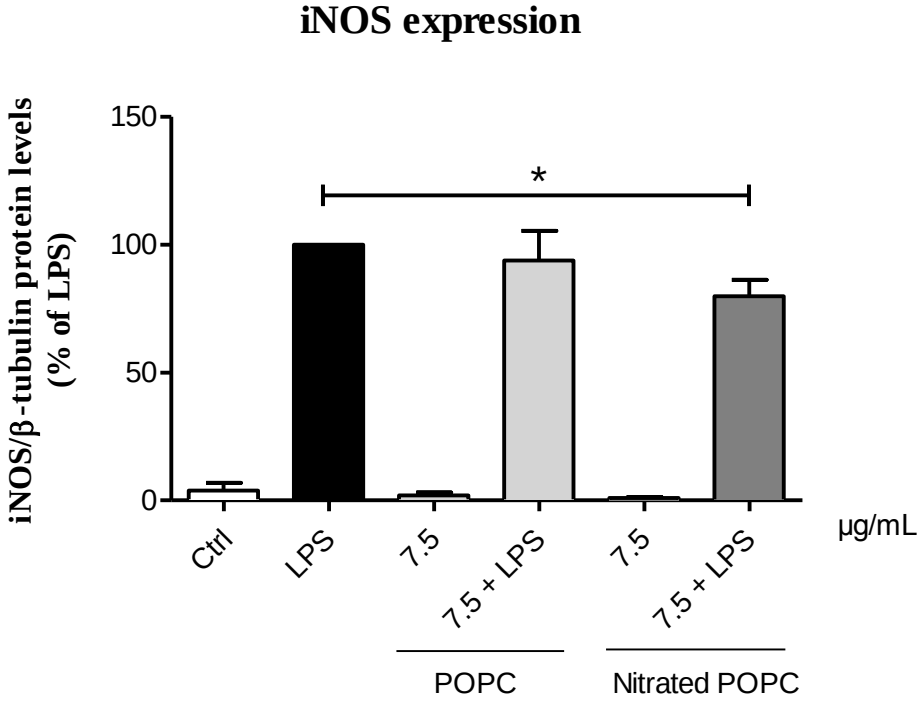

Figure III.12. Effect of non-modified POPC and nitrated POPC (7.5 µg/ml) on iNOS expression in raw 264.6 cells. Raw 264.6 cells ($0.6x10^6$ cells) were incubated for 24h in culture medium in the absence (control; white bar) or in the presence of LPS (1 µg/mL; black bar) or in the presence of LPS plus non-modified POPC (light grey bar) or nitrated POPC (dark grey bar). Data are mean ± SD values from three independent experiments.*$p<0.05$: LPS vs Nitrated POPC+LPS.

The results obtained in this work for nitrated POPC are somewhat in agreement with previous published work concerning the NO_2-FA. In a previous study, Ferreira *et al* [71] demonstrated that macrophage (J774.1 cells) inflammatory responses evoked by LPS 1 µg/mL were suppressed in the presence of NO_2-cLA (50 µmol/L) and NO_2-LA (20 µmol/L) namely through the inhibition of iNOS expression. Both nitroalkene derivatives down-regulate the NOS2 expression, however NO_2-LA demonstrated more potent inhibitory effects. Likewise, Trostchansky *et al* [10] demonstrated that, in activated macrophages, NO_2-AA also exert protective anti-inflammatory actions through the down-regulation of iNOS expression and diminishing the secretion of pro-inflammatory cytokines. The ability of NO_2-FA and NO_2-POPC to attenuate the iNOS expression during

macrophage activation should account for the resolution of inflammation, limiting the putative deleterious effects of pro-inflammatory stimuli.

NO_2-FA has been reported as a promising pharmacological tool to prevent and modulate inflammatory diseases associated with oxidative and nitroxidative stress conditions. The potential beneficial actions of the administration of NO_2-FA have been evaluated *in vivo* using murine models of several diseases and pathologies including diabetes and metabolic syndrome [135], nephropathy [101], ischemia-reperfusion injury [76, 77, 101], cardiovascular disease [96, 111], pulmonary inflammation [98, 102] and chronic inflammatory disease [100]. However, further studies are necessary to determine whether NO_2-FA supplementation would exert protective actions in human diseases, and to evaluate their potential toxicity when administrated for longer periods of time. The nitrated derivatives of POPC also demonstrated to be promising candidates as antioxidant and anti-inflammatory agents using *in vitro* model systems. These findings could be of utmost importance since the identification of nitrated derivatives of phospholipids was previously reported *in vivo* [175]. Besides, free NO_2-FA found endogenously can arise from nitrated phospholipids, and NO_2-PLs could be the first species to be formed *in vivo*. Nevertheless, future work may contemplate the elucidation of the biological properties of other nitrated phospholipids and the effects of specific nitrated products. The mechanisms underlying their antioxidant and anti-inflammatory actions namely the effects in the expression of antioxidant enzymes, in inhibition of pro-inflammatory signaling pathways and the effect of nitrated phospholipids on other key players of the inflammatory response, for instance cytokines, constitute key points that should be considered for further investigation. The effects of supplementation in human disease and their toxicity should also be evaluated for nitrated derivatives of phospholipids. This is an important topic since diet could contribute to increase the levels of NO_2-FA, and perhaps NO_2-PL, in tissues and plasma directly or through elevation of their endogenous generation.

III.2.1.3. Concluding Remarks

This study highlights for the first time the potential biological actions of nitrated phospholipids. Nitrated POPC revealed potential as anti-inflammatory and antioxidant agents, showing ability to reduce $ABTS^{\bullet+}$ and $DPPH^{\bullet}$ radicals and quench the $ROO^{\bullet}$ radicals in ORAC assay in a concentration-dependent way. The inhibition of iNOS expression in LPS-activated macrophages seems to be one of the molecular mechanisms accounting for their anti-inflammatory properties. The biological relevance of these findings needs to be deeply explored and validated in *in vivo* models.

CHAPTER III. RESULTS AND DISCUSSION

III.3. UNDERSTANDING THE CROSS REACTION BETWEEN NITRATED AND NITROXIDIZED DERIVATIVES OF PHOSPHOLIPIDS AND PROTEINS

CHAPTER III. RESULTS AND DISCUSSION

III.3. UNDERSTANDING THE CROSS REACTION BETWEEN NITRATED AND NITROXIDIZED DERIVATIVES OF PHOSPHOLIPIDS AND PROTEINS

III.3.1. MODIFICATION OF VIMENTIN BY NITRATED/NITROXIDIZED PRODUCTS OF POPC

The predominant molecular mechanism associated to NO_2-FA biological signaling actions is based on their electrophilic nature and reactivity toward proteins. NO_2-FAs interact with key target proteins inducing post-translational modifications that change protein structure and function leading to antioxidant and anti-inflammatory signaling effects. However, once again work focused on biological actions of nitrated phospholipids mediated by their adduction with key proteins remains undisclosed. Additionally, the structures and mechanisms involved in the formation of these adducts are far to be elucidated.

Aiming to contribute to knowledge regarding the ability of nitrated phospholipids to interact with target proteins, and the structures and mechanisms involved in the formation of the correspondent adducts, nitrated/nitroxidized phosphatidylcholine was incubated with well-known protein targets of electrophilic lipids, namely vimentin, using *in vitro* gel-based competition assays. Their interactions were evaluated using western blotting. It effects in the organization of vimentin network was also evaluated in SW13 adrenal carcinoma cell line expressing defined vimentin constructs using confocal microscopy (Section III.3.1).

III.3.1.1. Background and aim of the study

Nitrated and nitroxidized PLs were already identified in cardiac mitochondria from an animal model of type 1 diabetes and in cardiomyoblast cell line (H9c2) under starvation. However, the biological roles of these products still poorly explored. Nevertheless, as reported for nitro-fatty acids (NO_2-FA), nitro derivatives of PLs (NO_2-PLs) may also be able to interact with key proteins. Vimentin is an intermediate filament protein that possesses a single cysteine residue (Cys328), target for modifications by electrophiles.

In this study, the vimentin interactions with non-modified 1-palmitoyl-2-oleoyl-*sn*-glycero-3-phosphocholine (POPC) and nitrated POPC, namely the nitroalkene derivative (NO_2-POPC) that is the major product formed *in vitro* after biomimetic nitration of POPC with nitronium tetraflouroborate (NO_2BF_4), were assessed using an *in vitro* gel-based competition method. The effects of non-modified POPC and nitrated POPC in vimentin network organization were also evaluated using the human adrenal tumor SW13 cell line.

III.3.1.2. Results and discussion

Vimentin is the major intermediate filament protein expressed in mesenchymal cells where it forms the vimentin cytoskeletal network [213]. In cells, vimentin particles fuse into elongated structures known as squiggles that further assembly into intermediate filaments [214] which can further undergo polymerization [215-217]. This coiled coil protein is involved in physiological and pathological processes, such as embryogenesis, wound healing, autoimmune diseases, epithelial mesenchymal transition and therefore cancer cell dissemination and metastasis, among others.

Vimentin has been shown to play a number of critical functions. In spite of being a dynamic protein which provides flexibility to the cells, vimentin network whose robust filaments extended from the nuclear periphery to the cell membrane have important structural roles conferring mechanical resistance to cells and contributing to the maintenance of cell shape, architecture and integrity. Vimentin is the support for the correct anchorage of the position and function of cellular organelles in the cytosol such as nucleus, endoplasmic reticulum, and mitochondria where vimentin is usually attached to [218]. Besides, vimentin network promote the interaction with, regulation and organization of a number of proteins involved in attachment/adhesion, migration, and cell signaling

[219, 220]; promote a bidirectional cross-talk with other cytoskeletal structures and stabilize the cytoskeletal interactions [221, 222]. So, vimentin network play key roles in maintenance of cell homeostasis [221, 222]. Vimentin is also involved in the control of the transport of low-density lipoproteins-derived cholesterol from the lysosome to the site of the esterification. In cells with modified vimentin, the transport of LDL inside the cells is blocked and cells store a much lower amount of LDL. This is remarkably important in adrenal cells which rely on cholesteryl esters derived from LDL [223]. Vimentin also plays a role in aggresome formation, where it forms a cage surrounding a core of misfolded aggregated protein [224], which is formed when the protein-degradation system of cells (proteosomal degradation) is overloaded. Vimentin has another role as a mediator of the innate immune response.

In spite of its complete structural characterization remains undone, it is known that vimentin (55 kDa) possesses a single cysteine residue, Cys328. The highly conserved cysteine 328 residues is essential for vimentin stability, dynamics and correct function, being a requisite for optimal vimentin performance in network organization and expansion, organelle distribution and aggresome formation. Nevertheless, Cys328 is also considered as a noteworthy sensor for oxidative stress [225] being a target for numerous non-enzymatic oxidative modifications by several thiol-reactive compounds including glutathionylation, carbonylation, and nitrosylation [226-229]. Modifications of cys328 by different oxidants or electrophiles makes this modified vimentin not able to keep up with non-modified vimentin's demanding roles. Vimentin performance in network expansion, organization, and functions became compromised namely in achieving the appropriate distribution of cytoplasmic organelles, in formation of aggresomes upon inhibition of proteosomal degradation or extensive oxidative damage. However, these modifications may also be involved in regulation of response of vimentin network to oxidants and electrophiles under stress conditions [225, 230].

Since vimentin is a target for various electrophilic lipids [225], in this study we have explored the ability of vimentin to bind non-modified POPC and nitrated POPC (Figure III.13). Nitrated POPC was obtained after reaction between POPC and NO_2BF_4, previously reported [175], and the nitroalkene derivatives of POPC (NO_2-POPC), with electrophilic properties, were the major nitrated products identified (Figure III.13).

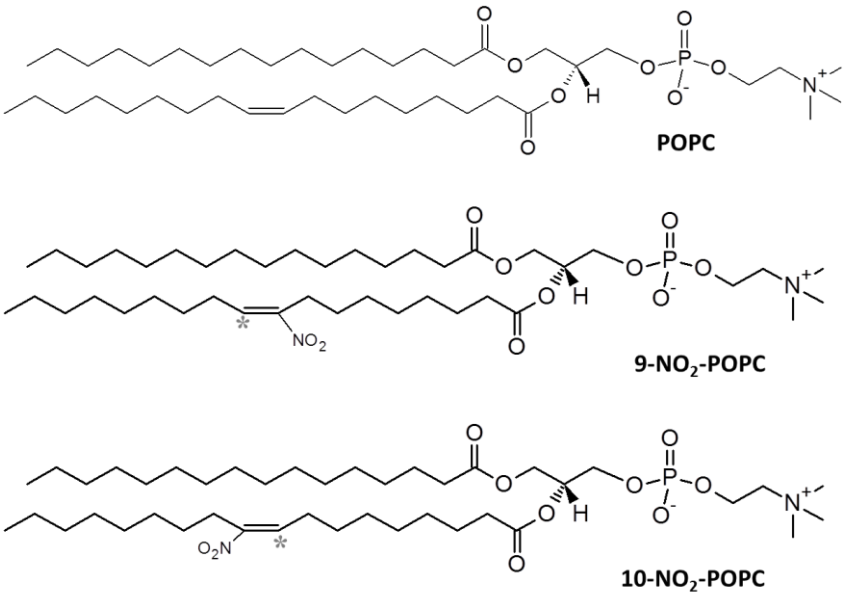

Figure III.13. Representative structure of the phospholipids used in this study. POPC, 1-palmitoyl-2-oleoyl-*sn*-glycero-3-phosphocholine (16:0/18:1). The structures of the two nitro derivatives of POPC (NO_2-POPC isomers), previously identified [175] are also presented: the 9-NO_2-POPC (nitro group in carbon 9, NO_2 in C9) e o 10-NO_2-POPC (nitro group in carbon 10, NO_2 in C10). *, specify the carbons susceptible to Michael addition.

We first performed a competition gel-based assay, as previously described in the work of Zorrilla and co-authors [231], based on the ability of compounds interacting with a given protein to shield its modifications by biotinylated iodoacetamide. In the presence of nitrated POPC de percentage of biotinylated iodoacetamide (Iac-B) binding to vimentin (21.9%) was significantly lower in comparison with POPC control (Figure III.14). Thus, incubation with nitrated POPC prevented vimentin modifications by Iac-B. This may point out a common site for electrophilic addition. In fact, the vimentin's Cys328 may be the common target for nitrated POPC-covalently binding.

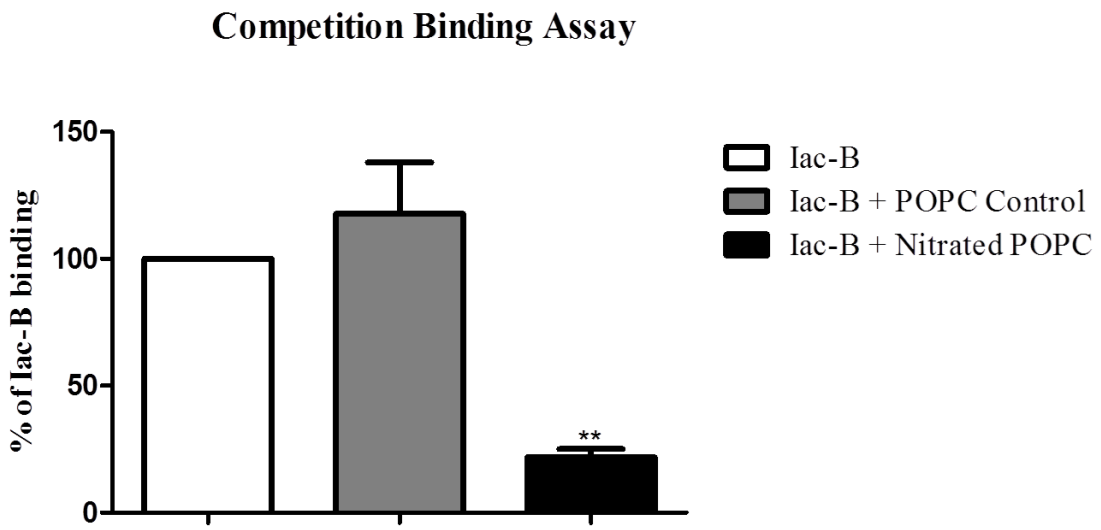

Figure III.14. Competition binding assay to evaluate the ability of non-modified POPC and nitrated POPC for binding to vimentin. Vimentin was pre-incubated with either 100 µmol/L non-modified POPC, nitrated POPC or vehicle (DMSO) for 4 h at room temperature before the addition of 20 µmol/L Iac-B and continued incubation for more 30 min at room temperature. Incorporation of non-modified POPC and nitrated POPC as well as the vimentin levels were obtained by western blotting. The graph presents results of three independent experiments performed in three different days (mean±SD, **$p<0.01$).

In order to obtain further support and to assess the functional effects of the interaction between nitrated POPC and vimentin, we explored the effects of non-modified POPC and nitrated POPC on cells expressing vimentin. We used the adrenal carcinoma cell line SW13/cl.2, a vimentin deficient cell model devoid of cytosolic intermediate filaments, which was previously stably transfected with several vimentin constructs using different plasmid-transfection strategies, as described in [225].

In the first place we used SW13/cl.2 cells stably transfected with bicistronic vectors coding for vimentin wt or C328S mutant and the red fluorescent protein RFP as a marker of transfection as separate products (RFP//vimentin wt or C328S). In these cells, both vimentin constructs form an extended radial network. Incubation of RFP//vimentin wt –expressing cells with 10 µmol/L nitrated POPC for 6h led to changes in vimentin filaments organization. A clear condensation of filaments at the cell periphery instead of the normal distribution was observed in 50.8% of cells. In the presence of 10 µmol/L non-modified

POPC, 98% of RFP//vimentin wt –expressing cells displayed the typical radial dispersion of vimentin filaments. However, for RFP//vimentin C328S – expressing cells, the effect of nitrated POPC was attenuated, and only in 34.7% of cells the vimentin filaments arrangement was changed. For RFP//vimentin C328S – expressing cells treated 10 µmol/L non-modified POPC, the majority of cells (96%) displayed the typical radial dispersion of vimentin filaments. Thus, RFP//vimentin C328S – expressing cells seem to be protected against the nitrated POPC-induced vimentin condensed filaments rearrangement at the cell periphery (Figure III.15). This may suggest that Cys328 has a key role in organization of vimentin filament network and in rearrangement of this network induced by nitrated POPC. These results are in agreement with the previously reported [225]. Treatment of RFP//vimentin wt – expressing cells with various electrophiles, such as HNE and diamide, was shown to induce modifications in vimentin cytoskeleton namely vimentin condensation in a higher proportion in comparison with C328-expressing cells.

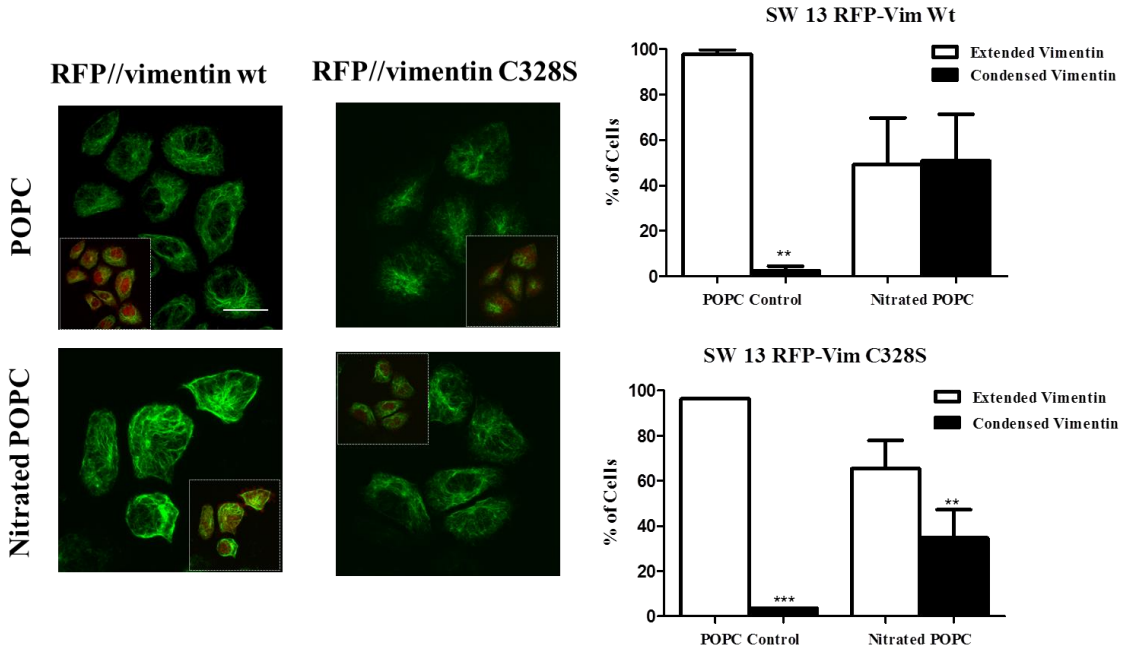

Figure III.15. Evaluation of effects of non-modified POPC and nitrated POPC in vimentin network in SW13 cells stably transfected with RFP//vimentin wt or C328S plasmids. Cells were treated with 10 µmol/L non-modified POPC or nitrated POPC for 6h, fixed and processed for immunofluorescence of vimentin. Inserts show overlays with RFP fluorescence as a control of transfection. Scale bar, 20 µm. The proportion of cells with

normal versus condensed vimentin was evaluated (mean±SD of two experiments, **p<0.01, ***p<0.001).

We next used a different cellular model, namely, SW13/cl.2 cells stably transfected with constructs expressing the green fluorescent protein fused to vimentin wt or C328S mutant (GFP-vimentin wt or C328S). These cells are characterized by the formation of filamentous structures with two free ends consistent with vimentin squiggles or short vimentin filaments in the case of wt, but only bright vimentin dots in the case of GFP-vimentin C328S, which is not competent for the formation of squiggles (not used in this work). The GFP-vimentin wt cells were treated with vehicle (DMSO), 10 or 30 µmol/L non-modified POPC, 10 or 30 µmol/L nitrated POPC, or 10 or 30 µmol/L GSNO (used as $NO^{\bullet}$ generator). Before being treated, cells were observed *in vivo* by confocal microscopy. After the treatments, cells were also immediately observed and followed during the 75 min of treatment. After 75 min of incubation, cells were fixed and processed for immunofluorescence. DSMO and 30 µmol/L non-modified POPC-treated cells displayed the short vimentin filaments (Figure III.16). For 10 µmol/L nitrated POPC-treated cells, a mix of cells showing vimentin filaments together with vimentin dots was observed. A small number of cells with rounded shape were also observed. Treatment with 30 µmol/L nitrated POPC also led to a disassembly of short filaments into dots. In fact, a great number of cells showing vimentin dots were observed. The aspect of dots mimics the distribution vimentin in of GFP-vimentin C328S cells. For cells treated with GSNO, no significant alterations were observed in vimentin filaments. All of these observations were similar in live cells before being fixed for immunofluorescence. Besides, an increased number of cells with rounded shape were observed, which may be related with the loss of cellular adhesion. In fact, we observed that cells treated with 30 µmol/L nitrated POPC seems to be in lower number after the immunofluorescence protocol, suggesting that cells could be lost during the experimental procedure due to the loss of cellular adhesion induced by treatment with 30 µmol/L nitrated POPC (Figure III.16).

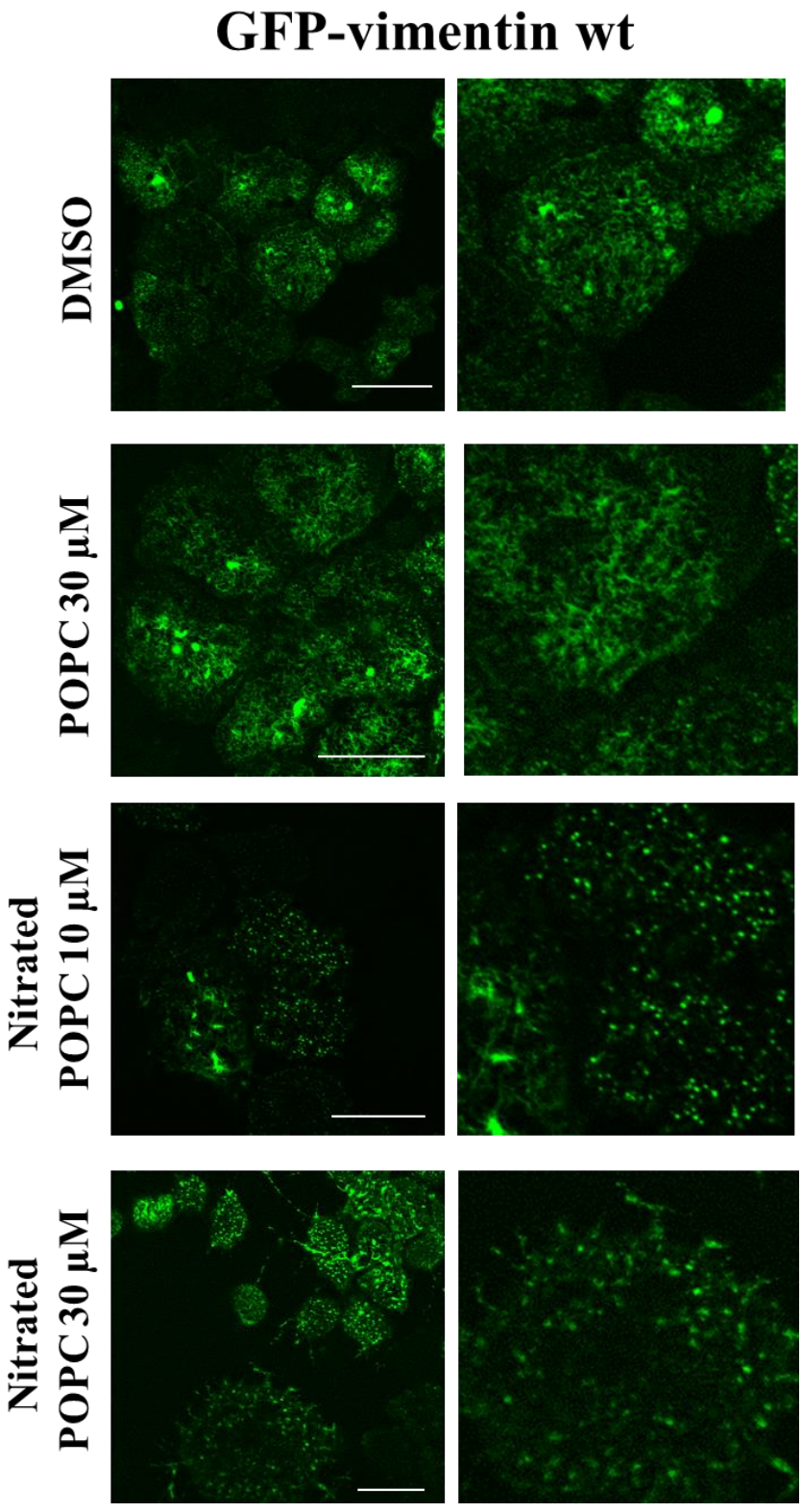

Figure III.16. Evaluation of effects of non-modified POPC and nitrated POPC in vimentin network in SW13 cells stably transfected with GFP-vimentin wt. Cells were treated with vehicle (DMSO), non-modified POPC (30 µmol/L) or nitrated POPC (10 or 30 µmol/L)

for 75 min. After that, cells were fixed and processed for immunofluorescence of vimentin. Scale bar, 20 μm. These images are representative of two experiments. Panels at the right shows enlarged areas of the images.

III.3.1.3. Concluding Remarks

In summary, Cys328 of vimentin seems to be a key residue for interaction with nitrated products of POPC, namely the NO_2-POPC derivative, which has a nitro group with electrophilic potential and ability to interact with Cys328 of vimentin leading to the formation of lipid-protein adducts. Nevertheless, these are preliminary results that need to be deeply explored. In fact, further studies based on MS approaches are needed to characterize vimentin-NO_2-POPC adducts and confirm the location of adduction.

CHAPTER IV. GENERAL CONCLUDING REMARKS

Lipids are privileged targets of reactive nitrogen species (RNS) under nitrative and nitroxidative stress conditions associated with disease. Nitro-fatty acids (NO_2-FA) have been the most reported products of the reaction between lipids and RNS, and have already been detected *in vivo* in plasma, urine and tissues, and are considered anti-inflammatory, anti-hypertensive, and anti-thrombotic agents. Although RNS can accumulate in the hydrophobic milieu of membranes, where phospholipids are abundant rather than free fatty, there is a lack of knowledge in what concern possible phospholipid (PL) nitration/nitroxidation and their putative biological roles. Having this in mind, the proposed aim of this thesis was to give some insights on the development of mass spectrometry strategies to identify nitrated/nitroxidized PL, and to search for their potential as anti-inflammatory and antioxidants agents together with their putative roles in post-translational modifications (PTM) of proteins.

To achieve the proposed aim, we used *in vitro* biomimetic model of nitroxidative stress conditions using pure PL standards and NO_2BF_4, and mass spectrometry (MS) analysis. Nitro derivatives of PL (NO_2-PL) were successfully identified by MS-based approaches (MS and MS/MS) also combined with liquid chromatography. The specific fragmentation pathways were assigned as the loss of HNO_2 and the formation of nitrated phospholipids as positive and negative ions. Interestingly, loss of HNO_2 was reported to be a typical neutral loss of nitro-fatty acids, and thus can be a general reporter neutral loss to nitro lipids. In addition, other forms of nitration and nitroxidation of phospholipids were also considered, and new mass spectrometry approaches were developed to identify by MS and MS/MS the nitroso, dinitroso, dinitro, nitronitroso and nitroxidized PL derivatives. Typical fragmentation pathways of nitrated and nitroxidized PL identified included the loss of HNO and HNO_2 for nitroso and nitro derivatives, respectively; the combined losses of HNO (or HNO_2) and polar head groups of PLs; and product ions corresponding to the modified fatty acyl chains ($[NO_n\text{-}FA+O_n+H]^+$ and $[NO_n\text{-}FA+O_n\text{-}H]^-$ ions (n=1-2)).

Using the defined fragmentation approaches, NO_2-PL were detected in this work and for the first time, both in biomimetic systems, *in vitro* in cell cultures, and *in vivo* in heart mitochondria from an animal model of type 1 diabetes mellitus. These results corroborate that besides the formation of NO_2-FA *in vivo*, our hypothesis of the chemical feasibility of nitration of phospholipids was confirmed, and their formation in biological conditions was also corroborated. Furthermore, NO_2-PL and the other modified PL were also detected in

cardiomyoblast H9c2 cells under starvation but not in ischemia or control revealing that modification of PL by RNS is a process dependent on other factors than their putative reactivity, and that can mirror the production of nitric oxide ($NO^{\bullet}$) and modulation of expression or activity of nitric oxide synthase (NOS).

These results highlight the importance of the PL nitration/nitroxidation and give the suggestion that, similarly as NO_2-FA, NO_2-PL or other nitrated/nitroxidized PL products, can be formed and can possess important biological roles, and beneficial health effects namely as cardioprotectors in cardiovascular diseases (CVD). This field of research needs to be explored considering that the biological role of nitrated lipids in CVD seems to be a join effect of cardioprotection, vasodilation and anti-inflammatory effects, among other. It is evident that future work is need in this field, either detecting nitrated PL in different pathological conditions, using a lipidomic approach, and to evaluate their biological effects.

Thus in this thesis, we also evaluate the potential of the nitrated/nitroxidized products of 1-plamitoyl-2-oleoyl-phosphatidylcholine (POPC) in immune/inflammatory response and as antioxidant agents. Nitrated/nitroxidized products of POPC revealed anti-inflammatory properties by decreasing the expression of the inducible nitric oxide synthase (iNOS) induced by LPS stimulation in macrophages (Raw 264.7). They also showed antioxidant properties, namely as scavenging agents, by reducing the $ABTS^{\bullet+}$, $DPPH^{\bullet}$ and peroxyl radicals. These findings highlight the potential role of nitrated/nitroxidized PLs as possible beneficial players in inflammatory and oxidative stress-related disorders.

Moreover, it was reported that NO_2-FA exerts their modulatory effects by the interaction with key proteins, forming intramolecular linkages by Michael addition with thiols group of cysteines or even with other amino acids, such as histidine. Nitrated/nitroxidized products of POPC, namely NO_2-POPC which is the major products formed, were incubated with vimentin, a protein that has a reactive cysteine able to from covalent adducts with other electrophilic lipids, and the results showed the ability of NO_2-POPC to interact with vimentin, demonstrating that similar with NO_2-FA, NO_2-PL are also very prone to protein PTM, and thus could exert similar signaling actions.

Overall, NO_2-PL and other nitrated/nitroxidized derivatives can be generated under biological conditions and can be considered lipid mediators during inflammatory and oxidative stress-related disorders, with signaling and modulatory properties that can be

important in diseases. Nevertheless, further research must be done in order to get more insights regarding the structural modifications and properties of nitrated/nitroxidized PL namely under nitroxidative stress conditions.

CHAPTER V. REFERENCES

[1] G.O. Fruhwirth, A. Loidl, A. Hermetter, Oxidized phospholipids: from molecular properties to disease, Biochimica et biophysica acta 2007, 1772: 718-36.
[2] P.A. Leventis, S. Grinstein, The distribution and function of phosphatidylserine in cellular membranes, Annual review of biophysics 2010, 39: 407-27.
[3] M.R.M. Domingues, A. Reis, P. Domingues, Mass spectrometry analysis of oxidized phospholipids, Chemistry and Physics of Lipids 2008, 156: 1-12.
[4] E. Niki, Y. Yoshida, Y. Saito, N. Noguchi, Lipid peroxidation: mechanisms, inhibition, and biological effects, Biochemical and biophysical research communications 2005, 338: 668-76.
[5] I. Milic, E. Griesser, V. Vemula, N. Ieda, H. Nakagawa, N. Miyata, J.M. Galano, C. Oger, T. Durand, M. Fedorova, Profiling and relative quantification of multiply nitrated and oxidized fatty acids, Analytical and Bioanalytical Chemistry 2015.
[6] H. Rubbo, R. Radi, M. Trujillo, R. Telleri, B. Kalyanaraman, S. Barnes, M. Kirk, B.A. Freeman, Nitric oxide regulation of superoxide and peroxynitrite-dependent lipid peroxidation. Formation of novel nitrogen-containing oxidized lipid derivatives, Journal of Biological Chemistry 1994, 269: 26066-75.
[7] P.R. Baker, F.J. Schopfer, S. Sweeney, B.A. Freeman, Red cell membrane and plasma linoleic acid nitration products: synthesis, clinical identification, and quantitation, Proceedings of the National Academy of Sciences of the United States of America 2004, 101: 11577-82.
[8] F. Blanco, A.M. Ferreira, G.V. López, L. Bonilla, M. González, H. Cerecetto, A. Trostchansky, H. Rubbo, 6-Methylnitroarachidonate: A novel esterified nitroalkene that potently inhibits platelet aggregation and exerts cGMP-mediated vascular relaxation, Free Radical Biology and Medicine 2011, 50: 411-418.
[9] E.S. Lima, P. Di Mascio, H. Rubbo, D.S. Abdalla, Characterization of linoleic acid nitration in human blood plasma by mass spectrometry, Biochemistry 2002, 41: 10717-22.
[10] A. Trostchansky, J.M. Souza, A. Ferreira, M. Ferrari, F. Blanco, M. Trujillo, D. Castro, H. Cerecetto, P.R. Baker, V.B. O'Donnell, H. Rubbo, Synthesis, isomer characterization, and anti-inflammatory properties of nitroarachidonate, Biochemistry 2007, 46: 4645-53.
[11] P.R. Baker, Y. Lin, F.J. Schopfer, S.R. Woodcock, A.L. Groeger, C. Batthyany, S. Sweeney, M.H. Long, K.E. Iles, L.M. Baker, B.P. Branchaud, Y.E. Chen, B.A. Freeman, Fatty acid transduction of nitric oxide signaling: multiple nitrated unsaturated fatty acid derivatives exist in human blood and urine and serve as endogenous peroxisome proliferator-activated receptor ligands, Journal of Biological Chemistry 2005, 280: 42464-75.
[12] F.J. Schopfer, C. Cipollina, B.A. Freeman, Formation and Signaling Actions of Electrophilic Lipids, Chemical Reviews 2011, 111: 5997-6021.
[13] T. Cui, F.J. Schopfer, J. Zhang, K. Chen, T. Ichikawa, P.R. Baker, C. Batthyany, B.K. Chacko, X. Feng, R.P. Patel, A. Agarwal, B.A. Freeman, Y.E. Chen, Nitrated fatty acids: Endogenous anti-inflammatory signaling mediators, Journal of Biological Chemistry 2006, 281: 35686-98.
[14] A.C. Geisler, T.K. Rudolph, Nitroalkylation--a redox sensitive signaling pathway, Biochimica et biophysica acta 2012, 1820: 777-84.
[15] B.A. Freeman, P.R. Baker, F.J. Schopfer, S.R. Woodcock, A. Napolitano, M. d'Ischia, Nitro-fatty acid formation and signaling, Journal of Biological Chemistry 2008, 283: 15515-9.
[16] A. Trostchansky, L. Bonilla, L. Gonzalez-Perilli, H. Rubbo, Nitro-fatty acids: formation, redox signaling, and therapeutic potential, Antioxidants and Redox Signaling 2013, 19: 1257-65.
[17] L.M. Baker, P.R. Baker, F. Golin-Bisello, F.J. Schopfer, M. Fink, S.R. Woodcock, B.P. Branchaud, R. Radi, B.A. Freeman, Nitro-fatty acid reaction with glutathione and cysteine. Kinetic analysis of thiol alkylation by a Michael addition reaction, Journal of Biological Chemistry 2007, 282: 31085-93.
[18] C. Batthyany, F.J. Schopfer, P.R. Baker, R. Duran, L.M. Baker, Y. Huang, C. Cervenansky, B.P. Branchaud, B.A. Freeman, Reversible post-translational modification of proteins by nitrated fatty acids in vivo, Journal of Biological Chemistry 2006, 281: 20450-63.
[19] P. Calcerrada, G. Peluffo, R. Radi, Nitric oxide-derived oxidants with a focus on peroxynitrite: molecular targets, cellular responses and therapeutic implications, Current pharmaceutical design 2011, 17: 3905-32.
[20] P. Pacher, J.S. Beckman, L. Liaudet, Nitric oxide and peroxynitrite in health and disease, Physiological reviews 2007, 87: 315-424.
[21] M. Valko, C.J. Rhodes, J. Moncol, M. Izakovic, M. Mazur, Free radicals, metals and antioxidants in oxidative stress-induced cancer, Chemico-biological interactions 2006, 160: 1-40.
[22] W.A. Pryor, K.N. Houk, C.S. Foote, J.M. Fukuto, L.J. Ignarro, G.L. Squadrito, K.J. Davies, Free radical biology and medicine: it's a gas, man!, American journal of physiology. Regulatory, integrative and comparative physiology 2006, 291: R491-511.

[23] M. Fazzari, A. Trostchansky, F.J. Schopfer, S.R. Salvatore, B. Sanchez-Calvo, D. Vitturi, R. Valderrama, J.B. Barroso, R. Radi, B.A. Freeman, H. Rubbo, Olives and olive oil are sources of electrophilic fatty acid nitroalkenes, PloS one 2014, 9: e84884.
[24] E. Weitzberg, J.O. Lundberg, Novel aspects of dietary nitrate and human health, Annual review of nutrition 2013, 33: 129-59.
[25] D.S. Bredt, S.H. Snyder, Isolation of nitric oxide synthetase, a calmodulin-requiring enzyme, Proceedings of the National Academy of Sciences of the United States of America 1990, 87: 682-5.
[26] H.H.H.W. Schmidt, F. Murad, Purification and characterization of a human NO synthase, Biochemical and biophysical research communications 1991, 181: 1372-1377.
[27] D.J. Stuehr, H.J. Cho, N.S. Kwon, M.F. Weise, C.F. Nathan, Purification and characterization of the cytokine-induced macrophage nitric oxide synthase: an FAD- and FMN-containing flavoprotein, Proceedings of the National Academy of Sciences of the United States of America 1991, 88: 7773-7.
[28] J.S. Pollock, U. Forstermann, J.A. Mitchell, T.D. Warner, H.H. Schmidt, M. Nakane, F. Murad, Purification and characterization of particulate endothelium-derived relaxing factor synthase from cultured and native bovine aortic endothelial cells, Proceedings of the National Academy of Sciences of the United States of America 1991, 88: 10480-4.
[29] P.C. Dedon, S.R. Tannenbaum, Reactive nitrogen species in the chemical biology of inflammation, Archives of biochemistry and biophysics 2004, 423: 12-22.
[30] W. Flores-Santana, C. Switzer, L.A. Ridnour, D. Basudhar, D. Mancardi, S. Donzelli, D.D. Thomas, K.M. Miranda, J.M. Fukuto, D.A. Wink, Comparing the chemical biology of NO and HNO, Archives of Pharmacal Research 2009, 32: 1139-1153.
[31] A. Pautz, J. Art, S. Hahn, S. Nowag, C. Voss, H. Kleinert, Regulation of the expression of inducible nitric oxide synthase, Nitric oxide: Biology and Chemistry / Official Journal of the Nitric Oxide Society 2010, 23: 75-93.
[32] W.H. Koppenol, The basic chemistry of nitrogen monoxide and peroxynitrite, Free Radical Biology and Medicine 1998, 25: 385-91.
[33] H. Rubbo, S. Parthasarathy, S. Barnes, M. Kirk, B. Kalyanaraman, B.A. Freeman, Nitric oxide inhibition of lipoxygenase-dependent liposome and low-density lipoprotein oxidation: termination of radical chain propagation reactions and formation of nitrogen-containing oxidized lipid derivatives, Archives of biochemistry and biophysics 1995, 324: 15-25.
[34] J.R. Lancaster, Jr., Simulation of the diffusion and reaction of endogenously produced nitric oxide, Proceedings of the National Academy of Sciences of the United States of America 1994, 91: 8137-41.
[35] A. Denicola, J.M. Souza, R. Radi, E. Lissi, Nitric oxide diffusion in membranes determined by fluorescence quenching, Archives of biochemistry and biophysics 1996, 328: 208-12.
[36] J.S. Beckman, W.H. Koppenol, Nitric oxide, superoxide, and peroxynitrite: the good, the bad, and ugly, The American journal of physiology 1996, 271: C1424-37.
[37] S.P. Goss, N. Hogg, B. Kalyanaraman, The effect of nitric oxide release rates on the oxidation of human low density lipoprotein, Journal of Biological Chemistry 1997, 272: 21647-53.
[38] D.A. Wink, J.B. Mitchell, Chemical biology of nitric oxide: Insights into regulatory, cytotoxic, and cytoprotective mechanisms of nitric oxide, Free Radical Biology and Medicine 1998, 25: 434-56.
[39] D.A. Wink, J.F. Darbyshire, R.W. Nims, J.E. Saavedra, P.C. Ford, Reactions of the bioregulatory agent nitric oxide in oxygenated aqueous media: determination of the kinetics for oxidation and nitrosation by intermediates generated in the NO/O2 reaction, Chem Res Toxicol 1993, 6: 23-7.
[40] J.R. Lancaster, Jr., Nitroxidative, nitrosative, and nitrative stress: kinetic predictions of reactive nitrogen species chemistry under biological conditions, Chem Res Toxicol 2006, 19: 1160-74.
[41] M. Ramalingam, S.-J. Kim, Reactive oxygen/nitrogen species and their functional correlations in neurodegenerative diseases, Journal of Neural Transmission 2012, 119: 891-910.
[42] R. Kohen, A. Nyska, Invited Review: Oxidation of Biological Systems: Oxidative Stress Phenomena, Antioxidants, Redox Reactions, and Methods for Their Quantification, Toxicologic Pathology 2002, 30: 620-650.
[43] A. Parihar, M.S. Parihar, S. Milner, S. Bhat, Oxidative stress and anti-oxidative mobilization in burn injury, Burns : journal of the International Society for Burn Injuries 2008, 34: 6-17.
[44] M. Kirsch, H. de Groot, Formation of peroxynitrite from reaction of nitroxyl anion with molecular oxygen, Journal of Biological Chemistry 2002, 277: 13379-88.
[45] J.S. Beckman, Oxidative damage and tyrosine nitration from peroxynitrite, Chem Res Toxicol 1996, 9: 836-44.
[46] C. Szabo, H. Ischiropoulos, R. Radi, Peroxynitrite: biochemistry, pathophysiology and development of therapeutics, Nature reviews. Drug discovery 2007, 6: 662-80.

[47] R. Radi, A. Denicola, B.A. Freeman, Peroxynitrite reactions with carbon dioxide-bicarbonate, Methods Enzymol 1999, 301: 353-67.
[48] X. Liu, M.J. Miller, M.S. Joshi, D.D. Thomas, J.R. Lancaster, Jr., Accelerated reaction of nitric oxide with O2 within the hydrophobic interior of biological membranes, Proceedings of the National Academy of Sciences of the United States of America 1998, 95: 2175-9.
[49] M.L. Brennan, W. Wu, X. Fu, Z. Shen, W. Song, H. Frost, C. Vadseth, L. Narine, E. Lenkiewicz, M.T. Borchers, A.J. Lusis, J.J. Lee, N.A. Lee, H.M. Abu-Soud, H. Ischiropoulos, S.L. Hazen, A tale of two controversies: defining both the role of peroxidases in nitrotyrosine formation in vivo using eosinophil peroxidase and myeloperoxidase-deficient mice, and the nature of peroxidase-generated reactive nitrogen species, Journal of Biological Chemistry 2002, 277: 17415-27.
[50] A. van der Vliet, J.P. Eiserich, B. Halliwell, C.E. Cross, Formation of reactive nitrogen species during peroxidase-catalyzed oxidation of nitrite. A potential additional mechanism of nitric oxide-dependent toxicity, Journal of Biological Chemistry 1997, 272: 7617-25.
[51] L. Gebicka, Kinetic studies on the oxidation of nitrite by horseradish peroxidase and lactoperoxidase, Acta biochimica Polonica 1999, 46: 919-27.
[52] J. Byun, D.M. Mueller, J.S. Fabjan, J.W. Heinecke, Nitrogen dioxide radical generated by the myeloperoxidase-hydrogen peroxide-nitrite system promotes lipid peroxidation of low density lipoprotein, FEBS letters 1999, 455: 243-6.
[53] J.P. Eiserich, M. Hristova, C.E. Cross, A.D. Jones, B.A. Freeman, B. Halliwell, A. van der Vliet, Formation of nitric oxide-derived inflammatory oxidants by myeloperoxidase in neutrophils, Nature 1998, 391: 393-7.
[54] K.J. Reszka, Z. Matuszak, C.F. Chignell, J. Dillon, Oxidation of biological electron donors and antioxidants by a reactive lactoperoxidase metabolite from nitrite (NO2-): an EPR and spin trapping study, Free Radical Biology and Medicine 1999, 26: 669-78.
[55] M. Mehl, A. Daiber, S. Herold, H. Shoun, V. Ullrich, Peroxynitrite reaction with heme proteins, Nitric oxide: Biology and Chemistry / Official Journal of the Nitric Oxide Society 1999, 3: 142-52.
[56] K.M. Robinson, J.S. Beckman, Synthesis of peroxynitrite from nitrite and hydrogen peroxide, Methods Enzymol 2005, 396: 207-14.
[57] J.S. Beckman, J. Chen, H. Ischiropoulos, J.P. Crow, Oxidative chemistry of peroxynitrite, Methods Enzymol 1994, 233: 229-40.
[58] V.B. O'Donnell, J.P. Eiserich, P.H. Chumley, M.J. Jablonsky, N.R. Krishna, M. Kirk, S. Barnes, V.M. Darley-Usmar, B.A. Freeman, Nitration of unsaturated fatty acids by nitric oxide-derived reactive nitrogen species peroxynitrite, nitrous acid, nitrogen dioxide, and nitronium ion, Chem Res Toxicol 1999, 12: 83-92.
[59] S.V.S. Chakravartula, M. Balazy, Characterization of Nitro Arachidonic Acid and Nitro Linoleic Acid by Mass Spectrometry, Analytical Letters 2012, 45: 2412-2424.
[60] E. Rivera-Tirado, M. Lopez-Casillas, C. Wesdemiotis, Characterization of diazeniumdiolate nitric oxide donors (NONOates) by electrospray ionization mass spectrometry, Rapid Communications in Mass Spectrometry 2011, 25: 3581-6.
[61] W.H. Koppenol, J.J. Moreno, W.A. Pryor, H. Ischiropoulos, J.S. Beckman, Peroxynitrite, a cloaked oxidant formed by nitric oxide and superoxide, Chem Res Toxicol 1992, 5: 834-42.
[62] R. Radi, Nitric oxide, oxidants, and protein tyrosine nitration, Proceedings of the National Academy of Sciences of the United States of America 2004, 101: 4003-8.
[63] W.A. Pryor, G.L. Squadrito, The chemistry of peroxynitrite: a product from the reaction of nitric oxide with superoxide, The American journal of physiology 1995, 268: L699-722.
[64] R. Radi, Protein tyrosine nitration: biochemical mechanisms and structural basis of functional effects, Accounts of chemical research 2013, 46: 550-9.
[65] M. Balazy, T. Iesaki, J.L. Park, H. Jiang, P.M. Kaminski, M.S. Wolin, Vicinal nitrohydroxyeicosatrienoic acids: vasodilator lipids formed by reaction of nitrogen dioxide with arachidonic acid, The Journal of pharmacology and experimental therapeutics 2001, 299: 611-9.
[66] M. Rudnicki, L.A. Faine, N. Dehne, D. Namgaladze, S. Ferderbar, R. Weinlich, G.P. Amarante-Mendes, C.Y. Yan, J.E. Krieger, B. Brune, D.S. Abdalla, Hypoxia inducible factor-dependent regulation of angiogenesis by nitro-fatty acids, Arteriosclerosis, thrombosis, and vascular biology 2011, 31: 1360-7.
[67] D. Tsikas, Methods of quantitative analysis of the nitric oxide metabolites nitrite and nitrate in human biological fluids, Free radical research 2005, 39: 797-815.
[68] D. Tsikas, A.A. Zoerner, J. Jordan, Oxidized and nitrated oleic acid in biological systems: analysis by GC-MS/MS and LC-MS/MS, and biological significance, Biochimica et biophysica acta 2011, 1811: 694-705.

[69] D. Tsikas, A.A. Zoerner, A. Mitschke, F.M. Gutzki, Nitro-fatty acids occur in human plasma in the picomolar range: a targeted nitro-lipidomics GC-MS/MS study, Lipids 2009, 44: 855-65.
[70] M.M. Wright, J. Kim, T.D. Hock, N. Leitinger, B.A. Freeman, A. Agarwal, Human haem oxygenase-1 induction by nitro-linoleic acid is mediated by cAMP, AP-1 and E-box response element interactions, The Biochemical Journal 2009, 422: 353-361.
[71] A.M. Ferreira, M.I. Ferrari, A. Trostchansky, C. Batthyany, J.M. Souza, M.N. Alvarez, G.V. Lopez, P.R. Baker, F.J. Schopfer, V. O'Donnell, B.A. Freeman, H. Rubbo, Macrophage activation induces formation of the anti-inflammatory lipid cholesteryl-nitrolinoleate, The Biochemical Journal 2009, 417: 223-34.
[72] S.R. Woodcock, S.R. Salvatore, G. Bonacci, F.J. Schopfer, B.A. Freeman, Biomimetic nitration of conjugated linoleic acid: formation and characterization of naturally occurring conjugated nitrodienes, The Journal of Organic Chemistry 2014, 79: 25-33.
[73] A. Trostchansky, H. Rubbo, Nitrated fatty acids: Mechanisms of formation, chemical characterization, and biological properties, Free Radical Biology and Medicine 2008, 44: 1887-1896.
[74] H. Rubbo, A. Trostchansky, V.B. O'Donnell, Peroxynitrite-mediated lipid oxidation and nitration: mechanisms and consequences, Archives of biochemistry and biophysics 2009, 484: 167-72.
[75] E.S. Lima, P. Di Mascio, D.S. Abdalla, Cholesteryl nitrolinoleate, a nitrated lipid present in human blood plasma and lipoproteins, Journal of lipid research 2003, 44: 1660-6.
[76] V. Rudolph, T.K. Rudolph, F.J. Schopfer, G. Bonacci, S.R. Woodcock, M.P. Cole, P.R.S. Baker, R. Ramani, B.A. Freeman, Endogenous generation and protective effects of nitro-fatty acids in a murine model of focal cardiac ischaemia and reperfusion, Cardiovascular Research 2010, 85: 155-166.
[77] S.M. Nadtochiy, P.R.S. Baker, B.A. Freeman, P.S. Brookes, Mitochondrial nitroalkene formation and mild uncoupling in ischaemic preconditioning: implications for cardioprotection, Cardiovascular Research 2009, 82: 333-340.
[78] P.R. Baker, F.J. Schopfer, V.B. O'Donnell, B.A. Freeman, Convergence of nitric oxide and lipid signaling: anti-inflammatory nitro-fatty acids, Free Radical Biology and Medicine 2009, 46: 989-1003.
[79] A. Napolitano, L. Panzella, M. Savarese, R. Sacchi, I. Giudicianni, L. Paolillo, M. d'Ischia, Acid-induced structural modifications of unsaturated Fatty acids and phenolic olive oil constituents by nitrite ions: a chemical assessment, Chem Res Toxicol 2004, 17: 1329-37.
[80] A. Napolitano, E. Camera, M. Picardo, M. d'Ischia, Acid-promoted reactions of ethyl linoleate with nitrite ions: formation and structural characterization of isomeric nitroalkene, nitrohydroxy, and novel 3-nitro-1,5-hexadiene and 1,5-dinitro-1, 3-pentadiene products, The Journal of Organic Chemistry 2000, 65: 4853-60.
[81] G. Bonacci, P.R.S. Baker, S.R. Salvatore, D. Shores, N.K.H. Khoo, J.R. Koenitzer, D.A. Vitturi, S.R. Woodcock, F. Golin-Bisello, M.P. Cole, S. Watkins, C. St. Croix, C.I. Batthyany, B.A. Freeman, F.J. Schopfer, Conjugated Linoleic Acid Is a Preferential Substrate for Fatty Acid Nitration, Journal of Biological Chemistry 2012, 287: 44071-44082.
[82] M. Delmastro-Greenwood, K.S. Hughan, D.A. Vitturi, S.R. Salvatore, G. Grimes, G. Potti, S. Shiva, F.J. Schopfer, M.T. Gladwin, B.A. Freeman, S. Gelhaus Wendell, Nitrite and nitrate-dependent generation of anti-inflammatory fatty acid nitroalkenes, Free Radical Biology and Medicine 2015, 89: 333-341.
[83] G. Bonacci, E.K. Asciutto, S.R. Woodcock, S.R. Salvatore, B.A. Freeman, F.J. Schopfer, Gas-phase fragmentation analysis of nitro-fatty acids, Journal of the American Society for Mass Spectrometry 2011, 22: 1534-51.
[84] R.L. Alexander, D.J. Bates, M.W. Wright, S.B. King, C.S. Morrow, Modulation of nitrated lipid signaling by multidrug resistance protein 1 (MRP1): glutathione conjugation and MRP1-mediated efflux inhibit nitrolinoleic acid-induced, PPARgamma-dependent transcription activation, Biochemistry 2006, 45: 7889-96.
[85] P. Manini, L. Capelli, S. Reale, M. Arzillo, O. Crescenzi, A. Napolitano, V. Barone, M. d'Ischia, Chemistry of nitrated lipids: remarkable instability of 9-nitrolinoleic acid in neutral aqueous medium and a novel nitronitrate ester product by concurrent autoxidation/nitric oxide-release pathways, The Journal of Organic Chemistry 2008, 73: 7517-25.
[86] A.A. Gallon, W.A. Pryor, The reaction of low levels of nitrogen dioxide with methyl linoleate in the presence and absence of oxygen, Lipids 1994, 29: 171-6.
[87] A.A. Gallon, W.A. Pryor, The identification of the allylic nitrite and nitro derivatives of methyl linoleate and methyl linolenate by negative chemical ionization mass spectroscopy, Lipids 1993, 28: 125-33.
[88] K. Jain, A. Siddam, A. Marathi, U. Roy, J.R. Falck, M. Balazy, The mechanism of oleic acid nitration by •NO2, Free Radical Biology and Medicine 2008, 45: 269-283.
[89] M. Balazy, S. Chemtob, Trans-arachidonic acids: new mediators of nitro-oxidative stress, Pharmacology and Therapeutics 2008, 119: 275-90.

[90] H. Jiang, N. Kruger, D.R. Lahiri, D. Wang, J.-M. Vatèle, M. Balazy, Nitrogen Dioxide Inducescis-trans-Isomerization of Arachidonic Acid within Cellular Phospholipids: DETECTION OF TRANS-ARACHIDONIC ACIDS IN VIVO, Journal of Biological Chemistry 1999, 274: 16235-16241.
[91] V. Rudolph, F.J. Schopfer, N.K. Khoo, T.K. Rudolph, M.P. Cole, S.R. Woodcock, G. Bonacci, A.L. Groeger, F. Golin-Bisello, C.S. Chen, P.R. Baker, B.A. Freeman, Nitro-fatty acid metabolome: saturation, desaturation, beta-oxidation, and protein adduction, Journal of Biological Chemistry 2009, 284: 1461-73.
[92] V.B. O'Donnell, B.A. Freeman, Interactions Between Nitric Oxide and Lipid Oxidation Pathways, Implications for Vascular Disease 2001, 88: 12-21.
[93] A. Trettin, A. Böhmer, A.A. Zoerner, F.-M. Gutzki, J. Jordan, D. Tsikas, GC–MS/MS and LC–MS/MS studies on unlabelled and deuterium-labelled oleic acid (C18:1) reactions with peroxynitrite (ONOO−) in buffer and hemolysate support the pM/nM-range of nitro-oleic acids in human plasma, Journal of Chromatography B 2014, 964: 172-179.
[94] F.J. Schopfer, Y. Lin, P.R. Baker, T. Cui, M. Garcia-Barrio, J. Zhang, K. Chen, Y.E. Chen, B.A. Freeman, Nitrolinoleic acid: an endogenous peroxisome proliferator-activated receptor gamma ligand, Proceedings of the National Academy of Sciences of the United States of America 2005, 102: 2340-5.
[95] F.J. Schopfer, C. Batthyany, P.R. Baker, G. Bonacci, M.P. Cole, V. Rudolph, A.L. Groeger, T.K. Rudolph, S. Nadtochiy, P.S. Brookes, B.A. Freeman, Detection and quantification of protein adduction by electrophilic fatty acids: mitochondrial generation of fatty acid nitroalkene derivatives, Free Radical Biology and Medicine 2009, 46: 1250-9.
[96] J. Zhang, L. Villacorta, L. Chang, Z. Fan, M. Hamblin, T. Zhu, C.S. Chen, M.P. Cole, F.J. Schopfer, C.X. Deng, M.T. Garcia-Barrio, Y.H. Feng, B.A. Freeman, Y.E. Chen, Nitro-oleic acid inhibits angiotensin II-induced hypertension, Circulation Research 2010, 107: 540-8.
[97] D.G. Lim, S. Sweeney, A. Bloodsworth, C.R. White, P.H. Chumley, N.R. Krishna, F. Schopfer, V.B. O'Donnell, J.P. Eiserich, B.A. Freeman, Nitrolinoleate, a nitric oxide-derived mediator of cell function: synthesis, characterization, and vasomotor activity, Proceedings of the National Academy of Sciences of the United States of America 2002, 99: 15941-6.
[98] N.K. Khoo, V. Rudolph, M.P. Cole, F. Golin-Bisello, F.J. Schopfer, S.R. Woodcock, C. Batthyany, B.A. Freeman, Activation of vascular endothelial nitric oxide synthase and heme oxygenase-1 expression by electrophilic nitro-fatty acids, Free Radic Biol Med 2010, 48: 230-9.
[99] B. Coles, A. Bloodsworth, S.R. Clark, M.J. Lewis, A.R. Cross, B.A. Freeman, V.B. O'Donnell, Nitrolinoleate inhibits superoxide generation, degranulation, and integrin expression by human neutrophils: novel antiinflammatory properties of nitric oxide-derived reactive species in vascular cells, Circulation Research 2002, 91: 375-81.
[100] S. Borniquel, E.A. Jansson, M.P. Cole, B.A. Freeman, J.O. Lundberg, Nitrated oleic acid up-regulates PPARgamma and attenuates experimental inflammatory bowel disease, Free Radical Biology and Medicine 2010, 48: 499-505.
[101] H. Liu, Z. Jia, S. Soodvilai, G. Guan, M.H. Wang, Z. Dong, J.D. Symons, T. Yang, Nitro-oleic acid protects the mouse kidney from ischemia and reperfusion injury, American Journal of Physiology. Renal Physiology 2008, 295: F942-9.
[102] A.T. Reddy, S.P. Lakshmi, R.C. Reddy, The nitrated fatty acid 10-nitro-oleate diminishes severity of LPS-induced acute lung injury in mice, PPAR Research 2012, 2012: 617063.
[103] S. Adamson, N. Leitinger, Phenotypic modulation of macrophages in response to plaque lipids, Current opinion in lipidology 2011, 22: 335-42.
[104] M.P. Cole, T.K. Rudolph, N.K. Khoo, U.N. Motanya, F. Golin-Bisello, J.W. Wertz, F.J. Schopfer, V. Rudolph, S.R. Woodcock, S. Bolisetty, M.S. Ali, J. Zhang, Y.E. Chen, A. Agarwal, B.A. Freeman, P.M. Bauer, Nitro-fatty acid inhibition of neointima formation after endoluminal vessel injury, Circulation Research 2009, 105: 965-72.
[105] E. Kansanen, H.K. Jyrkkanen, O.L. Volger, H. Leinonen, A.M. Kivela, S.K. Hakkinen, S.R. Woodcock, F.J. Schopfer, A.J. Horrevoets, S. Yla-Herttuala, B.A. Freeman, A.L. Levonen, Nrf2-dependent and -independent responses to nitro-fatty acids in human endothelial cells: identification of heat shock response as the major pathway activated by nitro-oleic acid, Journal of Biological Chemistry 2009, 284: 33233-41.
[106] J. Hwang, K.E. Lee, J.Y. Lim, S.I. Park, Nitrated fatty acids prevent TNFalpha-stimulated inflammatory and atherogenic responses in endothelial cells, Biochemical and biophysical research communications 2009, 387: 633-40.
[107] M.M. Wright, F.J. Schopfer, P.R. Baker, V. Vidyasagar, P. Powell, P. Chumley, K.E. Iles, B.A. Freeman, A. Agarwal, Fatty acid transduction of nitric oxide signaling: nitrolinoleic acid potently activates

endothelial heme oxygenase 1 expression, Proceedings of the National Academy of Sciences of the United States of America 2006, 103: 4299-304.
[108] T. Ichikawa, J. Zhang, K. Chen, Y. Liu, F.J. Schopfer, P.R. Baker, B.A. Freeman, Y.E. Chen, T. Cui, Nitroalkenes suppress lipopolysaccharide-induced signal transducer and activator of transcription signaling in macrophages: a critical role of mitogen-activated protein kinase phosphatase 1, Endocrinology 2008, 149: 4086-94.
[109] E.S. Lima, M.G. Bonini, O. Augusto, H.V. Barbeiro, H.P. Souza, D.S. Abdalla, Nitrated lipids decompose to nitric oxide and lipid radicals and cause vasorelaxation, Free Radical Biology and Medicine 2005, 39: 532-9.
[110] R.L. Charles, O. Rudyk, O. Prysyazhna, A. Kamynina, J. Yang, C. Morisseau, B.D. Hammock, B.A. Freeman, P. Eaton, Protection from hypertension in mice by the Mediterranean diet is mediated by nitro fatty acid inhibition of soluble epoxide hydrolase, Proceedings of the National Academy of Sciences of the United States of America 2014, 111: 8167-72.
[111] B. Coles, A. Bloodsworth, J.P. Eiserich, M.J. Coffey, R.M. McLoughlin, J.C. Giddings, M.J. Lewis, R.J. Haslam, B.A. Freeman, V.B. O'Donnell, Nitrolinoleate inhibits platelet activation by attenuating calcium mobilization and inducing phosphorylation of vasodilator-stimulated phosphoprotein through elevation of cAMP, Journal of Biological Chemistry 2002, 277: 5832-40.
[112] F.J. Schopfer, P.R. Baker, G. Giles, P. Chumley, C. Batthyany, J. Crawford, R.P. Patel, N. Hogg, B.P. Branchaud, J.R. Lancaster, Jr., B.A. Freeman, Fatty acid transduction of nitric oxide signaling. Nitrolinoleic acid is a hydrophobically stabilized nitric oxide donor, Journal of Biological Chemistry 2005, 280: 19289-97.
[113] L.A. Faine, D.M. Cavalcanti, M. Rudnicki, S. Ferderbar, S.M. Macedo, H.P. Souza, S.H. Farsky, L. Bosca, D.S. Abdalla, Bioactivity of nitrolinoleate: effects on adhesion molecules and CD40-CD40L system, The Journal of nutritional biochemistry 2010, 21: 125-32.
[114] S.P. Goss, N. Hogg, B. Kalyanaraman, The antioxidant effect of spermine NONOate in human low-density lipoprotein, Chem Res Toxicol 1995, 8: 800-6.
[115] M.J. Gorczynski, J. Huang, H. Lee, S.B. King, Evaluation of nitroalkenes as nitric oxide donors, Bioorganic and Medicinal Chemistry Letters 2007, 17: 2013-2017.
[116] A. Trostchansky, H. Rubbo, Lipid nitration and formation of lipid-protein adducts: biological insights, Amino acids 2007, 32: 517-22.
[117] E.E. Kelley, C.I. Batthyany, N.J. Hundley, S.R. Woodcock, G. Bonacci, J.M. Del Rio, F.J. Schopfer, J.R. Lancaster, Jr., B.A. Freeman, M.M. Tarpey, Nitro-oleic acid, a novel and irreversible inhibitor of xanthine oxidoreductase, Journal of Biological Chemistry 2008, 283: 36176-84.
[118] D. Lin, S. Saleh, D.C. Liebler, Reversibility of covalent electrophile-protein adducts and chemical toxicity, Chem Res Toxicol 2008, 21: 2361-9.
[119] K.E. Iles, M.M. Wright, M.P. Cole, N.E. Welty, L.B. Ware, M.A. Matthay, F.J. Schopfer, P.R. Baker, A. Agarwal, B.A. Freeman, Fatty acid transduction of nitric oxide signaling: nitrolinoleic acid mediates protective effects through regulation of the ERK pathway, Free Radical Biology and Medicine 2009, 46: 866-75.
[120] T.K. Rudolph, V. Rudolph, M.M. Edreira, M.P. Cole, G. Bonacci, F.J. Schopfer, S.R. Woodcock, A. Franek, M. Pekarova, N.K. Khoo, A.H. Hasty, S. Baldus, B.A. Freeman, Nitro-fatty acids reduce atherosclerosis in apolipoprotein E-deficient mice, Arteriosclerosis, thrombosis, and vascular biology 2010, 30: 938-45.
[121] L. Villacorta, J. Zhang, M.T. Garcia-Barrio, X.L. Chen, B.A. Freeman, Y.E. Chen, T. Cui, Nitro-linoleic acid inhibits vascular smooth muscle cell proliferation via the Keap1/Nrf2 signaling pathway, American journal of physiology. Heart and circulatory physiology 2007, 293: H770-6.
[122] E. Kansanen, G. Bonacci, F.J. Schopfer, S.M. Kuosmanen, K.I. Tong, H. Leinonen, S.R. Woodcock, M. Yamamoto, C. Carlberg, S. Ylä-Herttuala, B.A. Freeman, A.-L. Levonen, Electrophilic Nitro-fatty Acids Activate NRF2 by a KEAP1 Cysteine 151-independent Mechanism, Journal of Biological Chemistry 2011, 286: 14019-14027.
[123] A. Trostchansky, L. Bonilla, C.P. Thomas, V.B. O'Donnell, L.J. Marnett, R. Radi, H. Rubbo, Nitroarachidonic acid, a novel peroxidase inhibitor of prostaglandin endoperoxide H synthases 1 and 2, Journal of Biological Chemistry 2011, 286: 12891-900.
[124] T. Uchiyama, H. Atsuta, T. Utsugi, M. Oguri, A. Hasegawa, T. Nakamura, A. Nakai, M. Nakata, I. Maruyama, H. Tomura, F. Okajima, S. Tomono, S. Kawazu, R. Nagai, M. Kurabayashi, HSF1 and constitutively active HSF1 improve vascular endothelial function (heat shock proteins improve vascular endothelial function), Atherosclerosis 2007, 190: 321-9.
[125] E. Shin, E. Yeo, J. Lim, Y.H. Chang, H. Park, E. Shim, H. Chung, H.J. Hwang, J. Chun, J. Hwang, Nitrooleate Mediates Nitric Oxide Synthase Activation in Endothelial Cells, Lipids 2014, 49: 457-466.

[126] J.M. Souza, A. Trostchansky, C. Batthyany, R. Durán, B.A. Freeman, H. Rubbo, Posttranslational Modification of Human Alpha-Synuclein by Nitro-Oleic Acid, Free Radical Biology and Medicine 2010, 49, Supplement: S158.
[127] G. Bonacci, F.J. Schopfer, C.I. Batthyany, T.K. Rudolph, V. Rudolph, N.K. Khoo, E.E. Kelley, B.A. Freeman, Electrophilic fatty acids regulate matrix metalloproteinase activity and expression, Journal of Biological Chemistry 2011, 286: 16074-81.
[128] D.E. Artim, F. Bazely, S.L. Daugherty, A. Sculptoreanu, K.B. Koronowski, F.J. Schopfer, S.R. Woodcock, B.A. Freeman, W.C. de Groat, Nitro-oleic acid targets transient receptor potential (TRP) channels in capsaicin sensitive afferent nerves of rat urinary bladder, Experimental neurology 2011, 232: 90-9.
[129] X. Zhang, J.M. Beckel, S.L. Daugherty, T. Wang, S.R. Woodcock, B.A. Freeman, W.C. de Groat, Activation of TRPC channels contributes to OA-NO(2)-induced responses in guinea-pig dorsal root ganglion neurons, The Journal of Physiology 2014, 592: 4297-4312.
[130] X. Zhang, K.B. Koronowski, L. Li, B.A. Freeman, S. Woodcock, W.C. de Groat, Nitro-oleic acid desensitizes TRPA1 and TRPV1 agonist responses in adult rat DRG neurons, Experimental neurology 2014, 251: 12-21.
[131] A. Sculptoreanu, F.A. Kullmann, D.E. Artim, F.A. Bazley, F. Schopfer, S. Woodcock, B.A. Freeman, W.C. de Groat, Nitro-oleic acid inhibits firing and activates TRPV1- and TRPA1-mediated inward currents in dorsal root ganglion neurons from adult male rats, The Journal of pharmacology and experimental therapeutics 2010, 333: 883-95.
[132] Y. Li, J. Zhang, F.J. Schopfer, D. Martynowski, M.T. Garcia-Barrio, A. Kovach, K. Suino-Powell, P.R. Baker, B.A. Freeman, Y.E. Chen, H.E. Xu, Molecular recognition of nitrated fatty acids by PPAR gamma, Nature Structural and Molecular Biology 2008, 15: 865-7.
[133] F.J. Schopfer, M.P. Cole, A.L. Groeger, C.S. Chen, N.K. Khoo, S.R. Woodcock, F. Golin-Bisello, U.N. Motanya, Y. Li, J. Zhang, M.T. Garcia-Barrio, T.K. Rudolph, V. Rudolph, G. Bonacci, P.R. Baker, H.E. Xu, C.I. Batthyany, Y.E. Chen, T.M. Hallis, B.A. Freeman, Covalent peroxisome proliferator-activated receptor gamma adduction by nitro-fatty acids: selective ligand activity and anti-diabetic signaling actions, Journal of Biological Chemistry 2010, 285: 12321-33.
[134] M.J. Gorczynski, P.K. Smitherman, T.E. Akiyama, H.B. Wood, J.P. Berger, S.B. King, C.S. Morrow, Activation of peroxisome proliferator-activated receptor gamma (PPARgamma) by nitroalkene fatty acids: importance of nitration position and degree of unsaturation, Journal of medicinal chemistry 2009, 52: 4631-9.
[135] H. Wang, H. Liu, Z. Jia, G. Guan, T. Yang, Effects of endogenous PPAR agonist nitro-oleic acid on metabolic syndrome in obese Zucker rats, PPAR Research 2010, 2010: 601562.
[136] H. Nie, X. Xue, J. Li, X. Liu, S. Lv, G. Guan, H. Liu, G. Liu, S. Liu, Z. Chen, Nitro-Oleic Acid Attenuates OGD/R-Triggered Apoptosis in Renal Tubular Cells via Inhibition of Bax Mitochondrial Translocation in a PPAR-γ-Dependent Manner, Cellular Physiology and Biochemistry 2015, 35: 1201-1218.
[137] J.R. Koenitzer, G. Bonacci, S.R. Woodcock, C.-S. Chen, N. Cantu-Medellin, E.E. Kelley, F.J. Schopfer, Fatty acid nitroalkenes induce resistance to ischemic cardiac injury by modulating mitochondrial respiration at complex II, Redox Biology 2016, 8: 1-10.
[138] S.M. Nadtochiy, Q.M. Zhu, W. Urciuoli, R. Rafikov, S.M. Black, P.S. Brookes, Nitroalkenes confer acute cardioprotection via adenine nucleotide translocase 1, Journal of Biological Chemistry 2012, 287: 3573-80.
[139] G. Ambrozova, H. Martiskova, A. Koudelka, T. Ravekes, T.K. Rudolph, A. Klinke, V. Rudolph, B.A. Freeman, S.R. Woodcock, L. Kubala, M. Pekarova, Nitro-oleic acid modulates classical and regulatory activation of macrophages and their involvement in pro-fibrotic responses, Free Radical Biology and Medicine 2016, 90: 252-260.
[140] G. Ambrozova, T. Fidlerova, H. Verescakova, A. Koudelka, T.K. Rudolph, S.R. Woodcock, B.A. Freeman, L. Kubala, M. Pekarova, Nitro-oleic acid inhibits vascular endothelial inflammatory responses and the endothelial-mesenchymal transition, Biochimica et Biophysica Acta (BBA) - General Subjects 2016, 1860: 2428-2437.
[141] S. Liu, Z. Jia, L. Zhou, Y. Liu, H. Ling, S.F. Zhou, A. Zhang, Y. Du, G. Guan, T. Yang, Nitro-oleic acid protects against adriamycin-induced nephropathy in mice, American Journal of Physiology. Renal Physiology 2013, 305: F1533-41.
[142] H. Wang, H. Liu, Z. Jia, C. Olsen, S. Litwin, G. Guan, T. Yang, Nitro-oleic acid protects against endotoxin-induced endotoxemia and multiorgan injury in mice, American Journal of Physiology. Renal Physiology 2010, 298: F754-62.

[143] B. Sánchez-Calvo, A. Cassina, N. Rios, G. Peluffo, J. Boggia, R. Radi, H. Rubbo, A. Trostchansky, Nitro-Arachidonic Acid Prevents Angiotensin II-Induced Mitochondrial Dysfunction in a Cell Line of Kidney Proximal Tubular Cells, PloS one 2016, 11: e0150459.
[144] H. Wang, Z. Jia, J. Sun, L. Xu, B. Zhao, K. Yu, M. Yang, T. Yang, R. Wang, Nitrooleic Acid Protects against Cisplatin Nephropathy: Role of COX-2/mPGES-1/PGE(2) Cascade, Mediators of Inflammation 2015, 2015: 293474.
[145] B. Sanchez-Calvo, A. Cassina, N. Rios, G. Peluffo, J. Boggia, R. Radi, H. Rubbo, A. Trostchansky, Nitro-Arachidonic Acid Prevents Angiotensin II-Induced Mitochondrial Dysfunction in a Cell Line of Kidney Proximal Tubular Cells, PloS one 2016, 11: e0150459.
[146] A.T. Reddy, S.P. Lakshmi, R.R. Muchumarri, R.C. Reddy, Nitrated Fatty Acids Reverse Cigarette Smoke-Induced Alveolar Macrophage Activation and Inhibit Protease Activity via Electrophilic S-Alkylation, PloS one 2016, 11: e0153336.
[147] A. Klinke, A. Möller, M. Pekarova, T. Ravekes, K. Friedrichs, M. Berlin, K.M. Scheu, L. Kubala, H. Kolarova, G. Ambrozova, R.T. Schermuly, S.R. Woodcock, B.A. Freeman, S. Rosenkranz, S. Baldus, V. Rudolph, T.K. Rudolph, Protective Effects of 10-nitro-oleic Acid in a Hypoxia-Induced Murine Model of Pulmonary Hypertension, American Journal of Respiratory Cell and Molecular Biology 2014, 51: 155-162.
[148] P. Diaz-Amarilla, E. Miquel, A. Trostchansky, E. Trias, A.M. Ferreira, B.A. Freeman, P. Cassina, L. Barbeito, M.R. Vargas, H. Rubbo, Electrophilic nitro-fatty acids prevent astrocyte-mediated toxicity to motor neurons in a cell model of familial amyotrophic lateral sclerosis via nuclear factor erythroid 2-related factor activation, Free Radical Biology and Medicine 2016, 95: 112-120.
[149] B. Buszewski, S. Noga, Hydrophilic interaction liquid chromatography (HILIC)--a powerful separation technique, Analytical and Bioanalytical Chemistry 2012, 402: 231-47.
[150] B. Brugger, Lipidomics: analysis of the lipid composition of cells and subcellular organelles by electrospray ionization mass spectrometry, Annual review of biochemistry 2014, 83: 79-98.
[151] H.C. Kofeler, A. Fauland, G.N. Rechberger, M. Trotzmuller, Mass spectrometry based lipidomics: an overview of technological platforms, Metabolites 2012, 2: 19-38.
[152] M. Fazzari, N. Khoo, S.R. Woodcock, L. Li, B.A. Freeman, F.J. Schopfer, Generation and esterification of electrophilic fatty acid nitroalkenes in triacylglycerides, Free Radical Biology and Medicine 2015, 87: 113-24.
[153] S.R. Woodcock, G. Bonacci, S.L. Gelhaus, F.J. Schopfer, Nitrated fatty acids: synthesis and measurement, Free Radical Biology and Medicine 2013, 59: 14-26.
[154] A. Napolitano, E. Camera, M. Picardo, M. d'Ischia, Reactions of Hydro(pero)xy Derivatives of Polyunsaturated Fatty Acids/Esters with Nitrite Ions under Acidic Conditions. Unusual Nitrosative Breakdown of Methyl 13-Hydro(pero)xyoctadeca-9,11-dienoate to a Novel 4-Nitro-2-oximinoalk-3-enal Product, Journal of Organic Chemistry 2002, 67: 1125-1132.
[155] E.M. Bartlett, D.H. Lewis, Spectrophotometric determination of phosphate esters in the presence and absence of orthophosphate, Analitycal Biochemistry 1970, 36: 159-67.
[156] R. Ferreira, G. Guerra, A.I. Padrao, T. Melo, R. Vitorino, J.A. Duarte, F. Remiao, P. Domingues, F. Amado, M.R. Domingues, Lipidomic characterization of streptozotocin-induced heart mitochondrial dysfunction, Mitochondrion 2013, 13: 762-71.
[157] E.G. Bligh, W.J. Dyer, A RAPID METHOD OF TOTAL LIPID EXTRACTION AND PURIFICATION, Canadian Journal of Biochemistry and Physiology 1959, 37: 911-917.
[158] R.A. Gaussian 09, M. J. Frisch, G. W. Trucks, H. B. Schlegel, G. E. Scuseria, M. A. Robb, J. R. Cheeseman, G. Scalmani, V. Barone, B. Mennucci, G. A. Petersson, H. Nakatsuji, M. Caricato, X. Li, H. P. Hratchian, A. F. Izmaylov, J. Bloino, G. Zheng, J. L. Sonnenberg, M. Hada, M. Ehara, K. Toyota, R. Fukuda, J. Hasegawa, M. Ishida, T. Nakajima, Y. Honda, O. Kitao, H. Nakai, T. Vreven, J. A. Montgomery, Jr., J. E. Peralta, F. Ogliaro, M. Bearpark, J. J. Heyd, E. Brothers, K. N. Kudin, V. N. Staroverov, R. Kobayashi, J. Normand, K. Raghavachari, A. Rendell, J. C. Burant, S. S. Iyengar, J. Tomasi, M. Cossi, N. Rega, J. M. Millam, M. Klene, J. E. Knox, J. B. Cross, V. Bakken, C. Adamo, J. Jaramillo, R. Gomperts, R. E. Stratmann, O. Yazyev, A. J. Austin, R. Cammi, C. Pomelli, J. W. Ochterski, R. L. Martin, K. Morokuma, V. G. Zakrzewski, G. A. Voth, P. Salvador, J. J. Dannenberg, S. Dapprich, A. D. Daniels, Ö. Farkas, J. B. Foresman, J. V. Ortiz, J. Cioslowski, and D. J. Fox, Gaussian, Inc., Wallingford CT, 2009.
[159] E.D.G. NBO Version 3.1, A. E. Reed, J. E. Carpenter, and F. Weinhold.
[160] L.M. Magalhães, M.A. Segundo, S. Reis, J.L.F.C. Lima, Automatic method for determination of total antioxidant capacity using 2,2-diphenyl-1-picrylhydrazyl assay, Analytica Chimica Acta 2006, 558: 310-318.
[161] L.M. Magalhaes, L. Barreiros, M.A. Maia, S. Reis, M.A. Segundo, Rapid assessment of endpoint antioxidant capacity of red wines through microchemical methods using a kinetic matching approach, Talanta 2012, 97: 473-83.

[162] M. Ozgen, R.N. Reese, A.Z. Tulio, Jr., J.C. Scheerens, A.R. Miller, Modified 2,2-azino-bis-3-ethylbenzothiazoline-6-sulfonic acid (abts) method to measure antioxidant capacity of Selected small fruits and comparison to ferric reducing antioxidant power (FRAP) and 2,2'-diphenyl-1-picrylhydrazyl (DPPH) methods, Journal of Agricultural and Food Chemistry 2006, 54: 1151-7.
[163] V. Francisco, A. Figueirinha, B.M. Neves, C. Garcia-Rodriguez, M.C. Lopes, M.T. Cruz, M.T. Batista, Cymbopogon citratus as source of new and safe anti-inflammatory drugs: bio-guided assay using lipopolysaccharide-stimulated macrophages, Journal of Ethnopharmacology 2011, 133: 818-27.
[164] M. Pulfer, R.C. Murphy, Electrospray mass spectrometry of phospholipids, Mass Spectrometry Reviews 2003, 22: 332-64.
[165] S.M. Lam, G. Shui, Lipidomics as a Principal Tool for Advancing Biomedical Research, Journal of Genetics and Genomics 2013, 40: 375-390.
[166] Y.-P. Tu, K. Lu, S.-Y. Liu, Chemical ionization mass spectrometry of some nitro-containing bifunctional aromatic compounds. Location of protonation site, Rapid Communications in Mass Spectrometry 1995, 9: 609-614.
[167] J. Moolayil, M. George, R. Srinivas, D. Giblin, A. Russell, M. Gross, Protonated nitro group as a gas-phase electrophile: Experimental and theoretical study of the cyclization of o-nitrodiphenyl ethers, amines, and sulfides, Journal of the American Society for Mass Spectrometry 2007, 18: 2204-2217.
[168] P. Domingues, M.R. Domingues, F.M. Amado, A.J. Ferrer-Correia, Characterization of sodiated glycerol phosphatidylcholine phospholipids by mass spectrometry, Rapid Communications in Mass Spectrometry 2001, 15: 799-804.
[169] F.-F. Hsu, J. Turk, Studies on phosphatidylserine by tandem quadrupole and multiple stage quadrupole ion-trap mass spectrometry with electrospray ionization: Structural characterization and the fragmentation processes, Journal of the American Society for Mass Spectrometry 2005, 16: 1510-1522.
[170] F.-F. Hsu, J. Turk, Electrospray ionization with low-energy collisionally activated dissociation tandem mass spectrometry of glycerophospholipids: Mechanisms of fragmentation and structural characterization, Journal of Chromatography B 2009, 877: 2673-2695.
[171] C. Simões, V. Simões, A. Reis, P. Domingues, M.R. Domingues, Determination of the fatty acyl profiles of phosphatidylethanolamines by tandem mass spectrometry of sodium adducts, Rapid Communications in Mass Spectrometry 2008, 22: 3238-44.
[172] K.A. Al-Saad, W.F. Siems, H.H. Hill, V. Zabrouskov, N.R. Knowles, Structural analysis of phosphatidylcholines by post-source decay matrix-assisted laser desorption/ionization time-of-flight mass spectrometry, Journal of the American Society for Mass Spectrometry 2003, 14: 373-382.
[173] T. Melo, E.M. Silva, C. Simoes, P. Domingues, M.R. Domingues, Photooxidation of glycated and non-glycated phosphatidylethanolamines monitored by mass spectrometry, Journal of Mass Spectrometry 2013, 48: 68-78.
[174] A. Reis, P. Domingues, A.J. Ferrer-Correia, M.R. Domingues, Tandem mass spectrometry of intact oxidation products of diacylphosphatidylcholines: evidence for the occurrence of the oxidation of the phosphocholine head and differentiation of isomers, Journal of Mass Spectrometry 2004, 39: 1513-22.
[175] T. Melo, P. Domingues, R. Ferreira, I. Milic, M. Fedorova, S.M. Santos, M.A. Segundo, M.R. Domingues, Recent advances on mass spectrometry analysis of nitrated phospholipids, Analytical Chemistry 2016, 88: 2622-9.
[176] C.M. Spickett, A.R. Pitt, Oxidative lipidomics coming of age: advances in analysis of oxidized phospholipids in physiology and pathology, Antioxidants and Redox Signaling 2015, 22: 1646-66.
[177] B. Sousa, T. Melo, A. Campos, A.S. Moreira, E. Maciel, P. Domingues, R.P. Carvalho, T.R. Rodrigues, H. Girao, M.R. Domingues, Alteration in Phospholipidome Profile of Myoblast H9c2 Cell Line in a Model of Myocardium Starvation and Ischemia, Journal of cellular physiology 2016, 231: 2266-74.
[178] A. Denicola, C. Batthyány, E. Lissi, B.A. Freeman, H. Rubbo, R. Radi, Diffusion of Nitric Oxide into Low Density Lipoprotein, Journal of Biological Chemistry 2002, 277: 932-936.
[179] D.D. Thomas, X. Liu, S.P. Kantrow, J.R. Lancaster, Jr., The biological lifetime of nitric oxide: implications for the perivascular dynamics of NO and O2, Proceedings of the National Academy of Sciences of the United States of America 2001, 98: 355-60.
[180] L. Villacorta, Z. Gao, F.J. Schopfer, B.A. Freeman, Y.E. Chen, Nitro-fatty acids in cardiovascular regulation and diseases: characteristics and molecular mechanisms, Frontiers in bioscience 2016, 21: 873-89.
[181] L. Villacorta, L. Chang, S.R. Salvatore, T. Ichikawa, J. Zhang, D. Petrovic-Djergovic, L. Jia, H. Carlsen, F.J. Schopfer, B.A. Freeman, Y.E. Chen, Electrophilic nitro-fatty acids inhibit vascular inflammation by disrupting LPS-dependent TLR4 signalling in lipid rafts, Cardiovascular Research 2013, 98: 116-24.

[182] M. Abdelrahman, A. Sivarajah, C. Thiemermann, Beneficial effects of PPAR-gamma ligands in ischemia-reperfusion injury, inflammation and shock, Cardiovascular Research 2005, 65: 772-81.
[183] A.J. Gilde, M. Van Bilsen, Peroxisome proliferator-activated receptors (PPARS): regulators of gene expression in heart and skeletal muscle, Acta physiologica Scandinavica 2003, 178: 425-34.
[184] G.D. Lopaschuk, J.R. Ussher, C.D. Folmes, J.S. Jaswal, W.C. Stanley, Myocardial fatty acid metabolism in health and disease, Physiological reviews 2010, 90: 207-58.
[185] P.M. Barger, D.P. Kelly, PPAR signaling in the control of cardiac energy metabolism, Trends in cardiovascular medicine 2000, 10: 238-45.
[186] L.S. Golfman, C.R. Wilson, S. Sharma, M. Burgmaier, M.E. Young, P.H. Guthrie, M. Van Arsdall, J.V. Adrogue, K.K. Brown, H. Taegtmeyer, Activation of PPARgamma enhances myocardial glucose oxidation and improves contractile function in isolated working hearts of ZDF rats, American journal of physiology. Endocrinology and metabolism 2005, 289: E328-36.
[187] A.T. Reddy, S.P. Lakshmi, J.M. Kleinhenz, R.L. Sutliff, C.M. Hart, R.C. Reddy, Endothelial cell peroxisome proliferator-activated receptor gamma reduces endotoxemic pulmonary inflammation and injury, Journal of immunology 2012, 189: 5411-20.
[188] Y. Ren, C. Sun, Y. Sun, H. Tan, Y. Wu, B. Cui, Z. Wu, PPAR gamma protects cardiomyocytes against oxidative stress and apoptosis via Bcl-2 upregulation, Vascular pharmacology 2009, 51: 169-74.
[189] M. Asakawa, H. Takano, T. Nagai, H. Uozumi, H. Hasegawa, N. Kubota, T. Saito, Y. Masuda, T. Kadowaki, I. Komuro, Peroxisome proliferator-activated receptor gamma plays a critical role in inhibition of cardiac hypertrophy in vitro and in vivo, Circulation 2002, 105: 1240-6.
[190] A.T. Reddy, S.P. Lakshmi, S. Dornadula, S. Pinni, D.R. Rampa, R.C. Reddy, The nitrated fatty acid 10-nitro-oleate attenuates allergic airway disease, Journal of immunology 2013, 191: 2053-63.
[191] N.S. Dhalla, R.M. Temsah, T. Netticadan, Role of oxidative stress in cardiovascular diseases, Journal of hypertension 2000, 18: 655-73.
[192] G.D. Girnun, F.E. Domann, S.A. Moore, M.E. Robbins, Identification of a functional peroxisome proliferator-activated receptor response element in the rat catalase promoter, Molecular endocrinology 2002, 16: 2793-801.
[193] R. Schreck, K. Albermann, P.A. Baeuerle, Nuclear factor kappa B: an oxidative stress-responsive transcription factor of eukaryotic cells (a review), Free radical research communications 1992, 17: 221-37.
[194] X. Wang, S. Takeda, S. Mochizuki, R. Jindal, N.S. Dhalla, Mechanisms of Hydrogen Peroxide-Induced Increase in Intracellular Calcium in Cardiomyocytes, Journal of cardiovascular pharmacology and therapeutics 1999, 4: 41-48.
[195] T. Tsujita, L. Li, H. Nakajima, N. Iwamoto, Y. Nakajima-Takagi, K. Ohashi, K. Kawakami, Y. Kumagai, B.A. Freeman, M. Yamamoto, M. Kobayashi, Nitro-fatty acids and cyclopentenone prostaglandins share strategies to activate the Keap1-Nrf2 system: a study using green fluorescent protein transgenic zebrafish, Genes to Cells : Devoted to Molecular and Cellular Mechanisms 2011, 16: 46-57.
[196] M. Akerfelt, R.I. Morimoto, L. Sistonen, Heat shock factors: integrators of cell stress, development and lifespan, Nature reviews. Molecular cell biology 2010, 11: 545-55.
[197] E. Kansanen, H.K. Jyrkkanen, A.L. Levonen, Activation of stress signaling pathways by electrophilic oxidized and nitrated lipids, Free Radical Biology and Medicine 2012, 52: 973-82.
[198] J.J. Lum, D.E. Bauer, M. Kong, M.H. Harris, C. Li, T. Lindsten, C.B. Thompson, Growth factor regulation of autophagy and cell survival in the absence of apoptosis, Cell 2005, 120: 237-48.
[199] H. Kanamori, G. Takemura, R. Maruyama, K. Goto, A. Tsujimoto, A. Ogino, L. Li, I. Kawamura, T. Takeyama, T. Kawaguchi, K. Nagashima, T. Fujiwara, H. Fujiwara, M. Seishima, S. Minatoguchi, Functional significance and morphological characterization of starvation-induced autophagy in the adult heart, The American journal of pathology 2009, 174: 1705-14.
[200] A.B. Gustafsson, R.A. Gottlieb, Recycle or die: the role of autophagy in cardioprotection, Journal of molecular and cellular cardiology 2008, 44: 654-61.
[201] Y. Lee, H.Y. Lee, A.B. Gustafsson, Regulation of autophagy by metabolic and stress signaling pathways in the heart, Journal of cardiovascular pharmacology 2012, 60: 118-24.
[202] Z. Xia, H. Li, M.G. Irwin, Myocardial ischaemia reperfusion injury: the challenge of translating ischaemic and anaesthetic protection from animal models to humans, British journal of anaesthesia 2016, 117 Suppl 2: ii44-ii62.
[203] L.M. Magalhaes, M.A. Segundo, S. Reis, J.L. Lima, Methodological aspects about in vitro evaluation of antioxidant properties, Analytica Chimica Acta 2008, 613: 1-19.
[204] H. Yin, L. Xu, N.A. Porter, Free radical lipid peroxidation: mechanisms and analysis, Chemical Reviews 2011, 111: 5944-72.

[205] R.L. Prior, X. Wu, K. Schaich, Standardized methods for the determination of antioxidant capacity and phenolics in foods and dietary supplements, Journal of Agricultural and Food Chemistry 2005, 53: 4290-302.
[206] A. Khatchadourian, D. Maysinger, Lipid droplets: their role in nanoparticle-induced oxidative stress, Molecular Pharmaceutics 2009, 6: 1125-1137.
[207] A. Reis, M.R. Domingues, F.M. Amado, A.J. Ferrer-Correia, P. Domingues, Separation of peroxidation products of diacyl-phosphatidylcholines by reversed-phase liquid chromatography-mass spectrometry, Biomedical Chromatography 2005, 19: 129-37.
[208] M.G. Repetto, S.F. Llesuy, Antioxidant properties of natural compounds used in popular medicine for gastric ulcers, Brazilian Journal of Medical and Biological Research 2002, 35: 523-34.
[209] C.C. Lin, P.C. Huang, Antioxidant and hepatoprotective effects of Acathopanax senticosus, Phytotherapy Research 2000, 14: 489-94.
[210] E.K. Perry, A.T. Pickering, W.W. Wang, P.J. Houghton, N.S. Perry, Medicinal plants and Alzheimer's disease: from ethnobotany to phytotherapy, The Journal of Pharmacy and Pharmacology 1999, 51: 527-34.
[211] C. Mohanty, M. Das, S.K. Sahoo, Sustained wound healing activity of curcumin loaded oleic acid based polymeric bandage in a rat model, Molecular Pharmaceutics 2012, 9: 2801-11.
[212] A.A. Geronikaki, A.M. Gavalas, Antioxidants and inflammatory disease: synthetic and natural antioxidants with anti-inflammatory activity, Combinatorial Chemistry and High Throughput Screening 2006, 9: 425-42.
[213] L. Chang, R.D. Goldman, Intermediate filaments mediate cytoskeletal crosstalk, Nature reviews. Molecular cell biology 2004, 5: 601-13.
[214] R.D. Goldman, M.M. Cleland, S.N. Murthy, S. Mahammad, E.R. Kuczmarski, Inroads into the structure and function of intermediate filament networks, Journal of structural biology 2012, 177: 14-23.
[215] G. Colakoglu, A. Brown, Intermediate filaments exchange subunits along their length and elongate by end-to-end annealing, The Journal of cell biology 2009, 185: 769-77.
[216] K.L. Vikstrom, S.S. Lim, R.D. Goldman, G.G. Borisy, Steady state dynamics of intermediate filament networks, The Journal of cell biology 1992, 118: 121-9.
[217] M. Yoon, R.D. Moir, V. Prahlad, R.D. Goldman, Motile properties of vimentin intermediate filament networks in living cells, The Journal of cell biology 1998, 143: 147-57.
[218] T. Katsumoto, A. Mitsushima, T. Kurimura, The role of the vimentin intermediate filaments in rat 3Y1 cells elucidated by immunoelectron microscopy and computer-graphic reconstruction, Biology of the cell / under the auspices of the European Cell Biology Organization 1990, 68: 139-46.
[219] B. Eckes, D. Dogic, E. Colucci-Guyon, N. Wang, A. Maniotis, D. Ingber, A. Merckling, F. Langa, M. Aumailley, A. Delouvee, V. Koteliansky, C. Babinet, T. Krieg, Impaired mechanical stability, migration and contractile capacity in vimentin-deficient fibroblasts, Journal of cell science 1998, 111 (Pt 13): 1897-907.
[220] H. Kim, F. Nakamura, W. Lee, C. Hong, D. Perez-Sala, C.A. McCulloch, Regulation of cell adhesion to collagen via beta1 integrins is dependent on interactions of filamin A with vimentin and protein kinase C epsilon, Experimental cell research 2010, 316: 1829-44.
[221] J.E. Eriksson, T. Dechat, B. Grin, B. Helfand, M. Mendez, H.M. Pallari, R.D. Goldman, Introducing intermediate filaments: from discovery to disease, The Journal of clinical investigation 2009, 119: 1763-71.
[222] J. Lowery, E.R. Kuczmarski, H. Herrmann, R.D. Goldman, Intermediate Filaments Play a Pivotal Role in Regulating Cell Architecture and Function, Journal of Biological Chemistry 2015, 290: 17145-53.
[223] A.J. Sarria, S.R. Panini, R.M. Evans, A functional role for vimentin intermediate filaments in the metabolism of lipoprotein-derived cholesterol in human SW-13 cells, Journal of Biological Chemistry 1992, 267: 19455-63.
[224] J.A. Johnston, C.L. Ward, R.R. Kopito, Aggresomes: a cellular response to misfolded proteins, The Journal of cell biology 1998, 143: 1883-98.
[225] D. Perez-Sala, C.L. Oeste, A.E. Martinez, M.J. Carrasco, B. Garzon, F.J. Canada, Vimentin filament organization and stress sensing depend on its single cysteine residue and zinc binding, Nature communications 2015, 6: 7287.
[226] J. Chavez, W.G. Chung, C.L. Miranda, M. Singhal, J.F. Stevens, C.S. Maier, Site-specific protein adducts of 4-hydroxy-2(E)-nonenal in human THP-1 monocytic cells: protein carbonylation is diminished by ascorbic acid, Chem Res Toxicol 2010, 23: 37-47.
[227] M. Fratelli, H. Demol, M. Puype, S. Casagrande, I. Eberini, M. Salmona, V. Bonetto, M. Mengozzi, F. Duffieux, E. Miclet, A. Bachi, J. Vandekerckhove, E. Gianazza, P. Ghezzi, Identification by redox proteomics of glutathionylated proteins in oxidatively stressed human T lymphocytes, Proceedings of the National Academy of Sciences of the United States of America 2002, 99: 3505-10.
[228] B. Huang, S.C. Chen, D.L. Wang, Shear flow increases S-nitrosylation of proteins in endothelial cells, Cardiovascular Research 2009, 83: 536-46.

[229] M.B. West, B.G. Hill, Y.T. Xuan, A. Bhatnagar, Protein glutathiolation by nitric oxide: an intracellular mechanism regulating redox protein modification, FASEB journal : official publication of the Federation of American Societies for Experimental Biology 2006, 20: 1715-7.
[230] K. Stamatakis, F.J. Sanchez-Gomez, D. Perez-Sala, Identification of novel protein targets for modification by 15-deoxy-Delta12,14-prostaglandin J2 in mesangial cells reveals multiple interactions with the cytoskeleton, Journal of the American Society of Nephrology 2006, 17: 89-98.
[231] S. Zorrilla, B. Garzon, D. Perez-Sala, Selective binding of the fluorescent dye 1-anilinonaphthalene-8-sulfonic acid to peroxisome proliferator-activated receptor gamma allows ligand identification and characterization, Analitycal Biochemistry 2010, 399: 84-92.

SUPPLEMTARY FIGURES

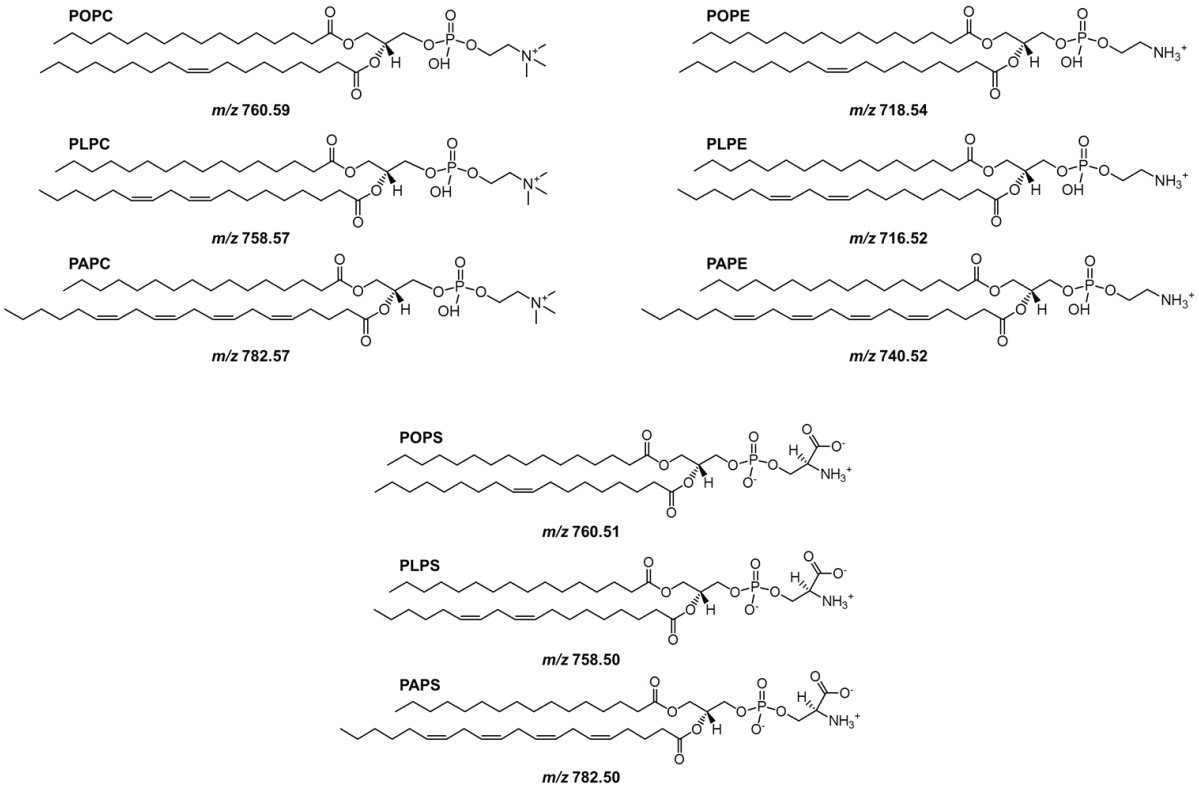

Figure S-1. Representative structure of the phospholipids used in this study. POPC, 1-palmitoyl-2-oleoyl-*sn*-glycero-3-phosphocholine (16:0/18:1); PLPC, 1-palmitoyl-2-linoleoyl-*sn*-glycero-3-phosphocholine (16:0/18:2); PAPC, 1-palmitoyl-2-arachidonoyl-*sn*-glycero-3-phosphocholine (16:0/20:4). POPE, 1-palmitoyl-2-oleoyl-*sn*-glycero-3-phosphoethanolamine (16:0/18:1); PLPE, 1-palmitoyl-2-linoleoyl-*sn*-glycero-3-phosphoethanolamine (16:0/18:2); PAPE, 1-palmitoyl-2-arachidonoyl-*sn*-glycero-3-phosphoethanolamine (16:0/20:4). POPS, 1-palmitoyl-2-oleoyl-*sn*-glycero-3-phosphoserine (16:0/18:1); PLPS, 1-palmitoyl-2-linoleoyl-*sn*-glycero-3-phosphoserine (16:0/18:2); PAPS, 1-palmitoyl-2-arachidonoyl-*sn*-glycero-3-phosphoserine (16:0/20:4).

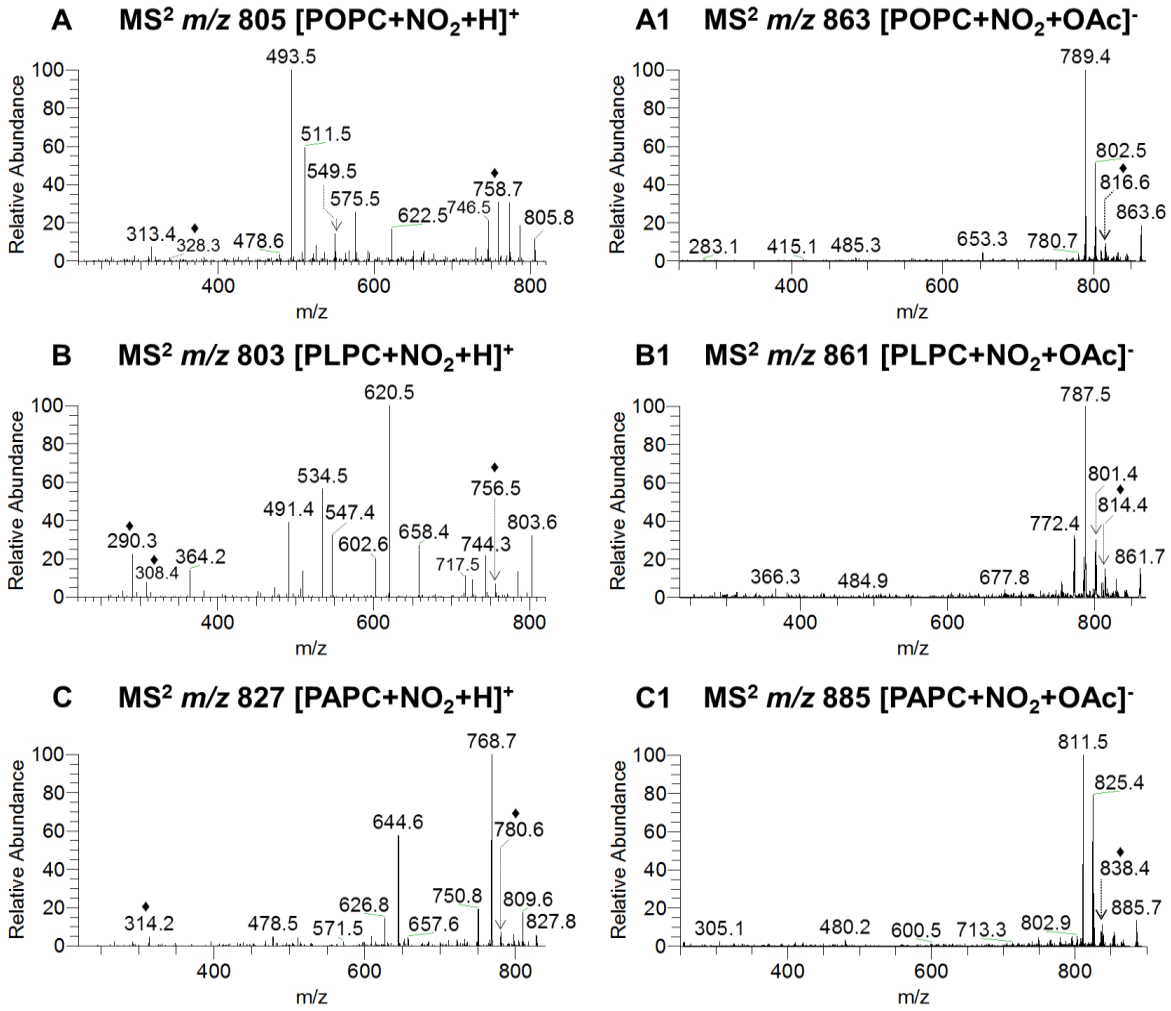

Figure S-2. ESI-MS/MS spectra of $[M+NO_2+H]^+$ and $[M+NO_2+OAc]^-$ molecular ions of: A) POPC ($[POPC+NO_2+H]^+$; A1, $[POPC+NO_2+OAc]^-$); B) PLPC ($[PLPC+NO_2+H]^+$; B1, $[PLPC+NO_2+OAc]^-$) and; C) PAPC ($[PAPC+NO_2+H]^+$; C1, $[PAPC+NO_2+OAc]^-$). Product ions indicating the presence of a NO_2 group are labeled with (♦).

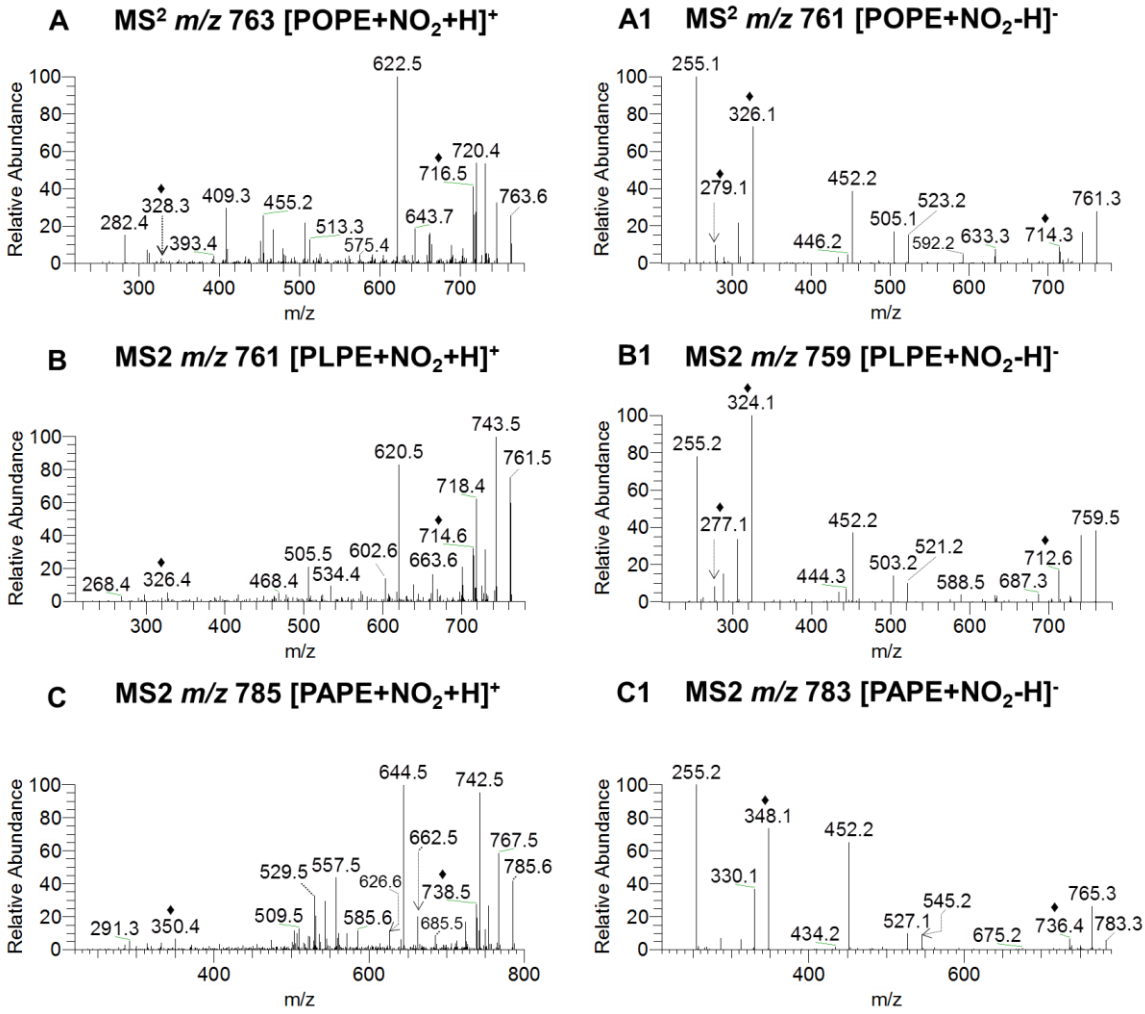

Figure S-3. ESI-MS/MS spectra of $[M+NO_2+H]^+$ and $[M+NO_2-H]^-$ molecular ions of: A) POPE ($[POPE+NO_2+H]^+$; A1, $[POPE+NO_2-H]^-$); B) PLPE ($[PLPE+NO_2+H]^+$; B1, $[PLPE+NO_2-H]^-$) and; C) PAPE ($[PAPE+NO_2+H]^+$; C1, $[PAPE+NO_2-H]^-$). Product ions indicating the presence of a NO_2 group are labeled with (♦).

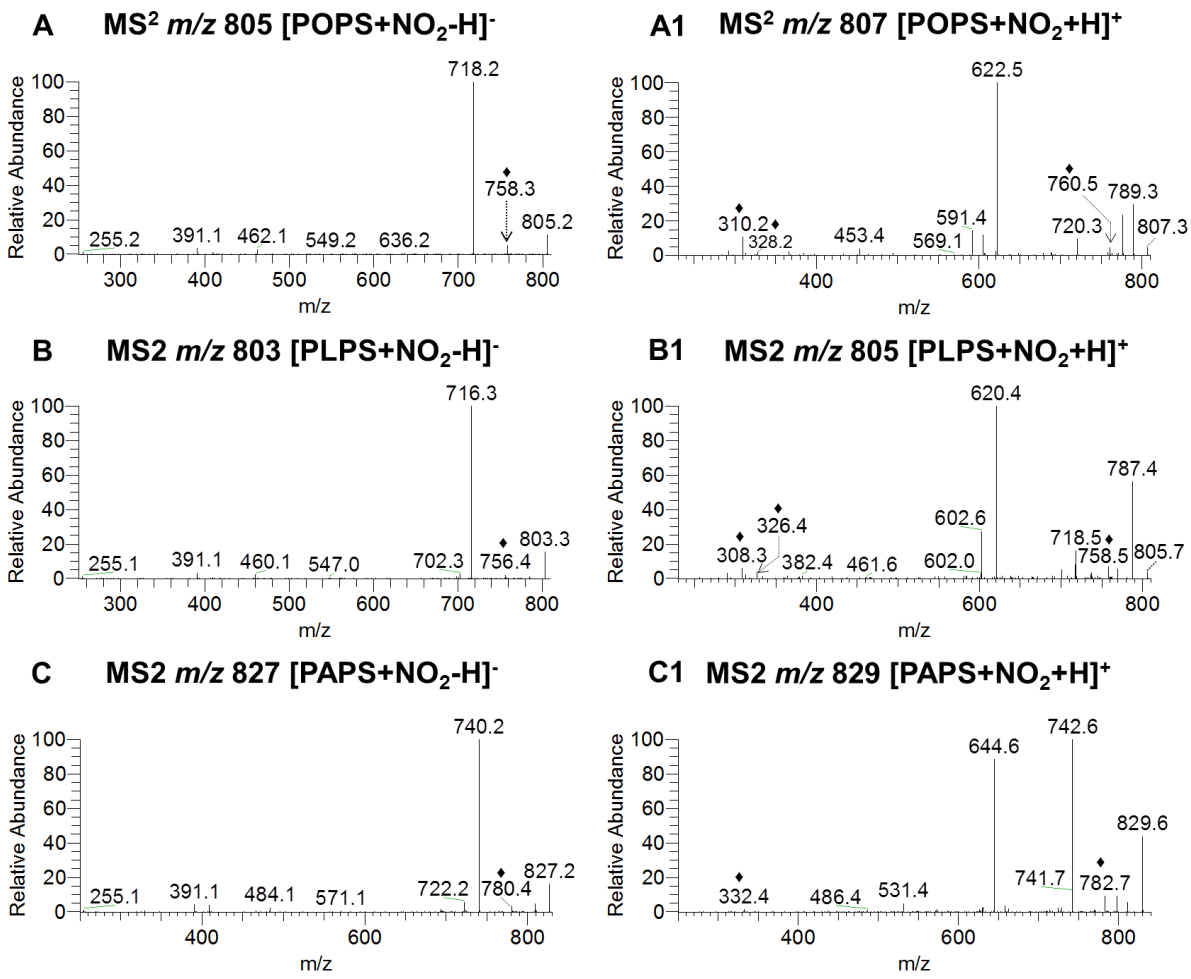

Figure S-4. ESI-MS/MS spectra of $[M+NO_2\text{-}H]^-$ and $[M+NO_2+H]^+$ molecular ions of: A) POPS ($[POPS+NO_2\text{-}H]^-$; A1, $[POPS+NO_2+H]^+$); B) PLPS ($[PLPS+NO_2\text{-}H]^-$; B1, $[PLPS+NO_2+H]^+$) and; C) PAPS ($[PAPS+NO_2\text{-}H]^-$; C1, $[PLPS+NO_2+H]^+$). Product ions indicating the presence of a NO_2 group are labeled with (♦).

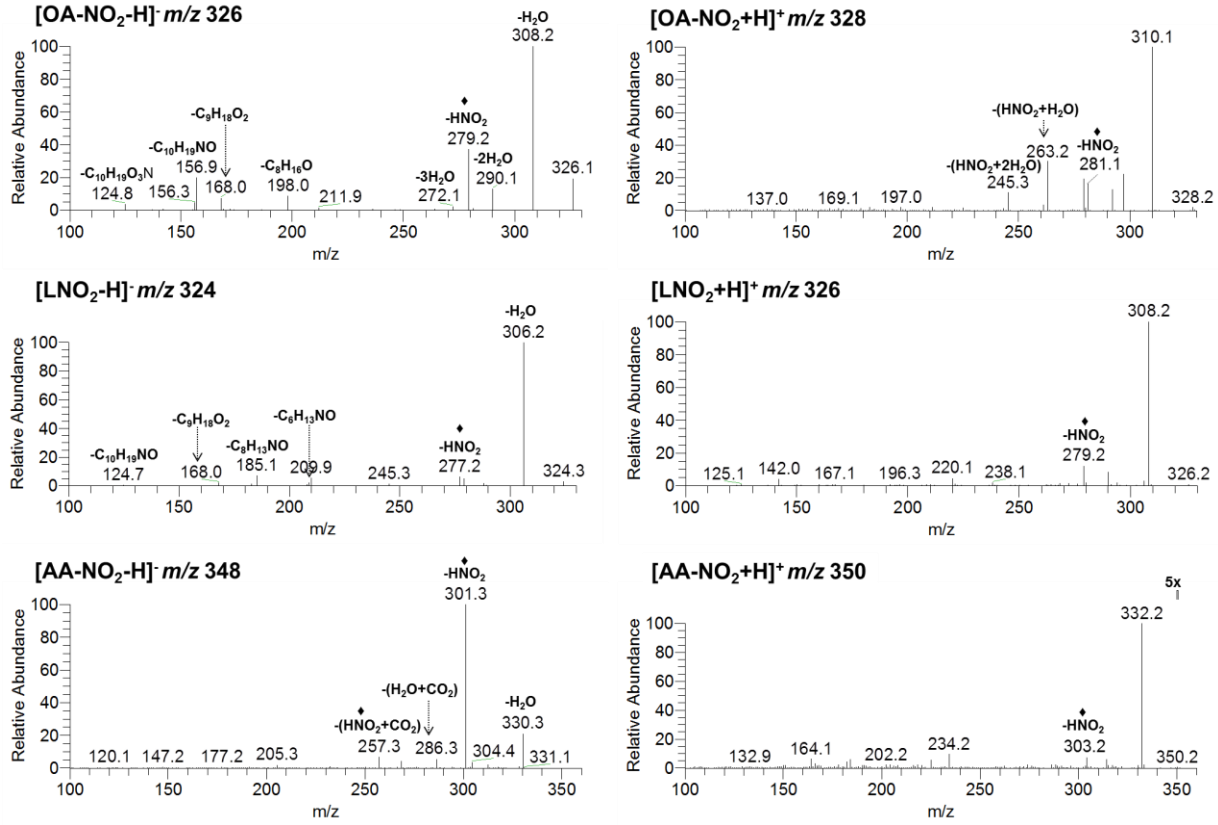

Figure S-5. MS^3 spectra of $[M+NO_2-H]^-$ and $[M+NO_2+H]^+$ ions of oleic acid ($[NO_2\text{-}OA\text{-}H]^-$ ions at *m/z* 326.1; $[NO_2\text{-}OA+H]^+$ ions at *m/z* 328.2), linoleic acid ($[NO_2\text{-}LA\text{-}H]^-$ ions at *m/z* 324.3; $[NO_2\text{-}LA+H]^+$ ions at *m/z* 326.2) and arachidonic acid ($[NO_2\text{-}AA\text{-}H]^-$ ions at *m/z* 348.2; ($[NO_2\text{-}AA+H]^+$ ions at *m/z* 350.2). Product ions indicating the presence of a NO_2 group are labeled with (♦).

Two major fragmentation pathways were proposed for the two distinct isomers NO_2-OA-PL. In the MS^3 of the NO_2-$OACOO^-$, the 9-NO_2-OA isomer gives specific signals at *m/z* 156.9 ($C_8H_{13}O_3^-$; loss of $C_{10}H_{19}ON$) and 168.0 ($C_9H_{14}O_2N^-$; loss of $C_9H_{18}O_2$), while 10-NO_2-OA was assigned based on product ions at *m/z* 124.9 ($C_8H_{13}O^-$; loss of $C_{10}H_{19}O_3N$) and 198.0 ($C_{10}H_{16}O_3N^-$; loss of) (Figure S-6 A and S-11). For NO_2-LA-PL, 9-NO_2-LA was assigned based on product ions at *m/z* 156.9 ($C_8H_{13}O_3^-$; loss of $C_{10}H_{19}ON$), *m/z* 168.0 ($C_9H_{14}O_2N^-$; loss of $C_9H_{16}O_2$) and *m/z* 209.9 ($C_{11}H_{16}O_3N^-$; loss of $C_7H_{17}O$), 10-NO_2-LA at *m/z* 124.7 ($C_8H_{13}O^-$; loss of $C_{10}H_{17}ON$), *m/z* 182.1 ($C_{10}H_{16}O_2N^-$; loss of $C_8H_{14}O_2$) and *m/z* 238.1 ($C_{13}H_{20}O_3N^-$; loss of $C_5H_{10}O$), 13- NO_2-LA at *m/z* 185.1 ($C_{10}H_{17}O_3^-$; loss of $C_8H_{13}ON$) and 208.9 ($C_{12}H_{17}O_3^-$; loss of $C_6H_{13}ON$). Low abundant product ions observed at *m/z* 195.1 ($C_{11}H_{15}O_3^-$; loss of $C_7H_{15}ON$) along with ions at *m/z* 156.9 ($C_8H_{13}O_3^-$; loss of $C_{10}H_{19}ON$) can be assigned as 12- NO_2-LA (Figure S-6 B and S-11). For NO_2-AA-PL, 14-NO_2-AA was assigned based on product ions at *m/z* 165.3 ($C_{10}H_{13}O_2^-$; loss of $C_{10}H_{17}O_2N$), 195.2 ($C_{11}H_{15}O_3^-$; loss of $C_9H_{15}ON$) and 177.2 ($C_{11}H_{13}O_2^-$; loss of $C_9H_{17}O_2N$) while 15-NO_2-AA was assigned based on product ions at *m/z* 191.3 ($C_{12}H_{15}O_2^-$; loss of $C_8H_{15}O_2N$), 147.2 ($C_{11}H_{15}^-$; loss of $C_9H_{15}O_4N$), 205.3 ($C_{13}H_{17}O_2^-$; loss of $C_7H_{13}O_2N$), 195.2 ($C_{11}H_{15}O_3^-$; loss of $C_9H_{15}ON$) and 177.2 ($C_{11}H_{13}O_2^-$; loss of $C_9H_{17}O_2N$). For 11- and 12-NO_2-AA assignment, product ions were observed at *m/z* 155.2 ($C_8H_{11}O_3^-$; loss of $C_{12}H_{19}ON$) (Figure S-6 C and S-11).

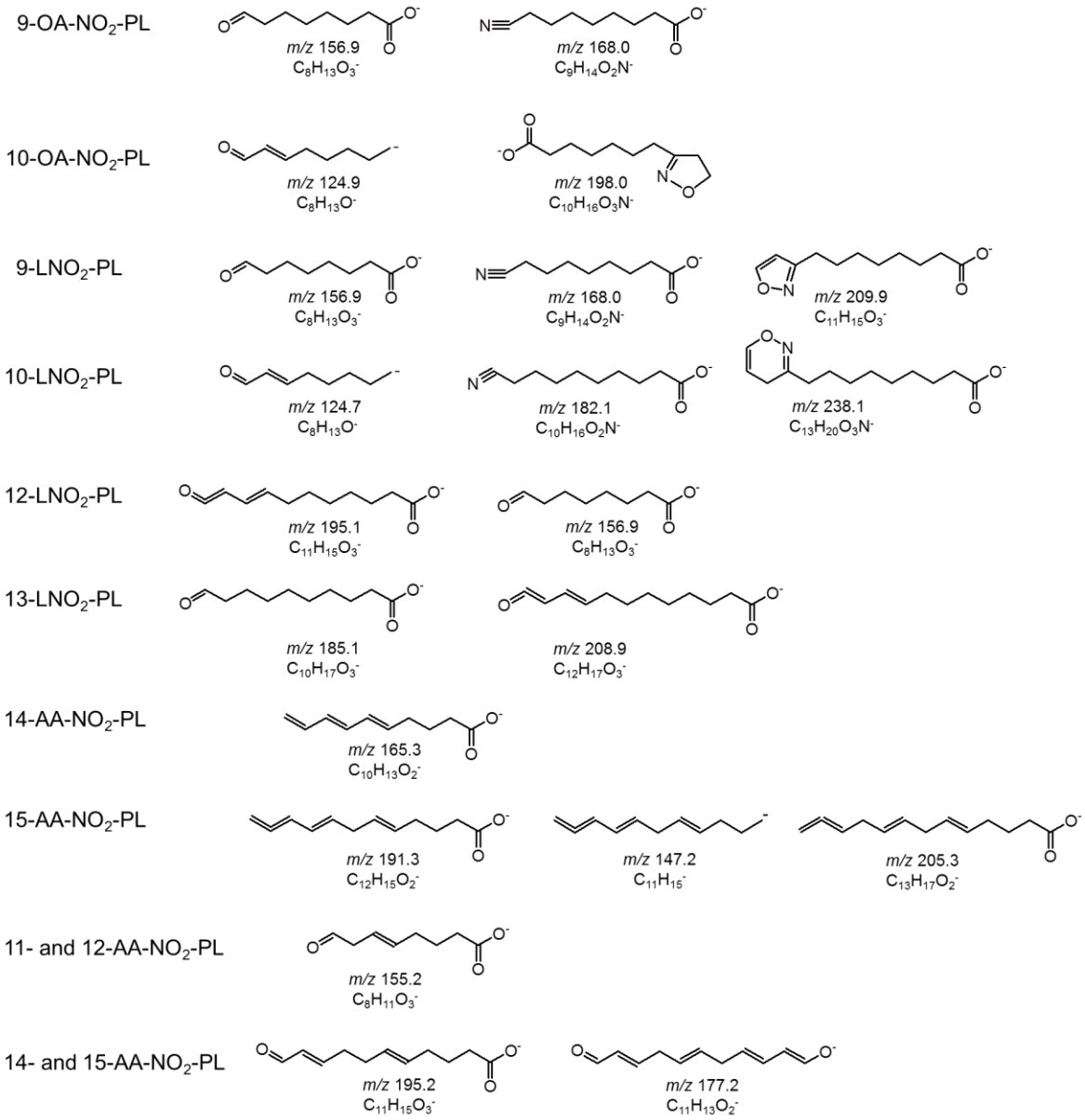

Figure S-6. Fragmentation products observed in the MS^3 spectra of the $[M-H]^-$ ions of NO_2-FA and proposed structural information for each nitroalkene isomer identified.

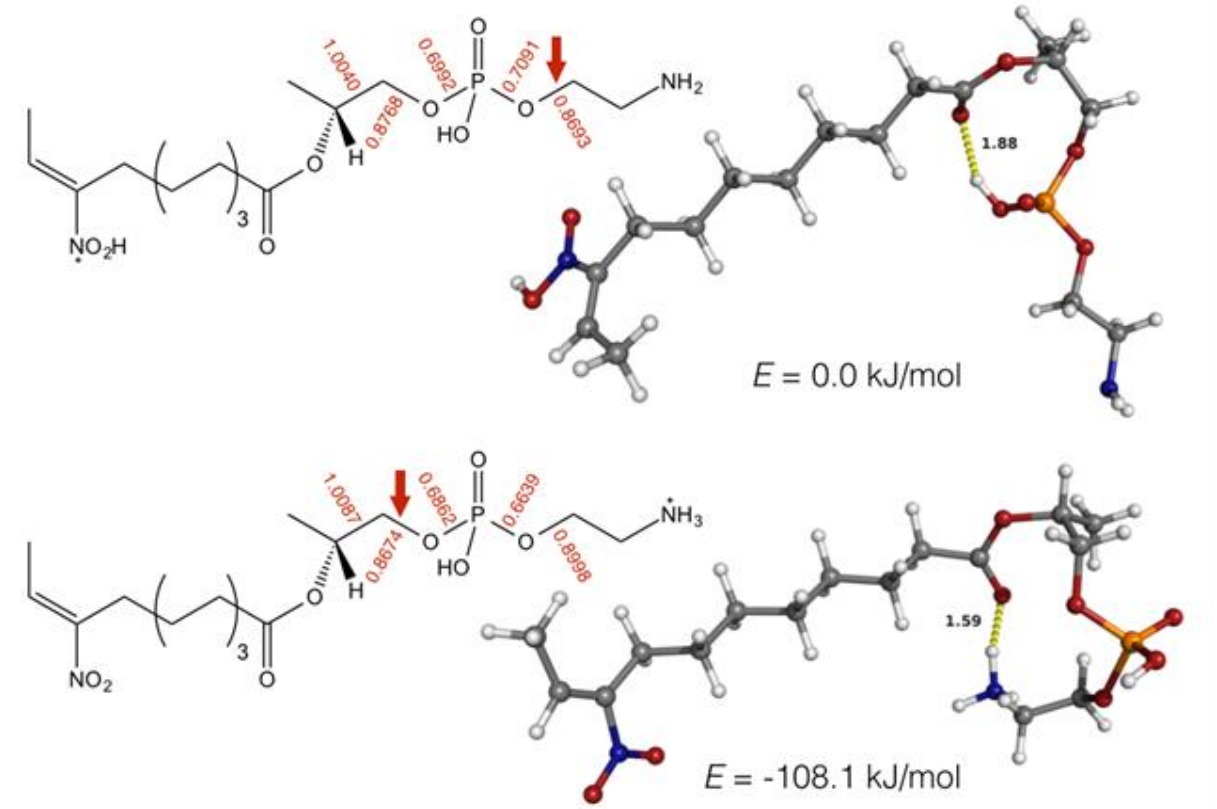

Figure S-7. Lowest energy conformations of the NO_2 and NH_2 protonated structures (top and bottom, respectively), obtained at the B3LYP/6-31G++** level, alongside the Wiberg bond indices of selected bonds discussed in the text. Color code - red: oxygen; blue: nitrogen; orange: phosphorus; gray: carbon; white: hydrogen.

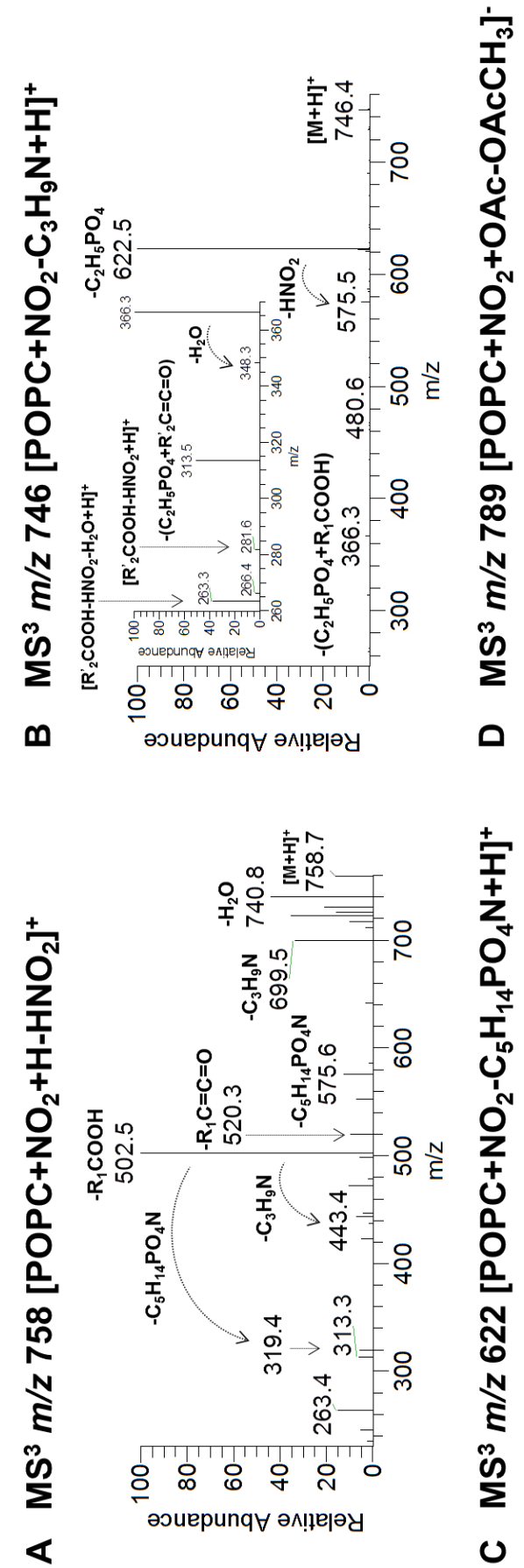

Figure S-8. MS^3 spectra of $[M+NO_2\text{-}HNO_2+H]^+$ (*m/z* 758.7), $[M+NO_2\text{-}C_3H_9N+H]^+$ (*m/z* 746.4), $[M+NO_2\text{-}C_5H_{14}PO_4N+H]^+$ (*m/z* 622.6) and $[M+NO_2+OAc\text{-}OAcCH_3]^-$ ions (*m/z* 789.6) of POPC. R'$_2$COOH and R'$_2$C=C=O correspond to the acid and ketene derivative of NO_2-FA, respectively.

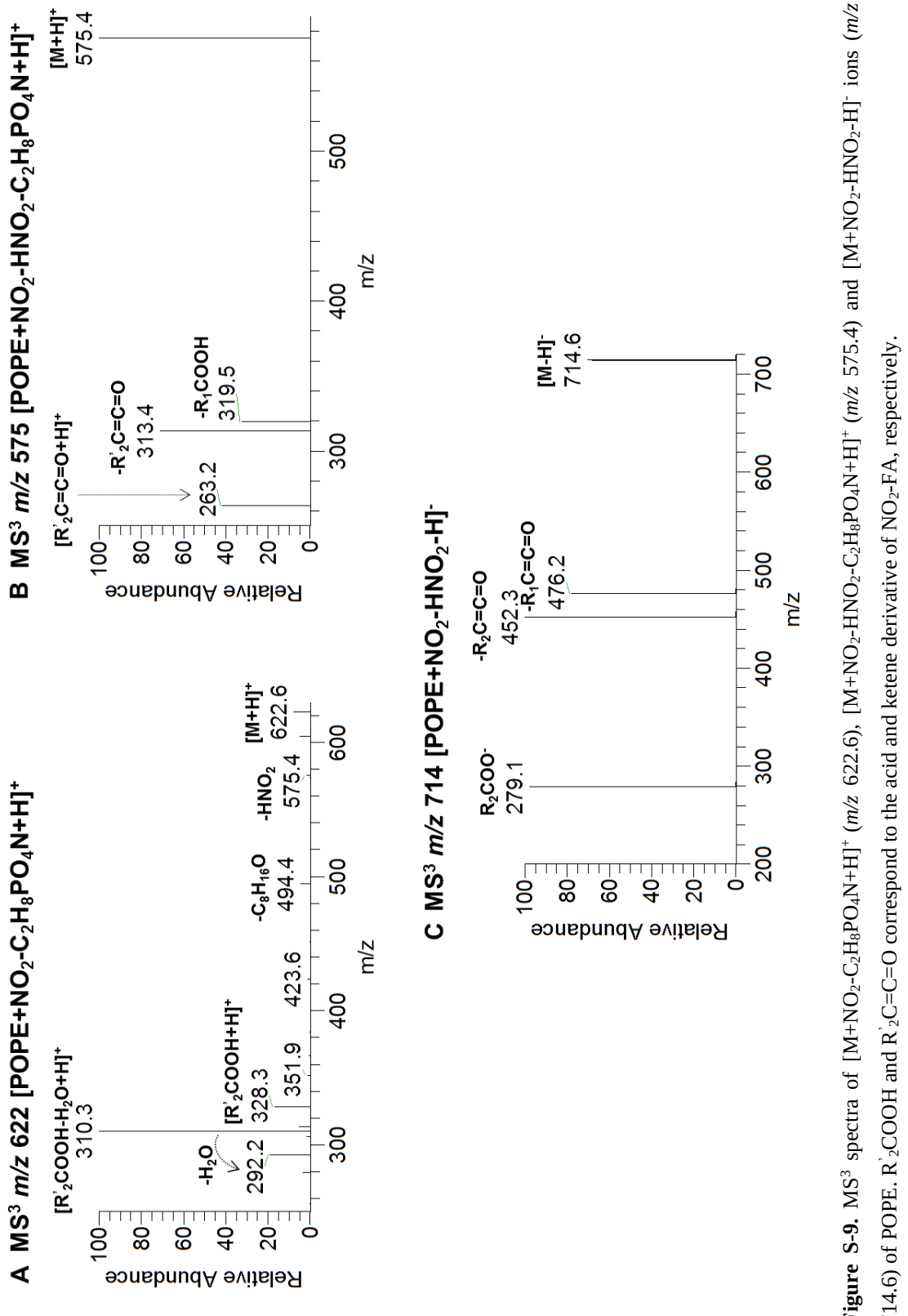

Figure S-9. MS^3 spectra of $[M+NO_2\text{-}C_2H_8PO_4N+H]^+$ (*m/z* 622.6), $[M+NO_2\text{-}HNO_2\text{-}C_2H_8PO_4N+H]^+$ (*m/z* 575.4) and $[M+NO_2\text{-}HNO_2\text{-}H]^-$ ions (*m/z* 714.6) of POPE. R'_2COOH and $R'_2C{=}C{=}O$ correspond to the acid and ketene derivative of NO_2-FA, respectively.

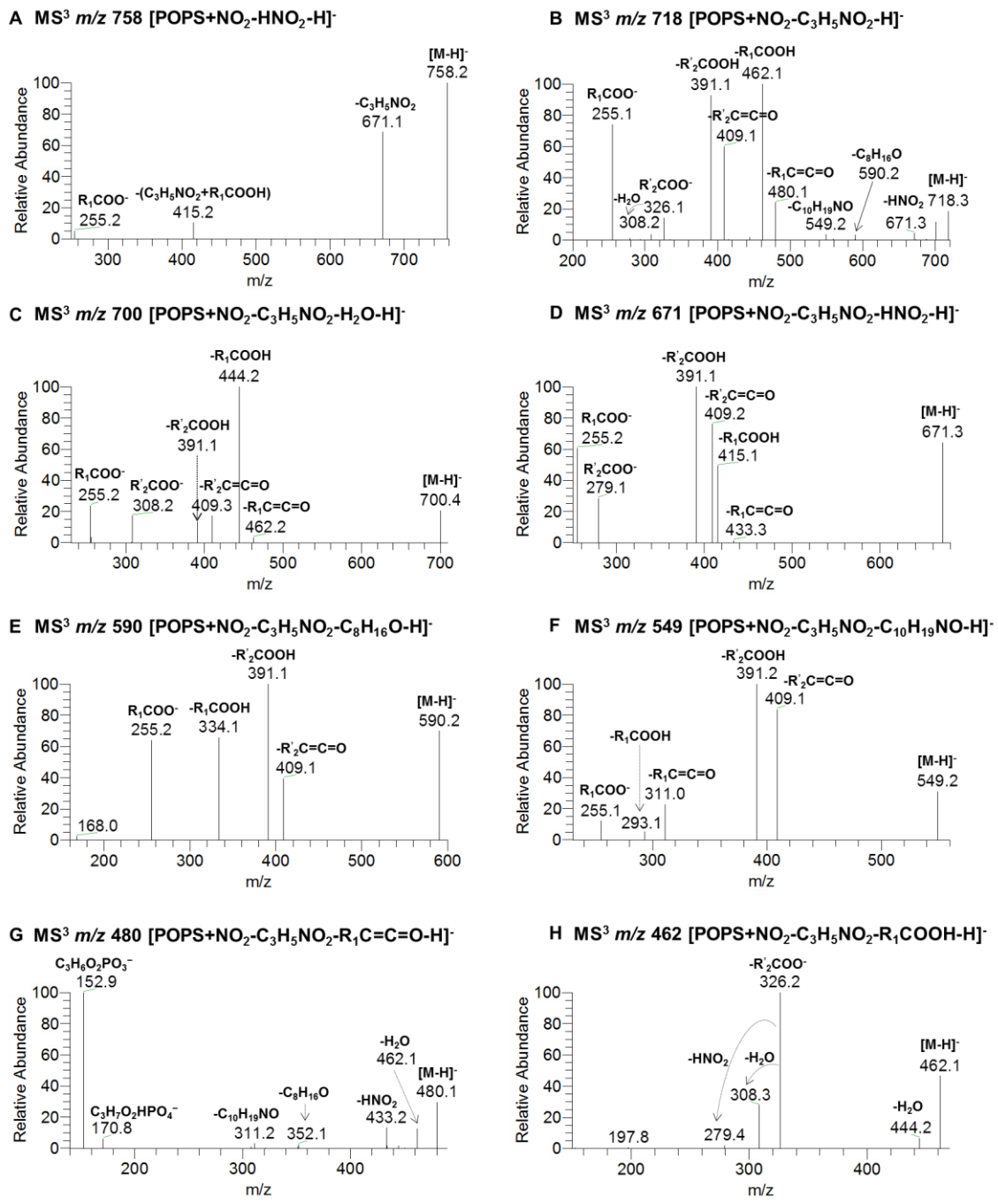

Figure S-10. MS^3 spectra of $[M+NO_2\text{-}HNO_2\text{-}H]^-$ (*m/z* 758.2), $[M+NO_2\text{-}C_3H_5NO_2\text{-}H]^-$ (*m/z* 718.3), $[M+NO_2\text{-}C_3H_5NO_2\text{-}H_2O\text{-}H]^-$ (*m/z* 700.4), $[M+NO_2\text{-}C_3H_5NO_2\text{-}HNO_2\text{-}H]^-$ (*m/z* 671.3), $[M+NO_2\text{-}C_3H_5NO_2\text{-}C_8H_{16}O\text{-}H]^-$ (m/z 590.2), $[M+NO_2\text{-}C_3H_5NO_2\text{-}C_{10}H_{19}NO\text{-}H]^-$ (*m/z* 549.2), $[M+NO_2\text{-}C_3H_5NO_2\text{-}R_1C{=}C{=}O\text{-}H]^-$ (*m/z* 480.1), $[M+NO_2\text{-}C_3H_5NO_2\text{-}R_1COOH\text{-}H]^-$ ions (*m/z* 462.1) of POPS. R'_2COOH and $R'_2C{=}C{=}O$ correspond to the acid and ketene derivative of NO_2-FA, respectively.

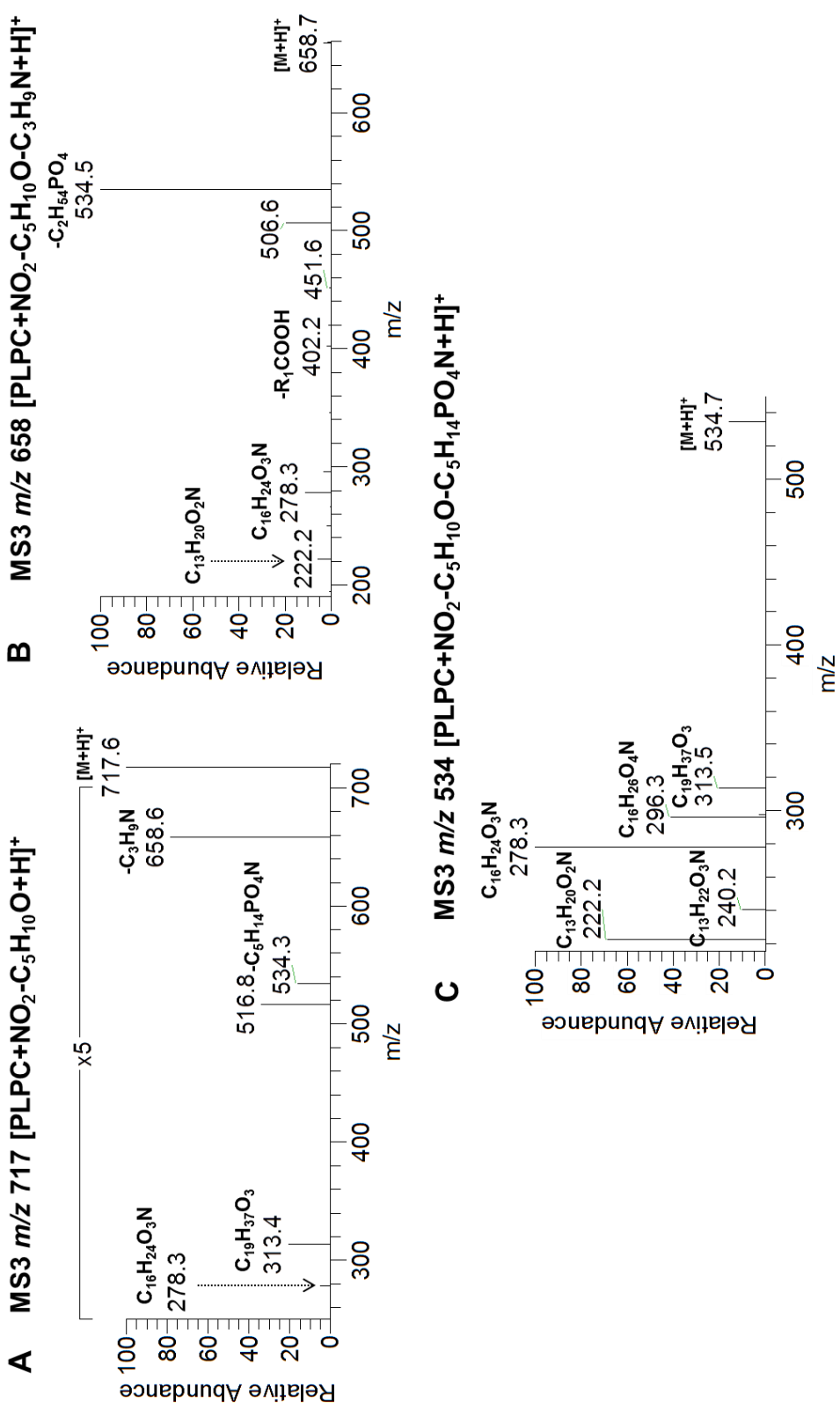

Figure S-11. MS^3 spectra of $[PLPC\text{-}NO_2+H]^+$ ions at *m/z* 717.6 ($[PLPC+NO_2\text{-}H\text{-}C_5H_{10}O]^+$), 658.7 ($[PLPC+NO_2\text{-}C_5H_{10}O\text{-}C_3H_9N+H]^+$), and 534.7 ($[PLPC+NO_2\text{-}C_5H_{10}O\text{-}C_5H_{14}PO_4N+H]^+$) corresponding to nitrated products with combined loss of polar head group and cleavage in the vicinity of the NO_2 group.

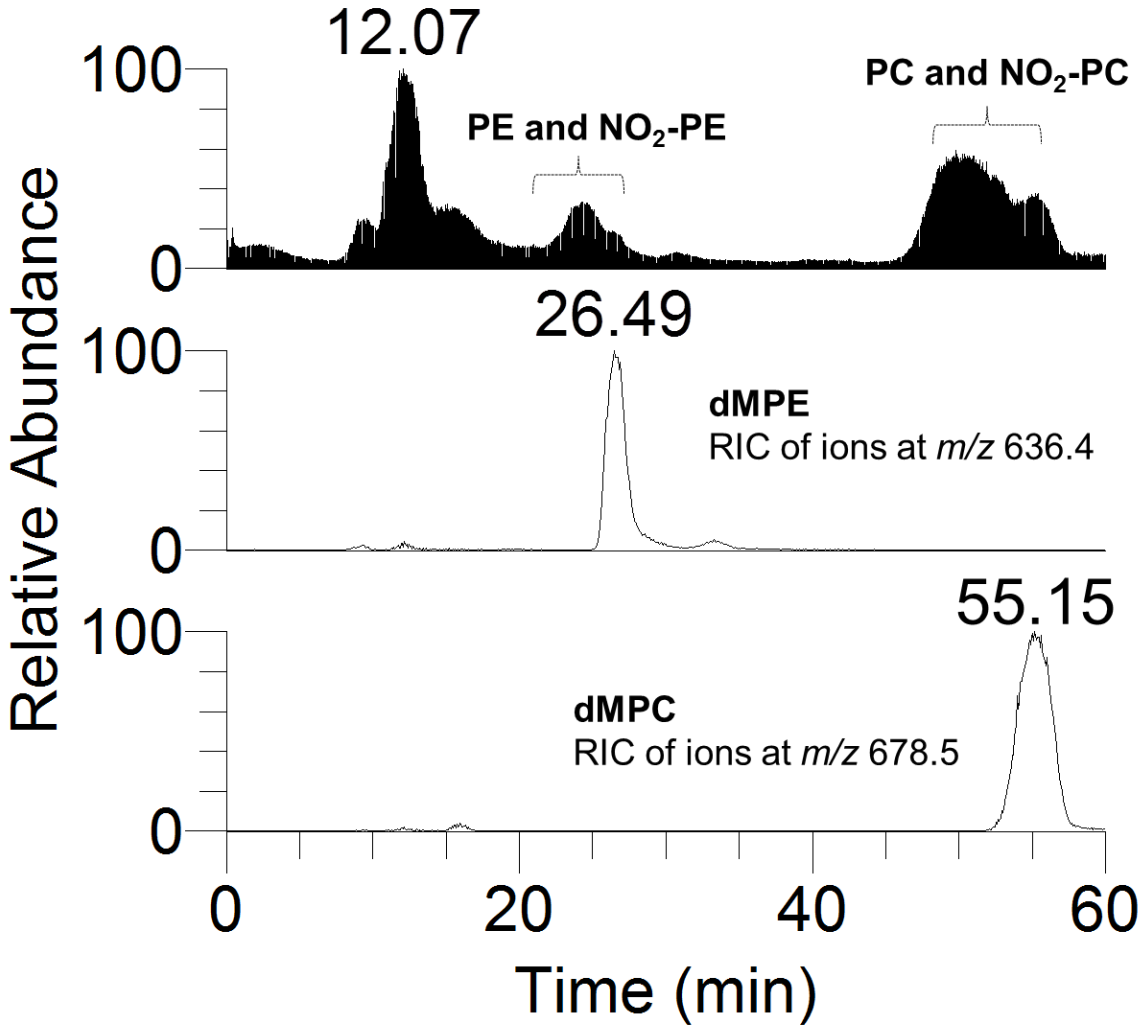

Figure S-12. HILIC-LC-MS chromatogram obtained for cardiac mitochondria of type 1 diabetes mellitus (T1DM) group with identification of retention time for phosphatidylethanolamine (PE) and nitrated PE (NO_2-PE) elution, and phosphatidylcholine (PC) and nitrated PC (NO_2-PC) elution. Reconstructed ion chromatogram (RIC) of ions at *m/z* 636.4 ($[dMPE+H]^+$), RT = 26.49 min, and ions at *m/z* 678.5 ($[dMPC+H]^+$), RT = 55.15 min.

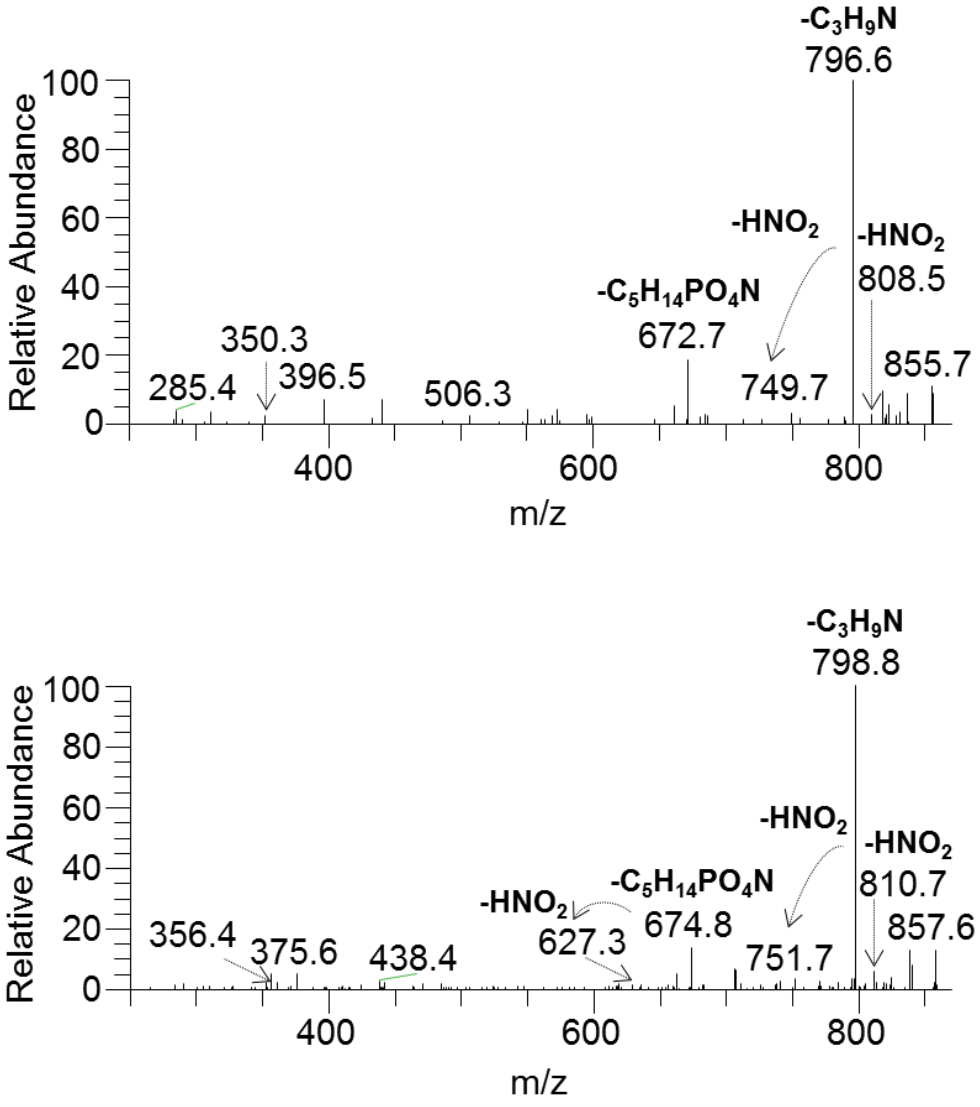

Figure S-13. HILIC-ESI-MS/MS spectra of ions at *m/z* 855.7 and 857.6 ($[M+H]^+$) observed in mitochondria from T1DM heart.

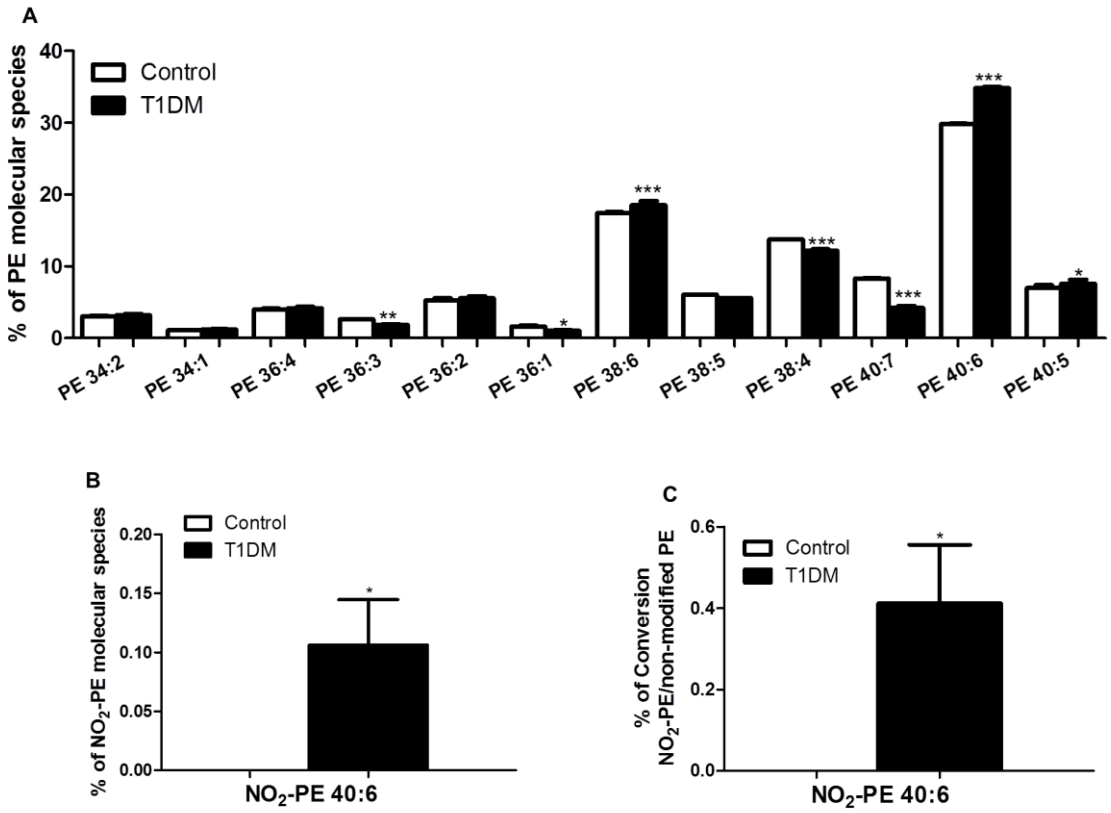

Figure S-14. A) Phosphatidylethanolamine (PE) molecular species profile observed for cardiac mitochondria of control group and type 1 diabetes mellitus (T1DM) group identified after LC-MS/MS analysis. B) NO_2-PE molecular species identified after LC-MS/MS analysis for cardiac mitochondria of control group and for type 1 diabetes mellitus (T1DM) group. The results were expressed as percentage obtained by dividing the ratio between the peak areas of each PE molecular specie and the PE internal standard (dMPE) and the total of all ratio. C) Ratio between non-modified PE molecular species and NO_2-PE in T1DM. The results were expressed as percentage determined by dividing the ratio between the peak areas of each NO_2-PE molecular specie and the PE internal standard (dMPE) and the ratio between the peak areas of the correspondent non-modified PE molecular specie and the PE internal standard (dMPE). Values are means±standard deviation. *p<0.05, **p<0.01 and ***p<0.0001, significantly different from control group.

SUPPLEMETARY TABLES

Table S-1. Summary of the nitroalkene products observed in the ESI-MS spectra, both in the positive- ($[M+H]^+$ ions for all PLs) and negative-ion mode ($[M-H]^-$ ions for PEs and PSs and $[M+OAc+NO_2]^-$ ions for PCs), after reaction of each phospholipid class with NO_2BF_4 with the identification and the indication of the respective *m/z* values. POPC, PC16:0/18:1; PLPC, PC16:0/18:2; PAPC, PC16:0/20:4; POPE, PE16:0/18:1; PLPE, PE16:0/18:2; PAPE, PE16:0/20:4; POPS, PS16:0/18:1; PLPS, PS16:0/18:2; PAPS, PS16:0/20:4.

PL Class	Non-modified			Nitroalkene Products (+NO_2, +45 u)		
	m/z $[M+H]^+$	*m/z* $[M-H]^-$	*m/z* $[M+OAc]^-$	*m/z* $[M+H+NO_2]^+$	*m/z* $[M-H+NO_2]^-$	*m/z* $[M+OAc+NO_2]^-$
POPC	760.59	--	818.33	805.67	--	863.33
PLPC	758.57	--	816.33	803.58	--	861.33
PAPC	782.57	--	840.33	827.50	--	885.33
POPE	718.54	716.52	--	763.62	761.43	--
PLPE	716.52	714.51	--	761.55	759.50	--
PAPE	740.52	738.51	--	785.63	783.27	--
POPS	762.53	760.51	--	807.58	805.27	--
PLPS	760.51	758.50	--	805.60	803.27	--
PAPS	784.51	782.50	--	829.58	827.25	--

Table S-2. Formula, calculated and observed mass and mass error of the NO_2-PLs derivatives formed due to reaction between NO_2BF_4 and each PL observed in the ESI-MS spectra. Data was acquired in the Q-TOF2 mass spectrometer, and lock mass was done in the $[M+H+\text{non-modified PL}]^+$. POPC, PC16:0/18:1; PLPC, PC16:0/18:2; PAPC, PC16:0/20:4; POPE, PE16:0/18:1; PLPE, PE16:0/18:2; PAPE, PE16:0/20:4; POPS, PS16:0/18:1; PLPS, PS16:0/18:2; PAPS, PS16:0/20:4.

Nitroalkene Products	Predicted formula $[M+NO_2+H]^+$	Calculated mass (Da)	Observed mass (Da)	Error (mDa)	Error (ppm)
POPC+NO_2	$C_{42}H_{82}N_2O_{10}P$	805.5707	805.5737	3.0	3.7
PLPC+NO_2	$C_{42}H_{80}N_2O_{10}P$	803.5551	803.5679	2.8	3.5
PAPC+NO_2	$C_{44}H_{80}N_2O_{10}P$	827.5551	827.5520	-3.1	-3.7
POPE+NO_2	$C_{39}H_{76}N_2O_{10}P$	763.5238	763.5251	1.3	1.8
PLPE+NO_2	$C_{39}H_{74}N_2O_{10}P$	761.5081	761.5065	-1.6	-2.1
PAPE+NO_2	$C_{41}H_{74}N_2O_{10}P$	785.5081	785.5099	1.8	2.3
POPS+NO_2	$C_{40}H_{76}N_2O_{12}P$	807.5136	807.5105	-3.1	-3.8
PLPS+NO_2	$C_{40}H_{74}N_2O_{12}P$	805.4979	805.4965	-1.4	-1.8
PAPS+NO_2	$C_{42}H_{74}N_2O_{12}P$	829.4979	829.4963	-1.6	-2.0

Table S-3. Summary of the major fragmentation pathways observed in the ESI-MS spectra, in the positive-ion mode ($[M+NO_2+H]^+$ ions) after reaction of each phospholipid class with NO_2BF_4 with the identification and the indication of the respective *m/z* values. POPC, PC16:0/18:1; PLPC, PC16:0/18:2; PAPC, PC16:0/20:4; POPE, PE16:0/18:1; PLPE, PE16:0/18:2; PAPE, PE16:0/20:4; POPS, PS16:0/18:1; PLPS, PS16:0/18:2; PAPS, PS16:0/20:4.

Typical neutral losses and product ions observed for NO_2-PL in positive-ion mode

Neutral Losses	Proposed Identification	$[POPC+NO_2+H]^+$	$[PLPC+NO_2+H]^+$	$[PAPC+NO_2+H]^+$
		805.75	803.58	827.75
18 u	$-H_2O$	787.63	785.54	809.58
47 u	$-HNO_2$	758.70	756.46	780.58
59 u	$-C_3H_9N$	746.52	744.34	768.67
106 u (59+47)	$-(C_3H_9N+HNO_2)$	699.62	697.42	721.50
183 u	$-C_5H_{14}PO_4N$	622.55	620.55	644.58
230 u (183+47)	$-(C_5H_{14}PO_4N+HNO_2)$	575.54	573.56	597.67
238 u	$-R_1C=C=O$	567.62	565.42	589.33
256 u	$-R_1COOH$	549.57	547.35	571.50
Product Ions				
$[NO_2-FA+H]^+$		328.26	326.41	350.33
$[NO_2-FA-H2O+H]^+$		310.27	308.35	332.25
$[NO_2-FA-2H_2O+H]^+$		292.30	290.26	314.17
$[NO_2-FA-NO_2+H]^+$		281.26	279.26	303.25

Neutral Losses	Proposed Identification	$[POPE+NO_2+H]^+$	$[PLPE+NO_2+H]^+$	$[PAPE+NO_2+H]^+$
		763.62	761.48	785.61
18 u	$-H_2O$	745.50	743.51	767.51
43 u	$-C_2H_5N$	720.41	718.38	742.51
47 u	$-HNO_2$	716.51	714.63	738.47
90 u (43+47)	$-(C_2H_5N+HNO_2)$	673.44	671.60	695.52
141 u	$-C_2H_8PO_4N$	622.51	620.47	644.51
188 u (141+47)	$-(C_2H_8PO_4N+HNO_2)$	575.44	573.44	597.57
238 u	$-R_1C=C=O$	525.37	523.33	547.36
256 u	$-R_1COOH$	507.44	505.48	529.47
Product Ions				
$[NO_2-FA+H]^+$		328.31	326.42	350.36
$[NO_2-FA-H_2O+H]^+$		310.30	308.38	332.33
$[NO_2-FA-2H_2O+H]^+$		292.41	290.24	314.27
$[NO_2-FA-NO_2+H]^+$		281.21	279.26	303.35

Neutral Losses	Proposed Identification	$[POPS+NO_2+H]^+$	$[PLPS+NO_2+H]^+$	$[PAPS+NO_2+H]^+$
		807.31	805.74	829.58
18 u	$-H_2O$	789.28	787.36	811.50
47 u	$-HNO_2$	760.52	758.46	782.68
87 u	$-C_3H_5NO_2$	720.26	718.46	742.56
134 u (87+47)	$-(C_3H_5NO_2+HNO_2)$	673.60	671.53	695.50
185 u	$-C_3H_8PO_6N$	622.52	620.42	644.56
232 u (185+47)	$-(C_3H_8PO_6N+HNO_2)$	575.43	573.43	597.32
238 u	$-R_1C=C=O$	569.15	567.44	591.63
256 u	$-R_1COOH$	551.57	549.40	573.46
Product Ions				
$[NO_2-FA+H]^+$		328.22	326.36	350.48
$[NO_2-FA-H_2O+H]^+$		310.24	308.29	332.37
$[NO_2-FA-2H_2O+H]^+$		292.33	290.47	314.23
$[NO_2-FA-NO_2+H]^+$		281.18	279.20	303.20

SUPPLEMTARY FIGURES

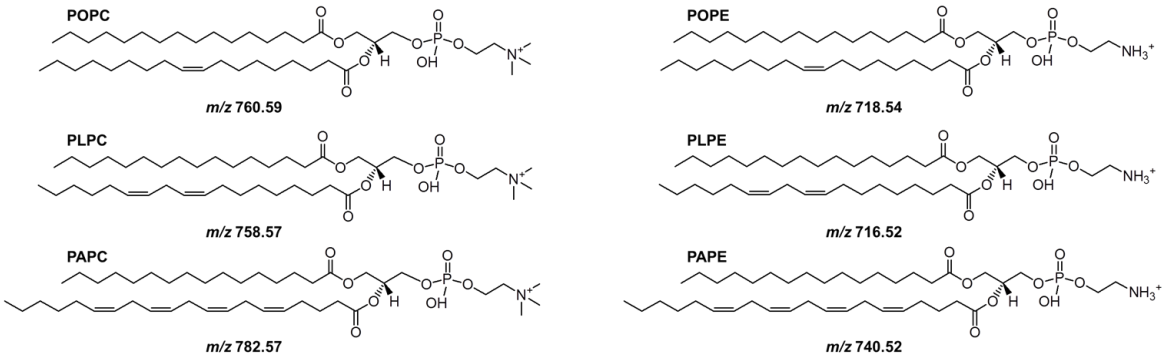

Figure S-1. Structure of the phosphatidylcholines (PCs) and phosphatidylethanolamines (PEs) used in this study. POPC, 1-palmitoyl-2-oleoyl-*sn*-glycero-3-phosphocholine; PLPC, 1-palmitoyl-2-linoleoyl-*sn*-glycero-3-phosphocholine; PAPC, 1-palmitoyl-2-arachidonoyl-*sn*-glycero-3-phosphocholine. POPE, 1-palmitoyl-2-oleoyl-*sn*-glycero-3-phosphoethanolamine; PLPE, 1-palmitoyl-2-linoleoyl-*sn*-glycero-3- phosphoethanolamine; PAPE, 1-palmitoyl-2-arachidonoyl-*sn*-glycero-3- phosphoethanolamine.

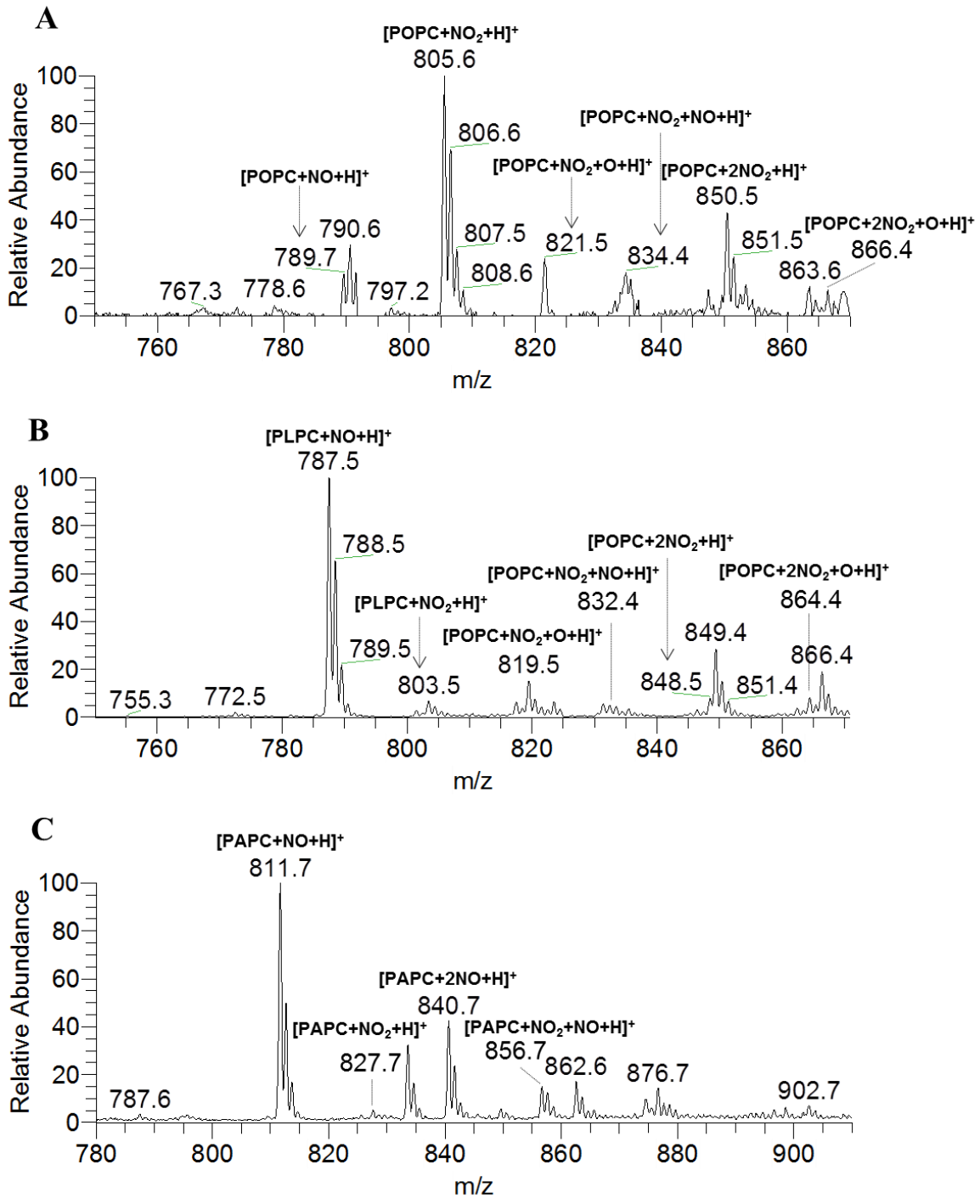

Figure S-2. ESI-MS spectra of POPC (A), PLPC (B) and PAPC (C) in positive-ion mode after incubation with NO_2BF_4.

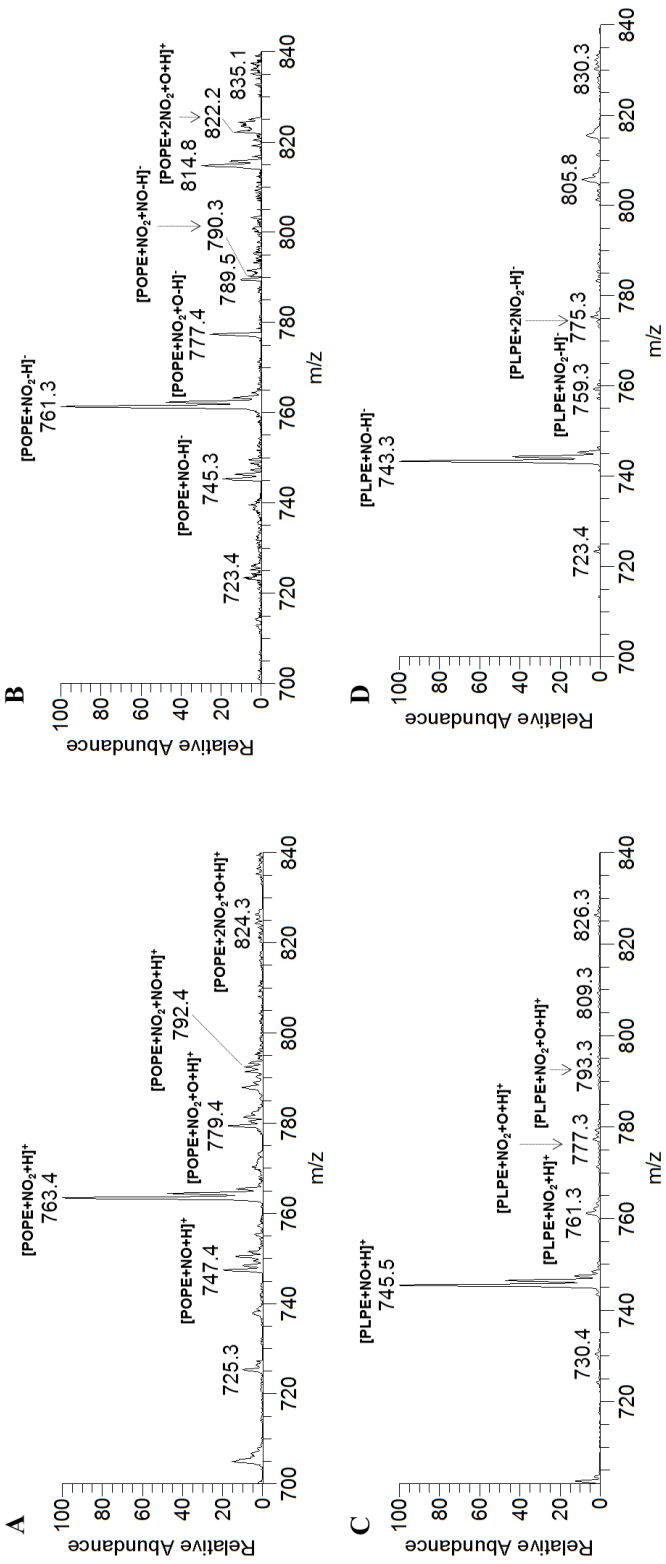

Figure S-3. ESI-MS spectra of POPE (A, B), PLPE (C, D) and PAPE (E, F) in positive- (A, C, E) and negative-ion mode (B, D, F) after incubation with NO_2BF_4.

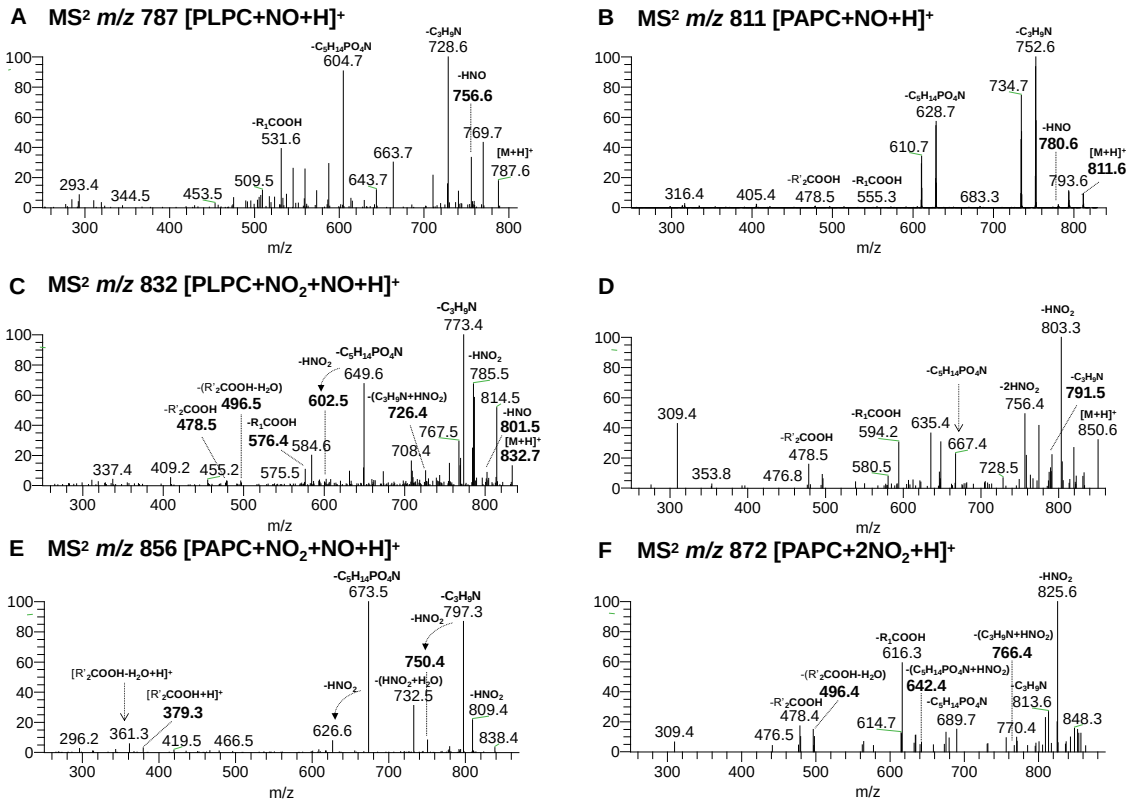

Figure S-4. LC-ESI-MS/MS spectra of $[M+H]^+$ ions at *m/z* 787.6 (PLPC+NO), 811.6 (PAPC+NO), 832.7 (PLPC+NO_2+NO), 850.5 (POPC+$2NO_2$), 856.4 (PAPC+NO_2+NO), and 872.6 (PAPC+$2NO_2$).

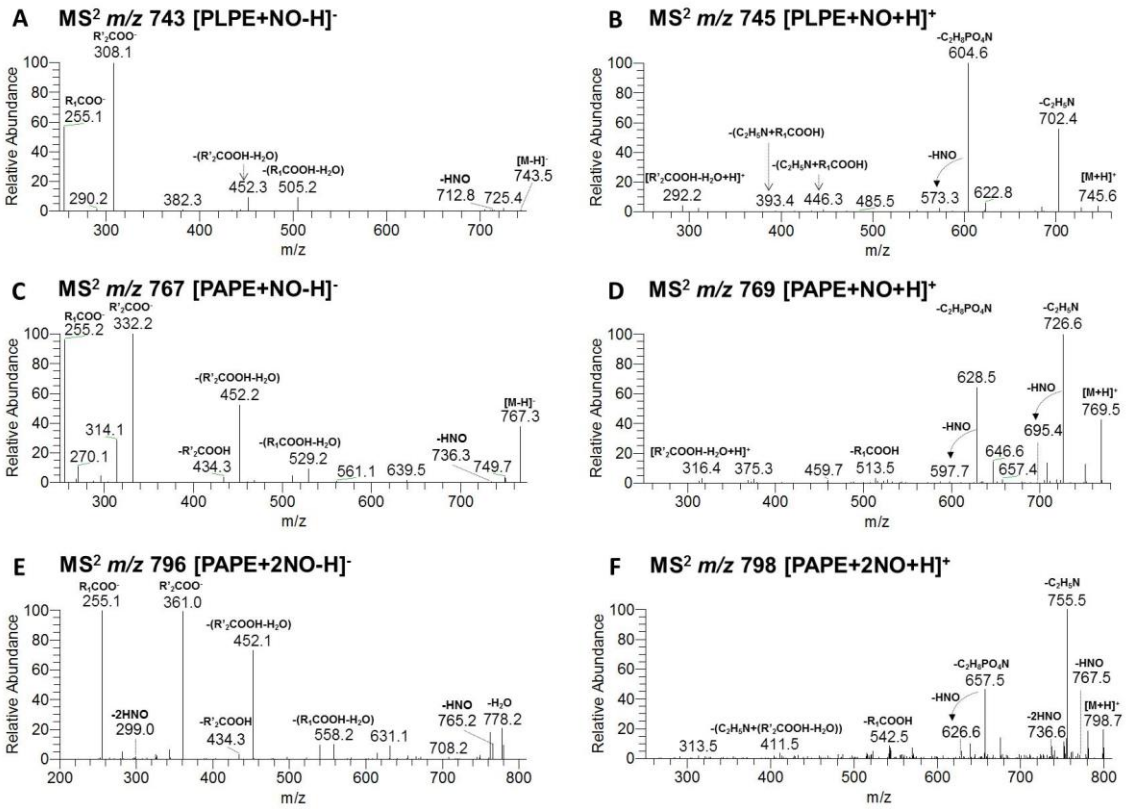

Figure S-5. LC-ESI-MS/MS spectra of $[M-H]^-$ ions at *m/z* 743.5 (PLPE+NO), 767.3 (PAPE+NO), 796.4 (PAPE+2NO). LC-ESI-MS/MS spectra of $[M+H]^+$ ions at *m/z* 745.6 (PLPE+NO), 769.5 (PAPE+NO), and 798.7 (PAPE+2NO).

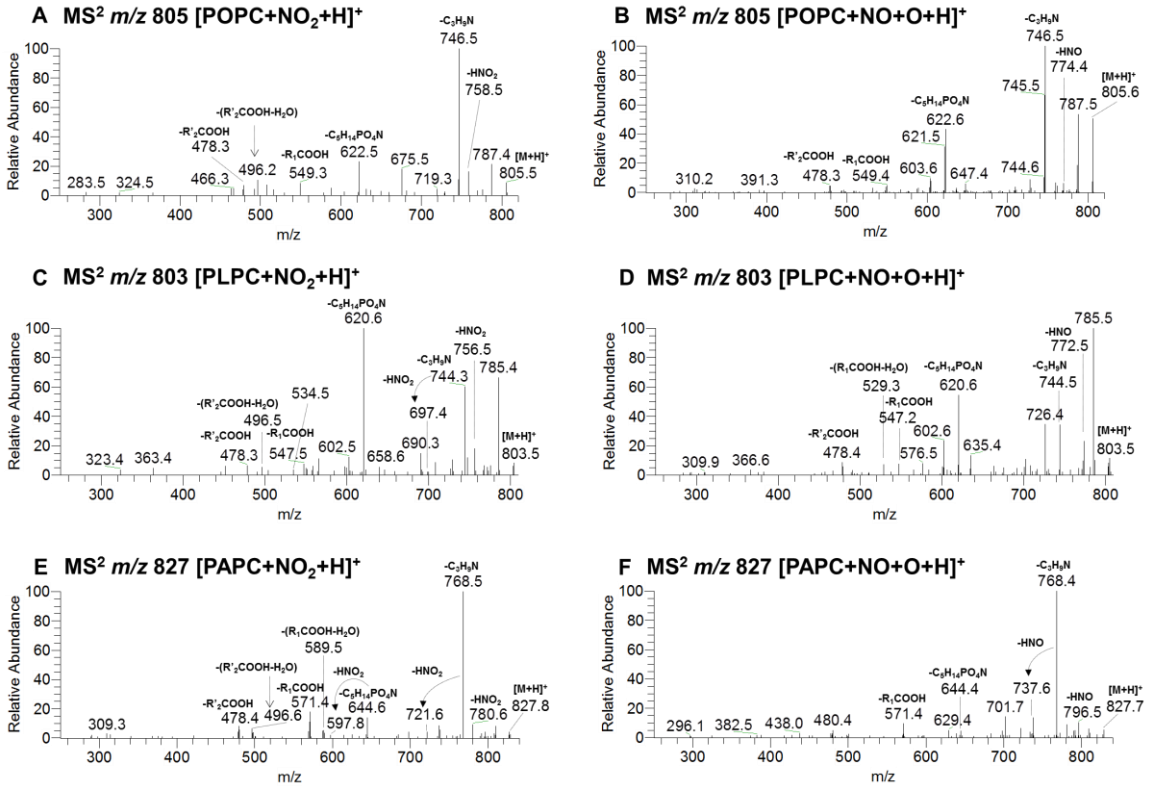

Figure S-6. LC-ESI-MS/MS spectra of $[M+H]^+$ ions at *m/z* 805.5 (POPC+NO_2), 805.6 (POPC+NO+O), 803.5 (PLPC+NO_2), 803.5 (PLPC+NO+O), 827.8 (PAPC+NO_2), 827.7 (PAPC+NO+O).

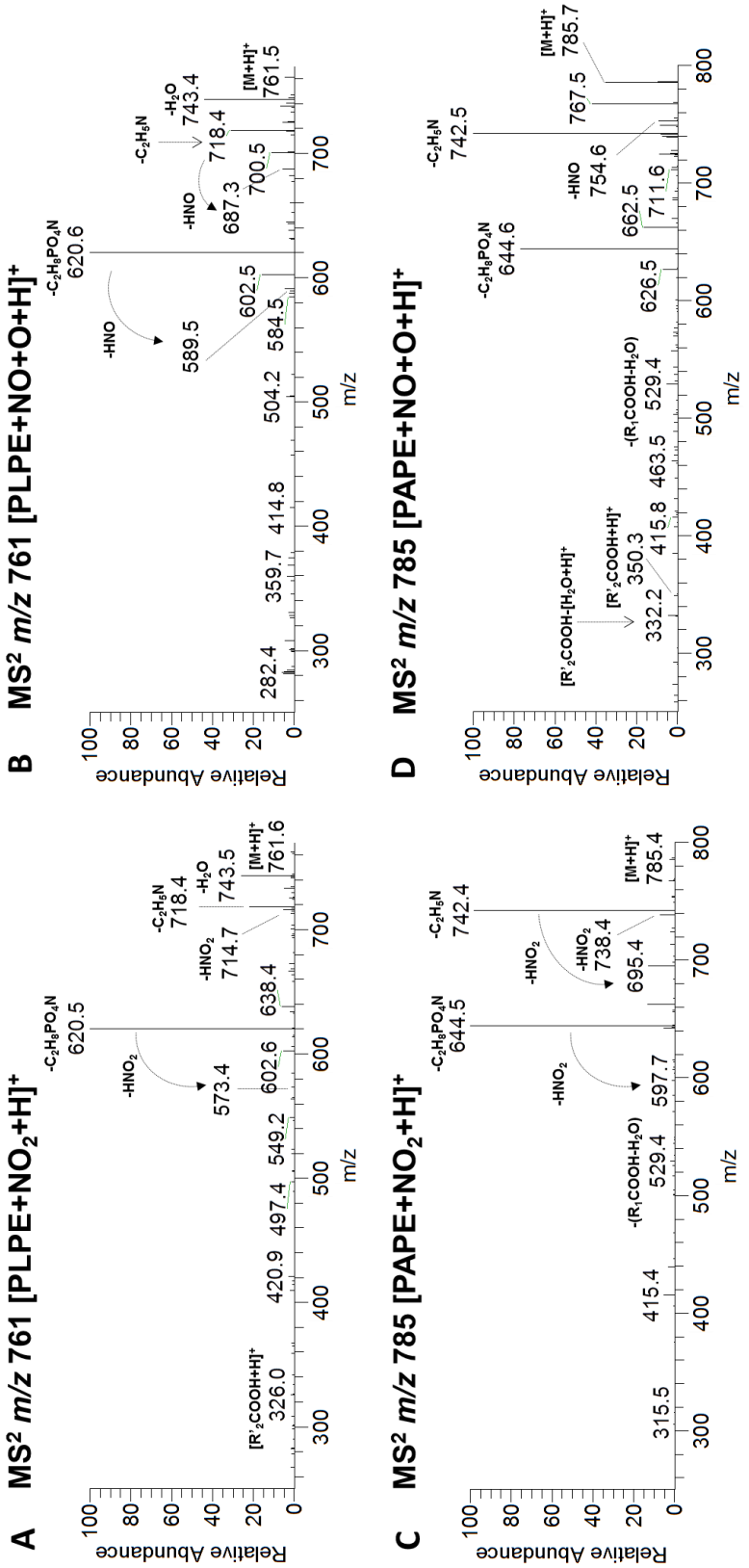

Figure S-7. LC-ESI-MS/MS spectra of $[M+H]^+$ ions at *m/z* 761.6 (PLPE+NO_2), 761.5 (PLPE+NO+O), 785.4 (PAPE+NO_2) and 785.7 (PAPE+NO+O).

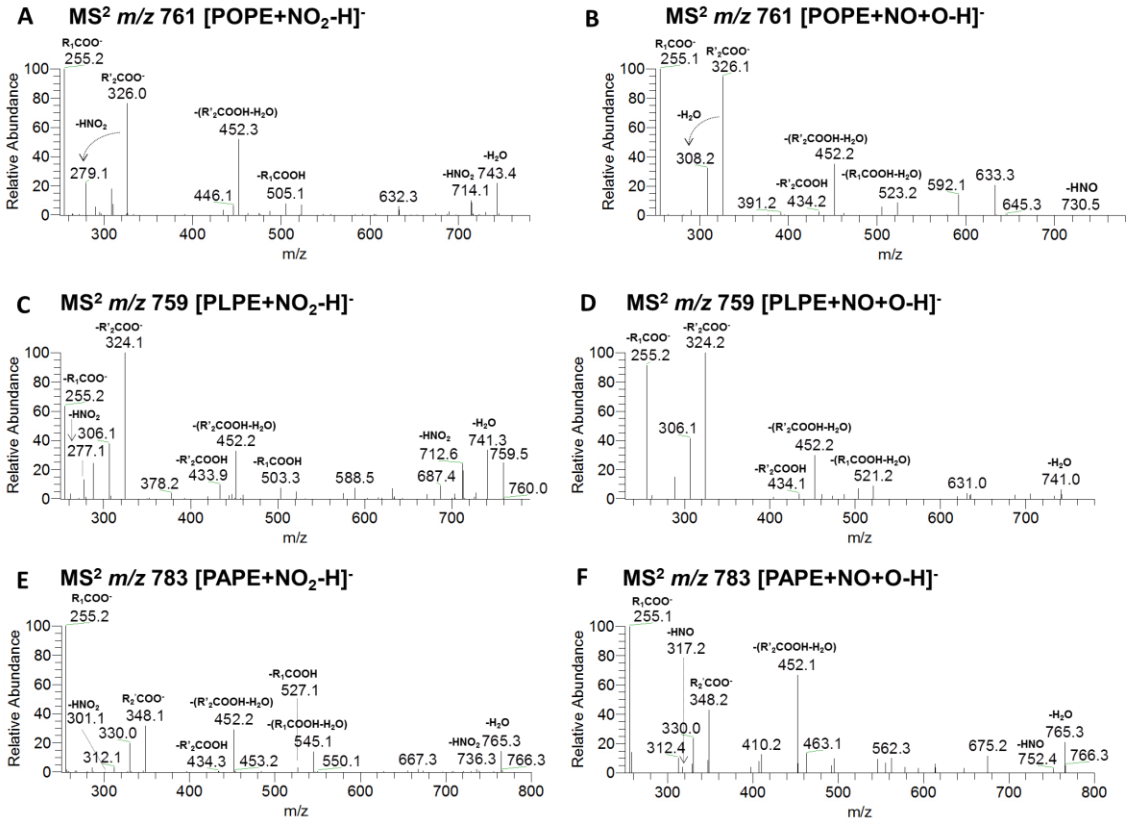

Figure S-8. LC-ESI-MS/MS spectra of $[M-H]^-$ ions at *m/z* 761.5 (POPE+NO_2), 761.4 (POPE+NO+O), 759.5 (PLPE+NO_2), 759.4 (PLPE+NO+O), 783.5 (PAPE+NO_2) and 783.4 (PAPE+NO+O).

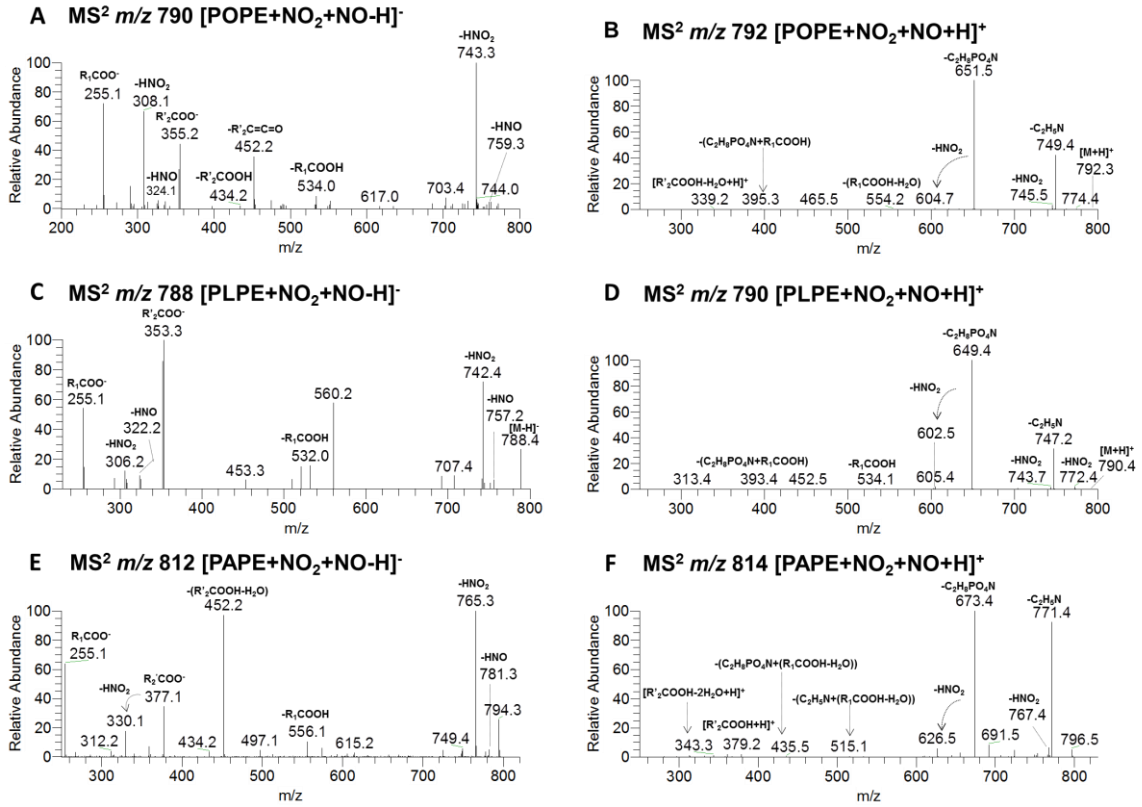

Figure S-9. LC-ESI-MS/MS spectra of $[M-H]^-$ ions at *m/z* 790.4 (POPE+NO_2+NO), 788.4 (PLPE+NO_2+NO), and 812.4 (PAPE+NO_2+NO). LC-ESI-MS/MS spectra of $[M+H]^+$ ions at *m/z* 792.3 (POPE+NO_2+NO), 790.4 (PLPE+NO_2+NO), and 814.5 (PAPE+NO_2+NO).

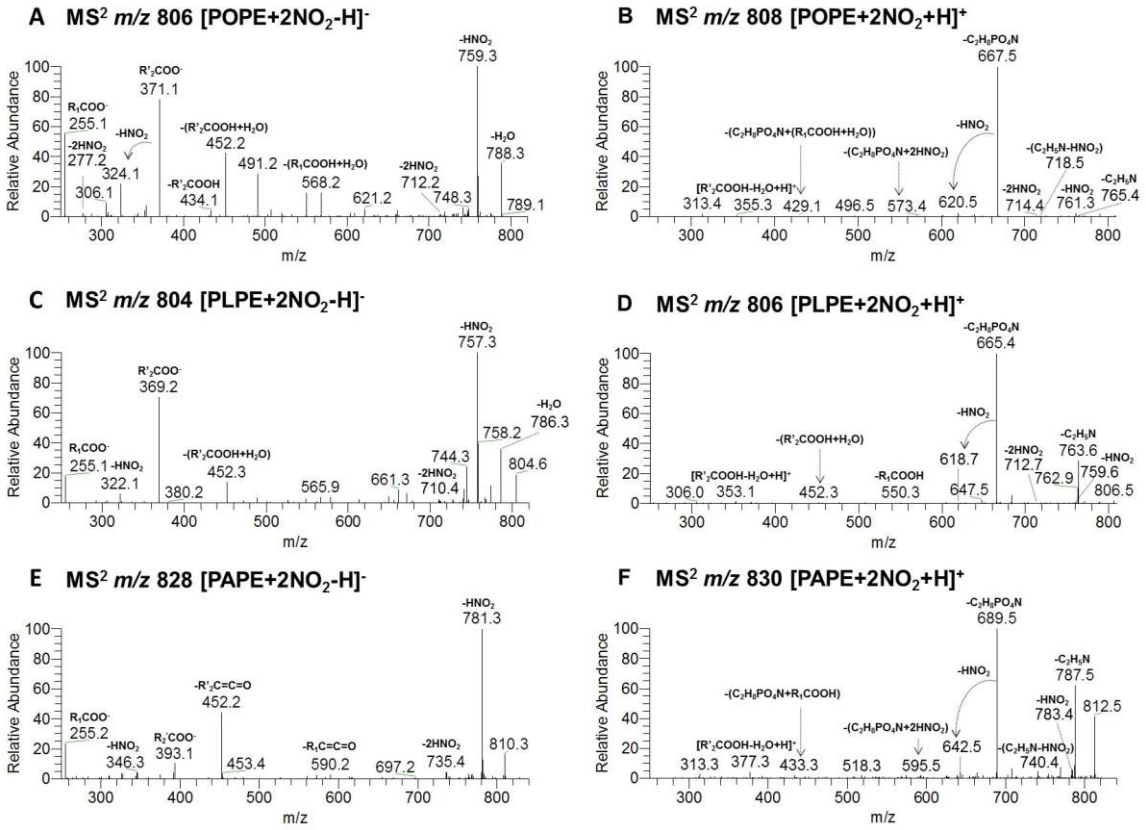

Figure S-10. LC-ESI-MS/MS spectra of $[M-H]^-$ ions at *m/z* 806.4 (POPE+2NO_2), 804.6 (PLPE+2NO_2), and 828.4 (PAPE+2NO_2). LC-ESI-MS/MS spectra of $[M+H]^+$ ions at *m/z* 808.5 (POPE+2NO_2), 806.5 (PLPE+2NO_2), and 830.5 (PAPE+2NO_2).

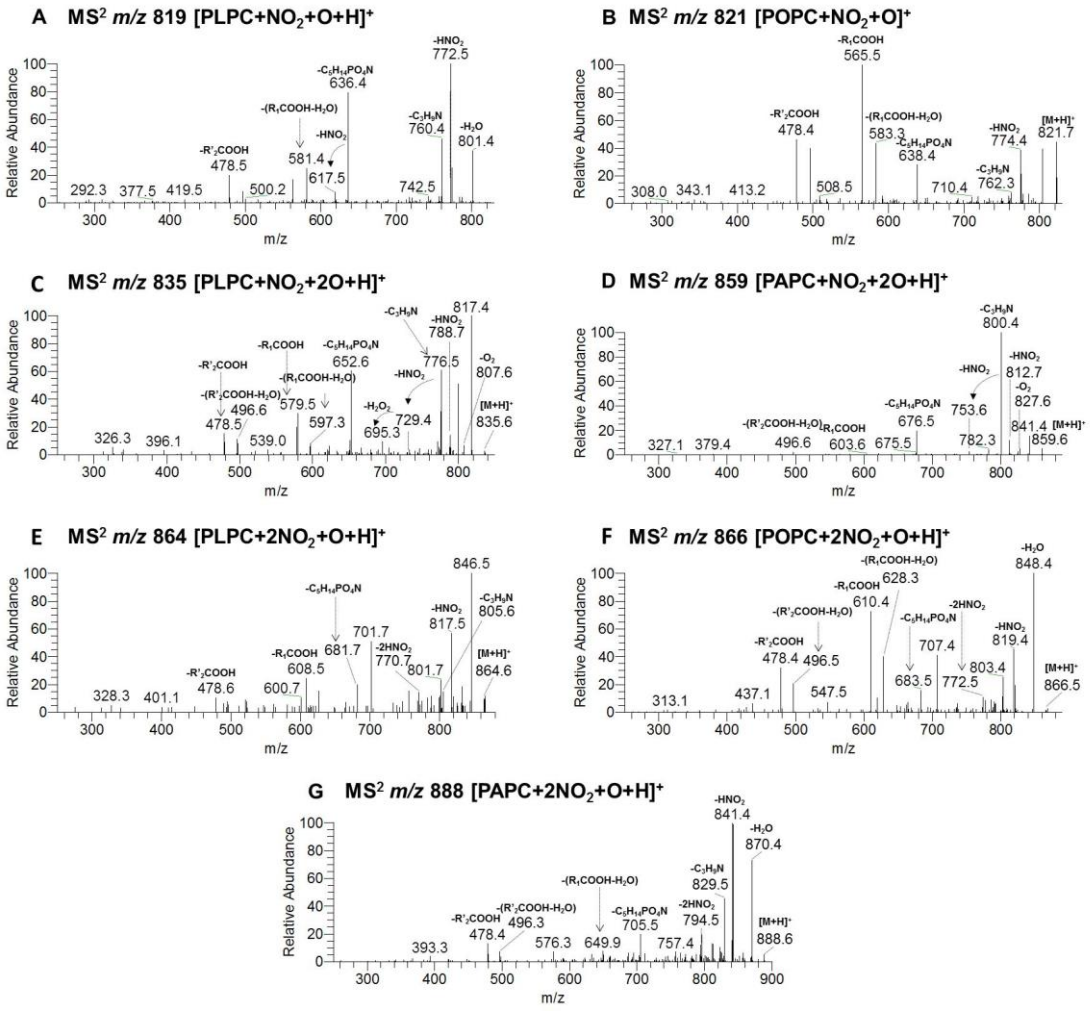

Figure S-11. LC-ESI-MS/MS spectra of $[M+H]^+$ ions at *m/z* 819.5 (PLPC+NO_2+O), 821.7 (POPC+NO_2+O), 835.6 (PLPC+NO_2+2O), 859.6 (PLPC+NO_2+2O), 864.6 (PLPC+2NO_2+O), 866.5(POPC+2NO_2+O), and 888.6 (PLPC+2NO_2+O).

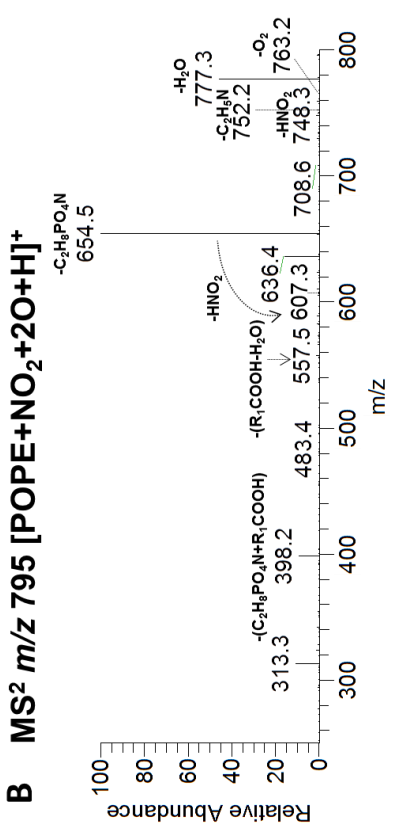

Figure S-12. LC-ESI-MS/MS spectra of $[M+H]^+$ ions at *m/z* 779.6 (POPE+NO_2+O), 795.4 (POPE+NO_2+2O), 824.4 (POPE+$2NO_2$+O), 840.4 (POPE+$2NO_2$+2O).

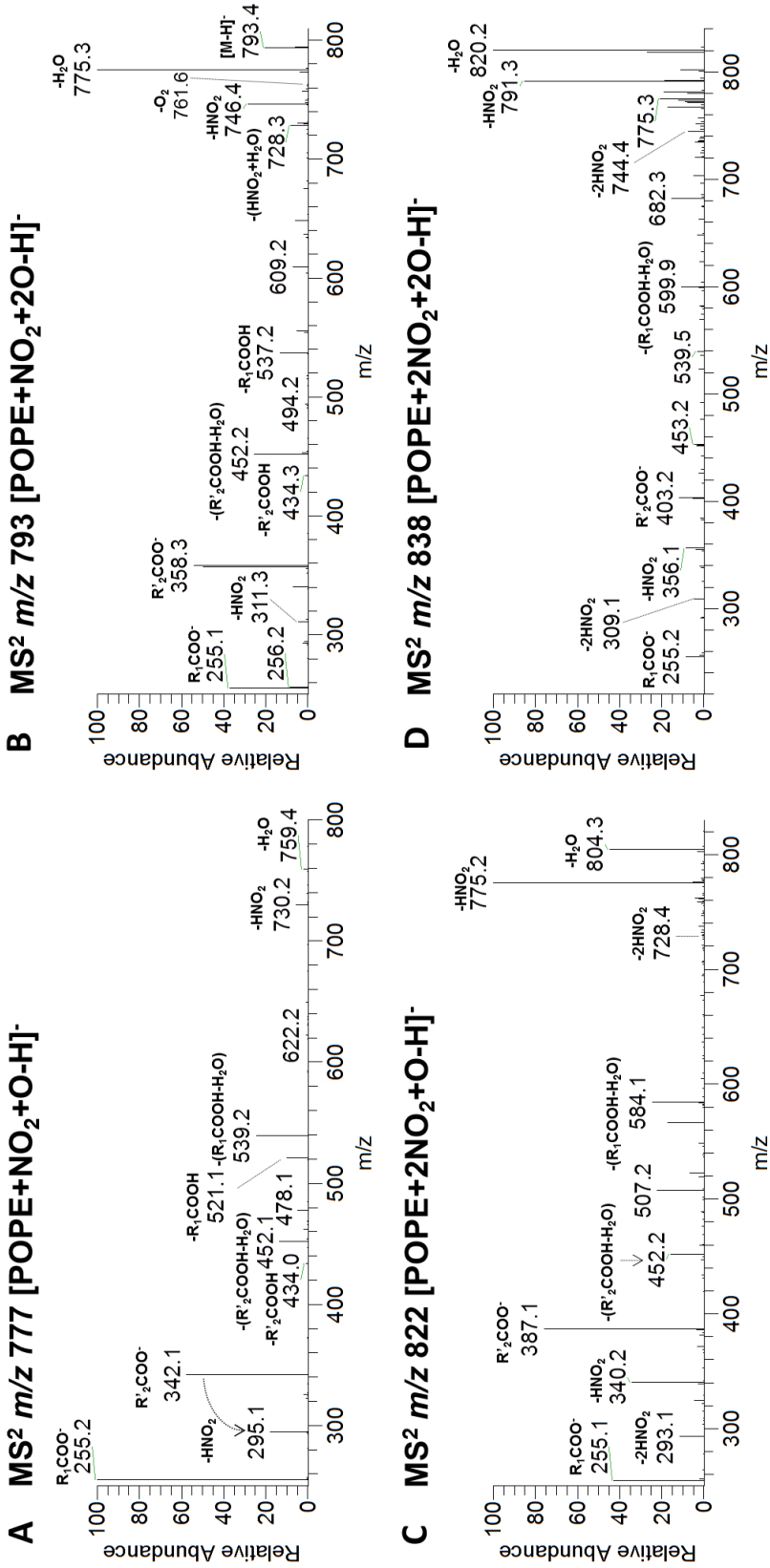

Figure S-13. LC-ESI-MS/MS spectra of $[M-H]^-$ ions at *m/z* 777.5 (POPE+NO_2+O), 793.4 (POPE+NO_2+2O), 822.4 (POPE+$2NO_2$+O), 838.4 (POPE+$2NO_2$+2O).

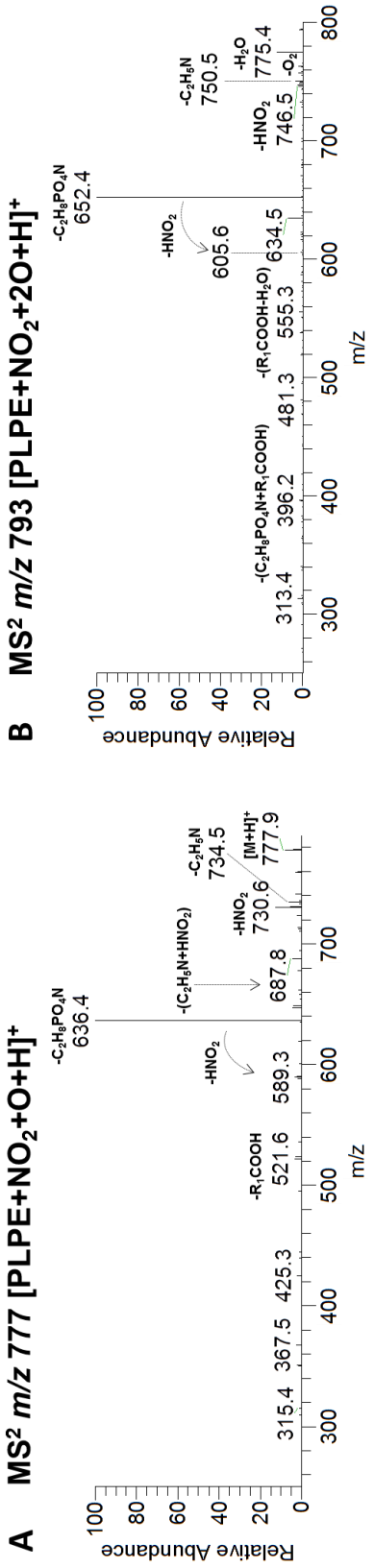

Figure S-14. LC-ESI-MS/MS spectra of $[M+H]^+$ ions at *m/z* 777.9 (PLPE+NO_2+O), 793.5 (PLPE+NO_2+2O), 838.5 (PLPE+$2NO_2$+2O).

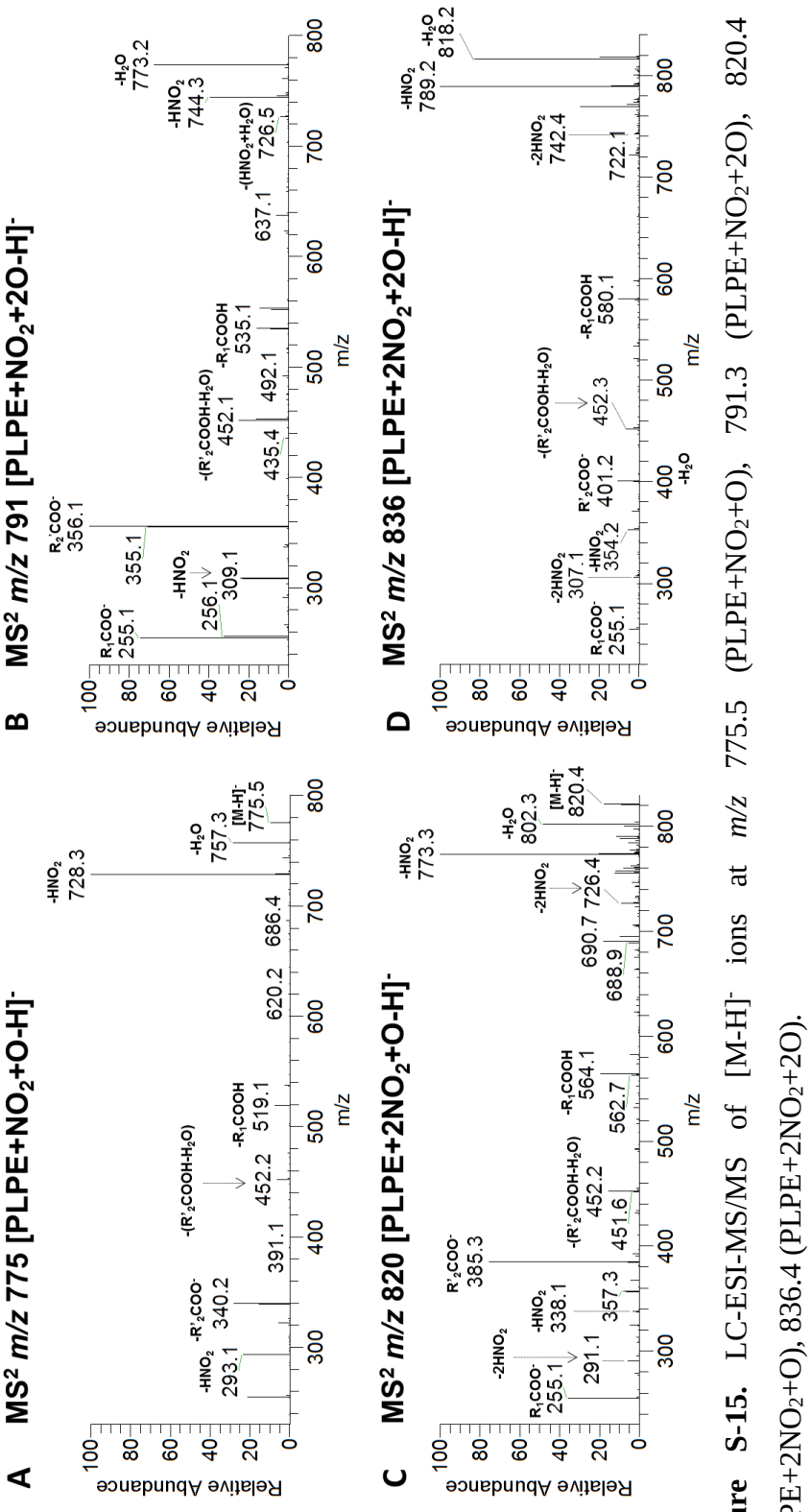

Figure S-15. LC-ESI-MS/MS of $[M-H]^-$ ions at *m/z* 775.5 (PLPE+NO_2+O), 791.3 (PLPE+NO_2+2O), 820.4 (PLPE+$2NO_2$+O), 836.4 (PLPE+$2NO_2$+2O).

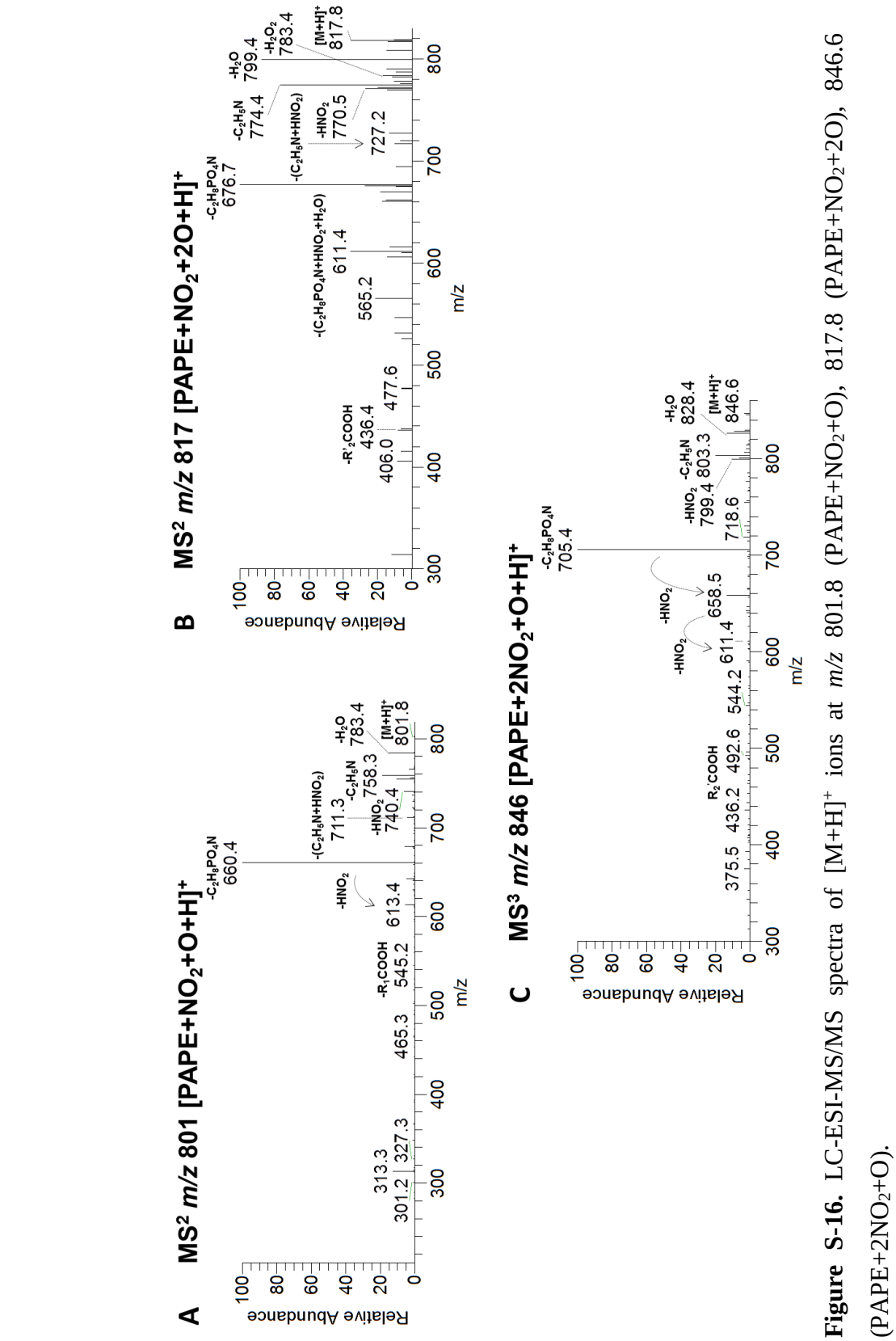

Figure S-16. LC-ESI-MS/MS spectra of $[M+H]^+$ ions at *m/z* 801.8 (PAPE+NO_2+O), 817.8 (PAPE+NO_2+2O), 846.6 (PAPE+2NO_2+O).

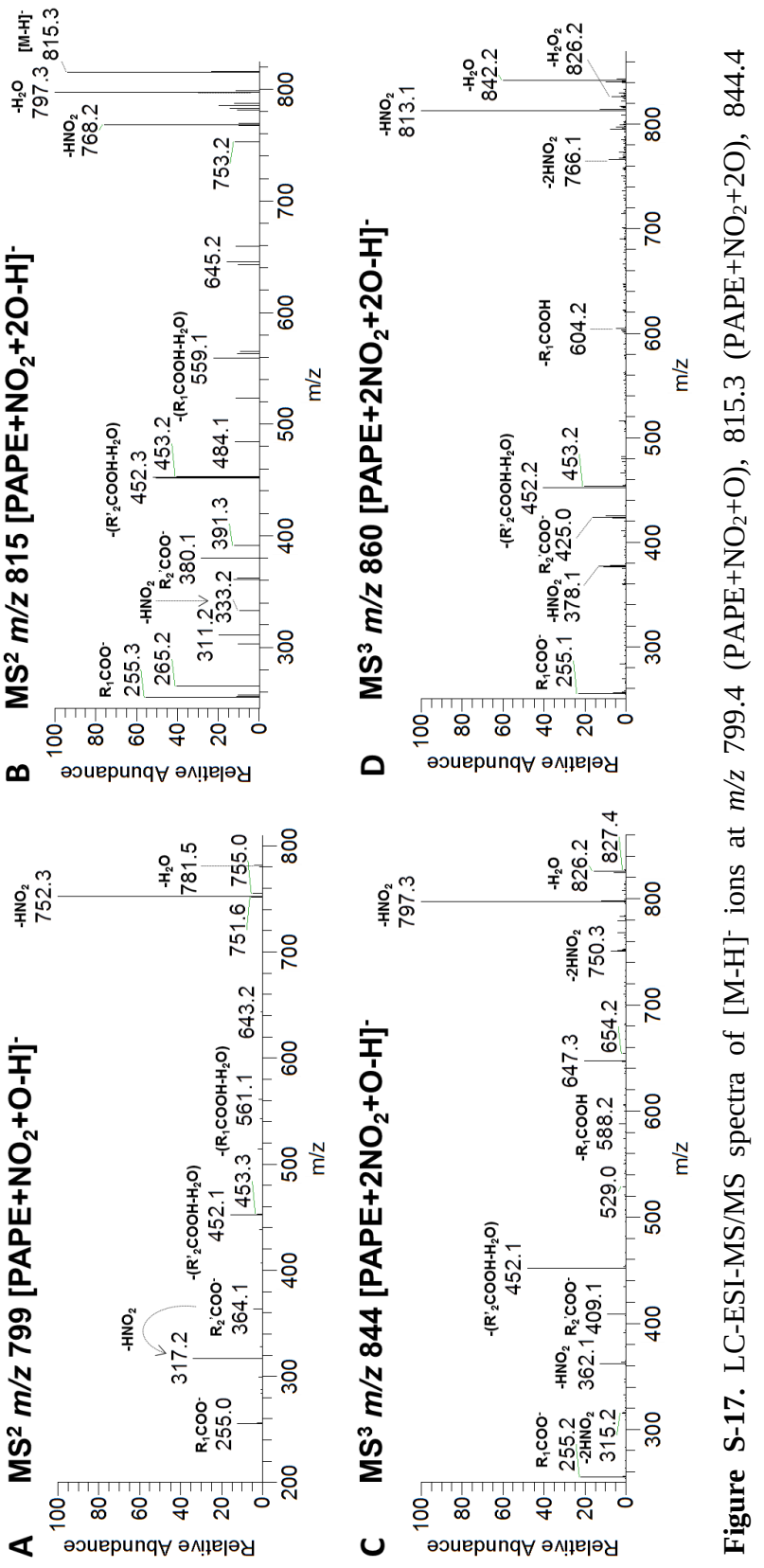

Figure S-17. LC-ESI-MS/MS spectra of $[M-H]^-$ ions at *m/z* 799.4 (PAPE+NO_2+O), 815.3 (PAPE+NO_2+2O), 844.4 (PAPE+2NO_2+O), 860.4 (PAPE+2NO_2+2O).

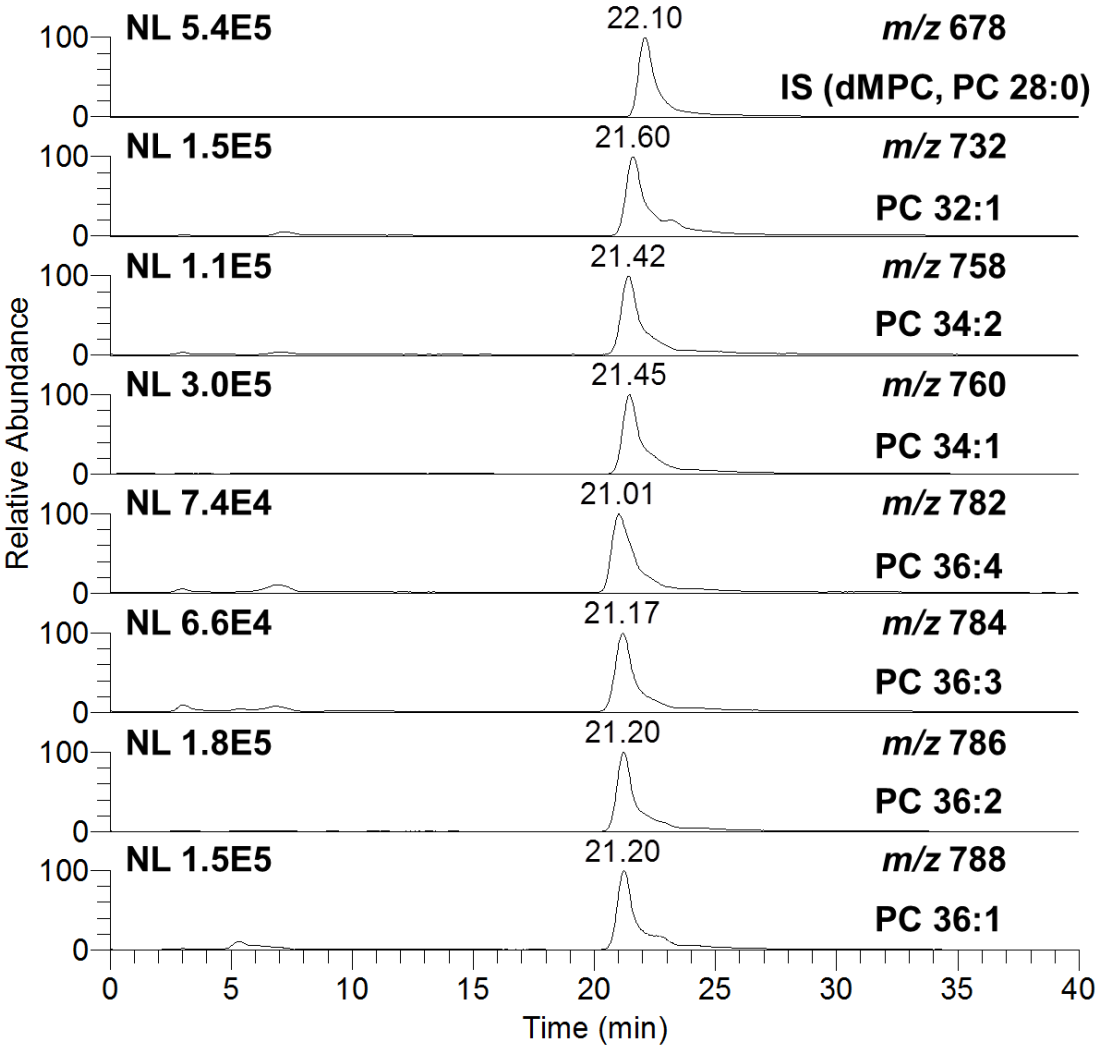

Figure S-18. Reconstructed ion chromatogram (RIC) of $[M+H]^+$ ion of the non-modified PC molecular species identified in H9c2 cardiomyoblast cells under starvation conditions. IS, internal standard.

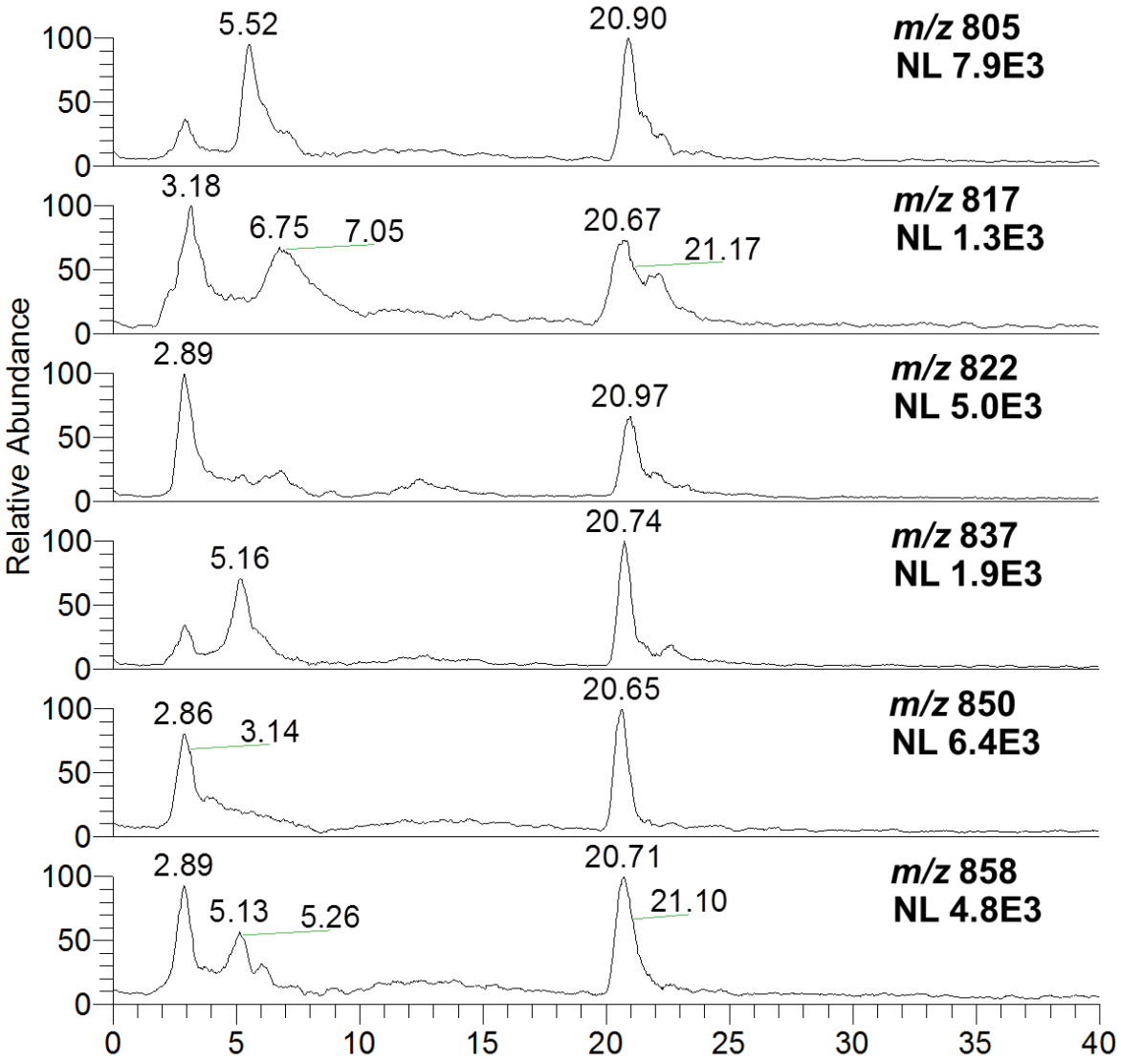

Figure S-19. Reconstructed ion chromatogram (RIC) of $[M+H]^+$ ions of the nitrated PC molecular species (*m/z* 805 NO_2-PC 16:0/18:1, *m/z* 822 $(NO_2)_2$-PC 16:0/16:1, *m/z* 817 NO-PC 18:0/18:1, *m/z* 850 $(NO_2)_2$-PC 16:0/18:1 and *m/z* 858 NO_2NO-PC 16:0/20:3) and nitroxidized PC molecular species (*m/z* 837.7 NO_2OOH-PC 16:0/18:1) identified in H9c2 cardiomyoblast cells under starvation condition.

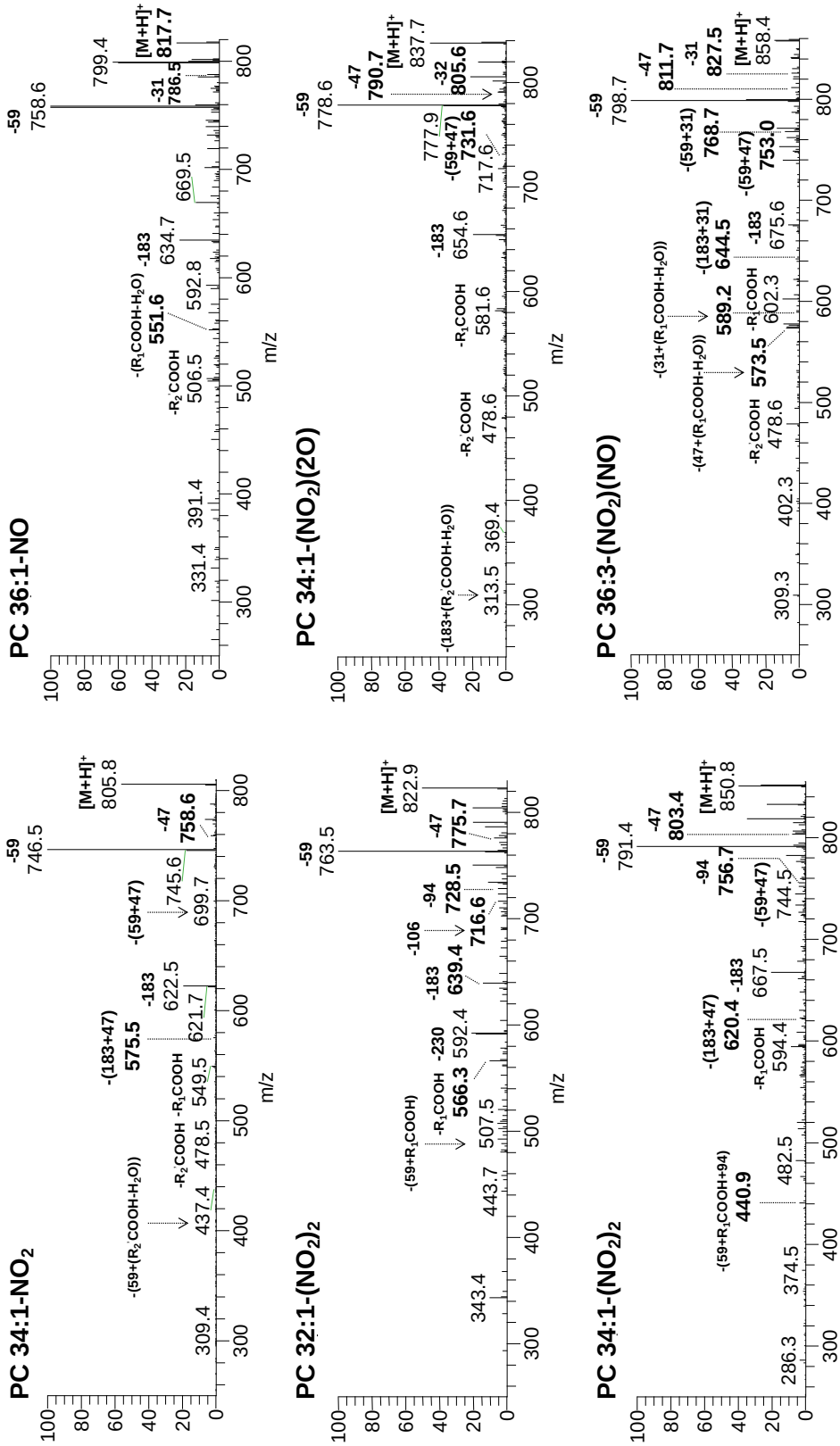

Figure S-20. HILIC-ESI-MS/MS spectra of $[M+H]^+$ ions at *m/z* 805.8 (NO_2-PC 16:0/18:1), 817.7 (NO-PC 18:0/18:1), 822.9 ($(NO_2)_2$-PC 16:0/16:1), 837.7 (NO_2OOH-PC 16:0/18:1), 850.8 ($(NO_2)_2$-PC 16:0/18:1), and 858.4 (NO_2NO-PC 16:0/20:3) observed in H9c2 cells under starvation condition.

Tandem mass spectra of ions at *m/z* 805.8 (NO_2-PC 16:0/18:1) showed neutral losses of 47 u (HNO_2, *m/z* 758.4) and combined losses of HNO_2 plus the polar head (*m/z* 699.8 (neutral loss of 106, corresponding to 59 u (C_3H_9N) + 47 u) and 575.5, neutral loss of 230, corresponding to 183 u ($C_5H_{15}O_4NP$) + 47 u). For ions *m/z* 822.9 ((NO_2)$_2$-PC 16:0/16:1) and 850.8 ((NO_2)$_2$-PC 16:0/18:1), their tandem mass spectra showed ions formed as a result of neutral losses of 47 u (775.7 and 803.4, respectively) and 94 u (*m/z* 728.5 and 756.7, respectively). Also, combined losses of 47 u and polar head were observed (-106 u (59+47): *m/z* 716.6 and 744.5, respectively; -230 (183+47): *m/z* 592.4 and 620.4, respectively). The nitronitroso derivative at *m/z* 858.4 (NO_2NO-PC 16:0/20:3) displayed neutral losses of 31 u (*m/z* 786.5), 47 u (*m/z* 790.7), 90 u (*m/z* 768.7), 106 u (*m/z* 753.0), 214 u (644.5). Nitrohydroxy derivative (*m/z* 837.7 (NO_2OOH-PC 16:0/18:1) showed neutral losses of 32 u (*m/z* 805.6), 47 u (*m/z* 790.7) and 106 u (*m/z* 731.6). tandem mass spectra of nitroso derivative *m/z* 817.7 (NO-PC 18:0/18:1) showed neutral losses of 31 u (*m/z* 786.5).

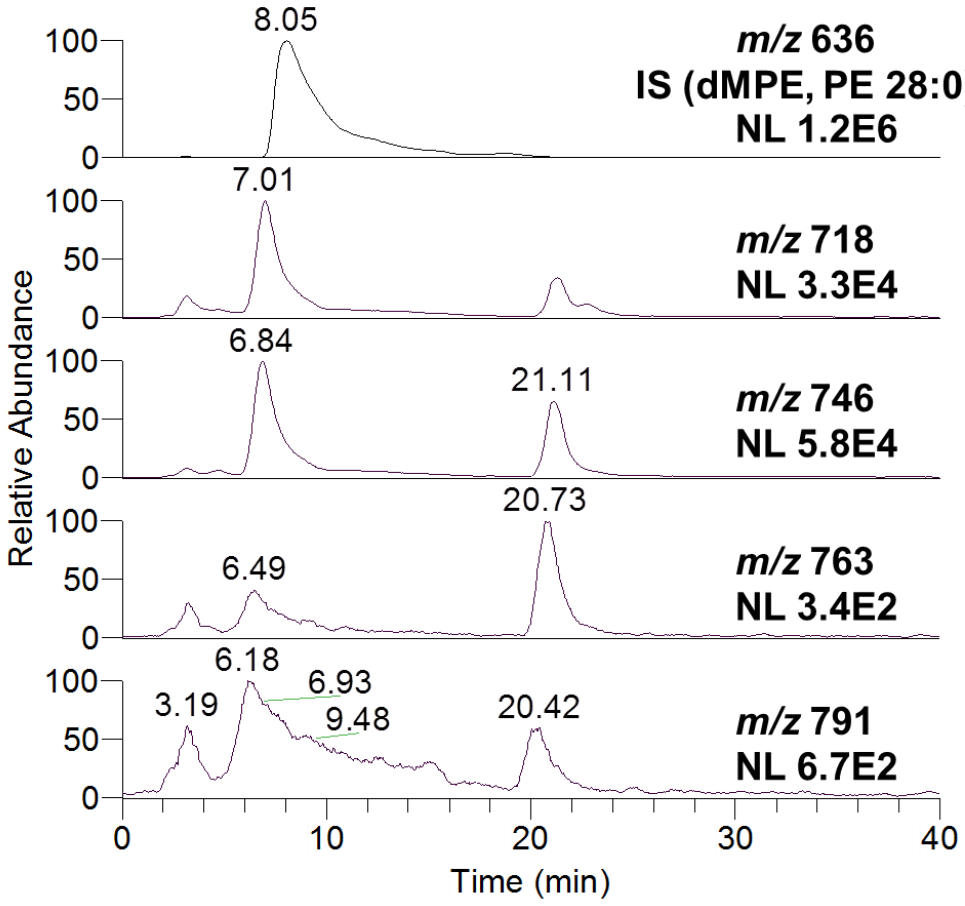

Figure S-21. Reconstructed ion chromatogram (RIC) of the protonated molecular ions $[M+H]^+$ of the non-modified (*m/z* 718 and 746) and nitrated and nitroxidized PE molecular species (*m/z* 763 NO_2-PE 16:0/18:1 and *m/z* 791 NO_2-PE 18:0/18:1) identified in H9c2 cardiomyoblast cells under starvation condition. IS, internal standard.

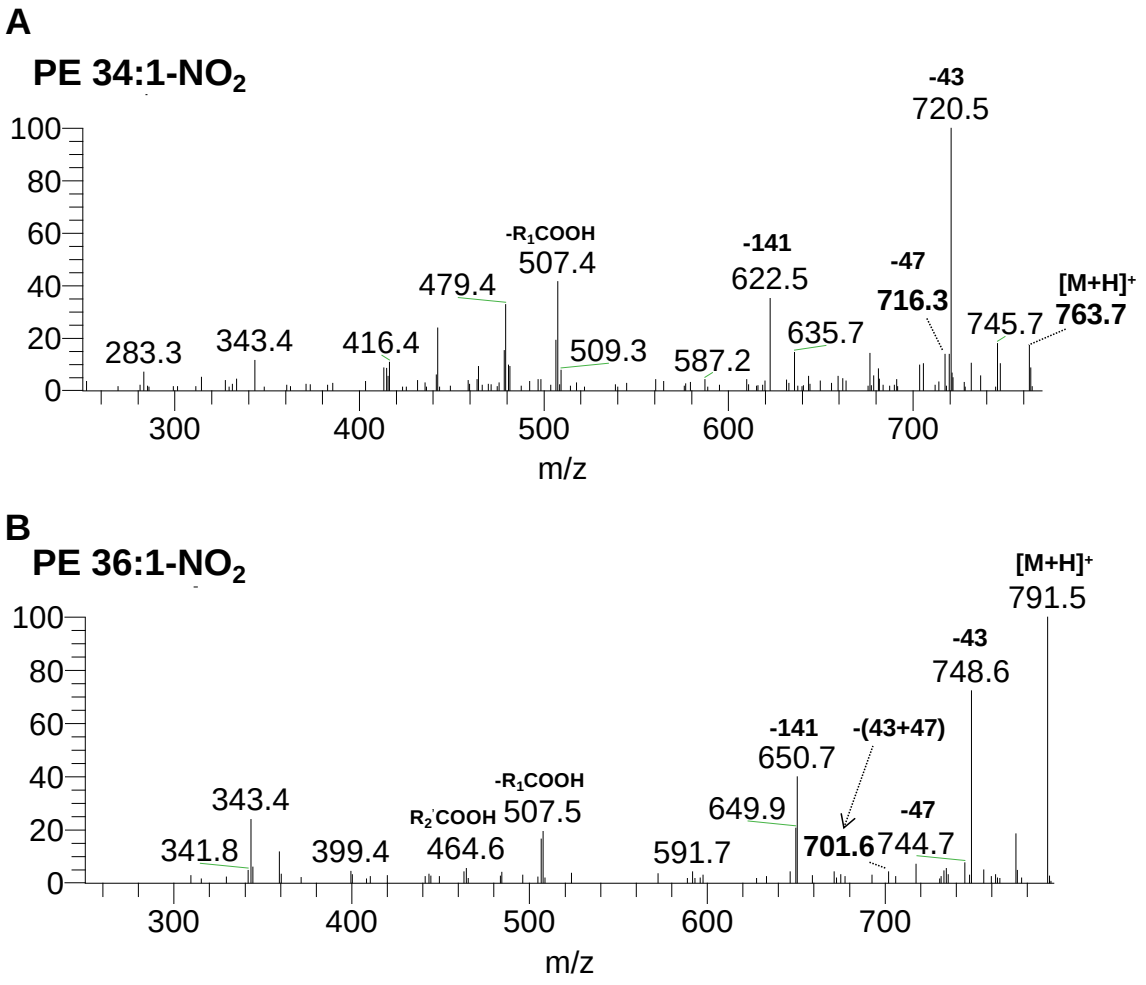

Figure S-22. HILIC-ESI-MS/MS spectra of $[M+H]^+$ ions at *m/z* 763 (NO_2-PE 16:0/18:1) and *m/z* 791 (NO_2-PE 18:0/18:1) observed in H9c2 cardiomyoblast cells under starvation condition.

SUPPLEMTARY TABLES

Table S1. Summary of the main nitrated and nitroxidized products observed in the positive ESI-MS spectra as $[M+H]^+$ ions of each PC after reaction with NO_2BF_4 with the identification and the indication of the respective *m/z* values. The corresponding retention time (RT) is also shown.

		POPC	**PLPC**	**PAPC**
		$[M+H]^+$	**$[M+H]^+$**	**$[M+H]^+$**
		$m/z_{(RT)}$	$m/z_{(RT)}$	$m/z_{(RT)}$
Non-modified		760.59	758.57	782.57
Nitration Derivatives				
NO-PL	+29, Nitroso	$789.58_{(35.1)}$	$787.56_{(20.8)}$	$811.56_{(26.4)}$
NO_2-PL	+45, Nitro	$805.57_{(44.8)}$	$803.56_{(39.3)}$	$827.56_{(43.0)}$
$(NO)_2$-PL	+58, Dinitroso	--	--	$840.55_{(11.6)}$
$(NO)(NO)_2$-PL	+74, Nitronitroso	$834.56_{(27.4)}$	$832.55_{(18.5)}$	$856.56_{(21.0)}$
$(NO_2)_2$-PL	+90, Dinitro	$850.56_{(39.0)}$	$848.54_{(32.6)}$	$872.54_{(35.3)}$
Nitration and Oxidation derivatives				
(NO)O-PL	+45, Nitrosohydroxy	$805.57_{(31.1)}$	$803.56_{(25.1)}$	$827.56_{(21.1)}$
(NO_2)O-PL	+61, Nitrohydroxy	$821.57_{(29.4)}$	$819.55_{(31.6)}$	$843.55_{(21.0)}$
(NO_2)(2O)-PL	+77, Nitrohydroperoxy	$837.56_{(22.6)}$	$835.54_{(24.8)}$	$859.54_{(21.5)}$
$(NO_2)_2$O-PL	+106, Dinitrohydroxy	$866.55_{(25.7)}$	$864.54_{(34.2)}$	$888.53_{(18.8)}$
$(NO_2)_2$(2O)-PL	+122, Dinitrohydroxy	$882.55_{(22.4)}$	$880.53_{(24.6)}$	$904.53_{(14.0)}$

Table S2. Summary of the main nitrated and nitroxidized products observed both in the positive-ion mode as $[M+H]^+$ ions and negative-ion mode as $[M-H]^-$ ions ESI-MS spectra from each PE, with the identification and the indication of the respective *m/z* values. The corresponding retention time (RT) is also shown.

		POPE		**PLPE**		**PAPE**	
		$[M+H]^+$	**$[M-H]^-$**	**$[M+H]^+$**	**$[M-H]^-$**	**$[M+H]^+$**	**$[M-H]^-$**
		$m/z_{(RT)}$	$m/z_{(RT)}$	$m/z_{(RT)}$	$m/z_{(RT)}$	$m/z_{(RT)}$	$m/z_{(RT)}$
Non-modified		718.54	716.53	716.52	714.52	740.52	738.52
Nitration Derivatives							
NO-PL	+29, Nitroso	$747.53_{(35.4)}$	$745.51_{(31.2)}$	$745.51_{(20.7)}$	$743.50_{(19.7)}$	$769.51_{(26.7)}$	$767.50_{(27.4)}$
NO_2-PL	+45, Nitro	$763.52_{(44.0)}$	$761.51_{(43.8)}$	$761.51_{(39.6)}$	$759.49_{(39.0)}$	$785.51_{(37.8)}$	$783.49_{(38.3)}$
$(NO)_2$-PL	+58, Dinitroso	--	--	--	--	$798.50_{(9.8)}$	$796.49_{(9.3)}$
$(NO)(NO_2)$-PL	+74, Nitronitroso	$792.51_{(26.5)}$	$790.50_{(25.9)}$	$790.50_{(19.1)}$	$788.48_{(18.3)}$	$814.50_{(21.9)}$	$812.48_{(22.8)}$
$(NO_2)_2$-PL	+90, Dinitro	$808.51_{(40.2)}$	$806.49_{(38.5)}$	$806.49_{(34.1)}$	$804.48_{(32.4)}$	$830.49_{(35.1)}$	$828.48_{(36.0)}$
Nitration and Oxidation derivatives							
(NO)O-PL	+45, Nitrosohydroxy	$763.52_{(31.3)}$	$761.51_{(30.7)}$	$761.51_{(24.5)}$	$759.49_{(23.7)}$	$785.51_{(21.6)}$	$783.49_{(22.0)}$
(NO_2)O-PL	+61, Nitrohydroxy	$779.52_{(29.6)}$	$777.50_{(27.5)}$	$777.50_{(32.2)}$	$775.49_{(30.9)}$	$801.50_{(21.3)}$	$799.49_{(21.4)}$
(NO_2)2O-PL	+77, Nitrohydroperoxy	$795.51_{(24.6)}$	$793.50_{(25.5)}$	$793.50_{(25.0)}$	$791.48_{(25.9)}$	$817.50_{(18.9)}$	$815.48_{(19.8)}$
$(NO_2)_2$O-PL	+106, Dinitrohydroxy	$824.50_{(25.4)}$	$822.49_{(25.2)}$	$822.49_{(33.4)}$	$820.47_{(33.2)}$	$846.49_{(14.4)}$	$844.47_{(15.3)}$
$(NO_2)_2$2O-PL	+122, Dinitrohydroperoxy	$840.50_{(23.4)}$	$838.48_{(24.6)}$	$838.48_{(23.9)}$	$836.47_{(25.1)}$	$862.48_{(11.7)}$	$860.47_{(12.6)}$

Table S3. Formula, calculated and observed mass and mass error of the nitrated and nitroxidized derivatives formed due to reaction between NO_2BF_4 and each PC observed in the ESI-MS spectra. Data was acquired in the Q-TOF2 mass spectrometer, and lock mass was done in the [M+H+non-modified PL]$^+$. POPC, PC16:0/18:1; PLPC, PC16:0/18:2; PAPC, PC16:0/20:4.

PC nitration products	Observed Mass (Da)	Calculated Mass (Da)	Error (mDa)	Error (ppm)	Predicted Formula $[M+H]^+$
[POPC+14u+H]+	774.5656	774.5649	0.7	0.9	$C_{42}H_{81}NO_9P$
[POPC+16u+H]+	776.5845	776.5805	-2.9	-3.8	$C_{42}H_{83}NO_9P$
[POPC+29u+H]+	789.5742	789.5758	-1.6	-2	$C_{42}H_{82}N_2O_9P$
[POPC+32u+H]+	792.5739	792.5755	-1.6	-2	$C_{42}H_{83}NO_{10}P$
[POPC+45u+H]+	805.5695	805.5707	-1.2	-1.5	$C_{42}H_{82}N_2O_{10}P$
[POPC+58u+H]+	818.5673	818.5660	1.3	1.6	$C_{42}H_{81}N_3O_{10}P$
[POPC+61u+H]+	821.5695	821.5656	3.9	4.7	$C_{42}H_{82}N_2O_{11}P$
[POPC+74u+H]+	834.5615	834.5609	0.6	0.7	$C_{42}H_{81}N_3O_{11}P$
[POPC+77u+H]+	837.5561	837.5605	-4.4	-5.3	$C_{42}H_{82}N_2O_{12}P$
[POPC+90u+H]+	850.5589	850.5558	3.1	3.7	$C_{42}H_{81}N_3O_{12}P$
[POPC+106u+H]+	866.5500	866.5507	-0.7	-0.8	$C_{42}H_{81}N_3O_{13}P$
[POPC+122u+H]+	882.5458	882.5456	0.2	0.2	$C_{42}H_{81}N_3O_{14}P$
[PLPC+14u+H]+	772.5483	772.5492	-0.9	-1.2	$C_{42}H_{79}NO_9P$
[PLPC+16u+H]+	774.5647	774.5649	-0.2	-0.3	$C_{42}H_{81}NO_9P$
[PLPC+29u+H]+	787.5597	787.5601	-0.4	-0.6	$C_{42}H_{80}N_2O_9P$
[PLPC+32u+H]+	790.5631	790.5598	3.3	4.2	$C_{42}H_{81}NO_{10}P$
[PLPC+45u+H]+	803.5565	803.5551	1.4	1.8	$C_{42}H_{80}N_2O_{10}P$
[PLPC+58u+H]+	816.5518	816.5503	1.5	1.8	$C_{42}H_{79}N_3O_{10}P$
[PLPC+61u+H]+	819.5507	819.5500	0.7	0.9	$C_{42}H_{80}N_2O_{11}P$
[PLPC+74u+H]+	832.5466	832.5452	1.4	1.7	$C_{42}H_{79}N_3O_{11}P$
[PLPC+77u+H]+	835.5397	835.5449	-5.2	-6.2	$C_{42}H_{80}N_2O_{12}P$
[PLPC+90u+H]+	848.5435	848.5401	3.4	4	$C_{42}H_{79}N_3O_{12}P$
[PLPC+106u+H]+	864.5383	864.5351	3.2	3.8	$C_{42}H_{79}N_3O_{13}P$
[PLPC+122u+H]+	880.5309	880.5300	0.9	1.1	$C_{42}H_{79}N_3O_{14}P$
[PAPC+14u+H]+	796.5513	796.5492	2.1	2.6	$C_{44}H_{79}NO_9P$
[PAPC+16u+H]+	798.5676	798.5649	2.7	3.4	$C_{44}H_{81}NO_9P$
[PAPC+29u+H]+	811.5589	811.5601	-1.2	-1.5	$C_{44}H_{80}N_2O_9P$
[PAPC+32u+H]+	814.5583	814.5598	-1.5	-1.9	$C_{44}H_{81}NO_{10}P$
[PAPC+45u+H]+	827.5578	827.5551	2.7	3.3	$C_{44}H_{80}N_2O_{10}P$
[PAPC+58u+H]+	840.5457	840.5503	-4.6	-5.5	$C_{44}H_{79}N_3O_{10}P$
[PAPC+61u+H]+	843.5463	843.5500	-3.7	-4.4	$C_{44}H_{80}N_2O_{11}P$
[PAPC+74u+H]+	856.5450	856.5452	-0.2	-0.3	$C_{44}H_{79}N_3O_{11}P$
[PAPC+77u+H]+	859.5413	859.5449	-3.6	-4.2	$C_{44}H_{80}N_2O_{12}P$
[PAPC+90u+H]+	872.5424	872.5401	2.3	2.6	$C_{44}H_{79}N_3O_{12}P$
[PAPC+106u+H]+	888.5349	888.5351	-0.2	-0.2	$C_{44}H_{79}N_3O_{13}P$
[PAPC+122u+H]+	904.5302	904.5300	0.2	0.3	$C_{44}H_{79}N_3O_{14}P$

Table S4. Formula, calculated and observed mass and mass error of the nitrated and nitroxidized derivatives formed due to reaction between NO_2BF_4 and each PE observed in the ESI-MS spectra. Data was acquired in the Q-TOF2 mass spectrometer, and lock mass was done in the $[M+H+\text{non-modified PL}]^+$. POPE, PE16:0/18:1; PLPE, PE16:0/18:2; PAPE, PE16:0/20:4.

PE nitration products	Observed Mass (Da)	Calculated Mass (Da)	Error (mDa)	Error (ppm)	Predicted Formula [M+H]+
$[POPE+14u+H]^+$	732.5200	732.5179	2.1	2.8	$C_{39}H_{75}NO_9P$
$[POPE+16u+H]^+$	734.5327	734.5336	-0.9	-1.2	$C_{39}H_{77}NO_9P$
$[POPE+29u+H]^+$	747.5297	747.5288	0.9	1.1	$C_{39}H_{76}N_2O_9P$
$[POPE+32u+H]^+$	750.5278	750.5285	-0.7	-0.9	$C_{39}H_{77}NO_{10}P$
$[POPE+45u+H]^+$	763.5236	763.5238	-0.2	-0.2	$C_{39}H_{76}N_2O_{10}P$
$[POPE+58u+H]^+$	776.5193	776.5190	0.3	0.4	$C_{39}H_{75}N_3O_{10}P$
$[POPE+61u+H]^+$	779.5203	779.5187	1.6	2.1	$C_{39}H_{76}N_2O_{11}P$
$[POPE+74u+H]^+$	792.5135	792.5139	-0.4	-0.5	$C_{39}H_{75}N_3O_{11}P$
$[POPE+77u+H]^+$	795.5125	795.5136	-1.1	-1.4	$C_{39}H_{76}N_2O_{12}P$
$[POPE+90u+H]^+$	808.5076	808.5088	-1.2	-1.5	$C_{39}H_{75}N_3O_{12}P$
$[POPE+106u+H]^+$	824.5029	824.5038	-0.9	-1	$C_{39}H_{75}N_3O_{13}P$
$[POPE+122u+H]^+$	840.4999	840.4987	1.2	1.5	$C_{39}H_{75}N_3O_{14}P$
$[PLPE+14u+H]^+$	730.5004	730.5023	-1.9	-2.6	$C_{39}H_{73}NO_9P$
$[PLPE+16u+H]^+$	732.5170	732.5179	-0.9	-1.3	$C_{39}H_{75}NO_9P$
$[PLPE+29u+H]^+$	745.5125	745.5132	-0.7	-0.9	$C_{39}H_{74}N_2O_9P$
$[PLPE+32u+H]^+$	748.5142	748.5129	1.3	1.8	$C_{39}H_{75}NO_{10}P$
$[PLPE+45u+H]^+$	761.5087	761.5081	0.6	0.8	$C_{39}H_{74}N_2O_{10}P$
$[PLPE+58u+H]^+$	774.5037	774.5034	0.3	0.4	$C_{39}H_{73}N_3O_{10}P$
$[PLPE+61u+H]^+$	777.5052	777.5030	2.2	2.8	$C_{39}H_{74}N_2O_{11}P$
$[PLPE+74u+H]^+$	790.5005	790.4983	2.2	2.8	$C_{39}H_{73}N_3O_{11}P$
$[PLPE+77u+H]^+$	793.4970	793.4979	-0.9	-1.2	$C_{39}H_{74}N_2O_{12}P$
$[PLPE+90u+H]^+$	806.4915	806.4932	-1.7	-2.1	$C_{39}H_{73}N_3O_{12}P$
$[PLPE+106u+H]^+$	822.4863	822.4881	-1.8	-2.2	$C_{39}H_{73}N_3O_{13}P$
$[PLPE+122u+H]^+$	838.4841	838.4830	1.1	1.3	$C_{39}H_{73}N_3O_{14}P$
$[PAPE+14u+H]^+$	754.5019	754.5023	-0.4	-0.5	$C_{41}H_{73}NO_9P$
$[PAPE+16u+H]^+$	756.5192	756.5179	1.3	1.7	$C_{41}H_{75}NO_9P$
$[PAPE+29u+H]^+$	769.5146	769.5132	1.4	1.8	$C_{41}H_{74}N_2O_9P$
$[PAPE+32u+H]^+$	772.5115	772.5129	-1.4	-1.8	$C_{41}H_{75}NO_{10}P$
$[PAPE+45u+H]^+$	785.5090	785.5081	0.9	1.1	$C_{41}H_{74}N_2O_{10}P$
$[PAPE+59u+H]^+$	798.5049	798.5034	1.5	1.9	$C_{41}H_{73}N_3O_{10}P$
$[PAPE+61u+H]^+$	801.5023	801.5030	-0.7	-0.9	$C_{41}H_{74}N_2O_{11}P$
$[PAPE+74u+H]^+$	814.4969	814.4983	-1.4	-1.7	$C_{41}H_{73}N_3O_{11}P$
$[PAPE+77u+H]^+$	817.4977	817.4979	-0.2	-0.3	$C_{41}H_{74}N_2O_{12}P$
$[PAPE+90u+H]^+$	830.4920	830.4932	-1.2	-1.4	$C_{41}H_{73}N_3O_{12}P$
$[PAPE+106u+H]^+$	846.4893	846.4881	1.2	1.4	$C_{41}H_{73}N_3O_{13}P$
$[PAPE+122u+H]^+$	862.4813	862.4830	-1.7	-2	$C_{41}H_{73}N_3O_{14}P$

Table S5. Typical modified carboxylate cations and anions of each fatty acids of each nitrated and nitroxidized PL molecular species observed in tandem mass spectra that can be used for diagnostic scan of nitrated and nitroxidized PLs in positive- and negative-ion mode.

Typical modified carboxylate cations and anions observed in MS^2						
	Oleic Acid		**Linoleic Acid**		**Arachidonic Acid**	
	$[R'COOH+H]^+$	$R'COO^-$	$[R'COOH+H]^+$	$R'COO^-$	$[R'COOH+H]^+$	$R'COO^-$
Nitrated derivatives						
Nitroso	312.3	310.2	310.2	308.2	334.2	332.2
Nitro	328.2	326.2	326.3	324.2	350.2	348.2
Dinitroso	--	--	--	--	363.2	361.2
Nitronitroso	357.2	355.2	355.2	353.2	379.2	377.2
Dinitro	373.2	371.2	371.2	369.2	395.2	393.2
Nitroxidized derivatives						
Nitrosohydroxy	328.2	326.2	326.3	324.2	350.2	348.2
Nitrohydroxy	344.2	342.2	342.2	340.2	366.2	364.2
Nitrohydroperoxy	360.2	358.2	358.2	356.2	382.2	380.2
Dinitrohydroxy	389.2	387.2	387.2	385.2	411.2	409.2
Dinitrohydroperoxy	405.2	403.2	403.2	401.2	427.2	425.2

SUPPLEMTARY FIGURES

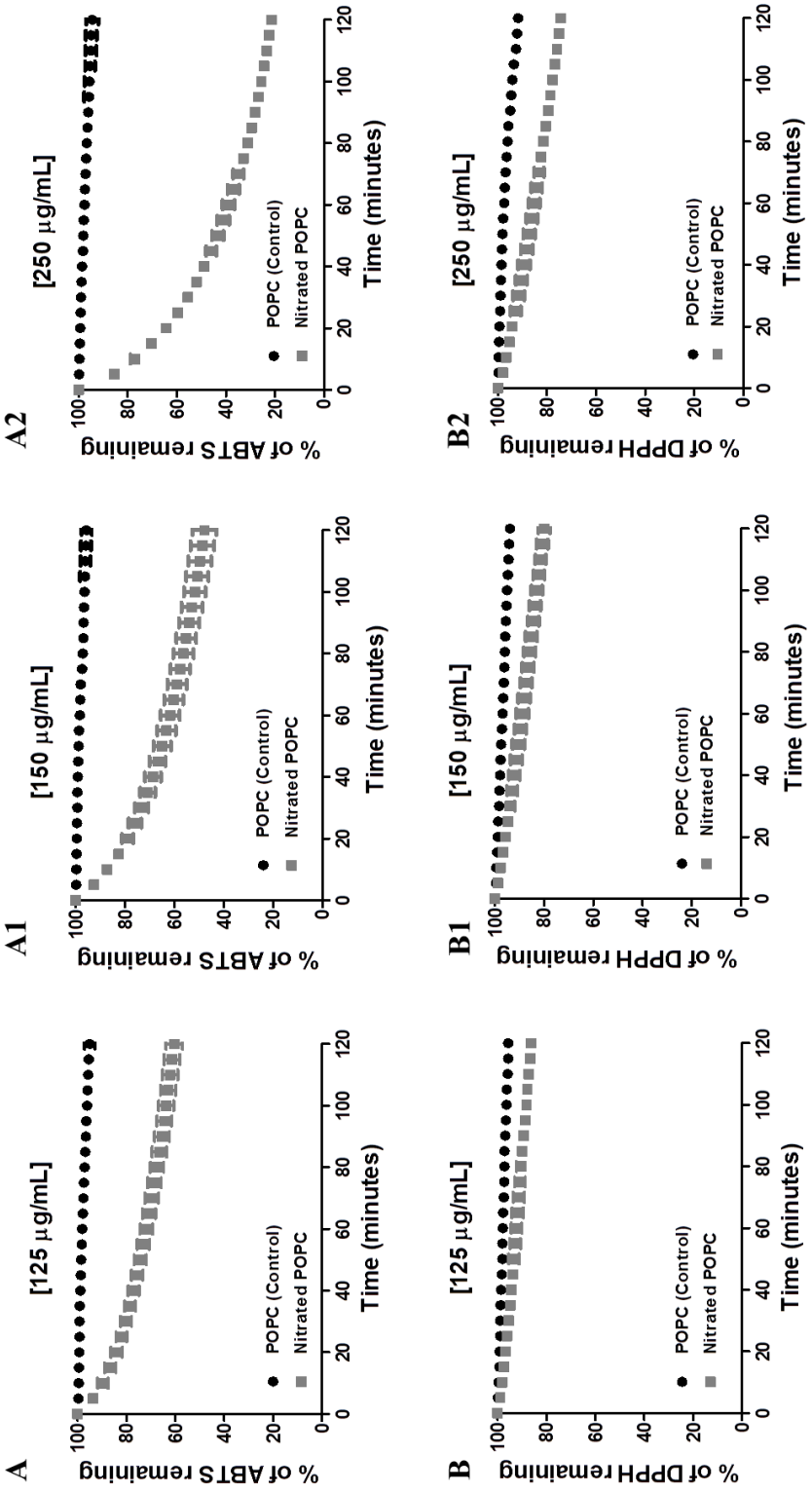

Figure S-1. Profile of $ABTS^{\bullet+}$ (A) and $DPPH^{\bullet}$ (B) radical consumption for non-modified POPC (control) and nitrated POPC.

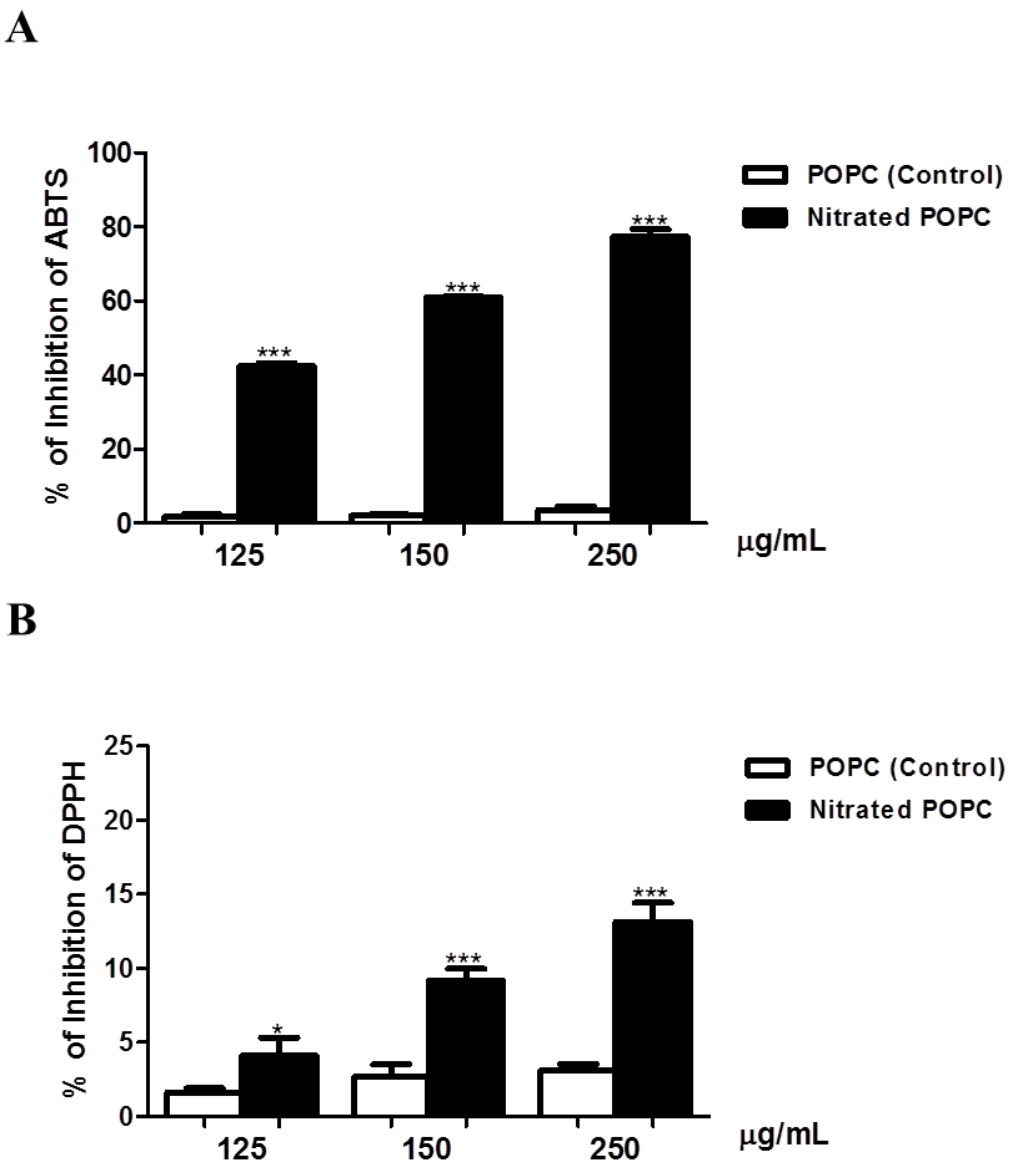

Figure S-2. (A) Percentage of inhibition of $ABTS^{\bullet+}$ (A) and $DPPH^{\bullet}$ radicals (B) obtained in the presence of non-modified POPC and nitrated POPC (125, 150 and 250 µg/mL) after 60 min of reaction. Values were the means±SD. ***, significantly different from control group ($P<0.0001$).

SUPPLEMTARY TABLES

Table S-1. Amount of the residual $ABTS^{\bullet+}$ and $DPPH^{\bullet}$ radicals after 60 min of reaction in the presence of non-modified POPC and nitrated POPC at the three concentrations tested (125, 150 and 250 µg/mL) prepared in ethanol. The results were expressed as percentage of $ABTS^{\bullet+}$ and $DPPH^{\bullet}$ remaining.

[Non-modified POPC] (µg/mL)	%ABTS Remaining	[Nitrated POPC] (µg/mL)	%ABTS Remaining
125	98.1±0.9	125	71.9±2.5
150	98.4±0.7	150	61.8±3.8
250	97.7±1.2	250	39.0±2.5
[Non-modified POPC] (µg/mL)	**%DPPH Remaining**	**[Nitrated POPC] (µg/mL)**	**%DPPH Remaining**
125	98.0±0.9	125	92.3±2.2
150	96.8±1.1	150	88.9±2.5
250	97.5±0.5	250	85.2±2.2